SKB

TECHNICAL REPORT 96-21

Boring of full scale deposition holes using a novel dry blind boring method

Jorma Autio, Timo Kirkkomäki

Saanio & Riekkola Oy, Helsinki, Finland

October 1996

SVENSK KÄRNBRÄNSLEHANTERING AB
SWEDISH NUCLEAR FUEL AND WASTE MANAGEMENT CO
P.O.BOX 5864 S-102 40 STOCKHOLM SWEDEN
PHONE +46 8 665 28 00
FAX +46 8 661 57 19

BORING OF FULL SCALE DEPOSITION HOLES USING A NOVEL DRY BLIND BORING METHOD

Jorma Autio, Timo Kirkkomäki

Saanio & Riekkola Oy, Helsinki, Finland

October 1996

BORING OF FULL SCALE DEPOSITION HOLES USING A NOVEL DRY BLIND BORING METHOD

Jorma Autio
Timo Kirkkomäki

Saanio & Riekkola Oy
Laulukuja 4
00420 Helsinki
Finland

October 1996

Keywords: Boring, shaft boring, blind boring, deposition hole boring, disturbed zone

ABSTRACT

Three holes the size of deposition holes (depth 7.5 m and diameter 1.5 m) were bored in the Research Tunnel at Olkiluoto in Finland. A novel full-face boring technique was used based on rotary crushing of rock and removal of crushed rock by vacuum flushing through the drill string. The purpose of the work was to demonstrate the feasibility of the technique. During the boring test procedures were carried out in order to determine the effect of changes in operating parameters on the performance of the boring machine and the quality of the hole.

The boring method was found to be technically feasible and efficient. The correlation between the rate of advance and the thrust used was established and this can be used to estimate the performance of a similar, but more powerful, boring machine.

Evaluation of the quality of the hole included studies of the geometry of the holes, measurements of surface roughness using a laser profilometer and study of excavation disturbances in the zone adjacent to the surface of the holes using two novel methods, the He-gas diffusion method and the ^{14}C-polymethyl-methacrylate method. It was found that there is a distinct disturbed zone adjacent to the surface of the full scale deposition holes which can be divided into three different zones. The zones are as follows: a crushed zone penetrating to a depth of about 3 mm from the surface, a fractured zone extending to a depth of 6 - 10 mm from the crushed zone and a microfractured zone extending to a depth of 15 - 35 mm from the fractured zone. The porosity of the rock in the disturbed zone measured using the ^{14}CPMMA-method was clearly greater than the porosity of undisturbed rock to a depth of about 11 mm. The values of permeability and diffusion coefficient in the disturbed zone measured in a direction perpendicular to the disturbed surface were found to be approximately one order of magnitude larger than those of undisturbed rock.

SAMMANFATTNING

Tre simulerade deponeringshål med diametern 1,5 m och djupet 7,5 m har borrats med en ny fullborrningsteknik i forskningstunnel i Olkiluoto på Finlands sydvästra kust. Metoden som användes bygger på krossande, roterande borrning med vakuumutsugning av borrkaxet via borrstången. Borrningen genomfördes för att demonstrera att metoden är tillämpbar i ett djupförvar. Under borrningen utfördes tester för att studera olika driftparametrars påverkan på borrmaskinens funktion och hålens kvalitet.

Borrmetoden visades vara tekniskt genomförbar och effektiv. Ett samband mellan borrsjunkning och matningskraft registrerades, vilket kan användas för att beräkna kapaciteten hos en liknande men kraftigare borrmaskin än den som användes. Utvärdering av hålens kvalitet inkluderade studier av hålens geometri, mätning av väggarnas ytråhet samt studier av borrpåverkan i bergväggen närmast hålet med hjälp av två nya metoder: He-gasdiffusion och ^{14}CPMMA (kol-14 polymetylmetakrylat) -autoradiografi.

Resultaten visar att det finns en distinkt störd zon närmast bergytan hos de fullstora deponeringshålen, som kan delas upp i tre mindre zoner. Dessa zoner är från hålet räknat en zon med krossat berg som sträcker sig ungefär 3 mm in, en uppsprucken zon som sträcker sig ytterligare ungefär 6 - 10 mm in samt en zon med mikrosprickor som sträcker sig ytterligare 15 - 35 mm in. Bestämningarna av bergets porositet med ^{14}CPMMA-metoden resulterade i förhöjda porositeter till ett djup av ungefär 11 mm. Uppmätta permeabiliteter och diffusions koefficienter radiellt in från borrhålet var ungefär 10 gånger så stora i den störda zon som i det intakta berget.

TABLE OF CONTENTS

SUMMARY

Three experimental full scale deposition holes were bored with a novel full-face boring technique in the Research Tunnel at Olkiluoto. The holes had a diameter of 1.527 m and an approximate depth of 7.5 m. The boring technique was based on rotary crushing of rock and dry removal of crushed rock by vacuum cleaning through the drill string. The boring experiment was carried out to demonstrate the feasibility of the technique especially in regard to the quality of the hole and performance of the boring equipment. During the boring process, tests were carried out to determine the effect of changes in operating parameters on the performance of the boring machine and on the quality of the hole.

Samples of the crushed rock were taken during boring and the particle size distribution and shape of particles were studied in relation to the boring parameters. The particle size distribution was found to be quite insensitive to the boring parameters.

The boring equipment used was found to be compact and easy to transfer. The occupational conditions were found satisfactory and the impact of the method on the environment was limited. The problems encountered in the work, which were manifested by a low degree of utilization of the equipment, were mainly related to the mechanical design and implementation of the boring machine and the vacuum suction system.

This study proved that deposition holes can be bored effectively using a boring machine based on full-face rotary crushing and removal of crushed rock by direct vacuum suction of air from the bottom of the hole. The average advance rate of the boring machine tested at the maximum machine thrust of about 600 kN and a rotation speed of 8 rpm was about 1.9 mm/rev. which is equivalent to 91 cm/h.

A correlation between the advance rate of boring and thrust was established which can be used to estimate the performance of a similar but more powerful boring machine. The efficiency of the vacuum flushing in keeping the bottom of the hole clean of crushed rock was assessed to be the most critical factor limiting the maximum advance rates achievable. The estimated maximum advance rate for a boring machine and cutter head with higher thrust and torque capacity and a suction system providing improved performance is estimated to be as high as 3 m/h for rock types similar to those in the Research Tunnel. The theoretical efficiency of a boring machine based on the concept introduced here and designed for the purpose of boring deposition holes as efficiently as technically possible suggests that a single deposition hole could be bored in one work shift.

The force per button row for the cutter configuration was calculated and it was estimated that for the 5 and 6 row cutter configuration the force per one button row is from 1.3 to 2.9 % of the total force depending on the position of the particular cutter. The correlation between the rate of advance and thrust was found to be exponential but could also be estimated fairly accurately with a linear expression. At the highest thrust level the maximum advance rate was approximately 2 mm/revolution, in which case the minimum advance rate of the multiple button rows was only 0.5 - 1.0 mm/revolution per cutter. Therefore the failure process of the rock and chip formation may not have been as effective as at higher thrust levels. The rate of penetration versus thrust behavior of the boring equipment was correlated against different types of rock with different drillability values and compressive strengths.

Interest in the quality of the hole focused on the surface roughness of the hole and the mechanical disturbance as specified by increased microfracturing and porosity in a zone close to the surface. The evaluation of the quality of the hole included studies of the geometry of the holes, measurement of surface roughness using a laser profilometer and study of excavation disturbance in the zone close to the surface of the holes by using two novel methods, the He-gas diffusion method and the ^{14}C-Polymethylmetacrylate method (^{14}CPMMA method). The excavation disturbance was studied in the laboratory using 98 mm diameter core samples taken from locations in the holes which represented the use of different boring parameters and penetration rates.

The straightness of the holes expressed as the deviation with respect to the depth of the hole was between 0.2 % and 0.4 %. This deviation was assumed to be caused primarily by deviation in the initial alignment of the boring machine.

The porosity of rock in the disturbed zone adjacent to the surface of the holes measured with the ^{14}CPMMA-method was clearly above the porosity of undisturbed rock to a depth of about 11 mm. The average values of porosity in a zone from the disturbed surface to a depth of 5 mm ranged from 0.2 to 1.2 vol.%. The porosity of the undisturbed rock ranged from 0.10 to 0.15 vol.%. Porous tracelines in the hole walls extended to depths of 15 - 30 mm from the disturbed surface depending on the orientation of the sample and the boring parameters.

The diffusion and permeability coefficients were measured with the He-gas method from 30 samples of both undisturbed and disturbed rock. A zone of higher radial conductivity and diffusivity was found next to the surface of the holes. The estimated thickness of this zone was between 17 and 21 mm from the surface. The maximum length of separate microcracks was estimated to be about 12 mm. The ratio of the diffusion coefficients between the disturbed zone and the intact rock was found to vary between 5 and 31, and the corresponding ratio of permeabilities varied between 10 and 90.

The novel boring method based on rotary crushing and removal of crushed rock by vacuum suction through the drill string was found to be technically feasible and efficient on the basis of the operational characteristics of the equipment and the boring parameters obtained in these tests. This study shows that further development of the boring equipment should be focused on improvement of the degree of utilization of the equipment and on increasing the efficiency of the vacuum cleaning system.

1 INTRODUCTION

According to the preliminary design for the final repository for spent fuel made by Swedish Nuclear Fuel and Waste Management Co (SKB) and Posiva Oy the repository is to be excavated at sufficient depth in the crystalline bedrock and the encapsulated spent fuel shall be emplaced in holes in the tunnel floor, see Figure 1-1. In the design proposed by SKB the total number of deposition holes is 4500 and the depth of the final repository for spent fuel ranges from 400 to 700 m. In the corresponding design proposed by Posiva Oy the depth of the repository is from 300 to 700 m and the number of deposition holes is 1530.

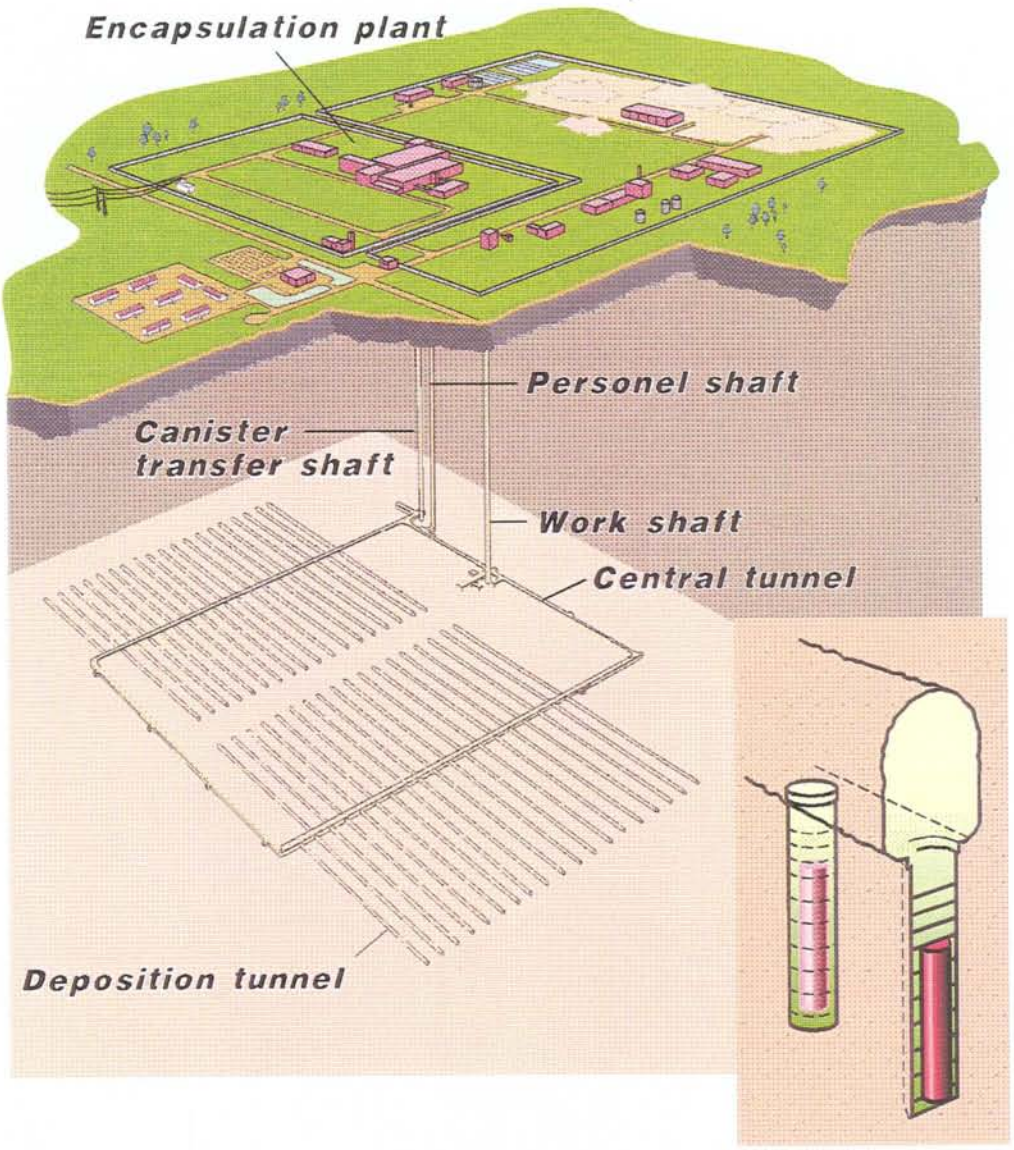

Figure 1-1. *Basic concept of the final repository for spent fuel. The spent fuel canisters will be emplaced in deposition holes in the tunnel floor (TVO 1992).*

The excavation of deposition holes has been one of the topics in the development of repository technology because the quality of the hole has an impact on the long-term safety of the disposal and the excavation of large number of holes in small tunnels at considerable depths is a challenging technical task.

Different alternative techniques for making the deposition holes have been proposed such as diamond coring, coring with abrasives, coring with water jets and conventional stitch drilling. Diamond coring was tested in the Stripa-project (Pusch & Nilsson 1982), by the Power Nuclear Reactor Company (PNC) of Japan in the Kamaishi research facility and in France (Boisson & Derlich 1994). Coring with abrasives is being used for making large diameter calender stacks of rock for paper mills. Coring with water jets has been tested by the Atomic Energy of Canada Limited (AECL) at the Underground Research Laboratory (ULR).

On the basis of previous studies (Nord 1980, Tahvanainen & Matikainen 1983, Autio 1992, Wichmann 1993, Øiseth 1995) full-face boring of deposition holes based on rotary crushing was a potential technique with certain obvious advantages but one which lacked references.

After a preliminary study and a review with different manufacturers and contractors, a machine design based principally on existing proven techniques suitable for boring holes of the size of the deposition holes in a small tunnel was developed. The novel boring technique was based on rotary crushing and removal of crushed rock by vacuum cleaning through the drill string. The principle of rotary crushing is well known and is in common use, for example in raise boring.

Three experimental full-scale deposition holes were bored in the Research Tunnel at Olkiluoto to demonstrate the feasibility of the technique with particular regard to the quality of the hole and performance of the boring equipment. The exact diameter of the hole resulted from the size of the available cutterhead, this being 1524 mm. The depth of the holes was 7.5 m. The novel boring equipment employed for this work had only been used previously for test boring a 2.7 m length of hole (Autio & Kirkkomäki 1996a, Johansson 1994).

The main objectives of the work were:

- to test the feasibility of the novel design of equipment which is based on rotary crushing and removal of rock using vacuum suction
- to produce a basis for future development of the equipment and performance evaluation
- to provide information about the performance of the boring machine and in particular about the parameters which govern boring performance so that the costs of using the method can be estimated
- to produce empirical data relating to the factors which affect the excavation disturbance caused by boring

- to characterize the boring process and its impact on the quality of the hole.

The evaluation of the quality of the holes included studies of the geometry of the holes, surface roughness and excavation disturbance in the zone adjacent to the surface of the holes. The quality of the hole received special attention since although it has an impact on the design and long term safety of the disposal and the extent of this impact has not been specified, existing information on the subject is very limited.

The excavation disturbance caused by boring is influenced by machine-related factors such as the shape of the cutters and thrust used, and rock-related factors such as uniaxial compressive strength and drillability index. Current estimates of the extent of the disturbance zone are in the main based on laboratory-based indentation experiments with single cutters. A recent review of the studies related to this subject and the latest achievements are reported by Tan et al. 1994, Lindqvist et al. 1994, Kou et al. 1994.

During boring, tests were carried out to determine the effect of changes in operating parameters on the performance of the boring machine and the quality of the hole. The main focus of interest in technical performance was the rate of penetration and the efficiency of the vacuum suction system. The main focus of interest in assessing the quality of the hole was surface roughness and mechanical disturbance, the latter being specified as the increase in microfracturing and porosity in a zone adjacent to the hole surface.

This report includes a description of the Research Tunnel, a description of the boring equipment and the results obtained. The Research Tunnel is described using parameters such as rock strength and drillability since these are of importance in the evaluation of the results of the boring demonstration.

A general description of the boring method is given, the main emphasis is placed on describing the cutter head and vacuum flushing system. In addition, a summary of the operational characteristics of the boring equipment is made, this includes evaluation of the occupational conditions and environmental emissions. The results of the determination of the boring parameters such as rate of penetration, cutter coefficient and specific energy are then presented. A more detailed description of the boring procedure and operational experiences is given elsewhere by Autio & Kirkkomäki 1996.

The particle size distribution and shape of the crushed rock resulting from the boring process is presented in general terms and in comparison to the thrust used as well as the properties of the hole such as dimensions, straightness, surface roughness and mechanical disturbance caused by boring.

The evaluation of the suitability of the method for producing deposition holes includes an estimate of the performance of the method using more effective boring equipment, an analysis of the effect of different rock types and some guidelines for future development.

2 DESCRIPTION OF THE RESEARCH TUNNEL

The three experimental full-scale deposition holes (diameter 1.5 m, depth 7.5 m) were bored in the Research Tunnel. This is located at a depth of 60 m in the VLJ repository which is an underground disposal facility for the low- and medium-level waste generated by the Olkiluoto nuclear power plant, see Figure 2-1. The repository is located 1 km from Olkiluoto 1 and Olkiluoto 2 powerplants on the Olkiluoto island on the southwest coast of Finland. The repository was taken into operation in 1992.

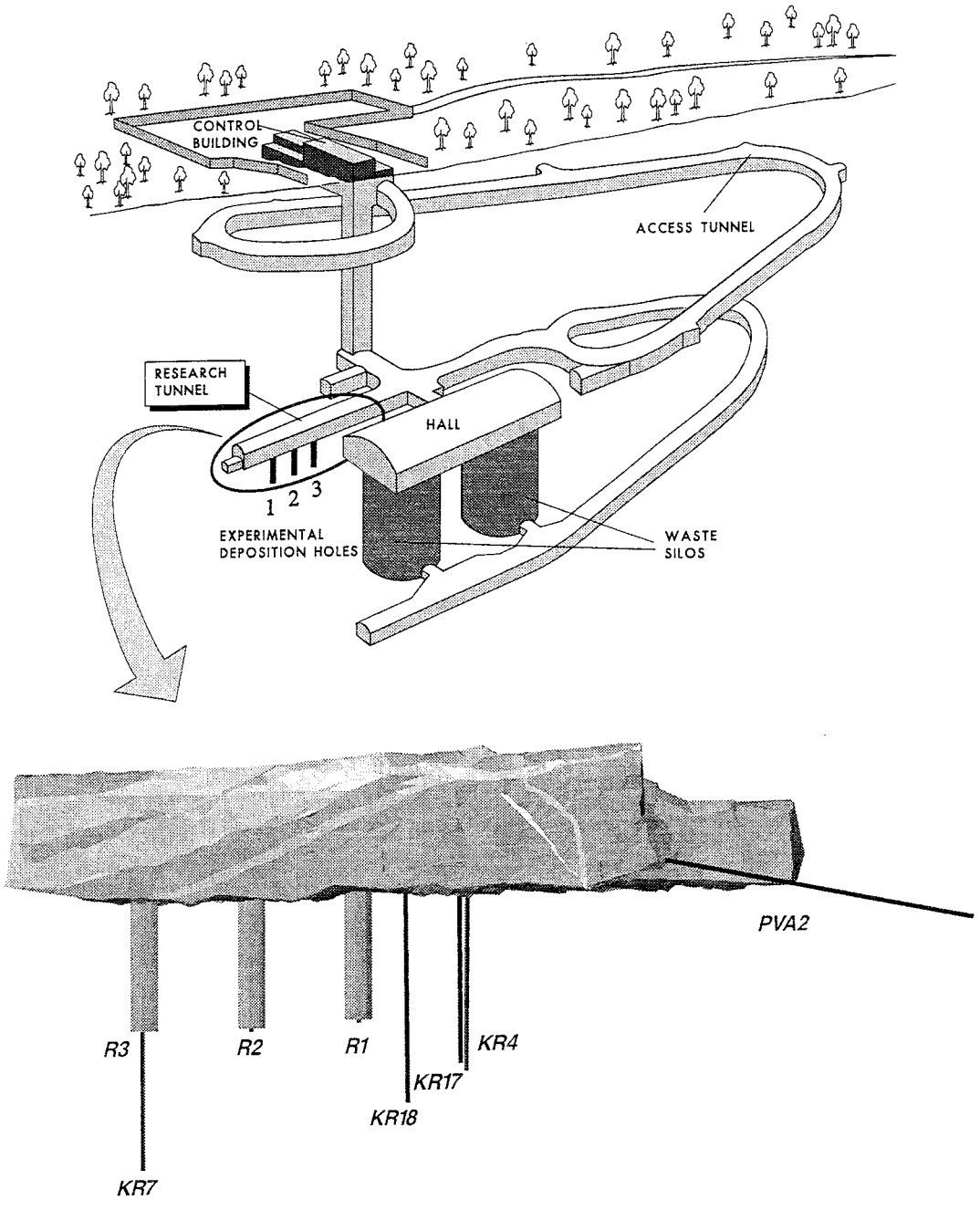

Figure 2-1. VLJ-repository and the Research Tunnel.

The Research Tunnel is 47 m long and from 4 to 7 m high. It was excavated using the conventional drill and blast technique. A charge density of approximately 1.1 kg-dyn/m (weight of charge per unit length of the stem section of the hole, equivalent to the charge density of dynamite) was used in the blasting of the floor section. The corresponding spacing between the perimeter holes was about 0.86 m.

Boring of the experimental full-scale deposition holes was accompanied by comprehensive pre-boring and post-boring characterization of the rock in the areas close to the holes using geophysical, geological, hydraulic and mechanical tests.

Before the boring began, investigative core holes KR5, KR6 and KR7 were drilled (Rautio & With 1993) in the position of the proposed full-scale experimental deposition holes to verify the quality of the rock, see Figures 2-1, 2-2 and 2-3. The inflow of water into the investigation holes was measured to be 0.05 - 13.00 l/h.

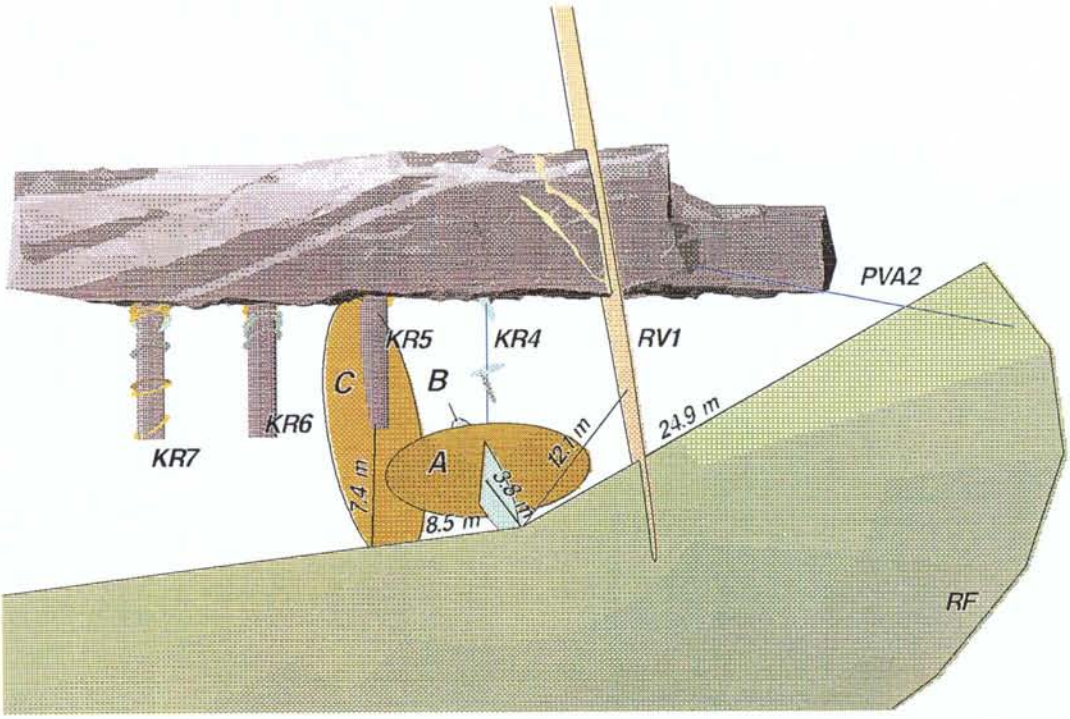

Figure 2-2. *3D model of the TVO Research Tunnel showing the hydraulically conductive fracture zones in the vicinity of the tunnel and the three full-scale experimental deposition holes.*

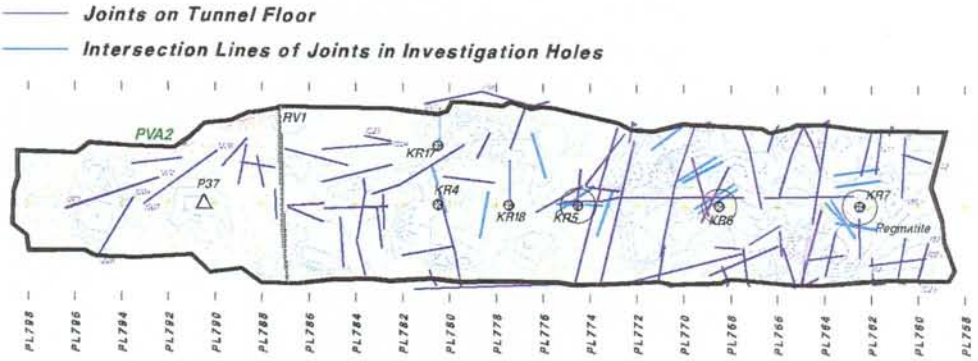

Figure 2-3. *Floor plane of the Research Tunnel showing the surface topography, geology and the location of the investigation holes KR5 - KR7 which were drilled in the proposed positions of the full-scale experimental deposition holes.*

The VLJ repository has been excavated in an east-west striking tonalite formation surrounded by mica gneiss. The rock types found in the Research Tunnel are gneissic tonalite and pegmatite. The tonalite is usually slightly foliated, medium-grained, massive and sparsely fractured as shown in Figure 2-4. Besides gneissic tonalite, which is referred to in this context as anisotropic tonalite, a fine-grained, homogeneous tonalite variant is met in minor sections of the hole. The pegmatite is non-foliated, coarse-grained, massive and sparsely fractured (Äikäs 1993).

According to the microscopic thin section examination and point counting method carried out by the Geological Survey of Finland, the main minerals in the anisotropic tonalite are quartz (16.4 %), plagioclase (37.2 %), biotite (29.6 %) and hornblende (11.0 %), making up about 94 % of the total content. The mafic minerals, especially oblong grains of biotite and hornblende are oriented. The grains are subhedral and the alteration to secondary minerals is insignificant.

The grain size of the quartz is 0.3 - 0.5 mm although the size of quartz clusters is 1 - 2 mm. The grain size of the plagioclase is larger, the largest grains being from 2 to 3 mm. The anorthic content of the plagioclase is 31 - 32 %. The biotite occurs as clusters of flaky grains of typical size from 1 to 3 mm.

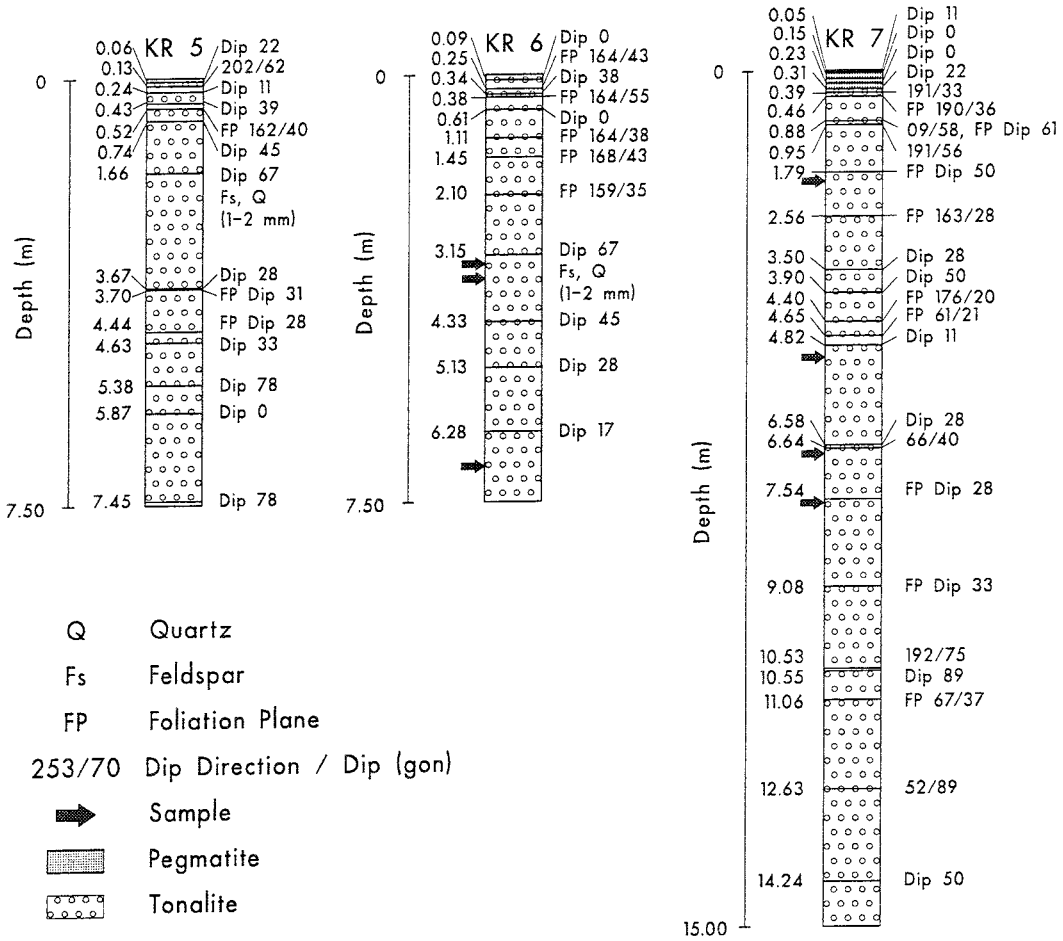

Figure 2-4. *Geology of core samples from boreholes KR5 - KR7 shown in Figures 2-2 and 2-3. The rock types, fractures, foliation planes and the directions of these are shown together with identified fracture fillings and sample positions.*

The state of stress at the VLJ-repository and Research Tunnel area is low according to stress measurements carried out before the construction of the VLJ-repository and the Research Tunnel (Kuula & Johansson 1991, Nykyri et al. 1991). The measured values of in-situ stress averaged 5 to 6 MPa at the level of the repository. The monitoring of rock displacements during and after construction of the repository conform to the stress measurements (Nykyri et al. 1994).

The mechanical properties of intact rock in the Research Tunnel were determined from irregular block samples of rock and from core samples taken from the investigation holes.

The average DRI-value, 55, for the anisotropic tonalite, the main rock type, is typical for this rock type, see Figure 2-5. The average brittleness value S_{20} was 51.5 and the Sievers' SJ value 32.4. The quartz content was 15 - 20 % and the Cerchar Abrasiveness Index (CAI) -value of the anisotropic tonalite was 3.8,

see Figure 2-6 (Johansson & Autio 1995). The average joint frequency was one fracture per metre.

The average DRI-value for pegmatite, 49.5, showed a value slightly lower than the values found in the literature. The DRI-values of the pegmatite are close to those of tonalite, and both rock types can be classified according to drillability as medium-hard rock (Lien 1980).

The strength and deformation properties of both the tonalite and the pegmatite showed very similar results when compared with the results obtained during the construction of the VLJ repository (Johansson & Autio 1993, Johansson & Autio 1995). The compressive strength value of 80 MPa for anisotropic tonalite is lower than that of typical granitic rocks, see Figure 2-7. The anisotropic tonalite shows clearly lower values than the isotropic tonalite which was only encountered in the upper part of borehole KR7 in the Research Tunnel. The tensile strength of ansiotropic tonalite, 9 MPa, and the deformation properties of the tonalite (Young's modulus 60 GPa) are typical for granitic rocks.

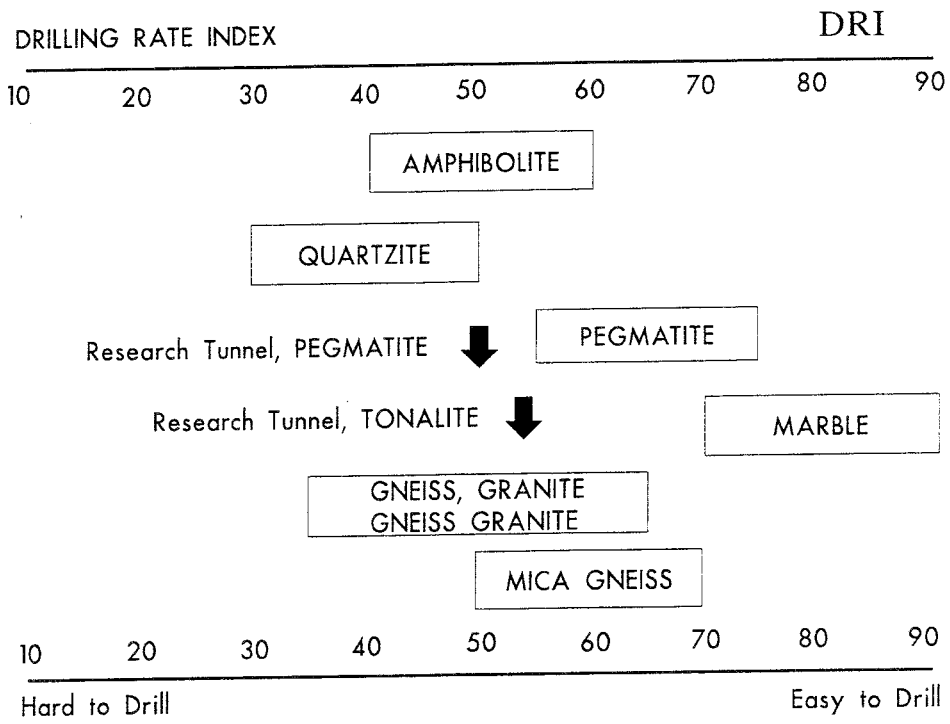

Figure 2-5. *Variation of DRI in various rock types and the average DRI-values determined for rock types in the Research Tunnel (Johansson & Autio 1993).*

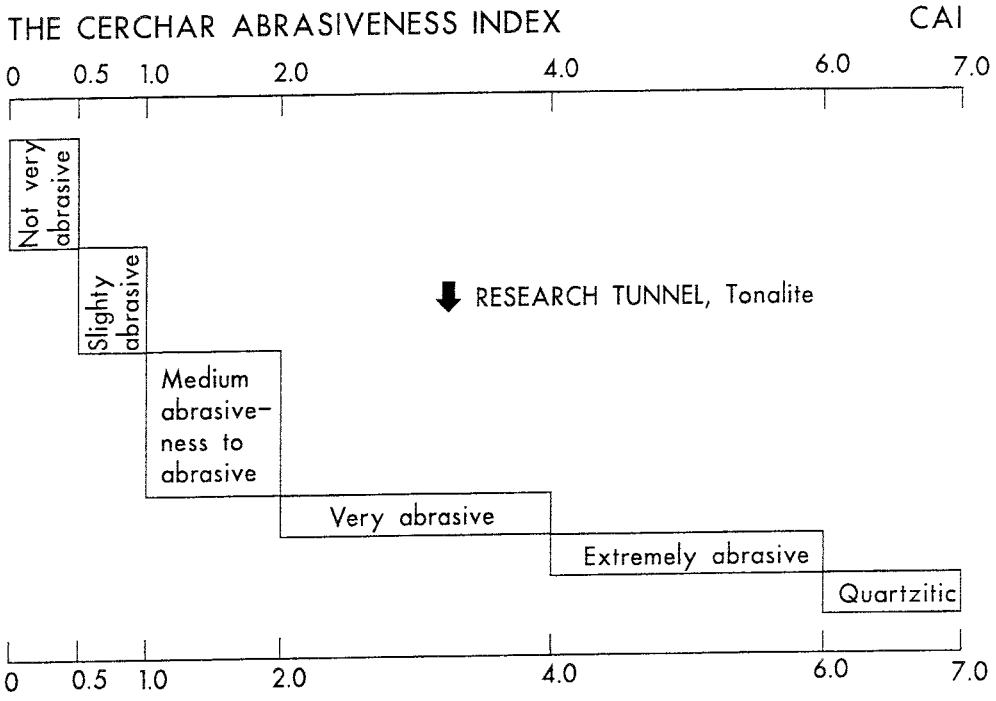

Figure 2-6. *The average CAI-value of anisotropic tonalite with respect to abrasiveness classification after CERCHAR 1986 (Johansson & Autio 1995).*

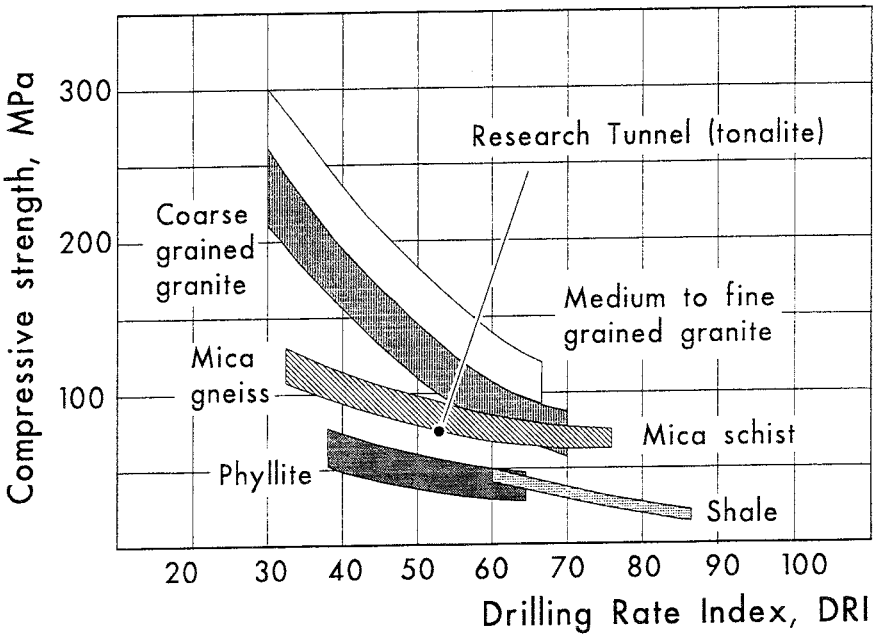

Figure 2-7. *Relation between Drilling Rate Index, DRI, and compressive strength in granitic rocks and in the Research Tunnel.*

3 DESCRIPTION OF THE BORING EQUIPMENT AND OPERATING PRINCIPLES

3.1 GENERAL

Boring was based on the rotary crushing of rock and removal of crushed rock by vacuum flushing and suction through the drill string. In principle, the process of crushing the rock is the same as used in conventional raise boring. The main difference lies in the method used to remove crushed rock from the bottom of the hole, see Figure 3.1-1. Vacuum cleaning was employed for this purpose.

The boring equipment comprised a raiseboring machine, frame, drillstring, cutter head and vacuum suction system, see Figures 3.1-2 and 3.1-3.

A separate pilot hole was bored before boring of the large hole began. The bit used for the boring of the pilot hole was then used in front of the large diameter cutter head as a guide and stabilizer.

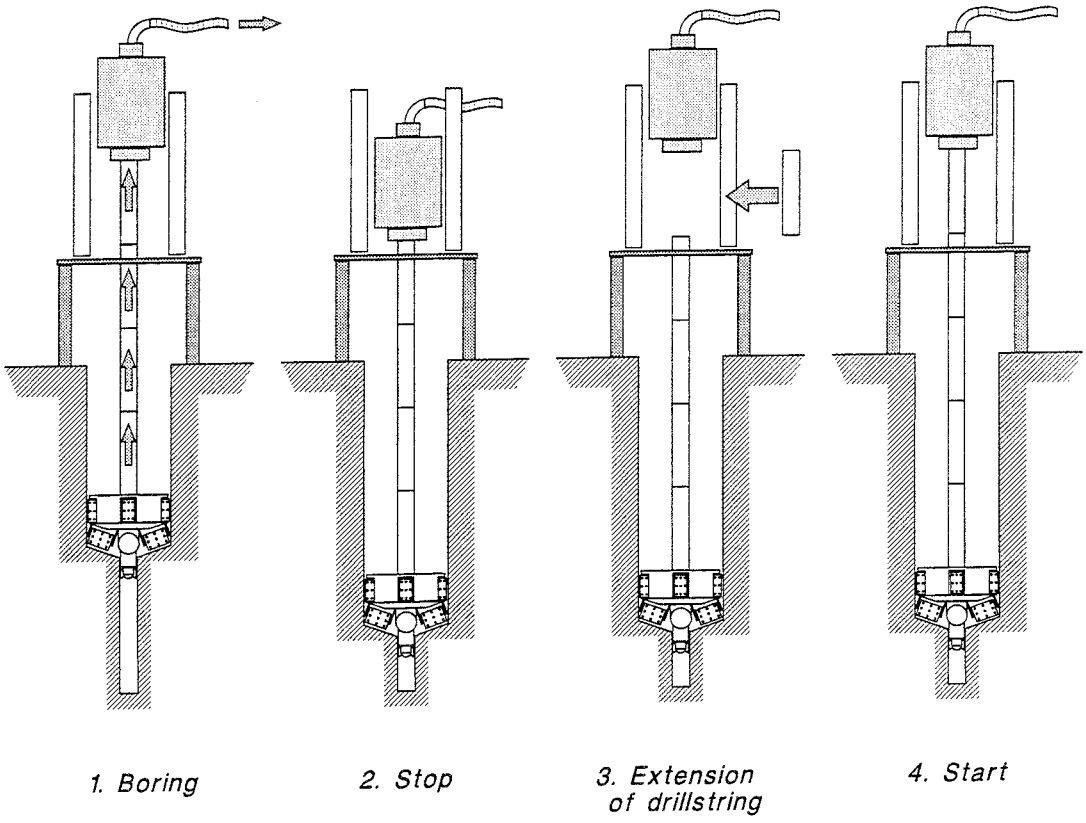

Figure 3.1-1. Operating principle of the boring method.

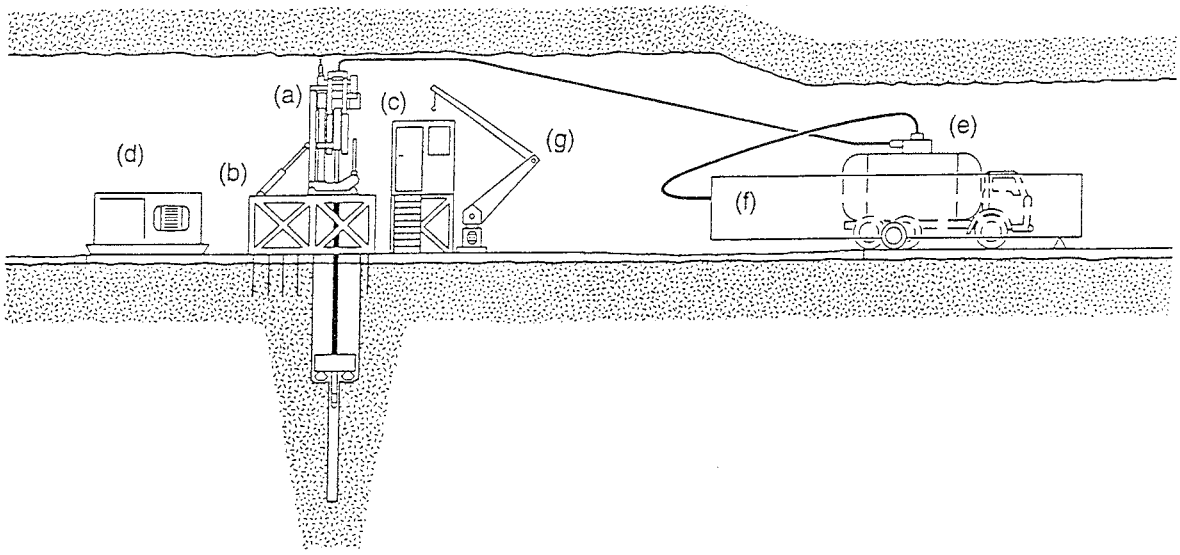

Figure 3.1-2. Drawing of the boring equipment showing the main components: a) the boring machine, b) frame, c) control container, d) electro-hydraulic power unit, e) cyclone and tank for crushed rock, f) vacuum unit, g) crane.

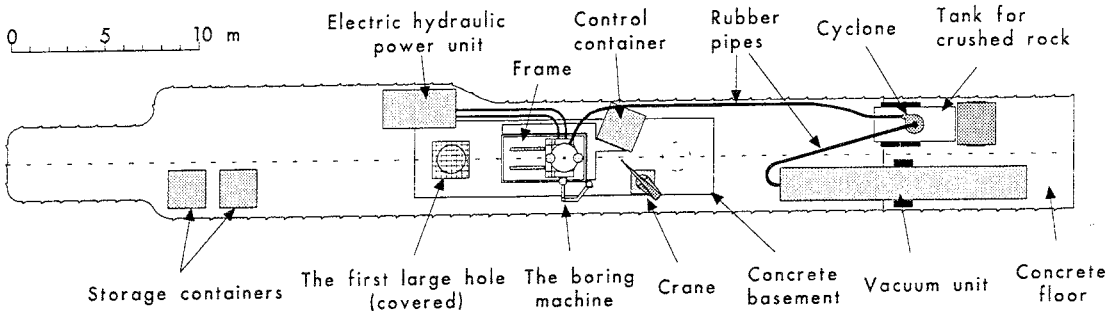

Figure 3.1-3. The layout of the boring equipment in the Research Tunnel.

3.2 THE BORING MACHINE

The raiseboring machine used to create the torque and thrust necessary for the rotary crushing was of type Subterranean-005L-137. The minimum height of the machine was about 3.2 m, the maximum height was about 3.6 m and the weight was 8890 kg.

The machine was electro- hydraulic and equipped with a power pack. The main components of the boring machine are shown in Figure 3.2-1.

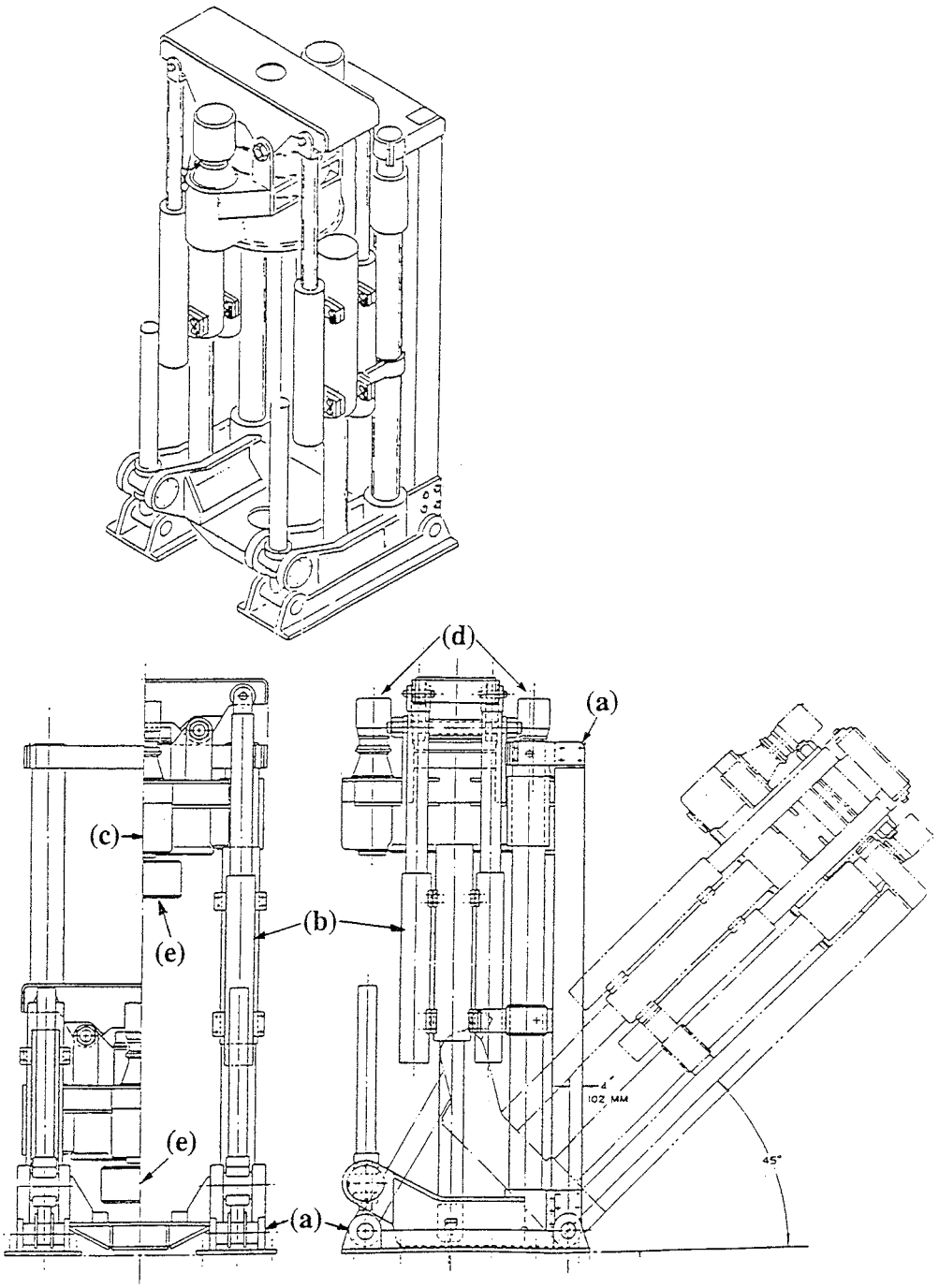

Figure 3.2-1. *Subterranean-005L-137 raiseboring machine. The main components of the machine are: a) base frame, b) hydraulic cylinders, c) gear box, d) rotation motors, e) fastening sleeve for drill string. The device for changing drill pipes and locking is not shown.*

The maximum thrust force exerted by the boring machine was measured to be from 500 to 630 kN depending on the position of the cutter head. The total installed electrical power of the boring machine was 151 kW (380 V and 50 Hz).

According to the manufacturer's specifications the machine's range of rotation speed was 0 - 98 rpm. The torque created by the machine was about 11 kNm at the maximum rotation speed of 98 rpm used for drilling of the pilot hole.

According to the manufacturer's specifications the range of rotation speed for reaming with the large cutter head was 0 - 14.6 rpm. The reaming torque at 14.6 rpm was 74 kNm. In practice, it was observed that the maximum rotation speed with the large cutter head was about 12 rpm.

The raiseboring machine was placed on a 1.8 m high base frame so that it was possible to lift the large cutter head for inspection, maintenance and transfer from hole to hole, see Figure 3.2-2.

The diameter of the drill pipes was 254 mm (10") and their length was 1520 mm. Standard stabilizer drill pipes were used behind the pilot bit.

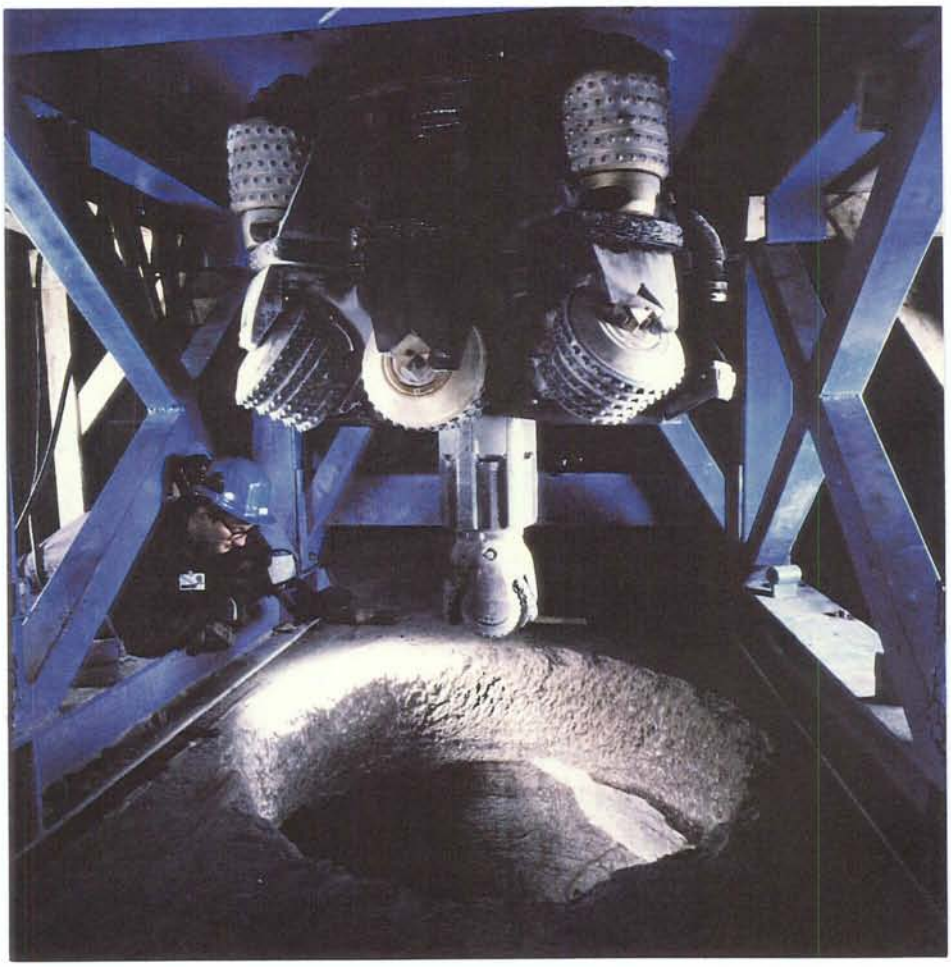

Figure 3.2-2. *Cutter head under the base frame and above a bored hole.*

3.3 THE PILOT BIT AND THE CUTTER HEAD

The pilot bit was a Sandvik Coromant Roller Bit, a standard three-cone bit with a diameter of 311 mm ($12^1/_4$") made for use in very hard rock (unconfined compressive strength, UCS, 250 - 700 MPa). The shape of the buttons was hemispherical, of type CH.

There were three openings for flushing channels in the bit. Vacuum suction nozzles were installed in these openings to remove the crushed rock when boring the pilot holes.

The large cutter head was a used Sandvik Coromant CBH-5 blind-hole head designed for boxhole boring with a hole diameter of 1524 mm, see Figures 3.3-1 and 3.3-2. The weight of the fully-dressed cutter head was 3800 kg.

The large cutter head was furnished with 8 roller button cutters of type Sandvik CMR and 4 gauge rollers. A combination of both 5- and 6-row cutters and 4- and 5-row cutters (see Figures 3.3-3 and 3.3-4) was used. The total number of button rows for the 5- and 6-row cutter dressing was 44 and the total for the 4- and 5-row cutter dressing was 36. The corresponding numbers of grooves on the bottom of the hole were 30 and 24 since some of the button rows followed the same groove.

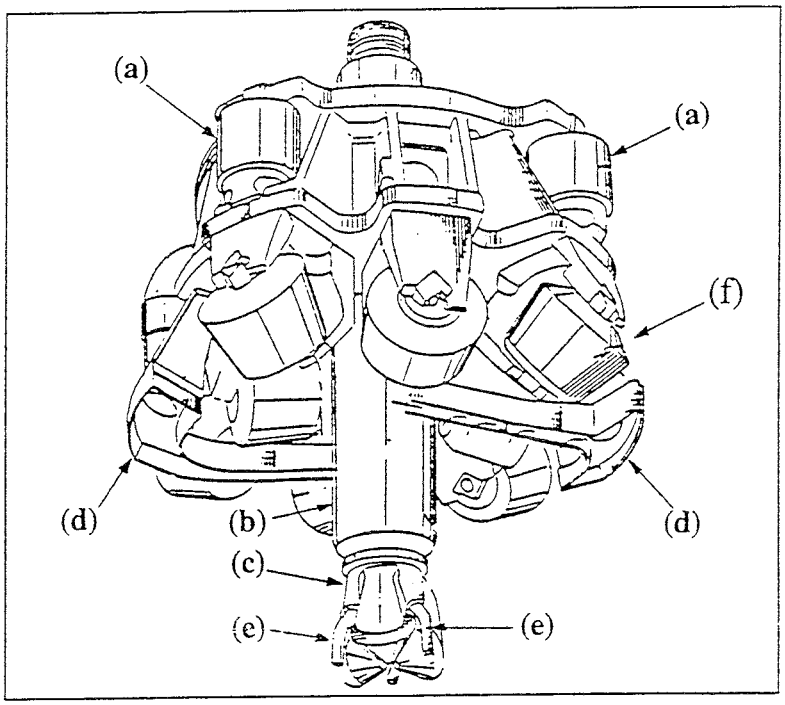

Figure 3.3-1. The Sandvik Coromant CBH-5 cutter head and the vacuum suction nozzles: a) gauge rollers, b) drill pipe and stem of pilot bit, c) pilot bit, d) nozzles in the cutter head, e) nozzles in the pilot bit, f) cutters.

The row spacing of the 5- and 6-row cutters was 39.6 mm and the spacing of the 4- and 5-row cutters was 51.0 mm. The corresponding spacing between the grooves on the bottom of the hole was 19.8 and 25.5 mm, see Figure 3.3-3.

The two nozzles which were used to suck the crushed rock were installed between the cutters in the cutter head.

With the cutter head rotating at 10 rpm the nozzles remained above each point on the bottom of the hole for 0.6 seconds. A rubber edging was fitted to the lower edge of the nozzles, the edge closest to the bottom of the hole.

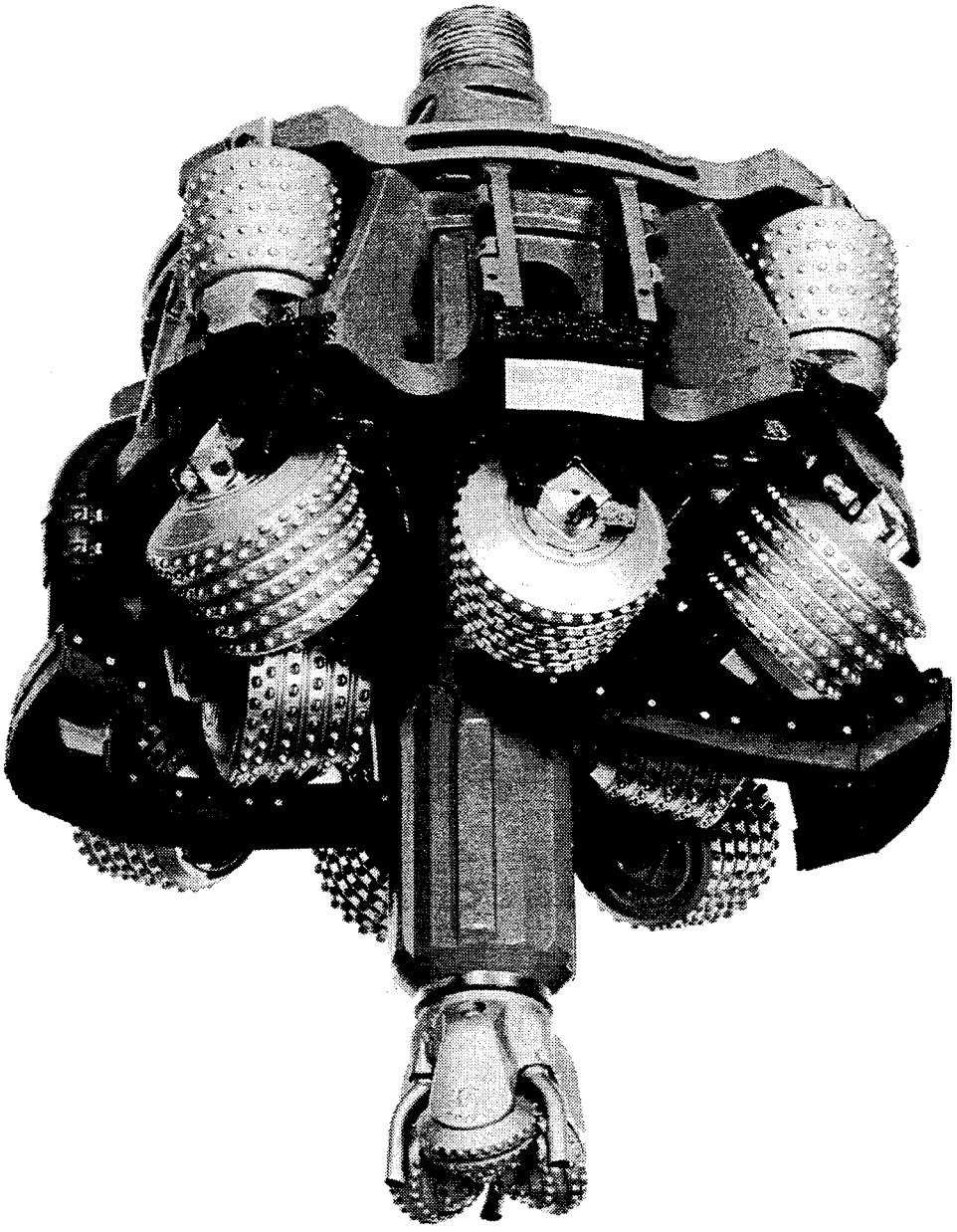

Figure 3.3-2. *The cutter head.*

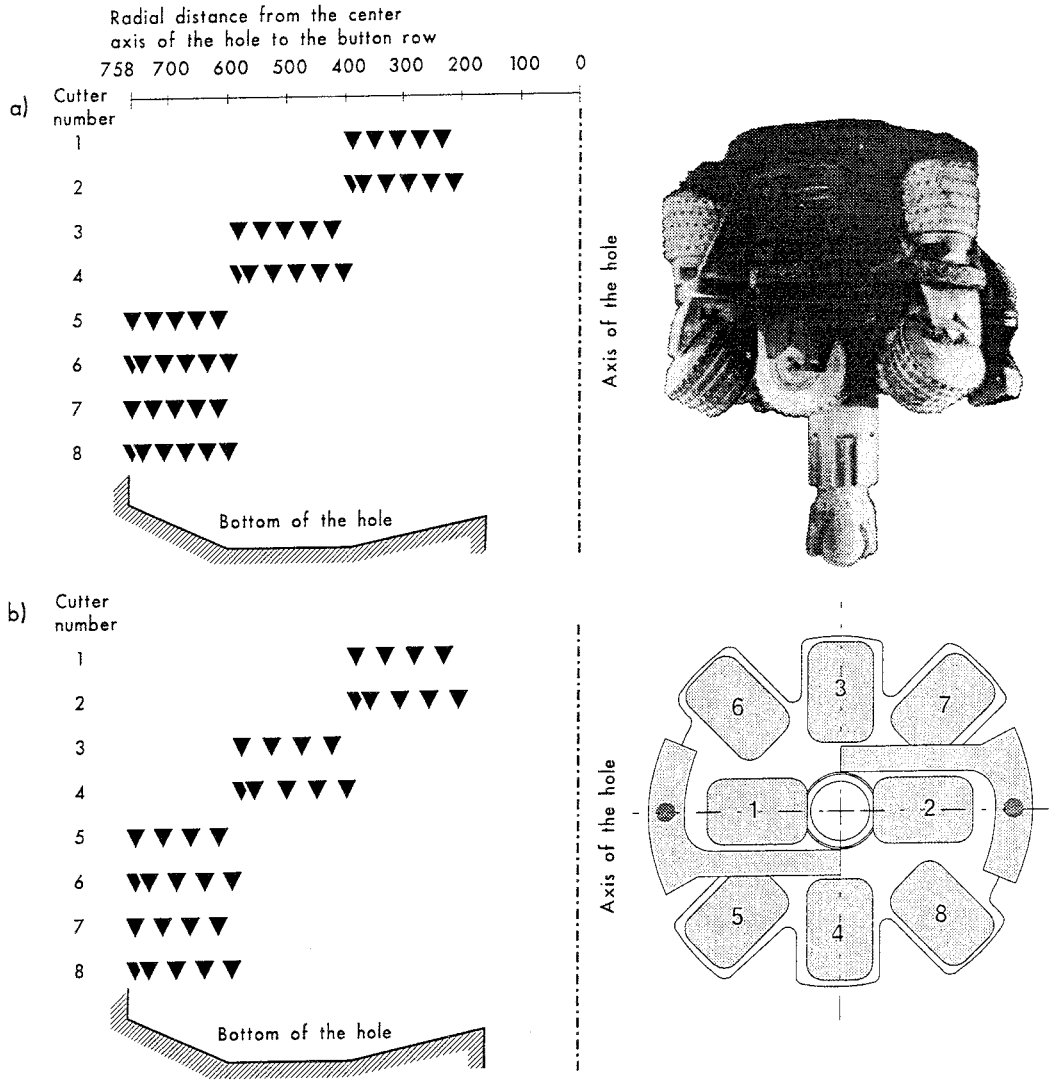

Figure 3.3-3. *The position of button rows in the cutters. The cutter head is furnished with cutters of type a) CMR-41 & -52, b) CMR-55 & -66.*

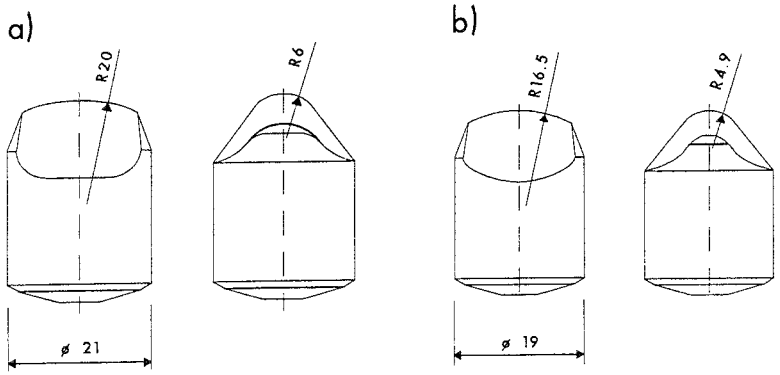

Figure 3.3-4. *The shape of the buttons in cutters of type a) CMR-41 & -52, b) CMR-55 & -66.*

3.4 THE VACUUM SUCTION SYSTEM

The crushed rock was sucked through the cutter head and drillstring to the suction line which consisted of the flow channels in the boring machine, the external transport pipes, the tank for crushed rock and the vacuum unit (see Figure 3.4-2).

Before entering the vacuum unit the air which contained the crushed rock passed through a cyclone to a tank used to separate and collect the crushed rock. The total volume of this tank was 8.2 m^3, providing an effective collection volume for crushed rock of 5 - 6 m^3. The tank was installed on a truck so that it could be driven out of the tunnel and inclined for emptying, see Figure 3.4-1.

The inner diameter of the drill pipes was not constant but contained "bottlenecks" which reduced the efficiency of vacuum suction. For this reason polyethylene casing was installed inside the pipes to form a flow path through the drill string with a constant diameter of about 120 mm.

The length of the crushed rock transportation line from the top of the boring machine to the vacuum unit was 24 m. The total length of the line from the cutter head to the vacuum unit was about 36 m when the 12 m vertical section of the drillstring is included.

The final design of the sampling tank for crushed rock was based on the use of the large collecting tank and three fine particle filters of the same type as those used in the vacuum unit, see Figure 3.4-3.

Figure 3.4-1. *The rock tank being emptied.*

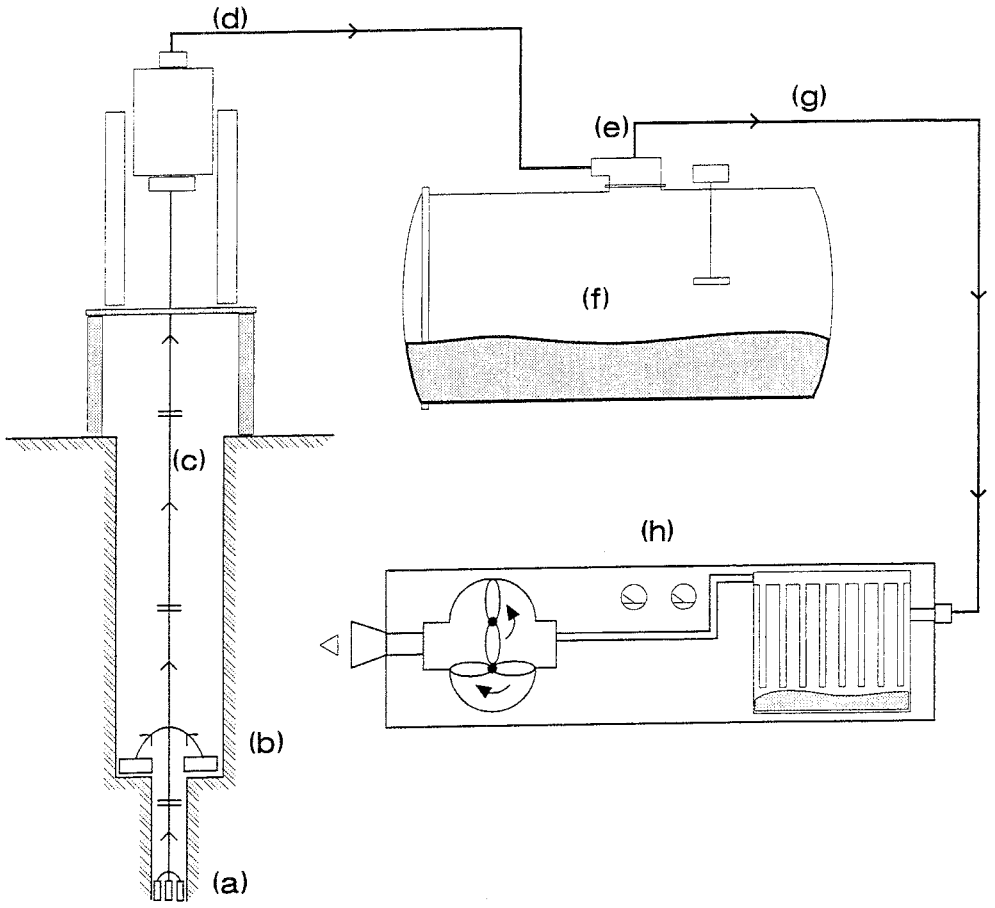

Figure 3.4-2. *Flow chart for the vacuum suction system: a) nozzles of the pilot bit, b) nozzles of the cutter head, c) drill pipes, d) pipe from the boring machine to the tank for crushed rock, e) cyclone, f) tank for crushed rock, g) pipe to the vacuum unit, h) vacuum unit.*

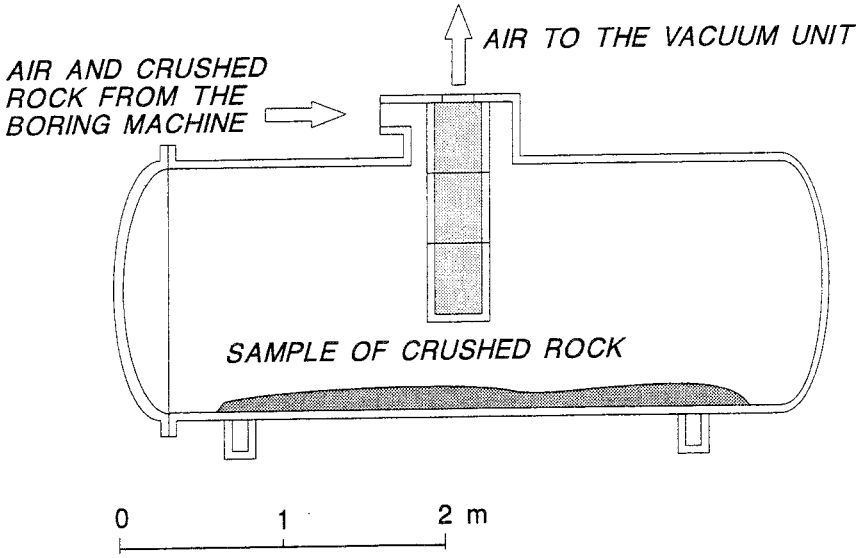

Figure 3.4-3. *The rock tank and the sampling system.*

4 OPERATIONAL CHARACTERISTICS OF THE BORING EQUIPMENT

4.1 FUNCTIONING OF THE EQUIPMENT

The boring of the three large holes (depth 7.5 m and diameter 1.5 m) showed that the principle of rock cutting based on rotary crushing and removal of crushed rock by vacuum suction functions well. Good boring performance close to that of raise boring was achieved when the equipment was in good operating condition. The total efficiency of the equipment was, however, hampered by the low degree of utilization caused by a large proportion of maintenance and repair work. A more detailed description of the boring procedure and operational experiences is given elsewhere by Autio & Kirkkomäki 1996.

The functioning of the pilot bit was characterized by wear, damage and clogging of the suction nozzles. The presence of small amounts of water also proved to be a problem. The design of the pilot bit and the method used for boring was shown to work well in dry competent rock without major fractures provided that care was taken to prevent overheating of the bit and bearings.

The functioning of the large diameter cutter head was characterized by problems related mainly to filling of the pilot hole during boring of the large hole, breaking of the rubber sleeves of the suction nozzles, clogging of the suction nozzles and wear of the vacuum suction pipes. The detachment of the cutter head for boring of the pilot hole and its subsequent reattachment were, in addition, labour-intensive tasks.

The principle of rock cutting and vacuum cleaning of the crushed rock from the bottom of the hole was shown to work well in competent rock without major fractures at a thrust of 600 kN and rotation speed of 8 rpm. The drawbacks in the method are related to the technical design and implementation.

The principle of boring a large diameter hole in a single run was demonstrated by the boring of a section of the second large hole without a separate pilot hole in a so called single-pass boring test. This boring method also functioned well from the technical point of view.

The vacuum unit functioned well although some particular problems were encountered. These were mainly related to monitoring of the equipment, extensive wear of the vacuum suction line and rapid filling of the dust compartment of the vacuum unit.

The principle of vacuum flushing and transport of crushed rock was found advantageous over traditional methods based on water flushing. Both direct and reverse flushing using either air or water as transport media can be used for the removal of crushed rock from beneath the cutter head. The advantages of air vacuum flushing compared to water flushing is that the equipment required is

compact and easy to move, and that the technique makes it possible to observe the surface and bottom of the hole during the boring process.

The boring had to be stopped while samples of crushed rock were taken during the boring. If similar sampling activities are to be carried out in future it will be worthwhile addressing the problem and designing an effective continuous sampling system.

The extensive wear of the vacuum suction line can be reduced by proper material selection and design of the vacuum flow system. From a practical point of view a reasonable goal would be that all parts of the line should withstand the abrasion and wear involved in the boring of a single 7.5 m deep hole in a single run.

The results of measurements of the wear on the cutters show that it is possible to measure the wear of cutters resulting from the boring of lengths of hole as short as those in the Research Tunnel.

On the basis of the boring work in the Research Tunnel the main problems which should be addressed to improve the feasibility of the method are:

- extensive wear of vacuum suction system including the suction nozzles
- set-up and transfer characteristics of the boring equipment
- cleaning of filters and emptying of the tank for crushed rock
- filling of the pilot hole.

4.2 WORK TIME ANALYSIS

The total time used for work in the tunnel was 64 workdays. About 13 % of the time spent on common basic activities in boring was used for the actual boring of pilot and large holes, see Figure 4.2-1. The novel boring equipment employed for this work had only been used previously for test boring a 2.7 m length of hole (Autio & Kirkkomäki 1996a). The nature of the work reduced the degree of utilization of the equipment for reasons which are not normally part of the activities involved in standard boring projects.

The repair of failures in the hydraulic system and repair and maintenance of the vacuum flushing system occupied a major portion of the time spent on repair and maintenance, which comprised 16.4 % of total man-hours, which is equal to approximately 24 % of the time spent on common basic activities in boring. The primary cause of the major portion of repair and maintenance work required during boring was extensive wear in the vacuum flushing system.

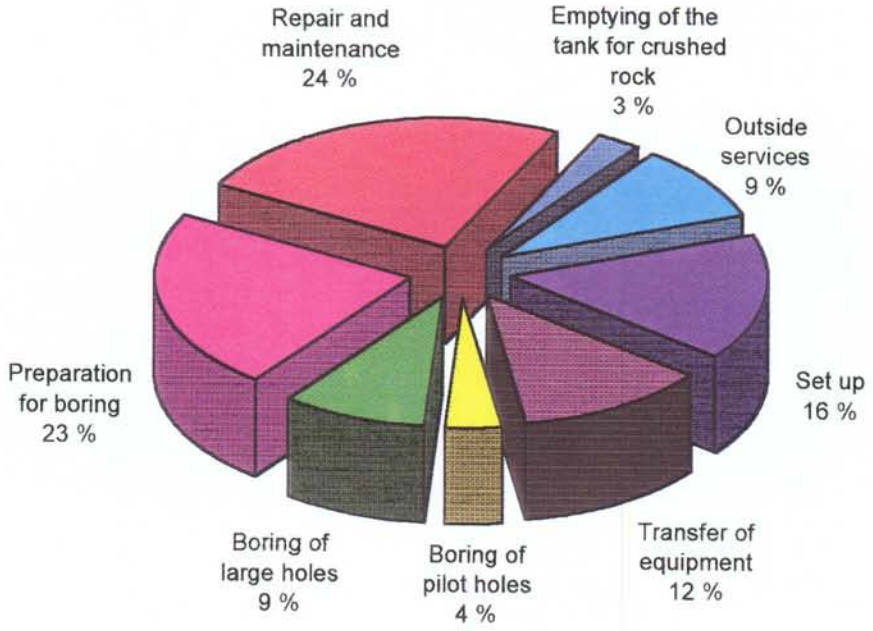

Figure 4.2-1. Division of the time between basic activities.

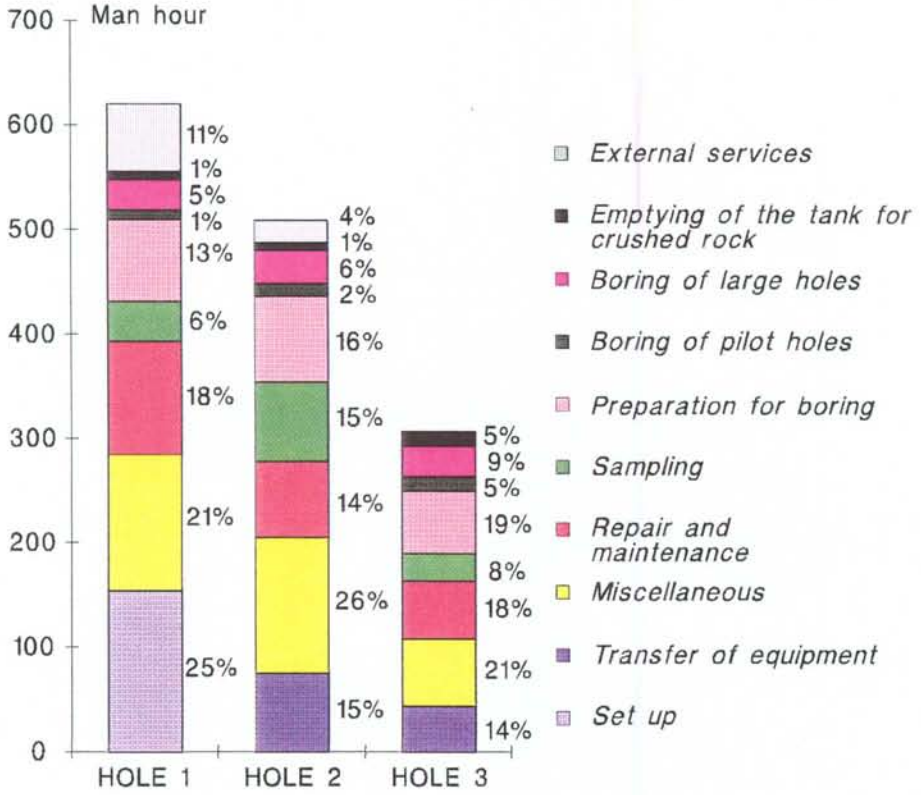

Figure 4.2-2. Time used for basic activities when boring the large holes. The time for large hole 1 does not include transfer of equipment which is included in set-up, correspondingly the times for holes 2 and 3 do not include set-up which is included in transfer of equipment.

The boring of the third hole took about 50 % of the time spent on the boring of the first hole as the operating procedures had become more familiar, see Figure 4.2-2. The activities where the greatest reductions in time spent were achieved were set-up, repair and maintenance, preparation for boring, and miscellaneous. The time spent on the actual boring of each of the large holes and for emptying of the tank for crushed rock was of the same order of magnitude.

The results of the worktime analysis imply that the best way of improving the degree of equipment utilization when boring relatively short holes is to reduce the time spent on set-up and transfer of equipment (19 %) and on preparation for boring (15 %) by carrying out maintenance and service work during these activities.

4.3 CONSUMABLES

Electricity consumption by the boring equipment is divided between the major elements as follows:

- power pack	installed power	151 kW
- vacuum unit	installed power	160 kW
- crane	installed power	20 kW
- other equipment	installed power	2 kW
Total installed power		333 kW

On average the boring machine took about 2 hours to bore one metre of hole. The estimated maximum consumption of electricity per meter of bored hole is therefore about 620 kWh.

A small amount of water (about 15 litres/min) was used in bursts for flushing during the boring of the first and third pilot holes and for cooling the hydraulic unit (1 - 5 litres/min).

4.4 EMISSIONS

Emissions occurring at the site can be divided into the following categories:

- emissions of hydraulic oil
- emissions of oil absorbant
- emissions of dust through the vacuum system
- emissions of fine-grained rock and dust
- emissions of water
- emissions of waste from construction work (sawdust, metal particles etc.)
- emission of heat.

The emissions of water, fine grained crushed rock and dust as well as the waste from construction work are avoidable by proper design.

Emissions of heat and dust in the outlet air of the vacuum unit did not pose a problem at the test site but in a production situation they will have an effect on the occupational conditions at the site. Possible problems can be resolved by good design of the equipment and ventilation of the site.

Emissions of oil in the form of hydraulic leakages and spillages are probably the most significant and the most difficult to avoid of all the emissions recorded when considering the future use of the method for the boring in small disposal tunnels.

Leakages of hydraulic fluid were a problem at the site even though the following precautions had been taken: the equipment was checked for leakages periodically during the operation; the equipment was provided with an oil spillage receptacle so that all oil leaking from the power pack and boring machine was collected. Oil absorbent material was placed by the boring unit for use in case of leakages. At a later stage, a plastic tarpaulin was wrapped around the hydraulic hoses to prevent leakages to tunnel walls. The floor of the tunnel was levelled with removable gravel which contained the finest gradings of particle to increase its absorbent capacity.

It is considered to be possible that all emissions could be avoided by proper design of the equipment and correct operating procedures. On the basis of the experience gained in this work all parts of the equipment which contain hydraulic oil should be covered by a protective shield and placed on oil spillage receptacles.

4.5 OCCUPATIONAL CONDITIONS

The occupational conditions at the site were monitored. Measurements were made of the quality of the inside air, temperature and acoustic noise.

The noise in the Research Tunnel was in the range 82 to 100 dB as shown in Figure 4.5-1. The level of noise insulation on the vacuum unit was low and could be raised to that of existing mobile units if necessary.

The normal temperature of the inside air in the Research Tunnel is about 14 °C. The temperature of the exhaust air from the vacuum unit was measured to be about 60 °C. An increase in the temperature of the inside air was observed after the vacuum unit had been running for several hours. The temperature of the inside air increased to a short-term maximum value of 18 to 21 °C, see Figure 4.5-2.

The free volume of the Research Tunnel is approximately 1900 m^3 and the air was changed once an hour in accordance with normal ventilation practice. The airflow through the vacuum unit was about 3240 m^3/h.

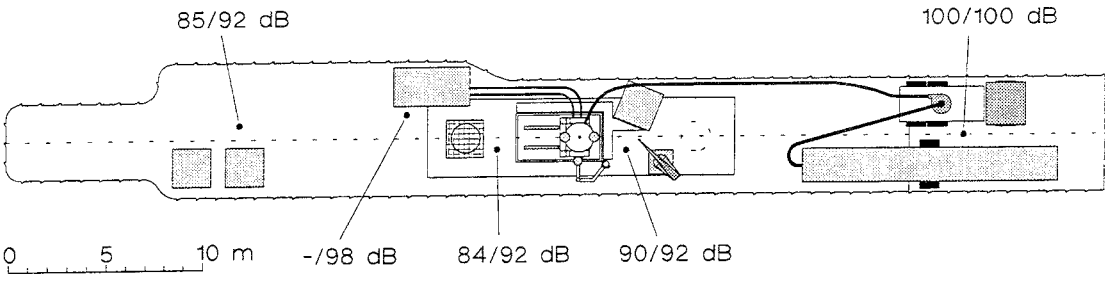

Figure 4.5-1. *The acoustic noise at different positions with only the vacuum unit running, and with all the equipment running.*

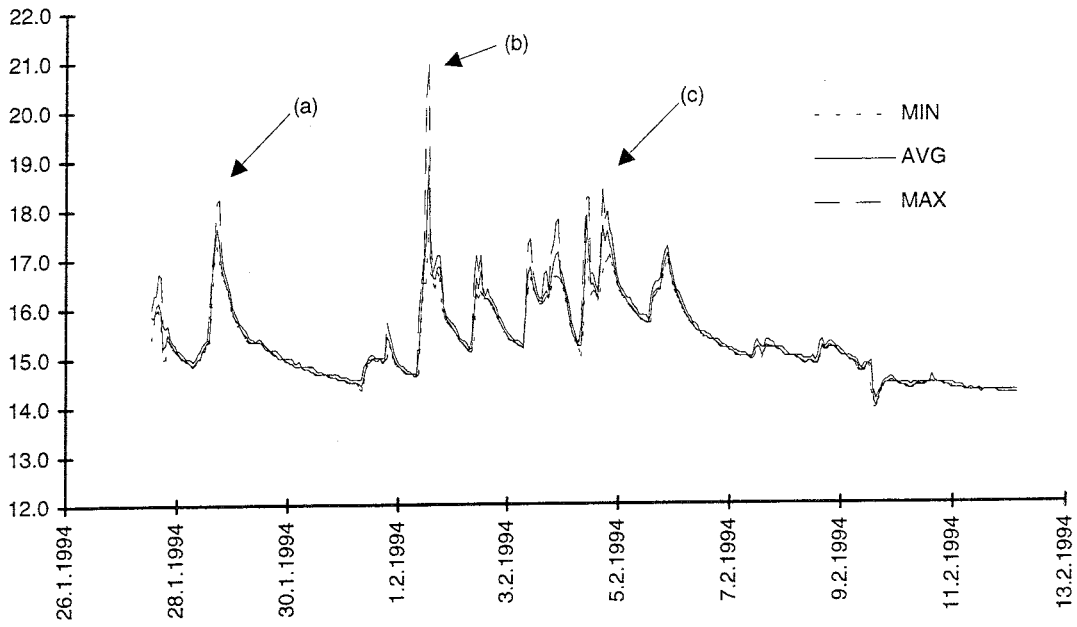

Figure 4.5-2. *The temperature of the inside air in the Research Tunnel. The peaks (a), (b), and (c) are caused by operation of the boring equipment continuously for several hours.*

The temperature of the inside air in the Research Tunnel during the boring work was kept close to normal working temperature. The only drawback of practical significance was that the warm air flowing out of the vacuum unit prevented the use of fire sensors in the vicinity of the vacuum unit.

The vacuum unit was the main source of the rise in temperature in the Research Tunnel. As this unit was operated for only relatively short lengths of time, continuous operation of similar equipment in a small tunnel such as during the construction of a repository for spent fuel may cause a heat load of practical significance.

The dust content of the inside air was measured to be 0.19 mg/m^3. This is about 2 % of the acceptable value for inorganic particles which is 10 mg/m^3. The amount of fine-grained quartz particles in the tunnel air was estimated to be 0.04 - 0.08 mg/m^3, corresponding to an estimated quartz content of 22 - 43 % for the dust. The HTP_{8h}-value is used to describe the acceptable limit of dust in the air. This figure is the known harmful concentration of contaminant in the air at the workplace averaged over eight hours (Työministeriö 1993). The acceptable HTP_{8h}-value for quartz content is 0.2 mg/m^3. The amount of fine quartz particles in the tunnel air was therefore estimated to be between 20 and 40 % of the hazardous value.

With regard to the future use of this boring method, the quality of the air, especially the dust content and content of fine quartz particles are important parameters.

The results of the measurements include inaccuracies with respect to long-term use of the equipment which result from the fact that the boring equipment was operated only for short periods. The results obtained may also be influenced by the nature of the work, so that the dust content of the inside air was different to what it would be during continuous construction work. The amount of fine quartz particles in the air must therefore be regarded as being a possible problem which could be addressed and solved, if necessary, by using current filtering techniques.

5 BORING PARAMETERS

5.1 GENERAL

Tests were carried out in addition to the normal follow-up of boring activities to determine the effect of changes in the operating parameters on the performance of the boring machine and the quality of the resulting hole.

The main areas of interest in technical performance were the penetration rate of the cutter head and the efficiency of the vacuum suction system. The tests included:

- testing the performance of the equipment at different operating parameters
- taking samples of the crushed rock at different operating parameters
- testing the effect of boring the large hole without a separate pilot hole
- testing different type of cutters.

The change of cutters from 5 and 6 row cutters to 4 and 5 row cutters before boring of the third hole took place was carried out to establish the effect of cutter size and shape on boring performance and the disturbance caused by boring. The same thrust and rotation tests were carried out with both sets of cutters.

During testing the thrust and rotation speed of the boring machine was varied in steps. Typically, the thrust was increased in four to five steps while the rotation speed was kept constant, as shown in Figure 5.1-1 for Test 3.7, and the rotation speed was then changed in three steps while the thrust was kept constant.

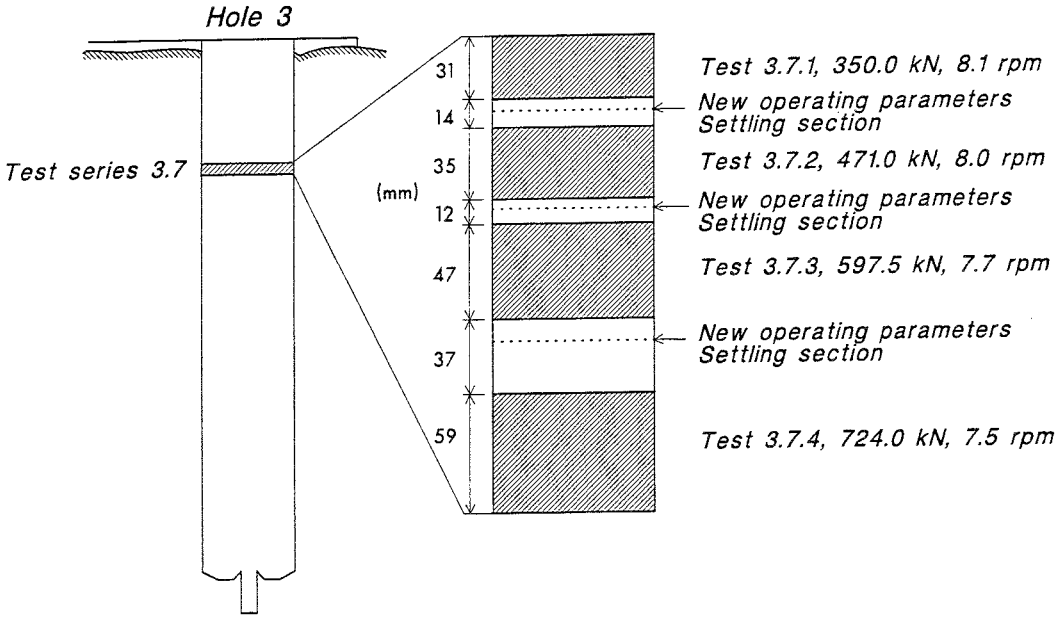

Figure 5.1-1. Example of a test section.

A summary of the 10 tests made during the boring of large holes which qualified to be used in further study are presented in Table 5.1-1. Three of the test were rotation tests. The positions of the test sections are shown in Figures 5.1-2 and 5.1-3. The results of the test measurements are shown in Tables 5.2-1 and 5.3-1.

The rotation speed was measured so that the time for at least ten rotations was measured manually with a stop watch with minimum accuracy of about ±2 %.

The advance of the cutter head was measured with a tape gauge (accuracy of one millimeter) and stop watch (accuracy of one second) with total accuracy of about ±1 %. The machine thrust and torque were measured manually from analog pressure gauges with an accuracy of 1 bar which gives a minimum total accuracy of ±1 %.

The parameters which were determined were:

- net advance rate, I
- advance per rotation, i
- penetration cofficient, b
- critical thrust, F_c
- cutter cofficient, k
- specific energy, E_s
- flow ratio, μ.

Table 5.1-1. Summary of the tests made during the boring of large holes

Test	Start depth (cm)	Stop depth (cm)	Thrust (kN)	Rotation speed (r/min)	Type of test
Series 2.4	261.9	318.8	719 - 305	8.5	Thrust test
Series 2.5	363.9	398	715	4.1-11.8	Rotation test
Series 2.6	539.9	586.2	731 - 312	8.0	Thrust test
Series 2.7	662	731.4	723 - 423	8.2	Thrust test
Series 3.7	197.5	221	724 - 471	7.8	Thrust test
Series 3.8	310	352.3	598 - 307	8.4	Thrust test
Series 3.9	448.4	483.1	599	4.4-11.8	Rotation test
Series 3.10	502.5	552.3	726	6.4-11.8	Rotation test
Series 3.11	561.5	592.7	607 - 307	8.3	Thrust test
Series 3.12	665	823.6	737 - 313	8.2	Thrust test

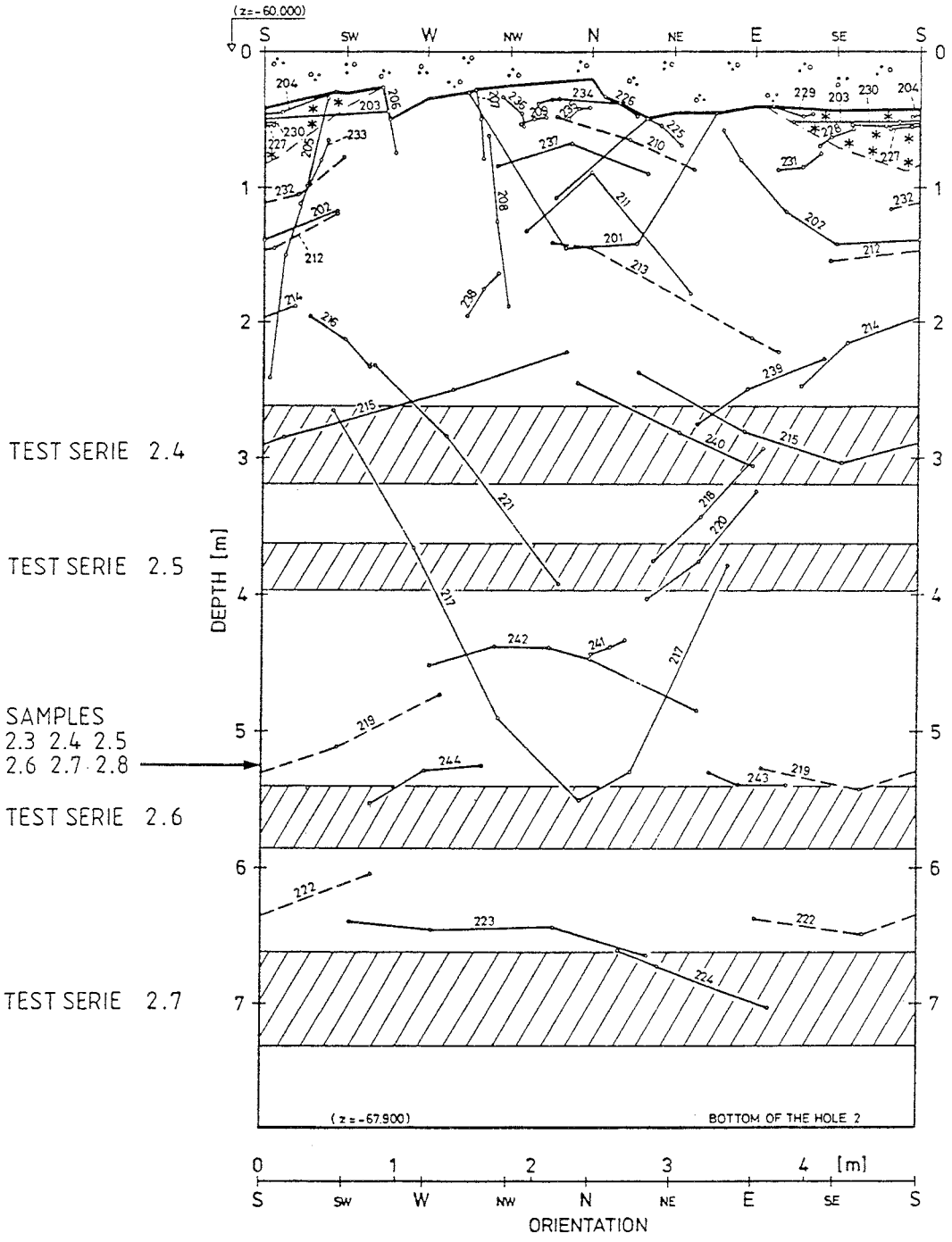

Figure 5.1-2. Positions of test sections in Hole 2.

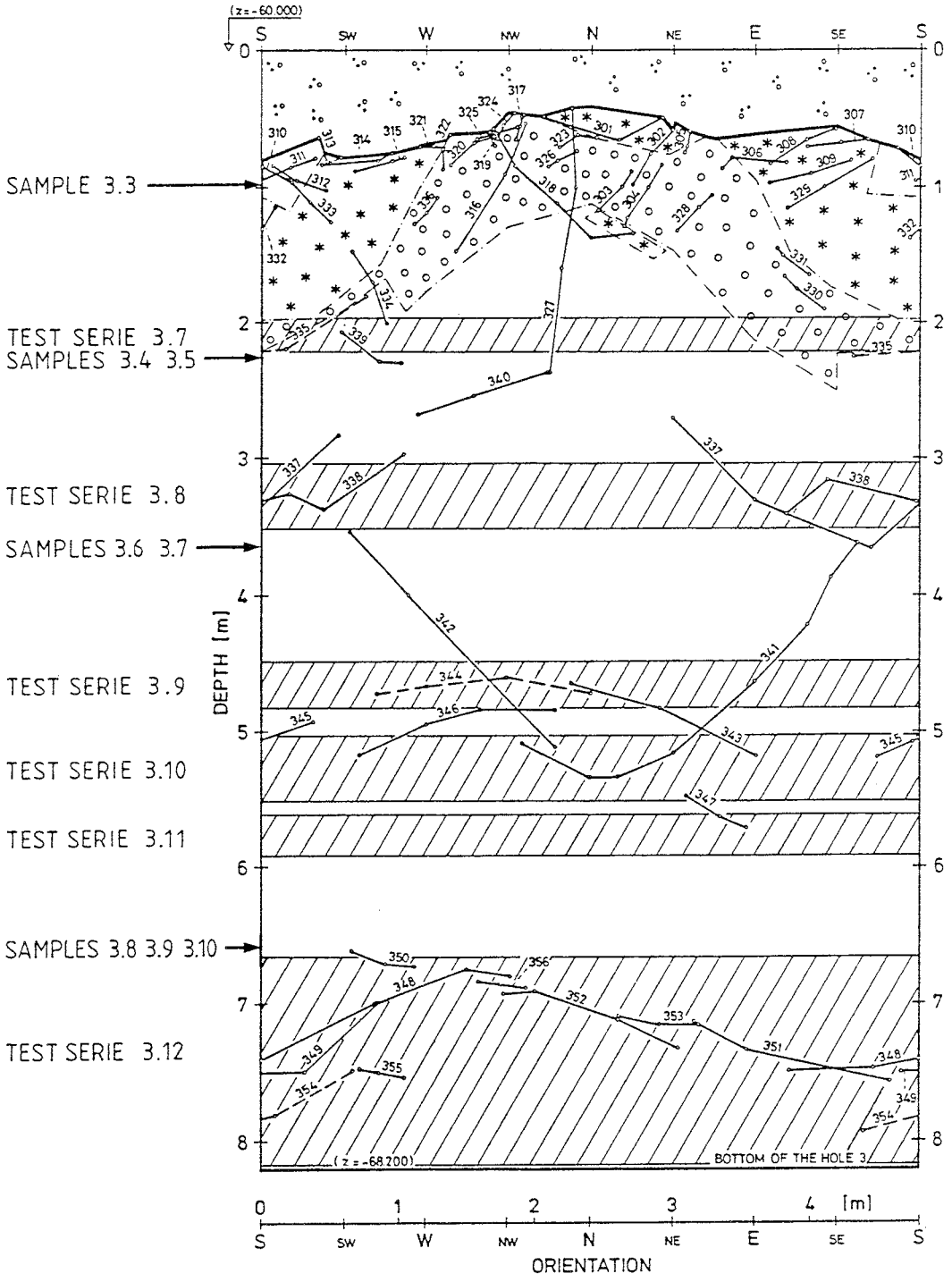

***Figure 5.1-3**. Positions of test sections in Hole 3.*

5.2 NET ADVANCE RATE (I) AND ADVANCE PER ROTATION (i) VERSUS THRUST

The net advance rate is the advance made by the cutter head during unit time. The advance rate is a function of the type of cutters (machine factors), the thrust being used, the rotation speed of the equipment and the properties of the rock. The net advance rate was determined at different thrusts and for the two different cutter head configurations.

If the vacuum flushing functions well, the net advance rate should increase in a linear fashion as the rotation speed is increased because the advance per rotation should be constant if the thrust is constant.

The maximum advance rate, I_{max} of 1.23 m/h was measured during the boring of the third large hole in Test 3.10.3 with a rotation speed of 12 rpm and thrust of 722 kN. The maximum advance rate of 0.88 m/h with the normal rotation speed of 8 rpm and maximum force of 700 kN was measured during Test 2.7.1.

The advance per rotation is equal to the net advance per unit time divided by the number of rotations per unit time if the rotation speed of the cutter head is constant. To illustrate the difference between net advance rate and the advance per rotation, both of these are shown in Figures 5.2-1 and 5.2-2 for Test Series 2.4.

The advance per rotation is a more accurate test parameter than the net advance rate since in practice it was difficult to manually adjust the rotation speed to an exact value and to keep it stable during the test.

The main importance of the advance per rotation lies in the fact that it is a parameter related to machine factors i.e. the type of cutters, the thrust used, and the flushing performance achieved. If the flushing functions well and the bottom of the hole is clean of crushed rock the advance per rotation should be constant regardless of the rotation speed used, which is discussed later in chapter 5.3.

A linear and exponential curve was fitted to the measured set of points according to the method of least squares. For comparative reasons a logarithmic fit was also made for Tests 2.4, 3.8 and 3.12. The R^2 regression coefficient, which is a measure of the goodness of fit, was also calculated for both curves and is shown in Figures 5.2-1 to 5.2-10 together with the results of the thrust tests and equations for the curves of best fit.

In general, measurements are shown using a logarithmic scale because this technique makes visual comparison of the results very simple - the slope of the curve represents the exponent of the exponential curve fit. The difference between the logarithmic and linear scale can be seen by comparing Figures 5.2-11, 5.2-12 and 5.2-13 (shown using linear scales) to the corresponding Figures 5.2-2, 5.2-6 and 5.2-8 (shown using logarithmic scales).

It should be noted that the differences between the exponential, linear, and logarithmic regression are very small in the measured range of thrusts. The differences are likely to became larger if the range of thrusts is extended beyond the upper values used in these tests.

While the exponential regression gives the best correlation for most of the tests, in Test 2.4 the best correlation is achieved using the exponential function while the linear and logarithmic functions give almost the same correlation result (see Figure 5.2-11). For Tests 3.8 and 3.12 the best fit is given by the logarithmic regression function and the poorest correlation is given by the exponential function, (see Figures 5.2-12 and 5.2-13).

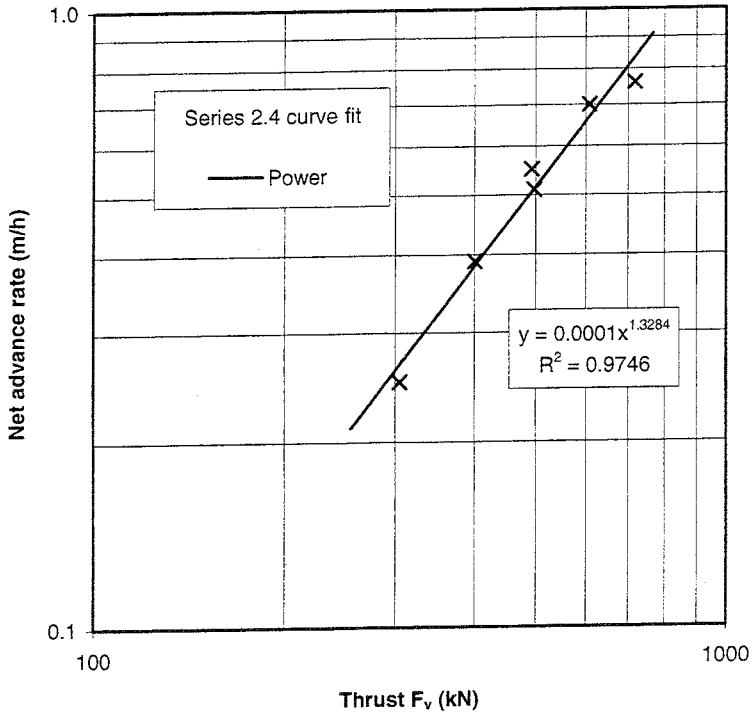

Figure 5.2-1. *The net advance rate as a function of thrust. Test 2.4, rotation speed 8 rpm, 5 & 6 row cutters.*

Table 5.2-1. The results of thrust test measurements carried out during the boring of large holes 2 and 3. The cutter coefficient is defined later in chapter 5.5.

Test	Thrust F_v (kN)	RPM (r/min)	Advance l (m/h)	Advance i (mm/rev)	Torque T (kNm)	Drag force F_r (kN)	Specific ener. E_s (MJ/m^3)	Cutter coeff. k	Airflow ϕ (m^3/s)
2.4.1	718.5	8.14	0.760	1.557	29.2	53.7	37.6	0.0748	0.853
2.4.2	608.8	8.14	0.700	1.434	28.9	53.1	40.3	0.0872	0.938
2.4.3	497.2	8.42	0.510	1.009	23.6	43.4	46.8	0.0872	1.013
2.4.4	492.9	8.57	0.550	1.069	24.3	44.7	45.5	0.0906	0.969
2.4.5	401.0	8.85	0.390	0.734	21.5	39.5	58.5	0.0985	1.017
2.4.6	401.0	8.85	0.390	0.734	21.1	38.8	57.6	0.0969	1.017
2.4.7	304.8	8.57	0.250	0.486	-	-	-	-	1.021
2.6.1	730.7	8.14	1.030	2.110	37.0	68.0	35.1	0.0930	0.687
2.6.2	503.9	8.14	0.490	1.004	25.0	46.0	49.8	0.0912	0.745
2.6.3	407.7	8.28	0.390	0.785	21.1	38.8	53.8	0.0953	0.741
2.6.4	311.5	7.62	0.260	0.569	18.7	34.3	65.7	0.1101	0.988
2.7.1	723.0	7.71	0.880	1.901	35.9	66.0	37.8	0.0913	0.894
2.7.2	668.0	8.31	0.820	1.645	31.7	58.3	38.6	0.0872	0.892
2.7.3	547.0	8.28	0.630	1.269	26.4	48.6	41.7	0.0888	0.909
2.7.4	423.3	8.42	0.440	0.871	22.5	41.4	51.8	0.0979	0.944
2.7.5	610.0	8.14	0.700	1.434	29.9	55.0	41.8	0.0902	0.927
3.7.2	471.0	8.00	0.350	0.729	22.2	40.8	60.9	0.0867	1.069
3.7.3	597.5	7.74	0.470	1.012	26.1	48.0	51.5	0.0803	1.017
3.7.4	724.0	7.50	0.590	1.311	29.9	55.1	45.7	0.0761	0.965
3.8.1	412.0	8.42	0.309	0.611	20.4	37.6	66.9	0.0913	1.101
3.8.2	497.2	8.28	0.410	0.826	22.5	41.5	54.6	0.0834	1.051
3.8.3	597.8	8.14	0.510	1.045	25.7	47.3	49.2	0.0792	1.002
3.8.4	307.0	8.42	0.200	0.396	18.0	33.1	90.8	0.1077	1.063
3.8.5	409.8	8.42	0.350	0.693	20.4	37.6	59.0	0.0917	1.023
3.8.6	497.2	8.28	0.450	0.906	22.5	41.5	49.8	0.0834	0.982
3.8.7	356.1	8.73	0.300	0.573	20.4	37.6	71.3	0.1056	1.009
3.11.1	606.7	8.14	0.694	1.422	28.5	52.5	40.1	0.0865	0.986
3.11.2	307.1	8.42	0.300	0.594	19.4	35.7	65.3	0.1161	1.048
3.11.3	407.7	8.28	0.410	0.826	21.8	40.2	52.9	0.0986	1.021
3.11.4	506.1	8.28	0.530	1.067	25.7	47.3	48.2	0.0935	0.971
3.12.1	728.5	8.00	0.780	1.625	31.7	58.3	39.0	0.0801	0.913
3.12.2	607.8	8.00	0.670	1.396	28.9	53.2	41.4	0.0874	0.957
3.12.3	507.3	8.00	0.530	1.104	24.7	45.4	44.7	0.0895	0.963
3.12.4	413.2	8.42	0.415	0.821	22.9	42.1	55.8	0.1020	1.028
3.12.5	312.7	8.57	0.270	0.525	19.4	35.7	73.8	0.1140	1.036
3.12.6	737.4	8.14	0.813	1.666	34.2	62.9	41.0	0.0853	0.829

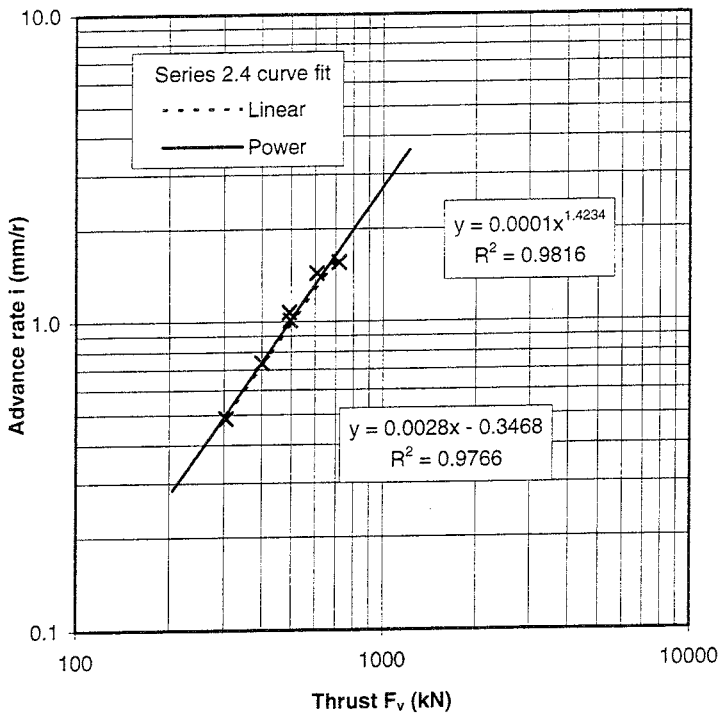

Figure 5.2-2. *Advance rate per rotation as a function of thrust. Test 2.4, rotation speed 8 rpm, 5 & 6 row cutters.*

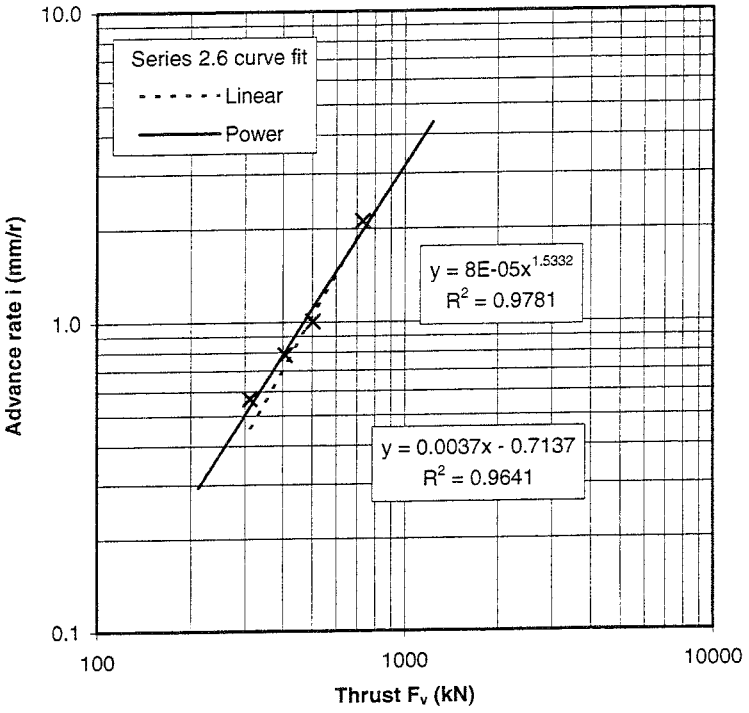

Figure 5.2-3. *Advance rate as a function of thrust. Test 2.6, rotation speed 8 rpm, 5 & 6 row cutters.*

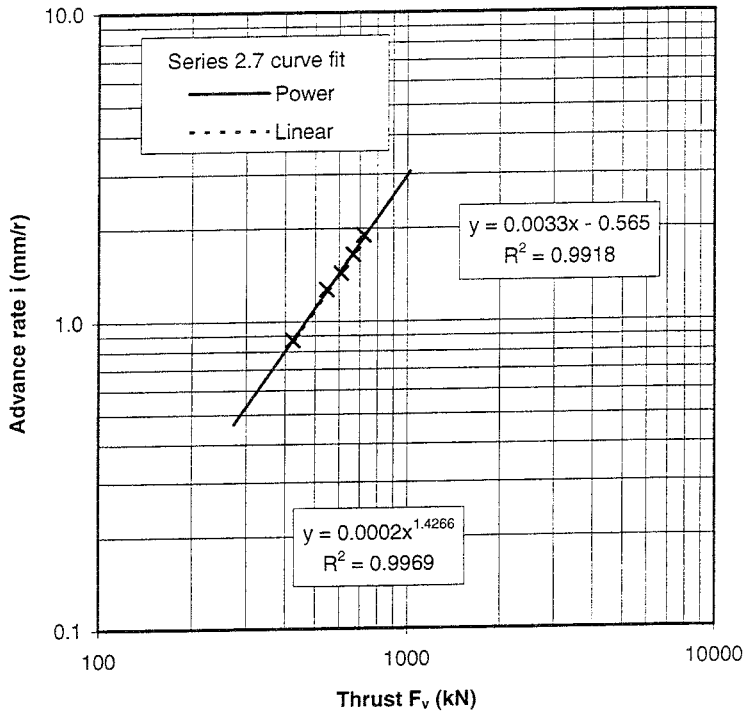

***Figure 5.2-4**. Advance rate as a function of thrust. Test 2.7, rotation speed 8 rpm, 5 & 6 row cutters.*

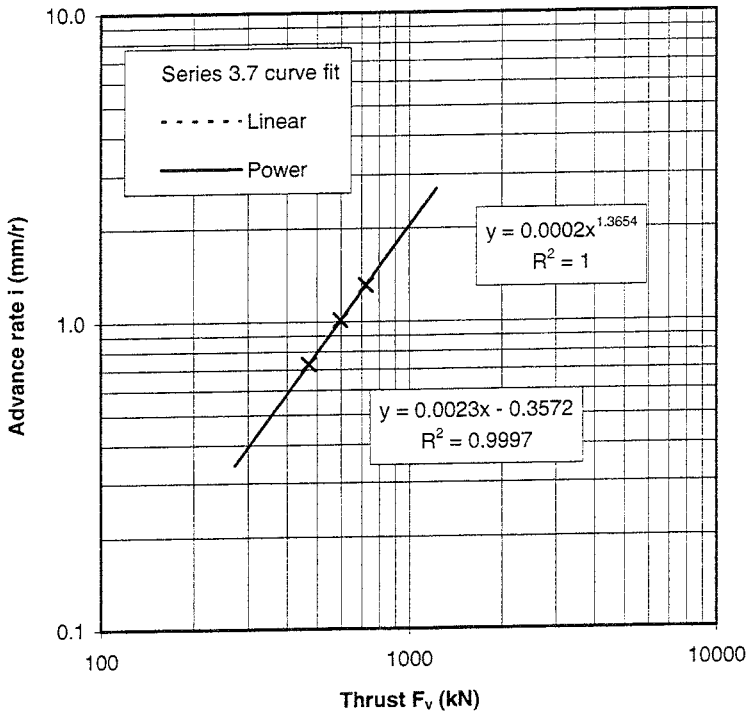

***Figure 5.2-5**. Advance rate as a function of thrust. Thrust Test 3.7, rotation speed 8 rpm, 4 & 5 row cutters.*

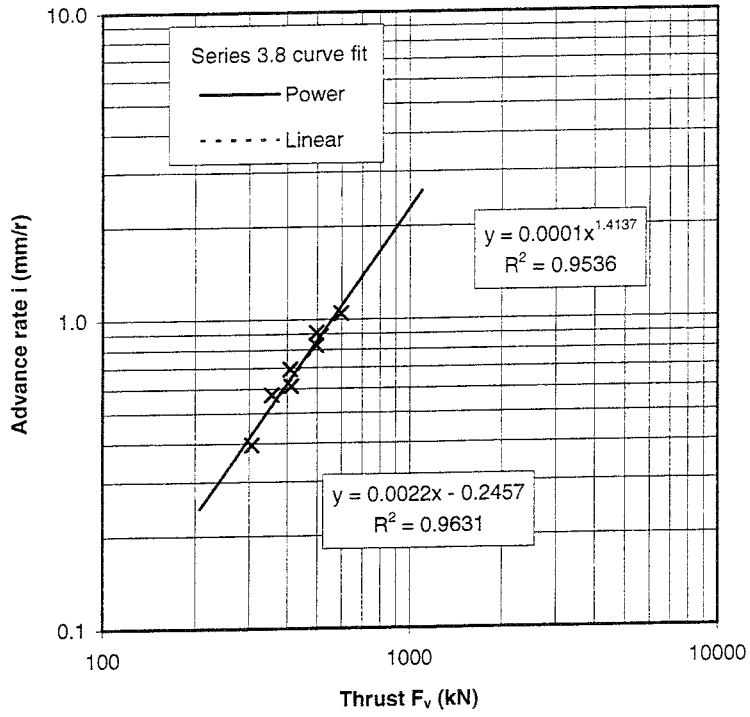

Figure 5.2-6. *Advance rate as a function of thrust. Test 3.8, rotation speed 8 rpm, 4 & 5 row cutters.*

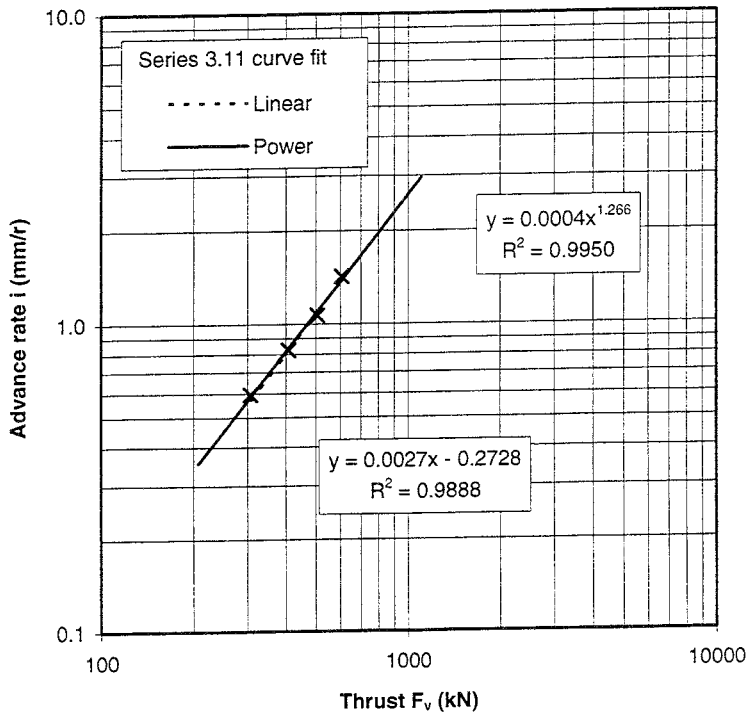

Figure 5.2-7. *Advance rate as a function of thrust. Test 3.11, rotation speed 8 rpm, 4 & 5 row cutters.*

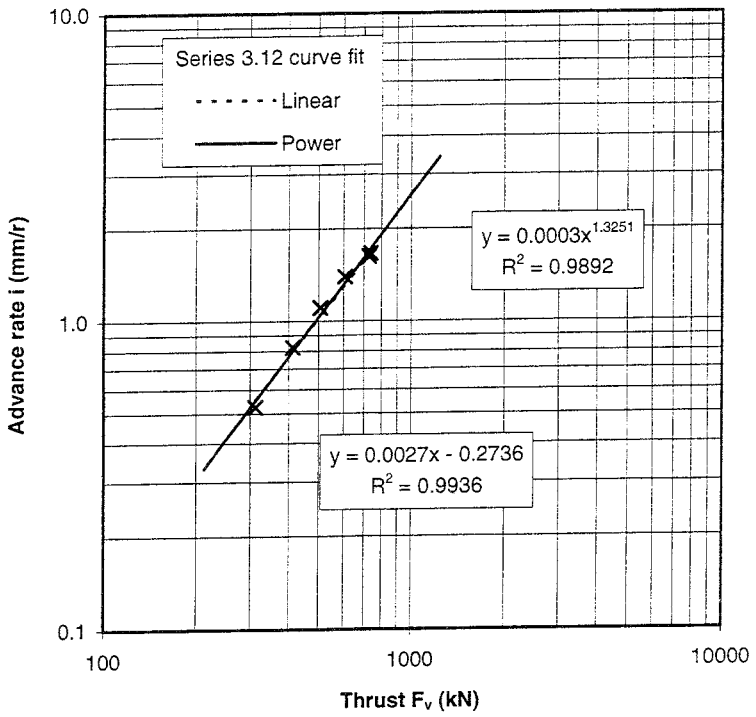

Figure 5.2-8. Advance rate as a function of thrust. Test 3.12, rotation speed 8 rpm, 4 & 5 row cutters.

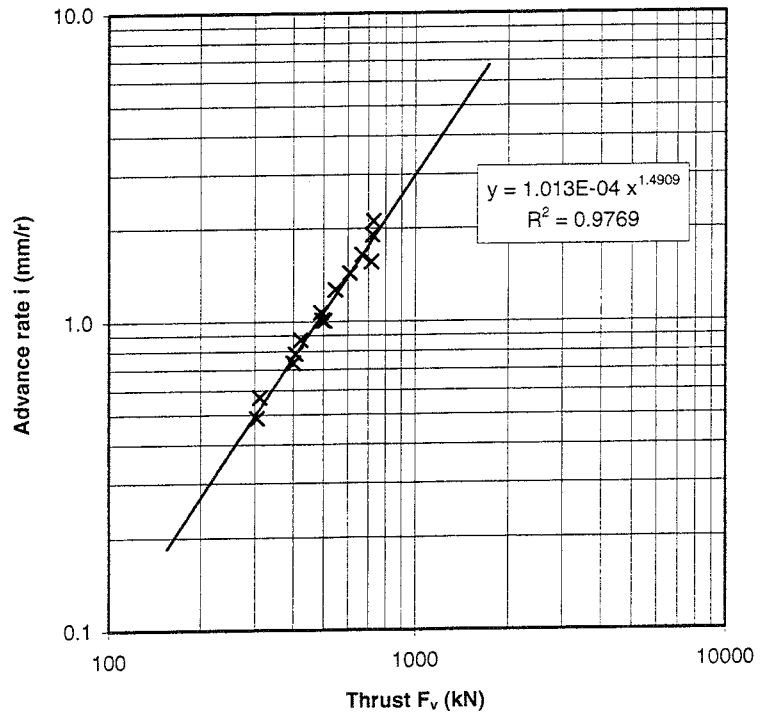

Figure 5.2-9 An estimate based on the least square curve fit of all data for advance rate per rotation as a function of thrust, rotation speed 8 rpm, 5 & 6 row cutters.

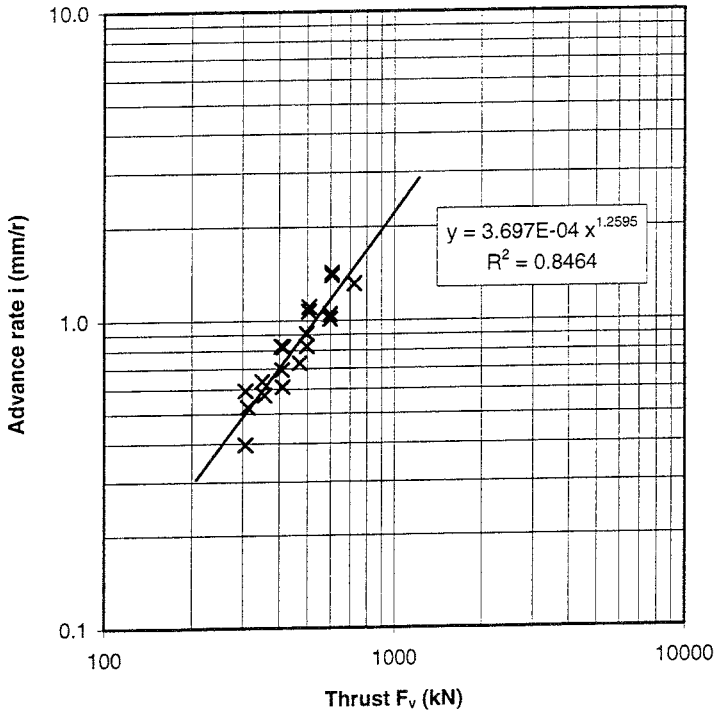

Figure 5.2-10. *An estimate based on the least square curve fit of all data for advance rate per rotation as a function of thrust, rotation speed 8 rpm, 4 & 5 row cutters.*

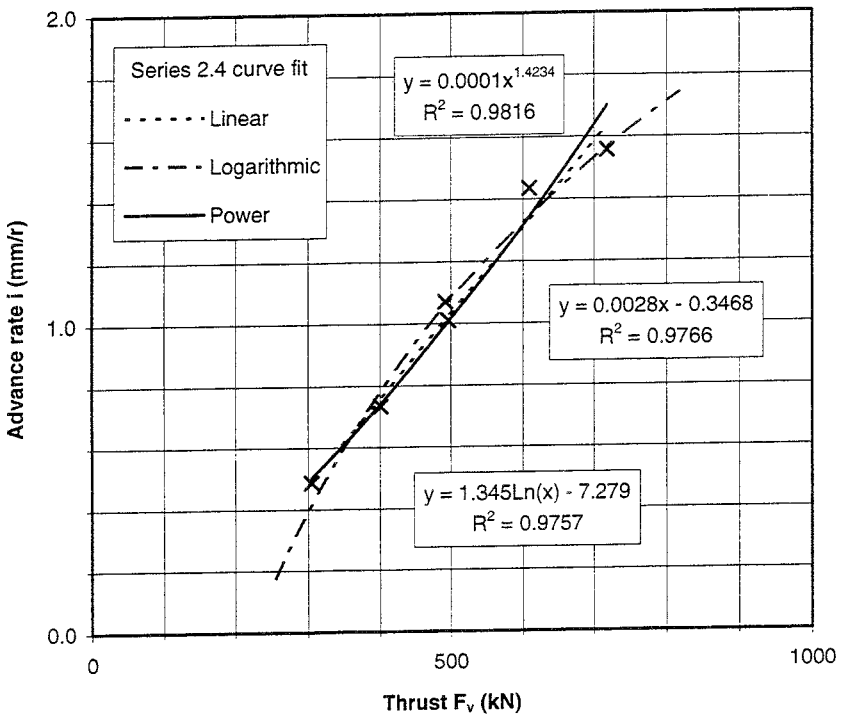

Figure 5.2-11. *Advance rate per rotation as a function of thrust. Test 2.4, rotation speed 8 rpm, 5 & 6 row cutters. This graph uses a linear scale and the exponential, linear and logarithmic regression functions are shown.*

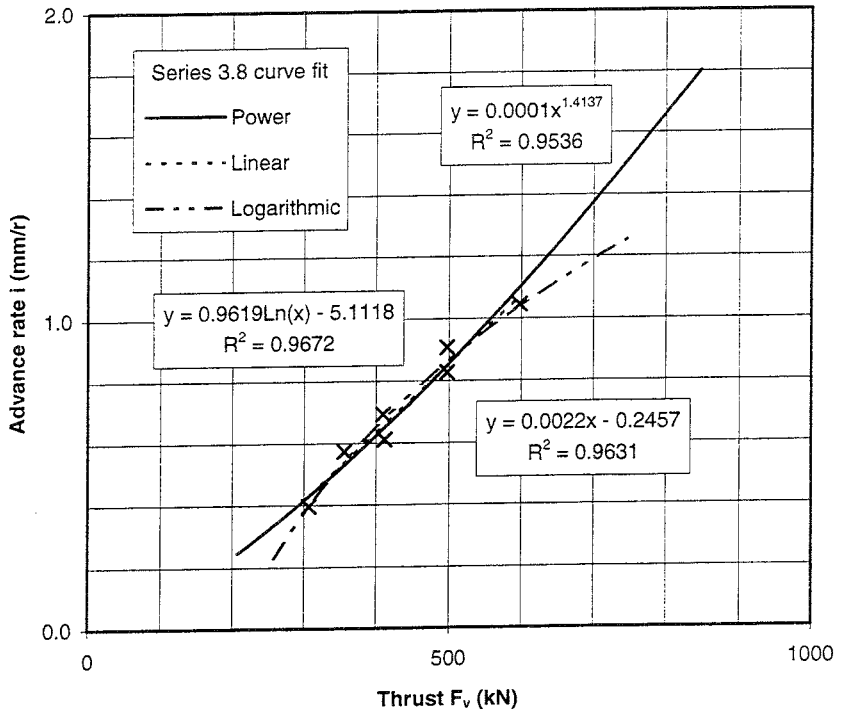

Figure 5.2-12. *Advance rate as a function of thrust. Test 3.8, rotation speed 8 rpm, 4 & 5 row cutters. This graph uses a linear scale and the exponential, linear and logarithmic regression functions are shown.*

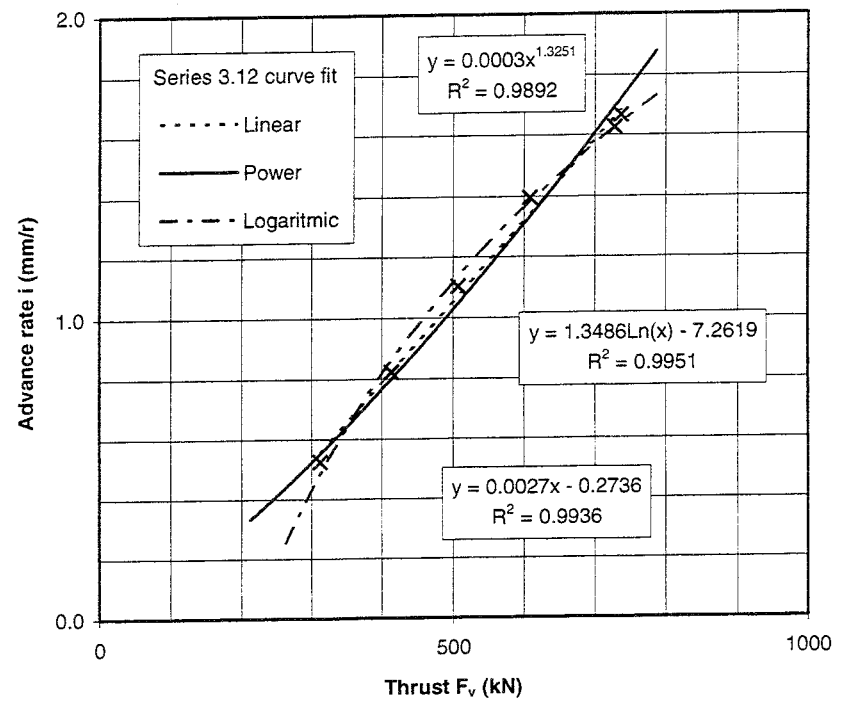

Figure 5.2-13. *Advance rate as a function of thrust. Test 3.12, rotation speed 8 rpm, 4 & 5 row cutters. This graph uses a linear scale and the exponential, linear and logarithmic regression functions are shown.*

5.3 ADVANCE RATE VERSUS ROTATION SPEED

The advance rates were measured using different rotation speeds and thrusts. One of the main objectives was to determine the effect of the rotation speed on the advance rate. This is most easily observed by measuring the advance per rotation for different rotation speeds. If the vacuum flushing can keep the bottom of the hole clean there should be no change in the advance per rotation if the thrust is kept constant. On this basis the extent of any difference should be a measure of the inefficiency of the vacuum cleaning system.

The results of the three Rotation Tests 2.5, 3.9 and 3.10 are shown in Table 5.3-1 and Figures 5.3-1 and 5.3-2 as advance rate versus rotation speed.

The result of Test 2.5 is consistent. The build-up of vacuum pressure and airflow during the test was steady and the rock in the test section is homogeneous. The result of the test, which shows a distinct drop of 25 % in the advance rate per rotation when the rotation speed was raised from 4 to 12 rpm can therefore be regarded as reliable.

The results of the Tests 3.9 and 3.10 are not consistent. The general trend is the same as in Test 2.5 but the behaviour of the advance per rotation with respect to build-up of vacuum pressure and airflow (shown in Table 5.3-1) is not conform as a function of thrust and therefore the absolute results are not considered to be reliable but merely to confirm the trend shown in Test 2.5.

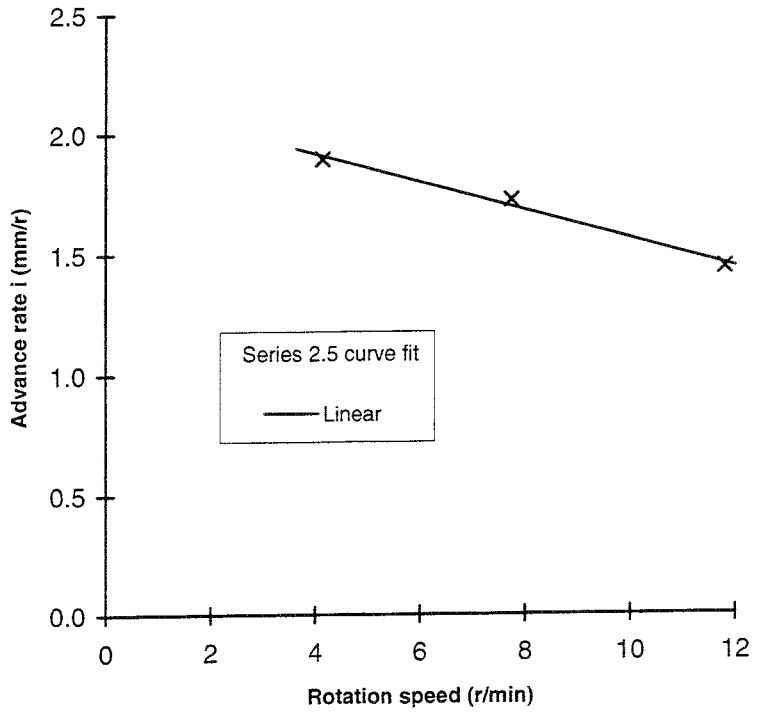

Figure 5.3-1. Advance rate as a function of rotation speed at a thrust of 710 kN. Test 2.5 with 5 & 6 row cutters.

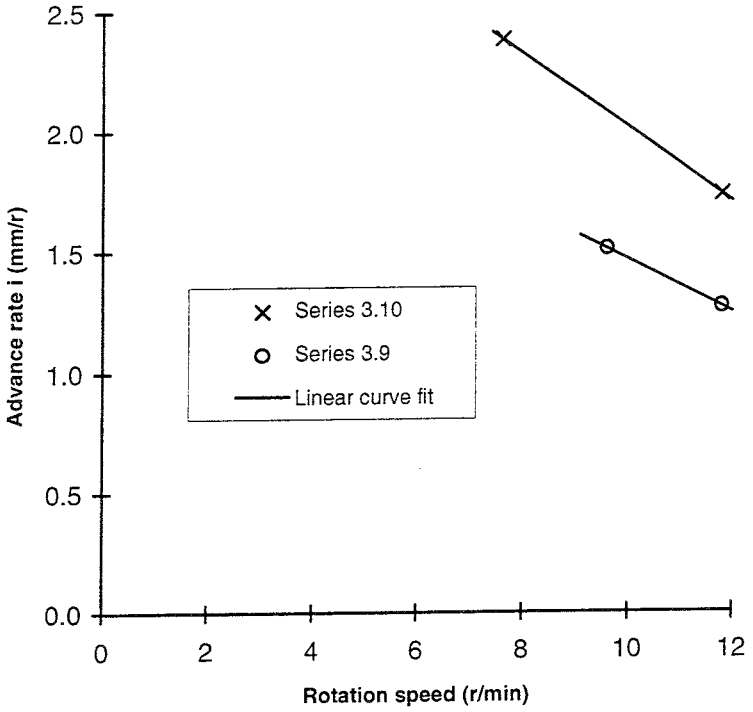

Figure 5.3-2. Advance *rate as a function of rotation speed at constant thrust. Tests 3.9 (points 1,2) and 3.10 (points 1,3) at thrusts of 600 and 720 kN correspondingly 4 & 5 row cutters. See comments in the text about the inconsistency of these results.*

Table 5.3-1. The results of the Rotation Test measurements carried out during the boring of large holes 2 and 3.

Test	Thrust F_v (kN)	RPM (r/min)	Advance l (m/h)	Advance i (mm/rev)	Torque T (kNm)	Drag force F_r (kN)	Specific energy (MJ/m^3)	Cutter coeff. k	Airflow ϕ (m^3/s)
2.5.1	724.6	4.14	0.470	1.893	32.8	60.2	34.6	0.0831	0.913
2.5.2	724.6	7.74	0.800	1.722	33.8	62.2	39.3	0.0858	0.874
2.5.3	694.4	11.80	1.020	1.440	37.3	68.6	51.9	0.0988	0.798
3.9.1	603.3	9.60	0.870	1.510	28.5	52.5	37.8	0.0870	0.952
3.9.2	596.8	11.80	0.900	1.271	28.9	53.2	45.5	0.0891	0.882
3.9.3	596.8	4.41	0.370	1.398	25.4	46.7	36.3	0.0782	0.932
3.10.1	730.7	7.62	1.090	2.384	34.2	62.9	28.7	0.0861	0.909
3.10.2	725.2	6.36	0.790	2.069	33.1	60.9	32.0	0.0840	0.896
3.10.3	722.4	11.80	1.230	1.737	37.0	68.1	42.6	0.0942	0.808

The test sections 3.9 and 3.10 are located in an slightly more fractured section of rock with some distinct inclined narrow schistosity planes. On visual inspection, the type of rock appears to be slightly different between the schistosity planes. The advance rates in Test 3.10 of 2.4 mm/rotation at a rotation speed of 7.6 rpm and 2 mm/rotation at 6.4 rpm are well above the average values for the hole and although the estimate of the quality of rock is based on visual observation, it is presumed that the higher level of advance can be significantly due to differences in the physical properties of the rock.

The large difference in Test 3.10 between the values of advance rate at 6.4 and 7.6 rpm could have been caused by machine factors or filling of the vacuum unit. The dust compartment of the vacuum unit and the filter were cleaned after Test 3.10 and after this cleaning the vacuum pressure level at 8 rpm and 700 kN dropped by about 14 % from 426 to 367 mbar during the boring of the test section.

It is also possible on the basis of the results obtained that the results could be affected by the direction of the change in rotation speed during the test. Both in Tests 3.9 and 3.10 the advance rate value measured after the rotation speed was decreased was not consistent with the advance behaviour when the rotation speed was increased.

It was observed that crushed rock remained on the bottom of the large hole during Test 3.9 at a rotation speed of 11.8 rpm. It is possible that insufficient time was allowed to elapse to enable the flushing process to stabilize after reducing the rotation speed to the test value of 4.4 rpm. It is therefore possible that some crushed rock accumulated during the boring at higher rotation speed was left in the centre part of the hole and therefore the result of the subsequent test section was disturbed.

The build-up of vacuum pressure during Test 3.9 was not consistent with the normal trend because the vacuum pressure of 398 mbar at 4.4 rpm was higher than the value of 388 mbar at 9.6 rpm. The normal trend is that the vacuum pressure increases as the rotation speed is raised. This supports the assumption that the inconsistency in the results of Tests 3.9 and 3.10 was caused by insufficient vacuum suction with a higher rotation speed. As the rotation speed is lowered the suction becomes more effective, the flow of crushed rock through the suction line increases, the vacuum pressure increases and the airflow is reduced.

5.4 PENETRATION COEFFICIENT (b) AND CRITICAL THRUST (F_c)

The critical thrust F_c is defined as the thrust required to maintain an advance of 1 mm/rotation. The relationship of the advance of boring versus the critical thrust and penetration coefficient in general can be described by Equation 5-1 (NTH 1994), which gives the critical thrust $F_c=F_v$ if i=1 mm.

$$F_v/F_c=i^{1/b} \qquad 5\text{-}1$$

which is equivalent to the Equation 5-2 presented for example by Hartman 1992 in the later more general form using the term load exponent instead of penetration coefficient.

$$i=(F_v/F_c)^b = F^b \qquad 5\text{-}2$$

where, b is the penetration coefficient
F_v is the thrust
F_c is the critical thrust
F is the total load (according to Hartman 1992)
i is the advance per rotation (referred also as advance rate).

$1/F_c^b$ is replaced by a constant "a" the result is:

$$i=a\,F_v b \qquad 5\text{-}3$$

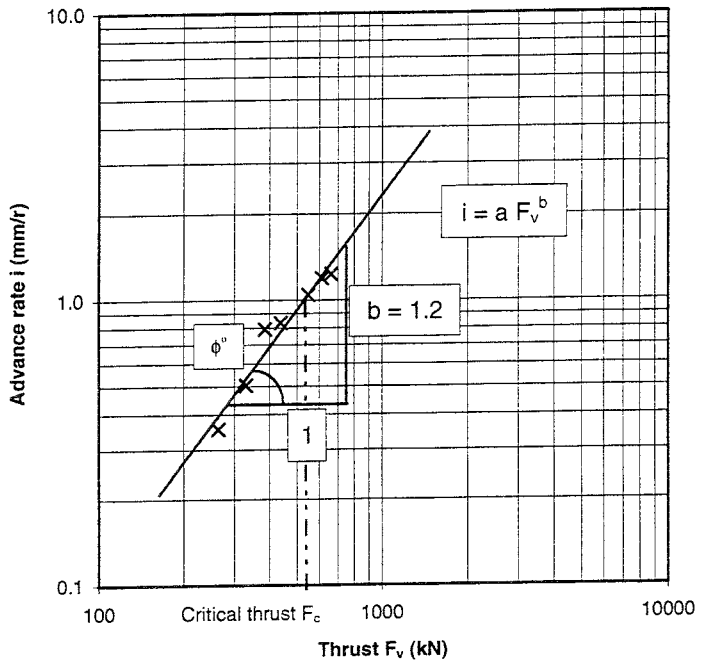

Figure 5.4-1. *Determination of the penetration coefficient b and critical thrust F_c. Parameter b is the slope of the regression line tan ϕ° as seen in this log-log diagram.*

The penetration coefficient b and critical thrust F_c, were calculated so that Equation 5-3 was fitted to the measured test series according to the sum of least squares as shown in figures in Section 5.2. The exponent of the curve was the penetration coefficient b, Figure 5.4-1.

The critical thrust F_c was determined as the value of the regression curve (both linear and exponential) which corresponds to an advance of 1 mm/rotation. A summary of the tests showing the calculated penetration coefficients and critical thrusts is presented in Table 5.4-1.

Both linear and exponential types of curve fit give very similar results for the average R^2 regression coefficient and critical thrust F_c as seen in Table 5.4-1. The average R^2 value for both types of curve fits is greater than 0.99. The exact average R^2 value for the exponential curve fit 0.994 is slightly higher than for the linear fit 0.990. The exponential curve fit was chosen for use in this study when analyzing the results since it corresponds to Equations 5-1, 5-2 and 5-3 and other test results with similar types of equipment (Lislerud 1994).

The penetration coefficient for the boring of large hole 2 with 5 and 6 row cutters is 1.42 - 1.53, the average value being 1.46. The critical thrust is 467 - 491 kN, the average value being 478 kN.

The penetration coefficient for the boring of large hole 3 with 4 and 5 row cutters is 1.27 - 1.47, the average value (excluding test 3.12, points 1 and 6) being 1.39. The critical thrust is 473 - 589 kN, the average value being 531 kN. Measuring points 1 and 6 represented a higher thrust and were suspected of being disturbed by inefficiency in vacuum flushing. The test result which does not include these points is defined as 3.12A.

Table 5.4-1. A summary of all tests and curve fits showing the calculated penetration coefficients and critical thrusts.

	Linear curve fit, $i = B F_v + A$				**Exponential curve fit,** $i = a F_v^{\ b}$			
Serie	multiplier B	constant A	R^2_{Lin}	F_{cLin} (kN)	constant a	b	R^2_{Exp}	F_{cExp} (kN)
2.4	0.0028	-0.3468	0.9766	481.0	1.47E-04	1.4234	0.9816	491.6
2.6	0.0037	-0.7137	0.9641	463.2	7.96E-05	1.5332	0.9781	471.5
2.7	0.0033	-0.5650	0.9918	474.2	1.55E-04	1.4266	0.9969	467.7
3.7	0.0023	-0.3572	0.9997	590.1	1.65E-04	1.3654	1.0000	588.8
3.8A	0.0023	-0.3031	0.9986	566.6	8.89E-05	1.4716	0.9987	566.0
3.8B	0.0024	-0.2739	0.9994	530.8	1.75E-04	1.3748	0.9999	539.8
3.11	0.0027	-0.2728	0.9888	471.4	4.06E-04	1.2660	0.9950	477.1
3.12	0.0027	-0.2736	0.9936	471.7	2.85E-04	1.3251	0.9892	473.4
3.12A	0.0030	-0.3987	1.0000	466.2	1.11E-04	1.4755	0.9977	479.9
Hole 2	0.0033	-0.5489	0.9514	469.4	1.01E-04	1.4909	0.9769	477.6
Hole 3	0.0023	-0.1932	0.8250	518.8	3.70E-04	1.2595	0.8464	530.9

Series Hole 2 and Hole 3 include all test results
3.8A include tests 1-4 and 3.8B include tests 5-7
3.12A include tests 2-5

An exponential curve was also fitted to the complete set of data. This gave a value of 1.49 for the penetration coefficient and a value of 478 kN for the critical thrust when boring with 5 and 6 row cutters, as shown in Figure 5.4-2. The corresponding values for boring with 4 and 5 row cutters were 1.26 and 531 kN, see Figure 5.4-3.

The value of the penetration coefficient (load exponent) is generally from 1.0 in harder rocks to 1.5 in soft rock, defined as rock with uniaxial compressive strength less than 100 MPa (Hartman 1992). The value given for full profile tunnel boring with disks is approximately 2 depending on the chipping efficiency (NTH 1994). The results of single cutter tests and test boring at Tamrock Test Mine (Lislerud 1994) using hemispherical buttons gave penetration coefficients ranging from 1.8 to 1.9.

The result obtained by curve fitting is consistent with the average values for 5 and 6 row cutters shown in Tables 5.4-1 and 5.4-2. It is therefore concluded that the thrust-advance behaviour of boring at a rotation speed of 8 rpm can be described by the exponential function shown in Figure 5.4-2.

The penetration coefficient obtained by curve fitting differs from the calculated average values for 4 and 5 row cutters as shown in Table 5.4-2. The results of the tests show a significant degree of scatter, as seen in Figure 5.4-3. Separate tests have produced consistent results in respect of penetration coefficient, which implies that the scattering is not a random effect but caused by differences in the rock or functioning of the machine.

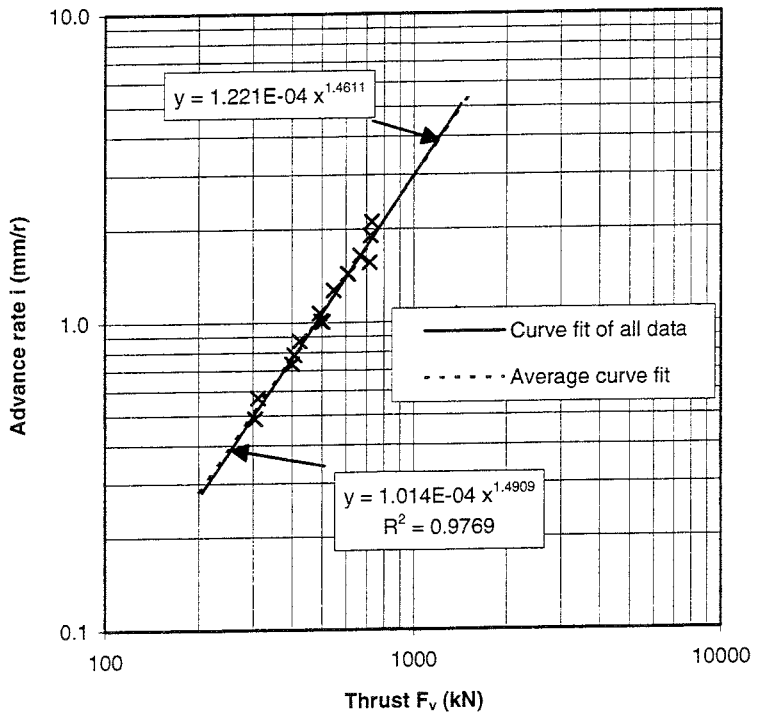

Figure 5.4-2. *All test results with 5 & 6 row cutters and the exponential curve fit to all data and average curve whose parameters are calculated as the average of all test results.*

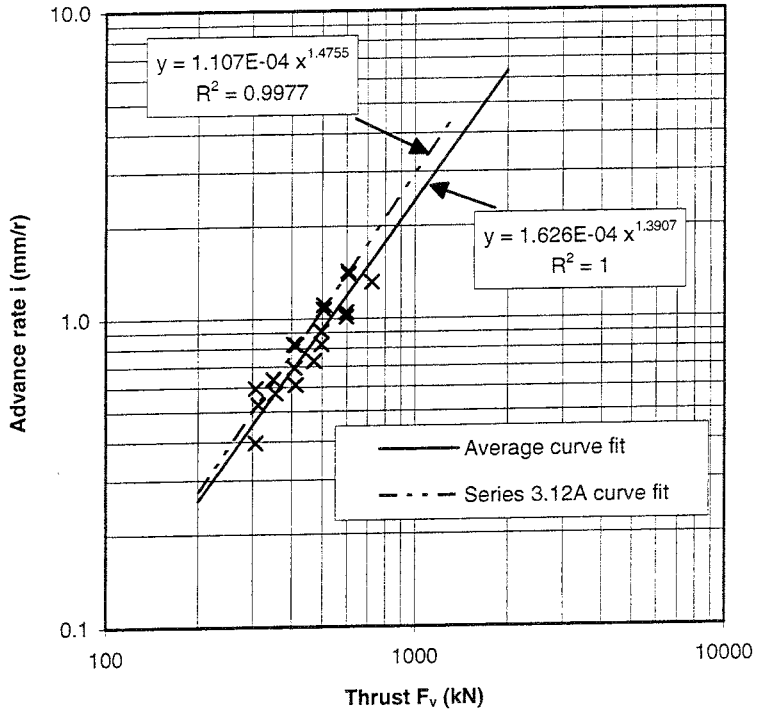

Figure 5.4-3. *All test results with 4 & 5 row cutters and the corresponding exponential curve with average parameter values. Fit for Test Series 3.12A is also shown.*

The texture of the rock in the lower section of the large hole 3 is similar to the rock texture in hole 2 but there is a difference in the upper part of the hole. The DRI-value of 56 in the lower section of hole 3 is also larger and close to the DRI-values of 57 in hole 2 in comparison to the DRI- value of 50 in the upper part of the hole 3 (above 5 m depth in the hole). The same trend is seen in the results of the critical thrust values. The average critical thrust in the upper part of the hole was 565 kN as it was 475 kN in the lower part of the hole.

It is therefore obvious that some of the scatter in the test results is caused by changes in the rock properties and it is concluded that the results obtained in tests 3.11 and 3.12 represent the average performance of the equipment used and the result of test 3.12A (points 2, 3, 4 and 5, critical thrust of 480 kN and penetration coefficient 1.48) shown in Table 5.4-2 and Figure 5.4-3 and 5.4-4, may represent the highest possible level of operating performance with 4 and 5 row cutters, comparable to the results from the boring of large hole 2 with 5 and 6 row cutters.

Table 5.4-2. The different values for penetration coefficient and critical thrust for both types of cutters.

Estimate	Penetration coefficient, b	Critical thrust, Fc (kN)
5&6 row cutters		
Average of all tests	1.46	477
Least square curve fit to all data	1.49	478
4&5 row cutters		
Average of tests 3.7, 3.8A, 3.8B, 3.11 and 3.12A	1.39	530
Least square curve fit to all data	1.26	531
Least square curve fit to series 3.12A	1.48	480
Least square curve fit to series 3.11 and 3.12	1.28	483
Estimated curve	1.39	475

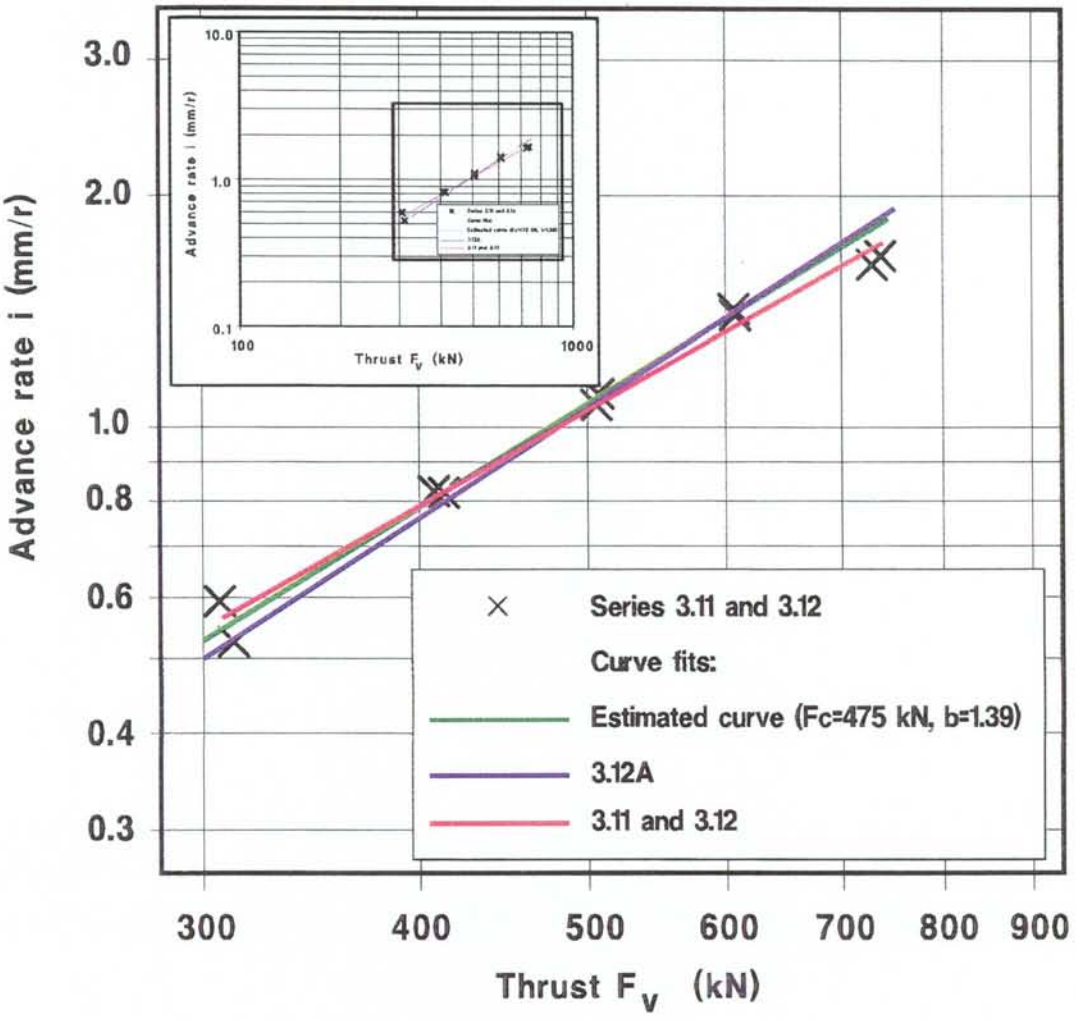

Figure 5.4-4. Results of Test Series 3.11 and 3.12 with 4 & 5 row cutters and the corresponding fit of exponential type. The estimated curve (F_c = 475 kN, b=1.39) and fit for Test Series 3.12A is also shown, see text for explanation.

A different approach to estimate the thrust advance behaviour of the 4 and 5 row cutters can be taken if it is assumed that the penetration coefficient is dependent on the machine factors and the critical thrust is dependent on rock factors. In that case the average critical thrust from tests 3.11 and 3.12 (475 kN) and the average penetration coefficient from all tests (1.39) can be used to describe the thrust advance behaviour of the 4 and 5 row cutters. The result, shown in Table 5.4-2 and Figure 5.4-4, is very close to the result achieved in test 3.12A.

When looking at the summary of the different values for penetration coefficient and critical thrust for both sets of cutters, shown in Table 5.4-2 and Figure 5.4-3, it should be noted that the measurements at low thrust values (well below the critical thrust) do not represent the performance of the boring method as well as the results obtained with higher thrust when considering practical applications.

5.5 CUTTER COEFFICIENT, k

The cutter coefficient is defined as the parameter k in equation

$$k=F_h/F_v \qquad 5\text{-}4$$

where, F_v is the thrust
F_h is the rotation force (Figure 5.5-1).

The importance of the cutter coefficient, which describes the rolling resistance with respect to the thrust of the cutter head, lies in the fact that it can be used to determine the torque demand on the boring machine according to Equation 5-5.

The rotation force was calculated from the rotation torque of the cutter head. The values for different tests at a rotation speed of 8 rpm are shown in Figures 5.5-2, 5.5-3 and 5.5-4 with respect to the advance rate. A second order polynomial fit is also shown. It should be noted that the shape of the regression curve at advance rates lower than 2 mm/r is governed by the free running torque of the boring machine and therefore the tail section of the regression curve at higher advance rates does not represent the true behaviour of the cutter coefficient and cannot be used to extrapolate to higher advance rates.

The values for the cutter coefficient are dependent on thrust and therefore also upon the rate of advance. The values found were in the range 0.075 - 0.14.

The cutter coefficient for 5 and 6 row cutters shown in Figure 5.5-2 shows typical behaviour. At first, the value for cutter coefficient falls until an advance rate of about 1.5 mm/rotation is reached. This is a consequence of the free running torque of the boring machine. At higher advance rates than 1.5 mm/rotation the value for cutter coefficient increases.

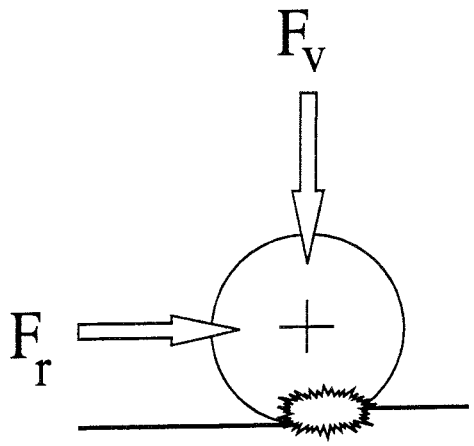

Figure 5.5-1. Determination of the cutter coefficient.

The cutter coefficient for 4 and 5 row cutters shown in Figures 5.5-3 and 5.5-4 has not reached the rising section of the curve.

The average value for the 4 and 5 row cutters was slightly smaller than the value for the 5 and 6 row cutters. With an advance rate of 1.5 mm/rotation the value for the 4 and 5 row cutters is about 0.080 and the value for the 5 and 6 row cutters is about 0.086.

The behaviour of the cutter coefficient compared to the rate of advance shows that the effect of the free running torque of the boring machine has a strong effect on the cutter coefficient and causes distortion in the forward end of the curve. A general trend is that an increase in thrust will produce a gradually increasing value for the cutter coefficient. The minimum values measured for the cutter coefficient are consistent with the typical range of values obtained elsewhere: 0.08 - 0.12 (NTH 1994). These values are also consistent with the results of raiseboring tests carried out in the Tamrock Test Mine (Lislerud 1994) when values of the cutter coefficient in the range of 0.08 - 1.44 were found.

$$F_{vmax}=M_{max}/(R_m*k) \qquad 5\text{-}5$$

where, R_m is the average radius of the button rows
M_{max} is the maximum torque of the boring machine
F_{vmax} is the maximum thrust of the machine.

The theoretical maximum thrust which could have been utilized by the equipment used in this work can be estimated on the basis of Equation 5-5 and by assuming that the cutter coefficient with the larger advance rate could take a value of 0.12, which is consistent with the typical values presented in the earlier paragraph. The maximum torque exerted by the boring machine was 73 kNm and therefore the theoretical maximum thrust which could have been utilized by the equipment used in this work was 1118 kN.

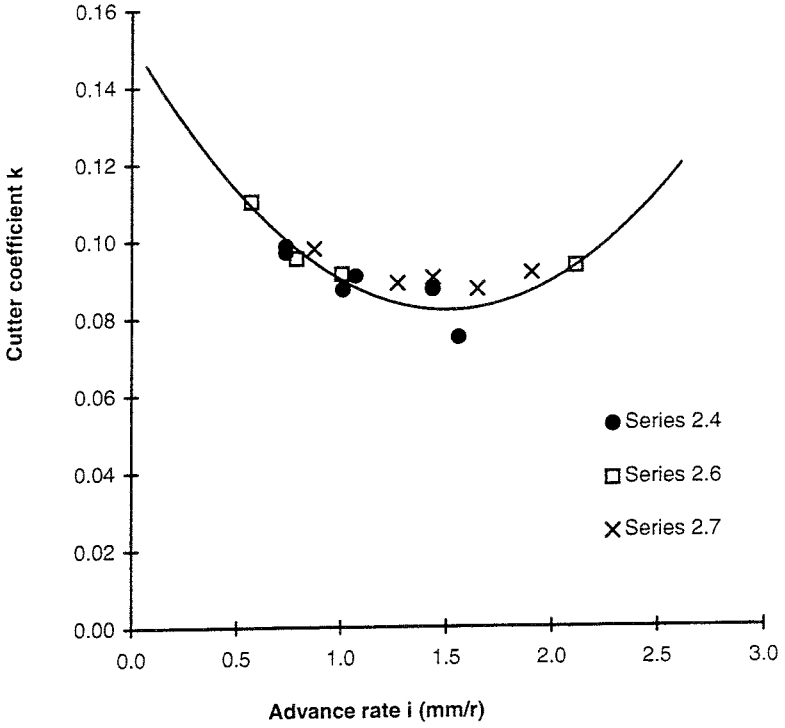

Figure 5.5-2. *Cutter coefficient plotted against advance rate, Tests 2.4, 2.6 and 2.7.*

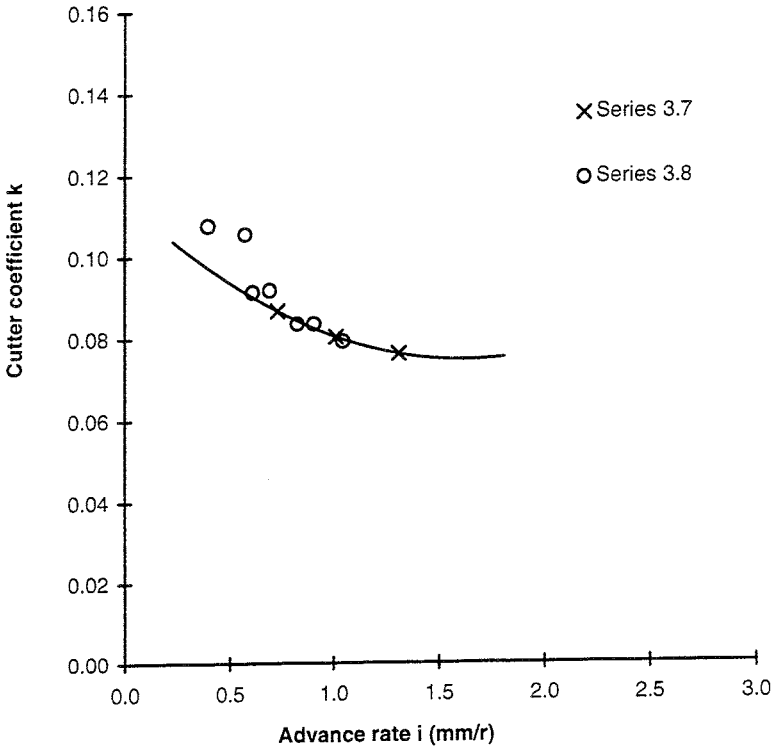

Figure 5.5-3. *Cutter coefficient plotted against advance rate, Tests 3.7 and 3.8.*

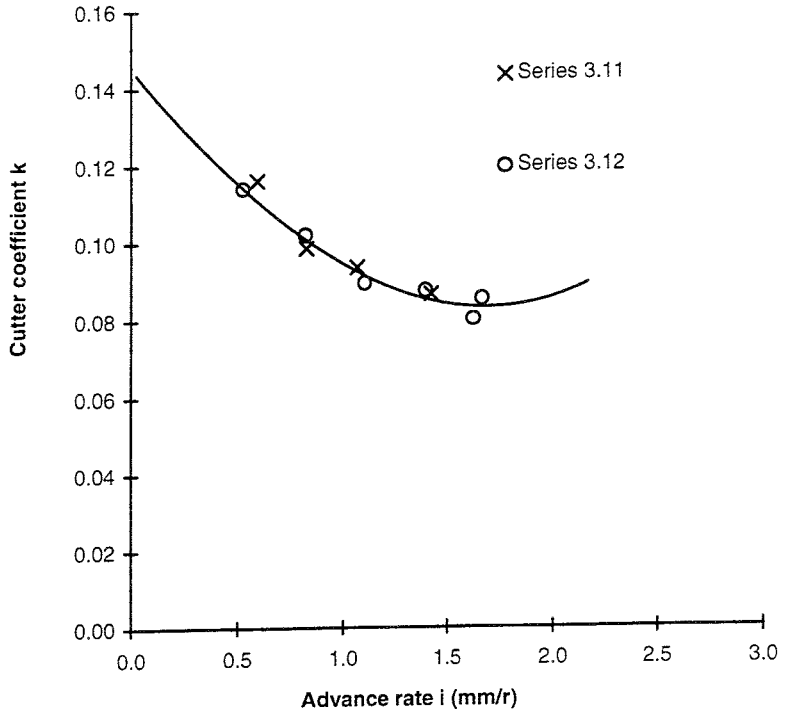

Figure 5.5-4. Cutter coefficient plotted against advance rate, Tests 3.11 and 3.12.

5.6 SPECIFIC ENERGY, E_S

The work and energy needed to crush the rock when boring comprises the work done by the thrust and the work done by the rotation force.

The specific energy, the energy needed to crush one cubic meter of solid rock, was calculated according to the generally used Equation 5-6 (given for example in NTH 1994) which gives the specific energy for the rotation force.

$$E_s = 2M/ir^2 \qquad 5\text{-}6$$

where, E_s is the specific energy required to crush one cubic meter of rock
M is the torque on the cutter head
i is the advance rate per rotation
r is the radius of the hole.

The amount of energy created by thrust is small in comparison to the amount of energy created by rotation and it is therefore neglected. The proportion of thrust energy lies in the range of 0.2 - 1.0 % of the total energy.

The specific energy value, E_s, for the boring of large holes was 35 - 91 MJ/m^3. This value decreases as the advance rate increases, as shown in Figures 5.6-1 to 5.6-7. Therefore the best advance rate is reached at the lowest specific energy.

Table 5.6-1. A summary of the tests and exponential curve fits showing the range of specific energy.

Serie	Tests	Specific energy (MJ/m3)	Eksponential curve fit of type $y = cx^d$ c	d	R^2_{Exp}
2.4	all	37 - 59	48.2	-0.5644	0.9876
2.6	all	35 - 66	49.5	-0.4678	0.9937
2.7	all	38 - 58	47.5	-0.4088	0.9483
3.7	2-4	46 - 61	52.2	-0.5147	0.9971
3.8A	1-4	49 - 91	49.4	-0.6414	0.9932
3.8B	5-7	50 - 70	48.8	-0.5416	0.9831
3.11	all	40 - 65	48.8	-0.5416	0.9908
3.12A	2-5	41 - 74	49.3	-0.6142	0.9882

The specific energy values are in the same range for both types of cutter arrangements even though the range of values for 4 and 5 row cutters (45 - 72 MJ/m^3) is slightly higher than that of the 5 and 6 row cutters (37 - 61 MJ/m^3), as seen in Table 5.6-1 and Figure 5.6-8.

Typical values of specific energy given by machine manufacturers for raise boring in granite with carbide insert button roller cutters fall in the range 68 - 186 MJ/m^3.

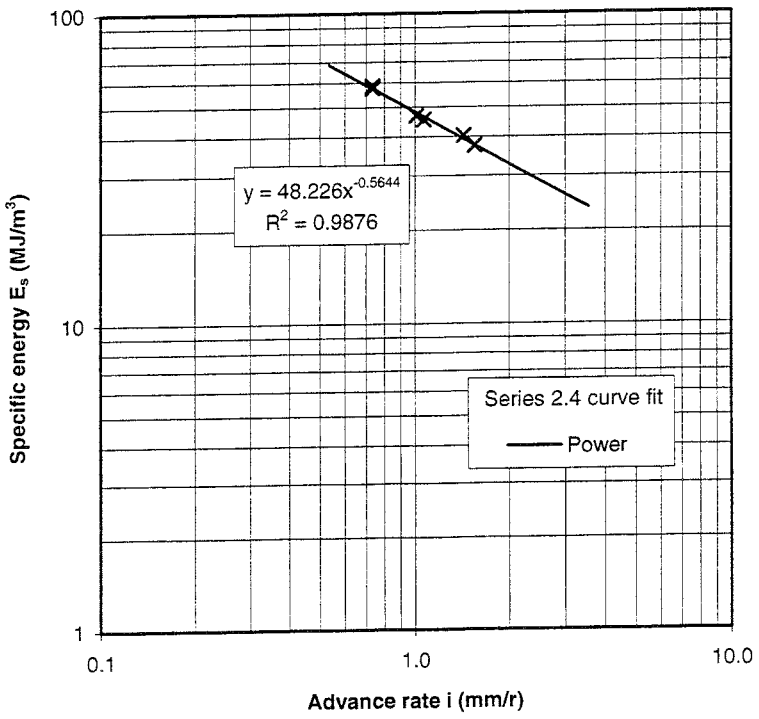

Figure 5.6-1. Specific energy plotted against advance rate for 5 & 6 row cutters, Test 2.4.

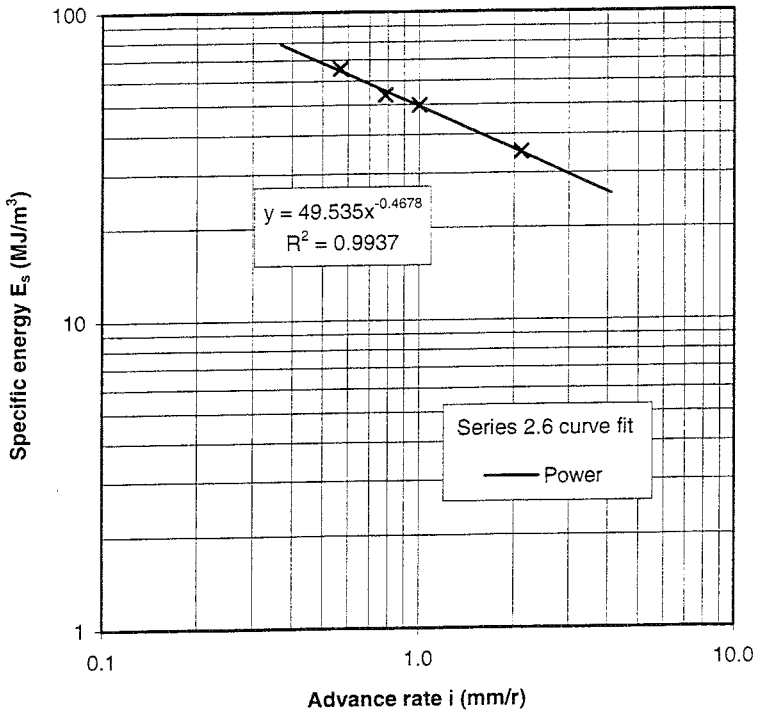

Figure 5.6-2. *Specific energy plotted against advance rate for 5 & 6 row cutters, Test 2.6.*

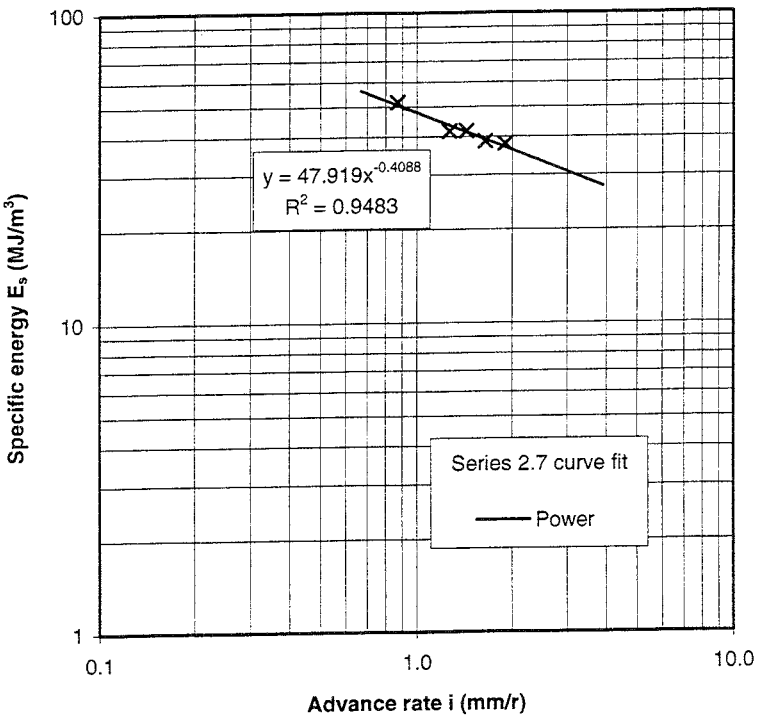

Figure 5.6-3. *Specific energy plotted against advance rate for 5 & 6 row cutters, Test 2.7.*

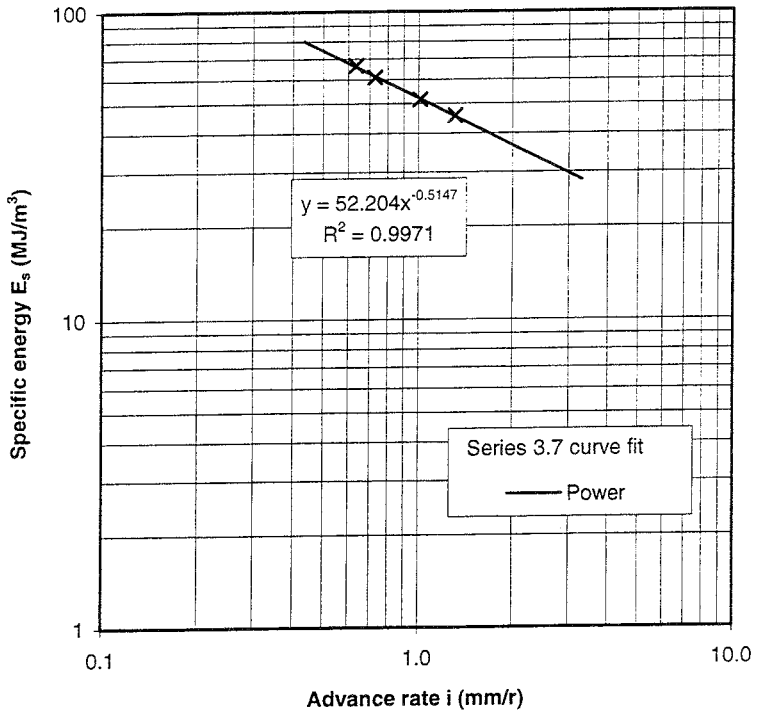

Figure 5.6-4. *Specific energy plotted against advance rate for 4 & 5 row cutters, Test 3.7.*

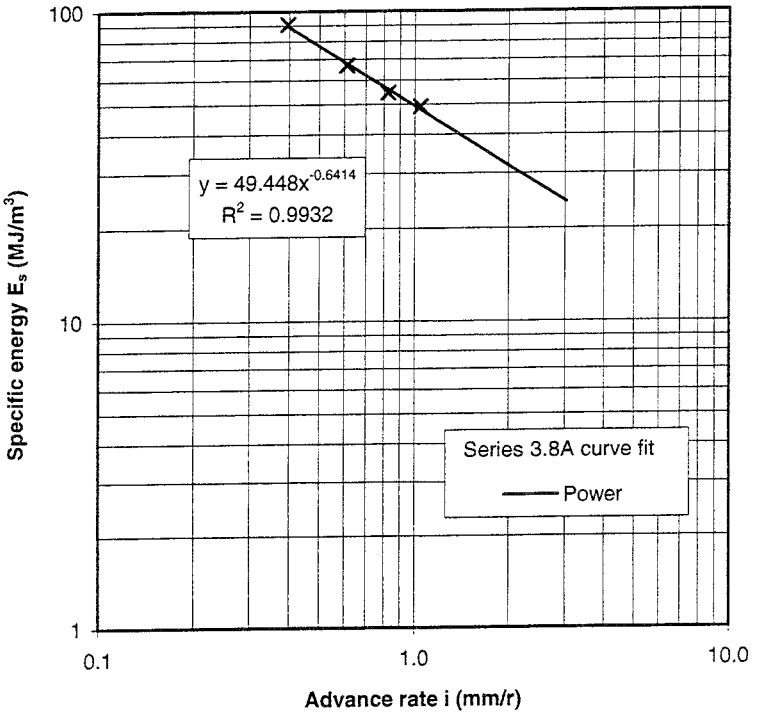

Figure 5.6-5. *Specific energy plotted against advance rate for 4 & 5 row cutters, Test 3.8A.*

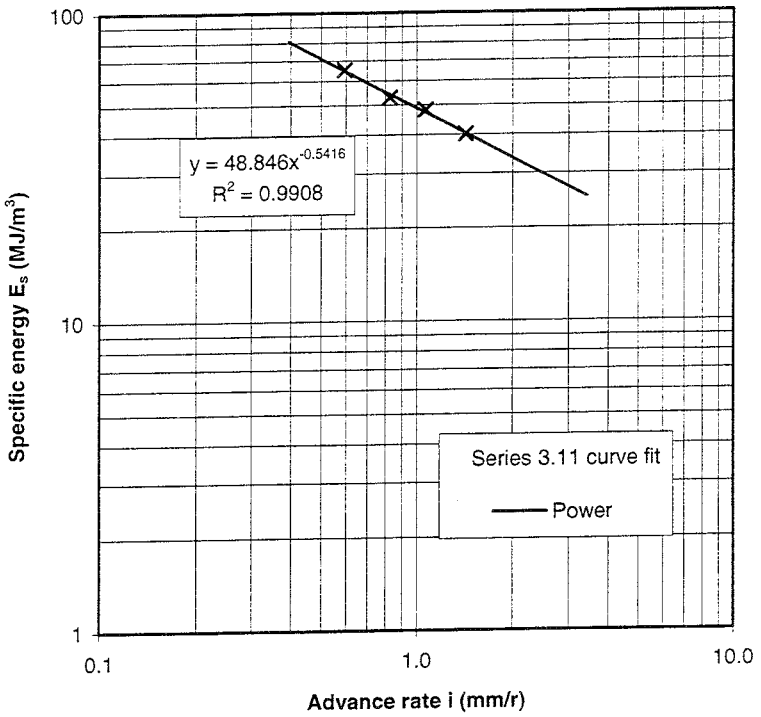

Figure 5.6-6. *Specific energy plotted against advance rate for 4 & 5 row cutters, Test 3.11.*

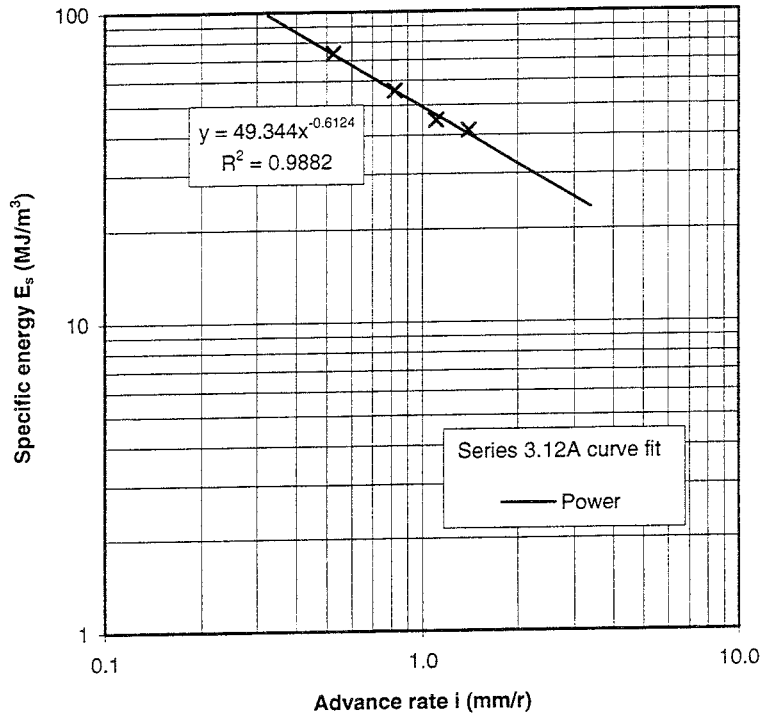

Figure 5.6-7. *Specific energy plotted against advance rate for 4 & 5 row cutters, Test 3.12A.*

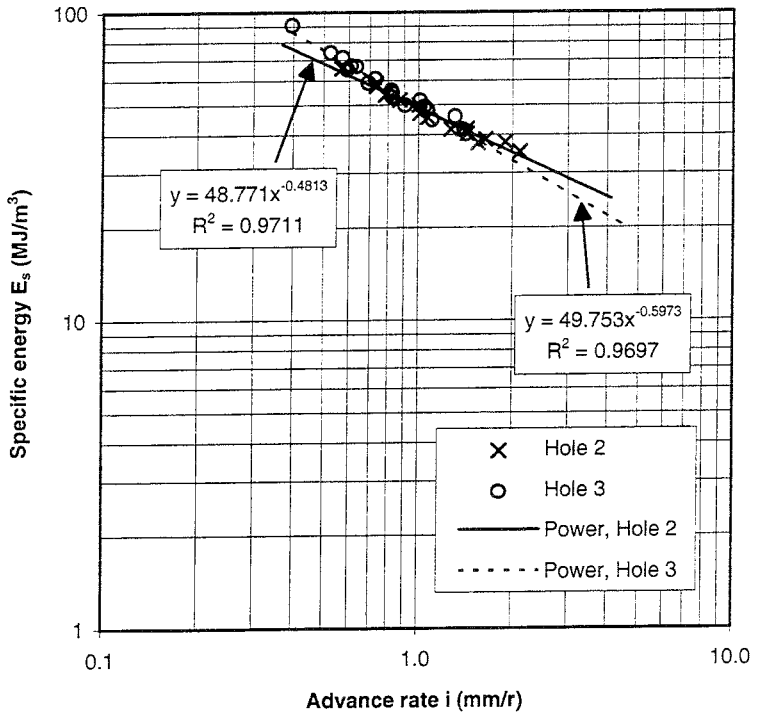

Figure 5.6-8. The average specific energy plotted against advance rate for both holes (both sets of cutters).

5.7 FLOW RATIO (μ) AND RATE OF AIRFLOW

The flow ratio for the vacuum suction was calculated as the ratio between the weight of crushed rock and the weight of the air at normal pressure. The density of air at normal pressure was assumed to be 1.2 kg/m^3 and the density of the crushed rock 2500 kg/m^3 when converting the volumetric flow to mass flow.

The flow ratio for the vacuum suction system when boring the large holes was in the range 0.3 - 1.6. This ratio is linearly dependent on the rate of advance and increases as the rate of advance increases, see Figure 5.7-1.

A vacuum system of the type employed with a flow ratio in the range 0 - 15 is called a dilute (lean) phase system. The values calculated from given data (Super Products 1993) for a similar type of vacuum suction equipment, type "Little Sucker"^{TM} Model 100 industrial vacuum loader, used for similar type of transport of crushed rock to that used in the current work give maximum flow ratios in the range 1.9 - 7.1.

The ideal flow ratio for a particular purpose is difficult to define accurately without testing since the flow ratio and the loading rate are functions of the suction line length, the diameter of the suction line and are also affected by factors such as material density, particle size, particle shape, coefficient of friction, and water content.

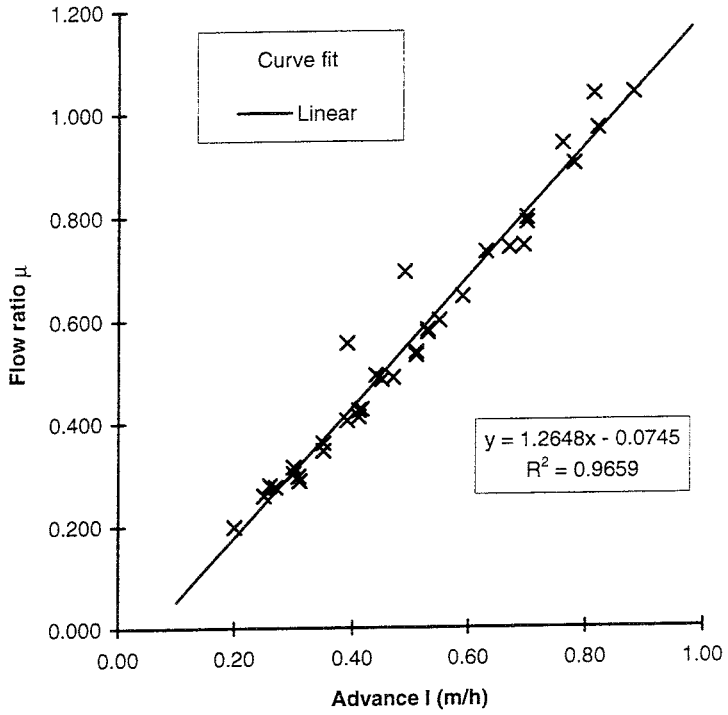

Figure 5.7-1. *Flow ratio plotted against advance rate for boring of a large hole.*

The measured airflow rate was found to be dependent on the advance rate as seen in Figure 5.7-2. As the advance rate is increased more material is conveyed with the flow and both the flow ratio and the vacuum pressure are increased while the airflow rate is reduced. The three measuring points (1, 2, 3) which are distinctly below the linear regression line for large hole 2 in Figure 5.7-2 were measured during Test 2.6. During this test, it was observed that the vacuum cleaning was not working efficiently and work was stopped. Point 4 was measured after the test had been restarted.

The results manifest, as discussed later in Chapter 8.5, the need to optimize the flow resistance in the suction line and to adjust the flow rate according to the flow ratio.

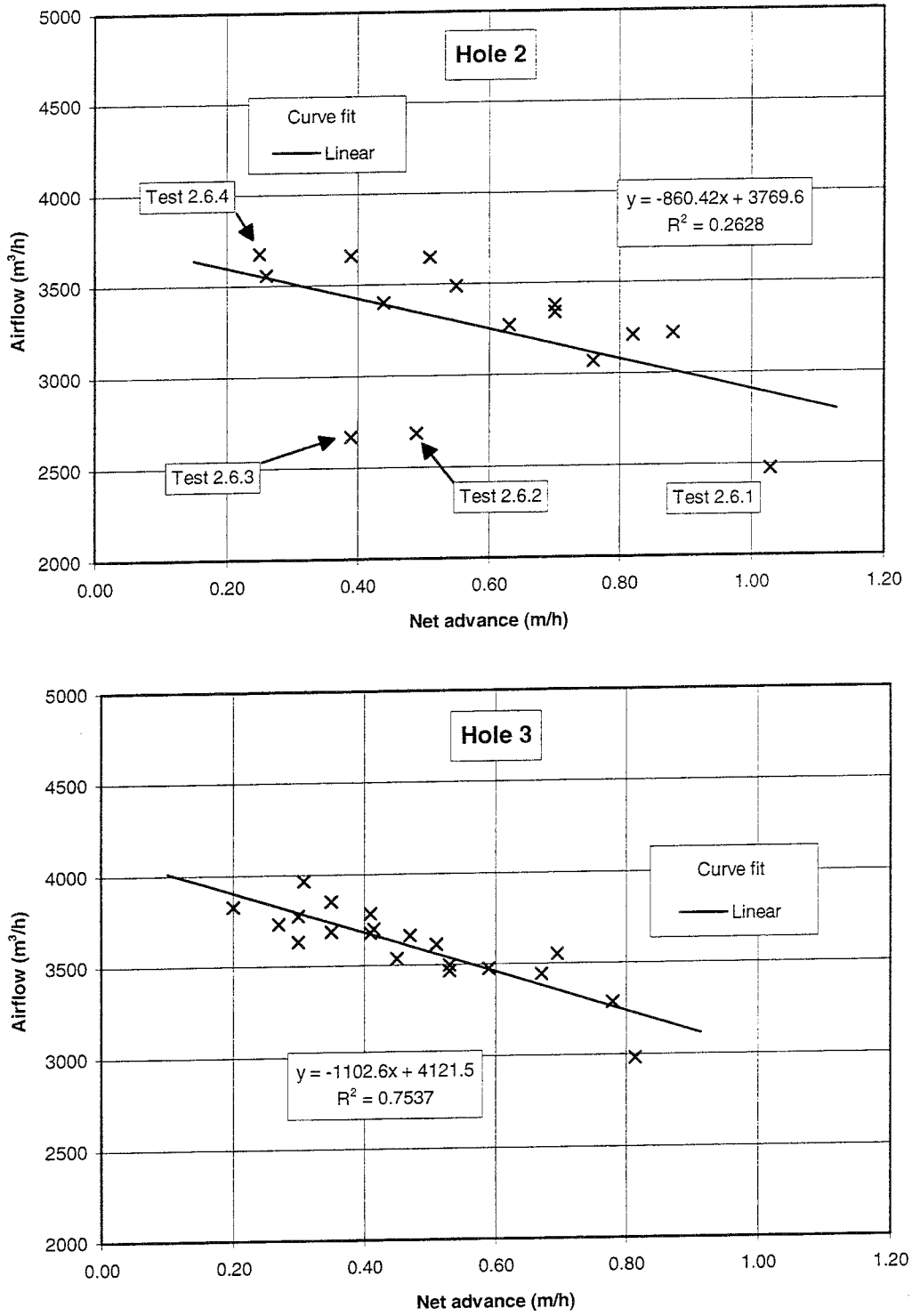

Figure 5.7-2. *The rate of airflow plotted against advance rate during the boring of test sections in large holes 2 and 3. As the advance rate is increased the flow ratio increases and the airflow is reduced.*

5.8 BORING OF THE PILOT HOLE AND THE LARGE HOLE AT THE SAME TIME IN A SINGLE OPERATION

A 1.3 metre length of large hole and pilot hole was bored at the same time in a single operation between the depths of 100.3 cm and 231.5 cm in large hole 2. This experiment was named a 'single pass' boring test since the complete hole was bored in a single operation.

No actual testing of the effect of changing the operating parameters was carried out in the manner described earlier, but the operating parameters were monitored and logged in the same manner as in the actual tests and the corresponding boring parameters were calculated.

A total of 11 different measurements were carried out between the hole depths of 106 cm and 226 cm as shown in Tables 5.8-1 and 5.8-2. Boring was carried out at a rotation speed of 8 rpm and thrust of 286 - 746 kN. The average advance rate versus thrust was calculated and is shown in Figures 5.8-1, 5.8-2 and 5.8-3. The specific energy of boring was plotted against thrust and the cutter coefficient plotted against rotation speed. These results are shown in Figures 5.8-4 and 5.8-5.

The first seven successive measurements 1, 2, 3, 4, 5, 6 and 7 (Table 5.8-1 and 5.8-2) give different and less effective thrust-advance behaviour (Figure 5.8-1 and 5.8-2) than the last four measurements 8, 9, 10 and 11 (Figure 5.8-3). The decreased advance rate performance could have been caused by a change in the vacuum flushing characteristics of the combined cutter head, a fault in the vacuum suction line or differences in the rock.

Table 5.8-1. Operating data during 'single pass' boring.

Test (No.)	Start depth (cm)	Stop depth (cm)	Advance (mm)	Time (min)	RPM (r/min)	Thrust (bar)	Torque (bar)	Vacuum (mbar)	Weight * (kg)
1	48.3	48.3	0	6	8	83	56	282	10680
2	48.3	48.3	0	6	8	83	50	277	10680
3	48.3	48.3	0	6	8	154	60	284	10680
4	48.3	48.3	0	6	8	175	60	330	10680
5	48.3	48.3	0	6	8	196	62	335	10680
6	48.3	48.3	0	6	8	215	60	346	10680
7	48.3	48.3	0	6	8	218	71	335	10680
8	48.3	48.3	0	12	8	219	69	355	10680
9	48.3	48.3	0	12	8	192	71	344	10680
10	48.3	48.3	0	7	8	194	65	356	10680
11	201.8	201.8	0	20	8	232	94	390	11020

* Weight of cutterhead and drillstring

Table 5.8-2. The calculated operating parameters of 'single pass' boring.

Test (No.)	Thrust F_v (kN)	Advance l (m/h)	ROP i (mm/r)	Torque T (kNm)	Drag force F_r (kN)	Specific energy E_s(MJ/m^3)	Cutter coefficient k	Air flow (m^3/s)	Flow ratio μ
1	286.2	0.15	0.31	19.7	36.3	126.3	0.1267	1.1744	0.1348
2	286.2	0.13	0.27	17.6	32.4	130.1	0.1131	1.1849	0.1158
3	441.4	0.20	0.42	21.1	38.8	101.5	0.0880	1.1702	0.1804
4	487.4	0.23	0.48	21.1	38.8	88.2	0.0797	1.0736	0.2261
5	533.3	0.28	0.58	21.8	40.1	74.9	0.0753	1.0632	0.2780
6	574.8	0.27	0.56	21.1	38.8	75.2	0.0676	1.0401	0.2740
7	581.4	0.41	0.85	25.0	46.0	58.6	0.0791	1.0632	0.4071
8	583.6	0.41	0.85	24.3	44.7	56.9	0.0766	1.0213	0.4238
9	524.5	0.38	0.80	25.0	46.0	62.4	0.0876	1.0443	0.3892
10	528.9	0.37	0.77	22.9	42.1	59.7	0.0796	1.0192	0.3818
11	746.0	0.65	1.34	33.1	60.9	49.3	0.0816	0.9482	0.7181

Visual inspection shows no significant differences in the rock and this is therefore considered to be an unlikely cause for the difference. According to the log book the following measures were taken prior to the boring of the eight measuring intervals:

- a hole worn in the bent pipe on top of the boring machine was repaired

- the nozzles of the pilot bit were extended to achieve a better cleaning effect.

It is most probable that these measures improved the performance of the cutter head and that the last four measurements 8, 9, 10 and 11 are therefore descriptive of the characteristics of this 'improved' operating state. The thrust-advance diagram and exponential curve fit of this set of measurements, as shown in Figure 5.8-3, is therefore presumed to characterize the boring process better than the earlier set of measurements 1-7.

The maximum advance rate measured during 'single pass' boring was 1.34 mm/rotation which is equal to 65 cm/h at a thrust of 746 kN and rotation speed of 8 rpm.

The actual thrust applied to the pilot bit and the division of thrust between the cutter head and the pilot bit can be calculated if the characteristic advance and thrust behaviour of both is known and the assumption made that the additional flow of crushed rock from the pilot bit does not affect the vacuum flushing characteristics of the large cutter head.

The mass flow during boring is divided between the pilot hole and large hole in the proportion 1:24 (4 % of flow through the pilot hole). The estimated flow of air is correspondingly divided in the proportion 1:5 (16 % of flow through pilot hole). Because of the relatively low flow ratio in the vacuum suction line and the small size of the mass flow from the pilot bit it is evident that it is possible to estimate the division of thrust with reasonable accuracy.

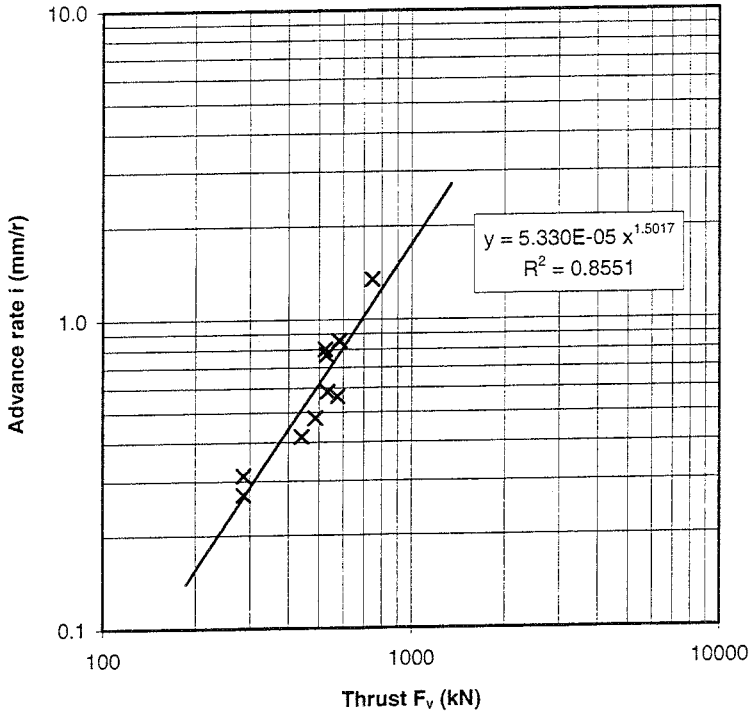

Figure 5.8-1. *All the measured advance rates plotted against thrust at a rotation speed of 8 rpm for 'single pass' boring, 5 & 6 row cutters and the pilot bit. The exponential curve fit is also shown.*

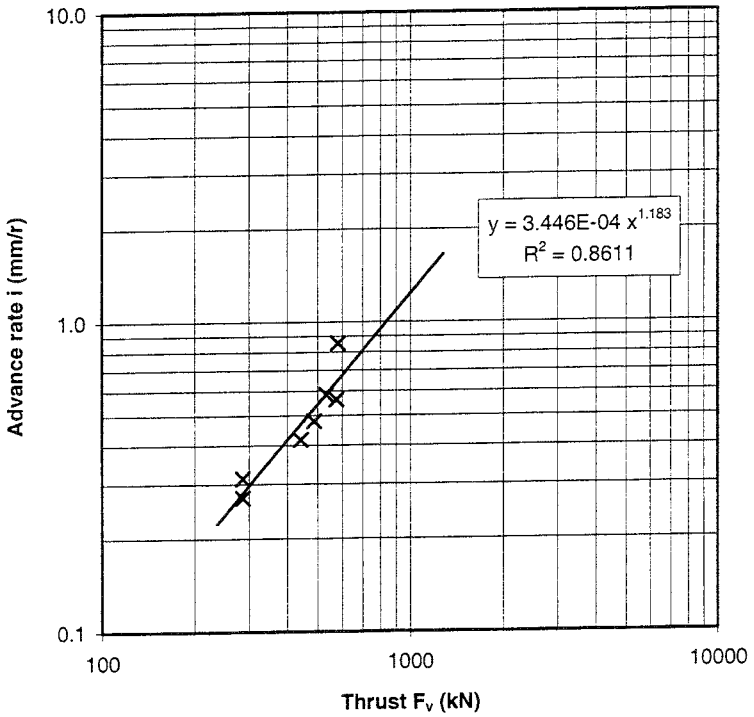

Figure 5.8-2. *The measured advance rates 1 - 7 plotted against thrust at a rotation speed of 8 rpm for 'single pass' boring, 5 & 6 row cutters and the pilot bit. The exponential curve fit is also shown.*

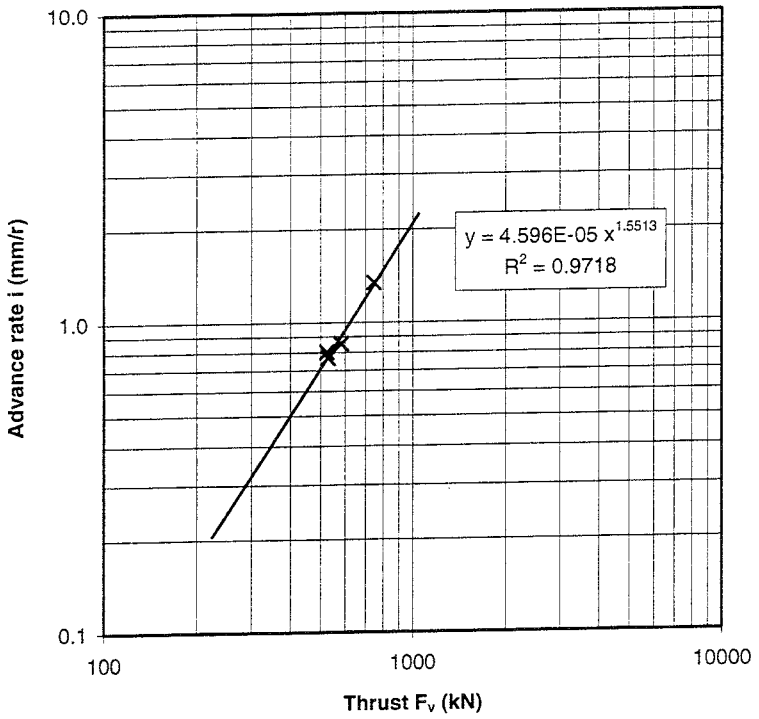

Figure 5.8-3. *The measured advance rates 8 - 11 plotted against thrust at a rotation speed of 8 rpm for 'single pass' boring, 5 & 6 row cutters and the pilot bit. The exponential curve fit is also shown.*

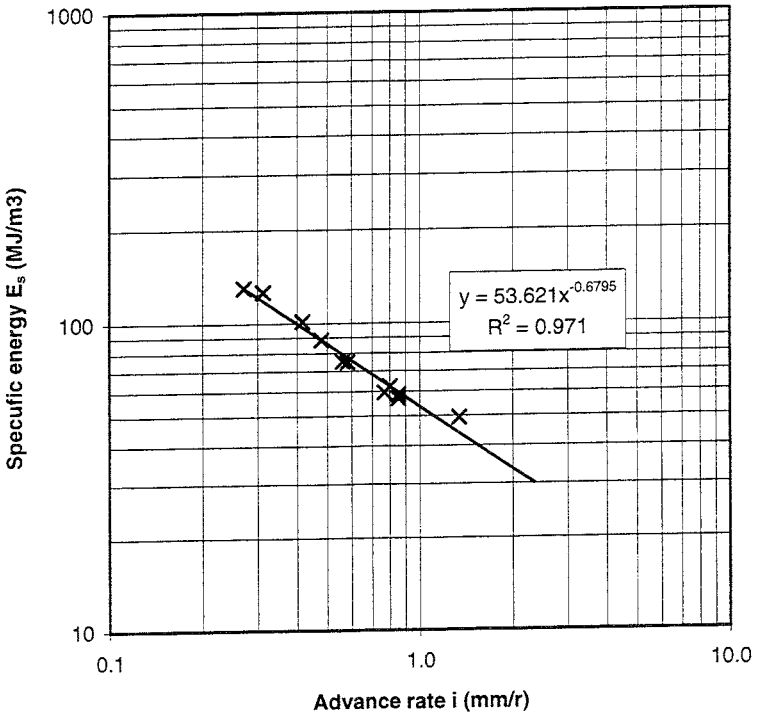

Figure 5.8-4. *Specific energy plotted against advance rate at a rotation speed of 8 rpm for 'single pass' boring, 5 & 6 row cutters and the pilot bit. The exponential curve fit is also shown.*

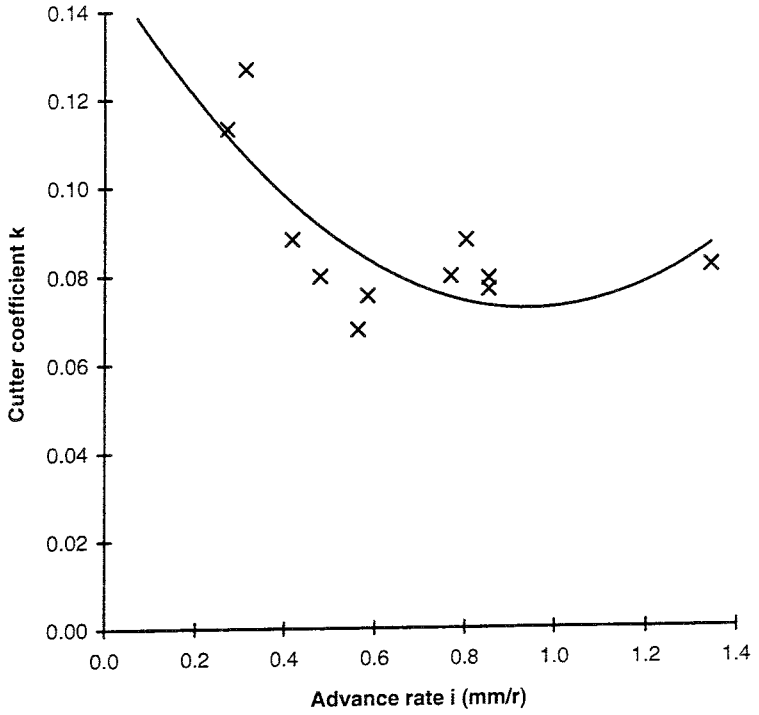

Figure 5.8-5. *Cutter coefficient plotted against advance rate at a rotation speed of 8 rpm for 'single pass' boring, 5 & 6 row cutters and the pilot bit.*

The advance rate compared to thrust was measured for the pilot bit in Test 2.2, see Figure 5.8-6. The effect of rotation speed on the rate of advance was measured for a thrust of about 131.5 kN in Test 2.1, see Figure 5.8-7.

From the linear curve least squares fit which describes the relationship between advance rate and rotation speed in Test 2.1 it can be estimated that a change in rotation speed of 1 rpm changes the advance rate by about 1.2 %. The advance rate of the pilot bit at low thrust levels is therefore not very sensitive to changes in rotation speed and the equation established in Test 2.2 can be used to estimate the thrust which should be applied to the pilot bit to achieve the penetration rate measured during the 'single pass' boring test.

The thrust on the pilot bit in normal pilot boring (Figure 5.8-6) which corresponds to the advance rate of 1.34 mm/rev achieved during 'single pass' boring at 8 rpm is 119 kN. The total thrust during 'single pass' boring at an advance rate of 1.34 mm/rev was 746 kN. If 119 kN was taken by the pilot bit then some 616 kN should have been acting on the large cutter head. According to the relationship established in Section 5.2 the minimum thrust which must be applied to the large cutter head to produce an advance rate of 1.34 mm/rev at 8 rpm is about 476 kN. The maximum thrust force which could have been acting on the pilot bit would therefore be some 259 kN, which is 140 kN more than the value predicted by the characteristic thrust-advance curve for pilot boring only.

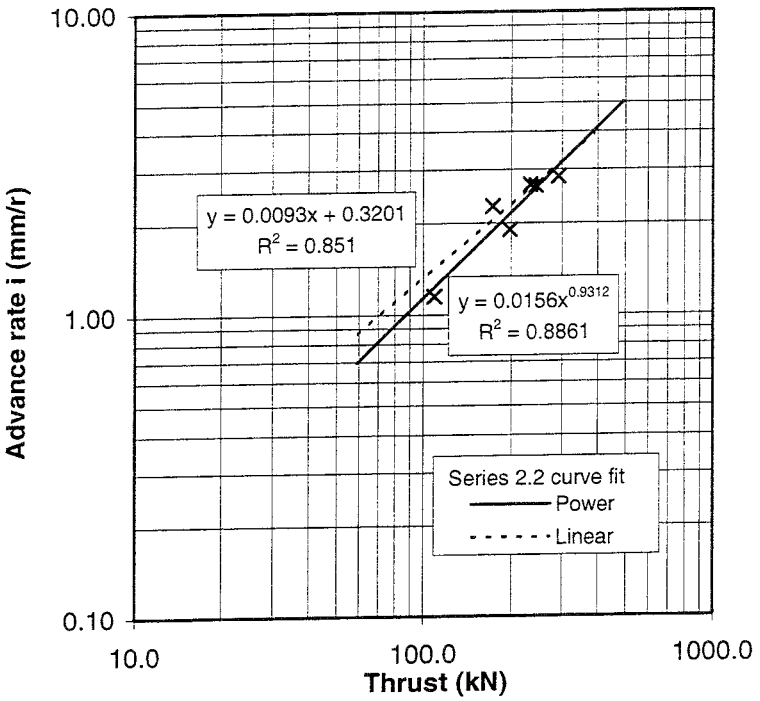

Figure 5.8-6. Advance rate plotted against thrust for the pilot bit in Test 2.2. Rotation speed 7.8 rpm, vacuum pressure 628 - 655 mbar.

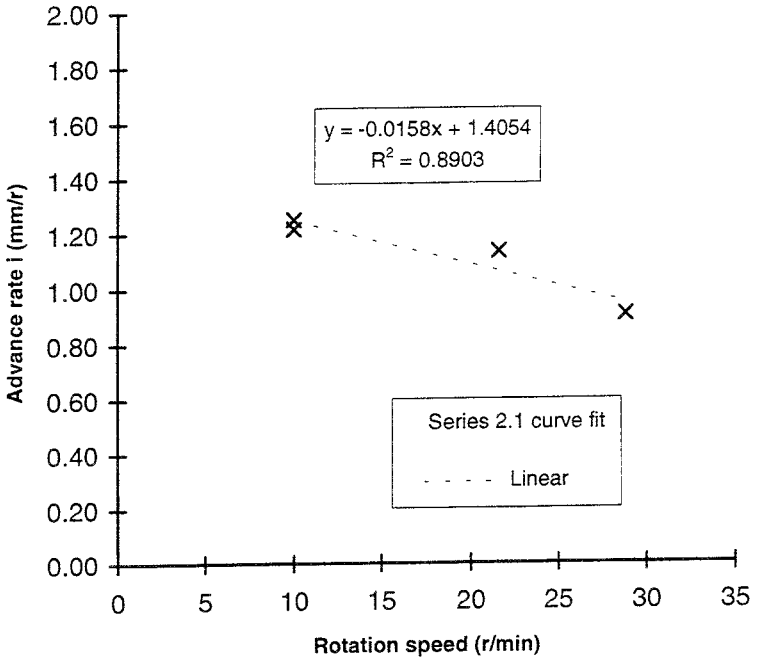

Figure 5.8-7. The effect of rotation speed on advance rate for a thrust of about 131.5 kN in Test 2.1, pilot bit.

According to other test results the estimated 16 % reduction in the airflow through the nozzles of the large cutter head does not have a significant effect on efficiency. The difference in the behaviour of the pilot bit when boring with the combined cutter head is therefore assumed to result from the reduced effectiveness of the vacuum flushing of crushed rock from the bottom of the pilot hole when this is compared to boring of the pilot hole alone. The estimated level of thrust applied to the pilot bit during the 'single pass' boring test was therefore about 259 kN, some 35 % of the total thrust.

The penetration rate of 4 mm/rev during boring of pilot hole, equivalent to 1.9 m/h, was reached at 8 rpm at a thrust of 400 kN on the pilot bit, see Figure 5.8 6, this is also the practical upper limit for use of the pilot bit. The corresponding value of thrust for the large cutter head is about 1200 kN and the total thrust needed to achieve such an advance rate with the combined cutter head used in the test is therefore 1600 kN, assuming that the vacuum flushing functions effectively. Using the value obtained from the test shown in Figure 5.8-3 in the regression Equation 5-7 would give a result of 1450 kN, which implies that at higher levels of thrust, the regression equation based on the 'single pass' boring test gives an advance rate which is too large in relation to thrust.

The limit for total thrust on the large cutter head is above 2000 kN but the maximum allowable thrust which can in theory be utilized with the combined cutter head is therefore limited by the capacity of the pilot bit to a total of 1600 kN which gives a maximum penetration rate of 1.9 m/h.

$$i = 0.0001\ F_v^{1.55} \qquad 5\text{-}7$$

where, i is the penetration rate of the combined cutter head
F_v is the total thrust force of the combined cutter head.

5.9 DISCUSSION OF RESULTS

The basic boring parameters established in this work are consistent with present day knowledge (NTH 1994, Hartman 1992, Lislerud 1994). The results obtained show that there is no significant difference between the performance of the two types of cutter configurations used, even though the measured data for the 4 and 5 row cutter configuration contains scatter, see Figure 5.9-1.

The thrust on the cutter head is quite often presented for comparative purposes as the thrust per button row. The total number of rows for the 5 and 6 row cutter configuration was 44, and for the 4 and 5 row cutters it was 36. The corresponding numbers of kerfs on the bottom of the hole were 30 and 24 respectively because some of the button rows followed the same path. The contact force on the different button rows depends on the number of successive rows which make the same kerf and can be estimated if the thrust-advance rate behaviour of the cutter is known. An exponential Equation 5-8, of same type as the Equation 5-3, was obtained with curve fitting from test results from the

same type of cutters as used in this work. This is shown in Figure 5.9-2. The value for penetration coefficient (b) obtained from the curve fit using least squares regression was 1.85.

$$i = 0.0075\ F_s^{1.85} = a\ F_s^{b} \qquad 5\text{-}8$$

where,
- b is the penetration coefficient for a single cutter
- a is a constant
- i is the advance rate (mm/rev)
- F_s is the thrust applied to a single row of buttons.

Equation 5-8 can be rewritten in a form which gives the thrust of single button row as a function of the advance rate per rotation:

$$F_s(i) = (i/a)^{1/b} \qquad 5\text{-}9$$

If there are n button rows in a series, the corresponding thrust is

$$F_s(i/n) = (i/na)^{1/b} = (1/n)^{1/b}\ (i/a)^{1/b} = (1/n)^{1/b}\ F_s(i) \qquad 5\text{-}10$$

where,
- b is the penetration coefficient for a single cutter
- a is a constant
- i is the advance rate of the cutter (mm/rev)
- n number of button rows in series
- $F_s(i)$ is the thrust applied to a single row of buttons.

Equation 5-10 can be rewritten in form which gives the thrust applied to button rows which are followed by one and three rows of buttons:

$$F_{2s}(i) = (i/2)^{1/b}\ Fs(i) \qquad 5\text{-}11$$

$$F_{4s}(i) = (i/4)^{1/b}\ Fs(i) \qquad 5\text{-}12$$

where,
- b is the penetration coefficient for a single cutter,
- $F_{2s}(i)$ is the thrust applied to one button row of two successive rows (kN)
- $F_{4s}(i)$ is the thrust applied to one button row of four successive rows (kN)
- i is the advance rate of the cutter head (mm/rev)
- $F_s(i)$ is the thrust applied to a single row of buttons.

When Equations 5-11 and 5-12 are applied to every button row in the cutter head, the following Equations 5-13 and 5-14 are obtained. These give the relationship between advance rate, total thrust and thrust per button row for the 5 and 6 row cutter configuration and the 4 and 5 row cutter configuration accordingly,

$$F_t(i) = 18F_s(i)+22\,(1/2)^{1/b}F_s(i)+4(1/4)^{1/b}F_s(i)$$
$$= F_s(i)(18+22\,(1/2)^{1/b}+4\,(1/4)^{1/b}) \qquad 5\text{-}13$$

$$F_t(i) = 14F_s(i)+18\,(1/2)^{1/b}F_s(i)+4(1/4)^{1/b}F_s(i)$$
$$= F_s(i)(14+18\,(1/2)^{1/b}+4\,(1/4)^{1/b}) \qquad 5\text{-}14$$

where,
- b is the penetration coefficient for a single cutter
- $F_t(i)$ is the total thrust applied to the cutter head (kN)
- i is the advance rate of the cutter head (mm/rev)
- $F_s(i)$ is the thrust applied to a single row of buttons.

The results presented in Table 5.9-1 show that the thrust per single button row with the 5 and 6 row configuration is the total force divided by 35. This equals 2.86 %. The value for a button row which is followed by another was 69 % of the force per single row and the value for a button row followed by three rows is 47 % of the force per single row.

Table 5.9-1. The division of thrust between different types of button rows.

Cutter set up, penetration coefficient 1.85	Force per single row button row F_s, as procentage of the total thrust force	Force per button row F_{2s} which is followed by another row, as procentage of the force per single row F_s	Force per button row F_{4s} which is followed by three rows, as procentage of the force per single row F_s
4&5 row cutters	3.54%	69%	47%
5&6 row cutters	2.86%	69%	47%

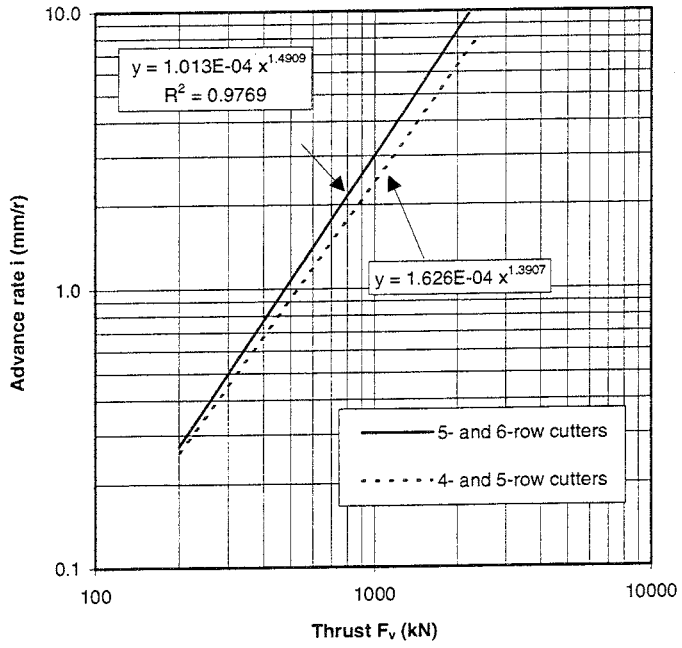

Figure 5.9-1. Advance rate plotted against thrust for both type of cutters at a rotation speed of about 8 rpm.

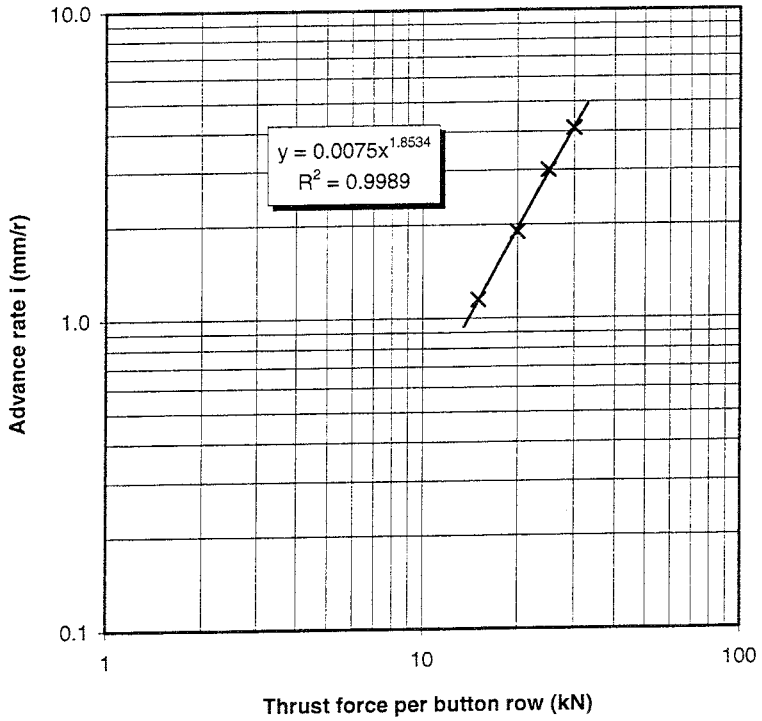

Figure 5.9-2. *Estimated advance rate plotted against thrust expressed as thrust per button row for the same type of cutters as the 5 & 6 row cutters used in this study.*

For example, if the total thrust applied to the cutter head is 600 kN, then the thrust on a single button row is 17 kN, the thrust on one row followed by another row is 12 kN, and the thrust applied to one row followed by three other rows is 8 kN.

In the reverse manner the results presented for the force per single button row can be transformed to present the results for the complete cutter head.

The thrust-advance rate diagrams for different types of rock for both complete cutter head configurations used were calculated using Equations 5-13 and 5-14 on the basis of the thrust-advance behaviour of single cutters. These diagrams, together with the results from the boring in the Research Tunnel are shown in Figures 5.9-3 and 5.9-4. Soft rock is defined as rock with unconfined compressive strength equal to or lower than 100 MPa. The corresponding value for medium rock is 140 MPa and for hard rock 250 MPa.

The thrust-advance behaviour observed in this boring experiment lies between the curves for soft and medium rock which is consistent with the fact that the compressive strength of the rock in the Research Tunnel is 75 - 112 MPa.

The relationship between advance rate and thrust at different rock strengths was also calculated after Hartman 1992 in a similar manner, as shown in Figures 5.9-5 and 5.9-6.

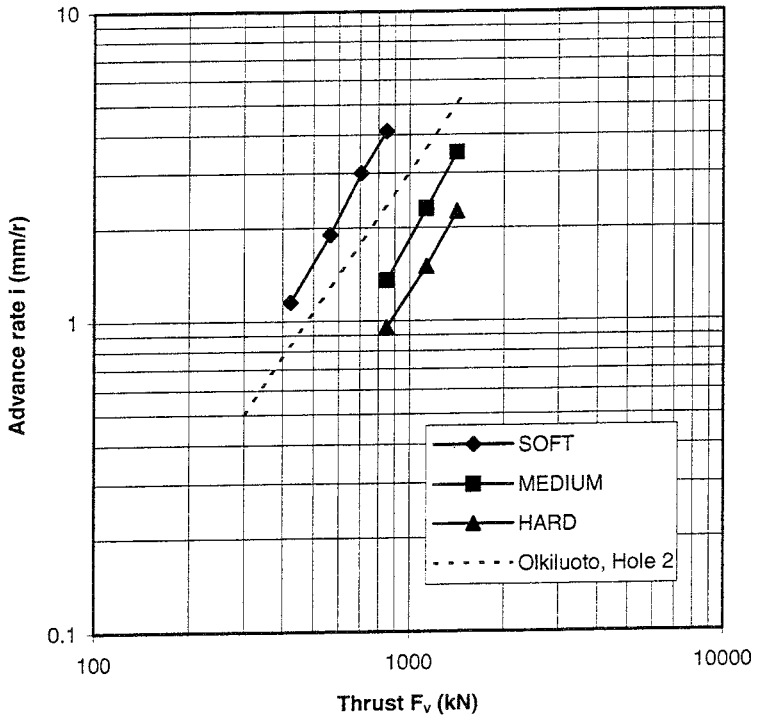

***Figure 5.9-3**. Measured advance rates plotted against total thrust applied to the cutter head for 5 & 6 row cutters (large hole 2).*

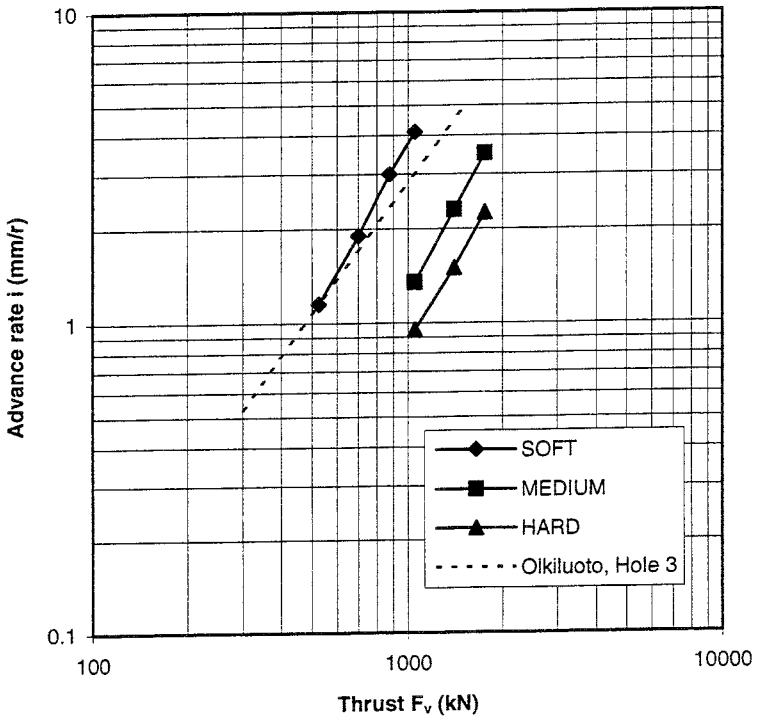

***Figure 5.9-4**. Measured advance rates plotted against total thrust applied to the cutter head for 4 & 5 row cutters (large hole 3).*

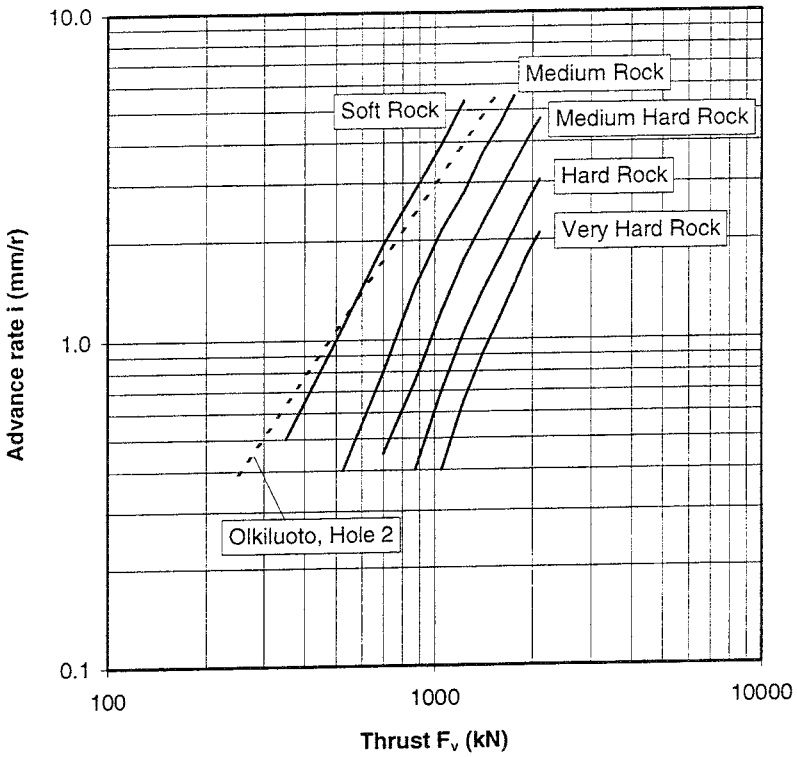

***Figure 5.9-5**. Measured advance rates plotted against total thrust applied to the cutter head for 5 & 6 row cutters (large hole 2) calculated from Hartman 1992.*

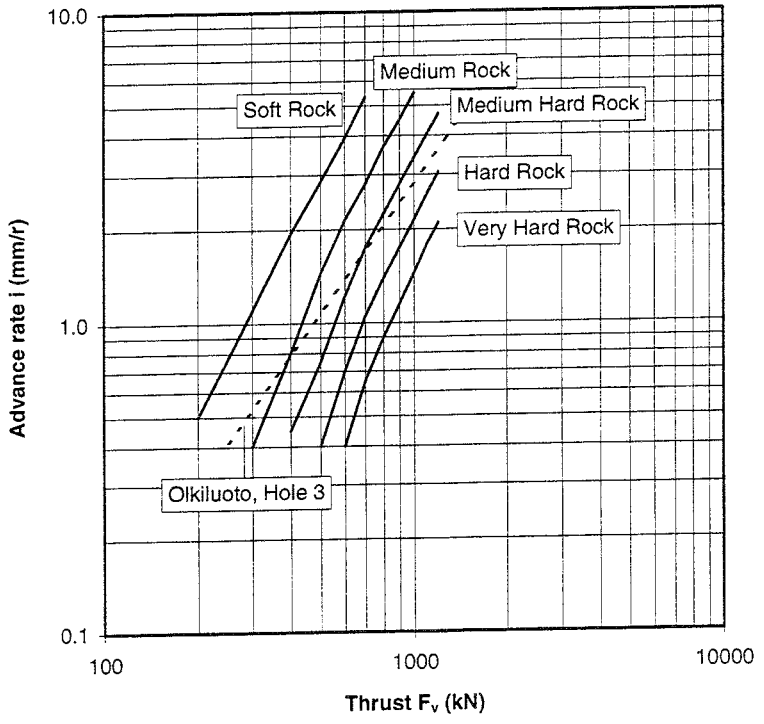

***Figure 5.9-6**. Measured advance rates plotted against total thrust applied to the cutter head for 4 & 5 row cutters (large hole 3) calculated from Hartman 1992.*

6 PARTICLE SIZE DISTRIBUTION OF CRUSHED ROCK

6.1 GENERAL

Samples were taken during boring to establish the effect of different levels of thrust and different rotation speeds on the quality of the crushed rock.

The boring of the large holes is based on rotary crushing of rock, the specific energy of which is used for:

- crack formation in solid rock
- crack formation which loosens chips
- crushing of the rock to powder
- crushing and regrinding of the loosened rock particles.

The degree of grinding and chipping is affected by the average brittleness value S_{20} and the Sievers' SJ value which are also used to determine the drillability value DRI. The corresponding values for the main rock type, anisotropic tonalite, were 55 for the average DRI-value, 51.5 for the average brittleness value S_{20}, and 32.4 for the Sievers' SJ value. Rocks with low surface hardness (which are characterised by having SJ-values as high as the anisotropic tonalite), are observed to result in a lot of crushed rock powder in the cutter grooves (NTH 1994). In rock with low brittleness values the chips have a tendency to be thicker (NTH 1994), see Figure 6.1-1. The above-mentioned observations are relevant for cutting with roller buttons even though they are based on observations made using disc cutting.

If no significant regrinding of rock is taking place it is estimated that about 90 % of the specific energy is used for crushing the rock and 10 % is used for creating cracks (NTH 1994).

Regrinding of the loosened rock particles takes place if material is not removed by the flushing. The energy used for this regrinding results in a low total efficiency for the boring system. The particle size distribution and shape of particles is therefore dependent on the type of rock and machine factors such as the flushing technique and cutter positioning. The major difference in the particle size distribution and shape of the crushed rock produced by the boring equipment used in this work compared to the results achieved with normal raiseboring is caused by the method of removing rock by vacuum flushing.

The shape of the larger particles (chips) and the amount of fine-grained rock is a measure of the efficiency of the chipping mechanism. A particular design can be optimized for different types of rock.

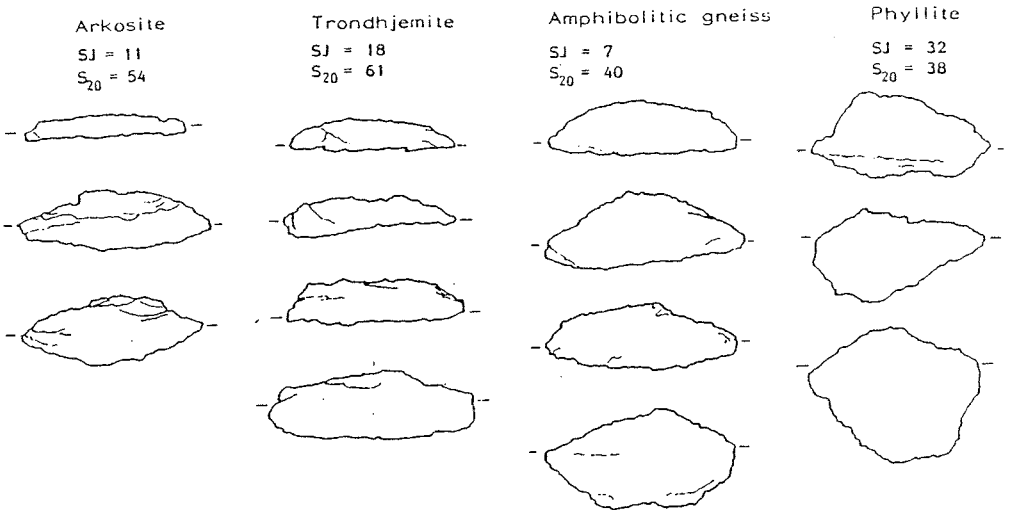

Figure 6.1-1. Typical chip shapes for different types of rock (NTH 1988).

Table 6.1-1. Samples taken and corresponding operating data for the boring machine.

Sample	Start depth (cm)	Stop depth (cm)	Rotation speed (rpm)	Thrust (kN)	Weigth of sample (kg)
2.3	520.7	522.4	7.4	736	79.7
2.4	522.4	523.5	7.2	596	64.3
2.5	523.4	524.6	7.7	486	60.8
2.6	524.6	526.3	10.0	700	71.4
2.7	526.3	527.8	4.1	736	76.6
2.8	527.8	529.6	7.7	731	82.2
3.3	98.2	99.4	8.0	718	62.1
3.4	225.0	226.0	8.0	474	52.4
3.5	226.0	227.1	7.9	721	47.4
3.6	363.5	364.6	7.4	477	49.1
3.7	364.6	365.9	7.9	722	61.3
3.8	657.0	658.1	5.9	734	51.9
3.9	658.1	659.2	7.5	730	56.4
3.10	659.2	660.4	11.7	734	59.0

The particle size and shape distribution of the crushed rock was determined (Lappalainen 1994). The work included:

- determination of particle size distribution by dry sieving
- determination of particle size by aerometer
- determination of shape factors
- photographing of fractions of the samples.

In this study, the total number of samples from the large holes was 14. Of these, 6 samples were from large hole 2 and 8 samples were taken from large hole 3. The samples were taken at different levels of thrust and different rotation speeds of the boring machine. A summary of the samples taken is shown in Table 6.1-1.

6.2 PREPARATORY TREATMENT OF THE SAMPLES

The samples were stored and transported to the laboratory in plastic containers. Preparatory treatment of the samples consisted of drying for 12 hours at 85 °C, homogenization and partitioning of the samples into smaller final samples.

The samples were weighed in the Research Tunnel and in the laboratory. The weight of the initial samples taken while boring large holes 2 and 3 was 47 - 82 kg. After preparatory treatment the weight of the final sample used for determinations was in the range 2.0 - 2.9 kg.

6.3 DETERMINATIONS

Dry sieving of the samples was carried out in accordance with current specification TIE201 (Lappalainen 1994).

The determination of the distribution of fine particles (particle size under 0.074 mm) by the aerometer method was carried out in accordance with current specification TIEL 732816 (Lappalainen 1994).

The shape factors of the samples were determined according to current specification TIE233 (Lappalainen 1994). Measurement of the dimensions of the particles was carried out using an electronic slide gauge connected to a computer. The shape factor was determined from particles whose size was larger than 8 mm. The number of particles measured was 100 per sample.

The thickness (a), length (c) and width (b) of each particle was measured and the flakiness (b/a) and elongation (c/a) was calculated.

6.4 RESULTS

6.4.1 Particle size distribution

On average the particle size of 56 - 64 weight-% of the crushed rock was less than 1 mm. Both types of cutters with maximum thrust and a rotation speed of about 8 rpm produced an average of about 60 weight-% of particles smaller than 1 mm in size. The average particle size, d_{50}, of the crushed rock was 0.4 - 0.6 mm, see Figures 6.4-1 and 6.4-2.

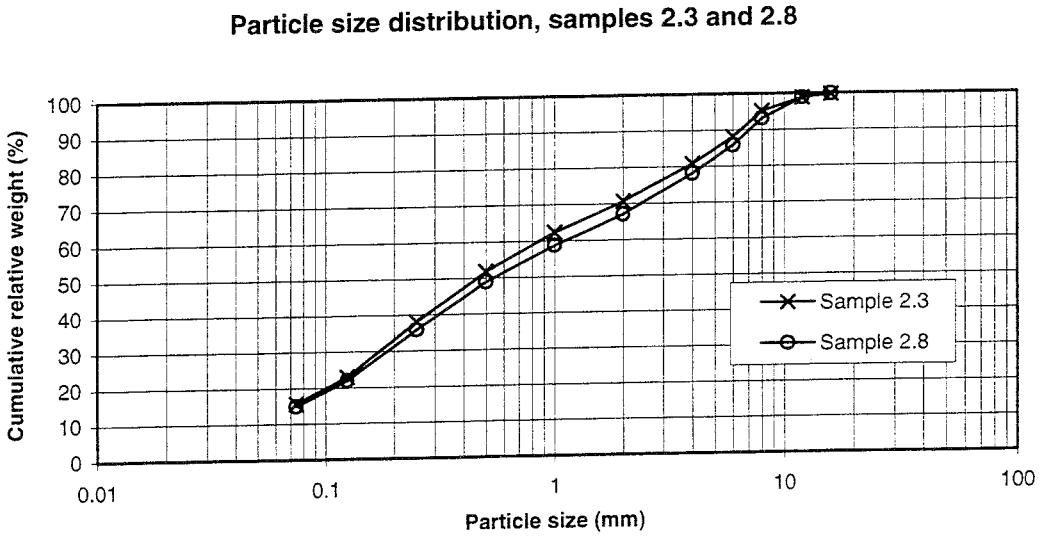

Figure 6.4-1. Particle size distribution for the Samples 2.3 and 2.8. 5 & 6 row cutters, rotation speed 8 rpm and maximum thrust of about 700 kN.

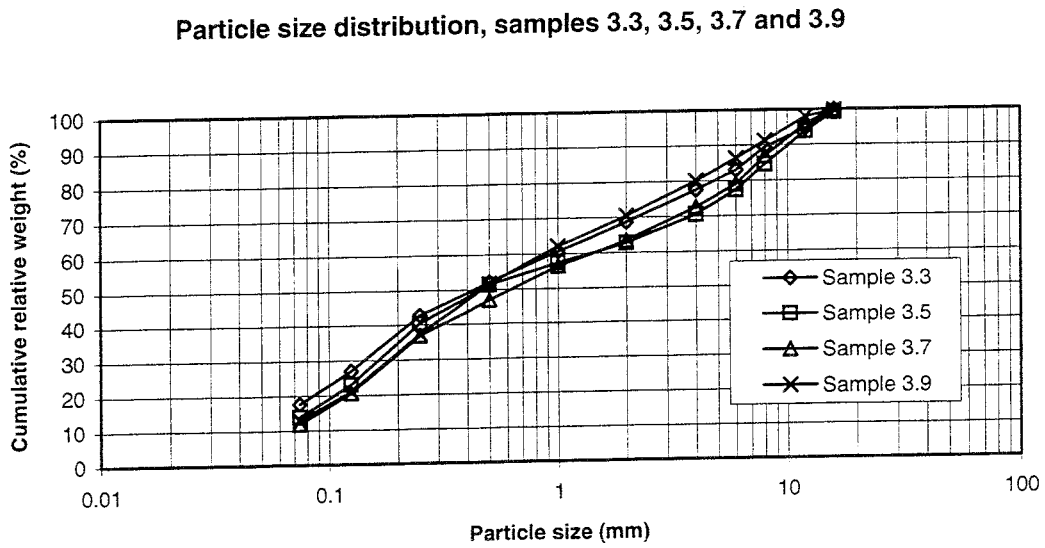

Figure 6.4-2. Particle size distribution for Samples 3.3, 3.5, 3.7 and 3.9, 4 & 5 row cutters, rotation speed 8 rpm and maximum thrust of about 700 kN.

The difference in particle size distribution resulting from the use of the two types of cutters is small and can be seen in particle sizes over 1 mm. With 5 and 6 row cutters the amount of particles of size 10 mm or smaller is 97 % of the total weight of the sample. The corresponding figure with 4 and 5 row cutters is 92 %, see Figure 6.4-3.

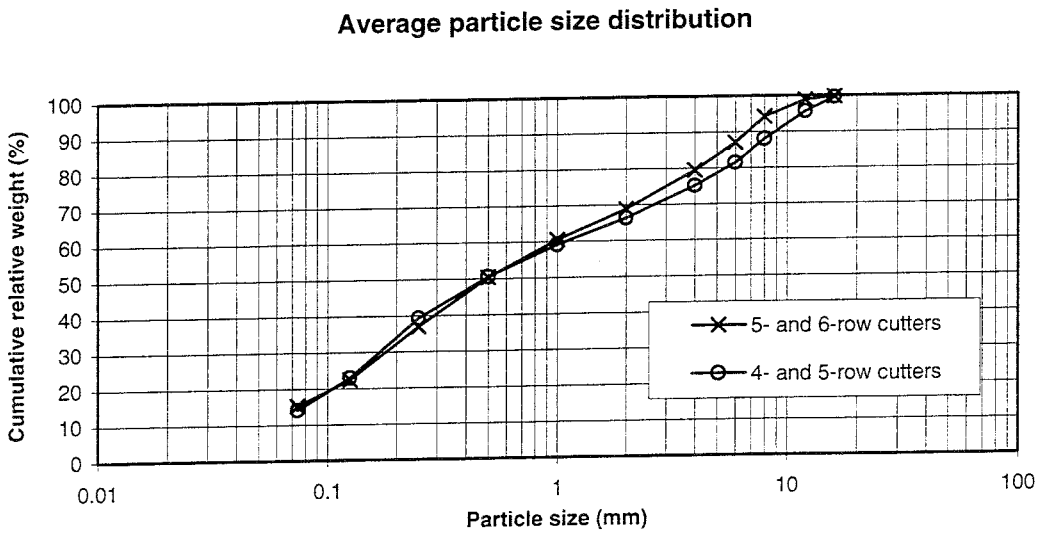

***Figure 6.4-3**. Particle size distribution for the samples. Averages of 4 & 5 row cutters and 5 & 6 row cutters, rotation speed 8 rpm and maximum thrust of about 700 kN.*

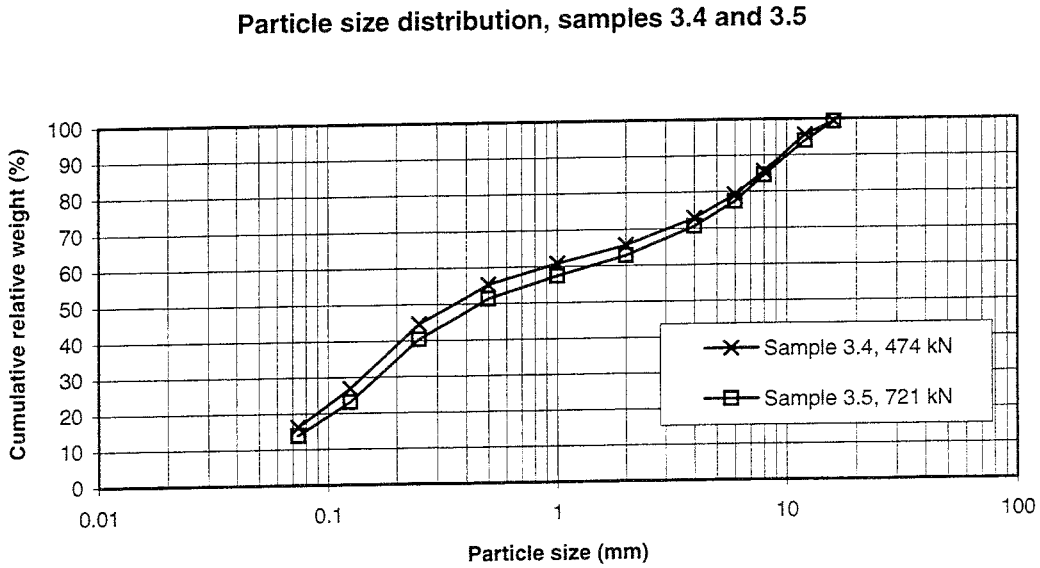

***Figure 6.4-4**. Particle size distribution for samples using different thrusts, 4 & 5 row cutters, rotation speed about 8 rpm and maximum thrust of 474 - 721 kN. Samples 3.4 and 3.5.*

The difference in particle size resulting from the use of different thrust levels is small, see Figure 6.4-4, 6.4-5 and 6.4-6. In general, the average particle size increases slightly as the thrust is raised. The difference is more evident with 5 and 6 row cutters. Although the amount of data is limited, the trend is clear.

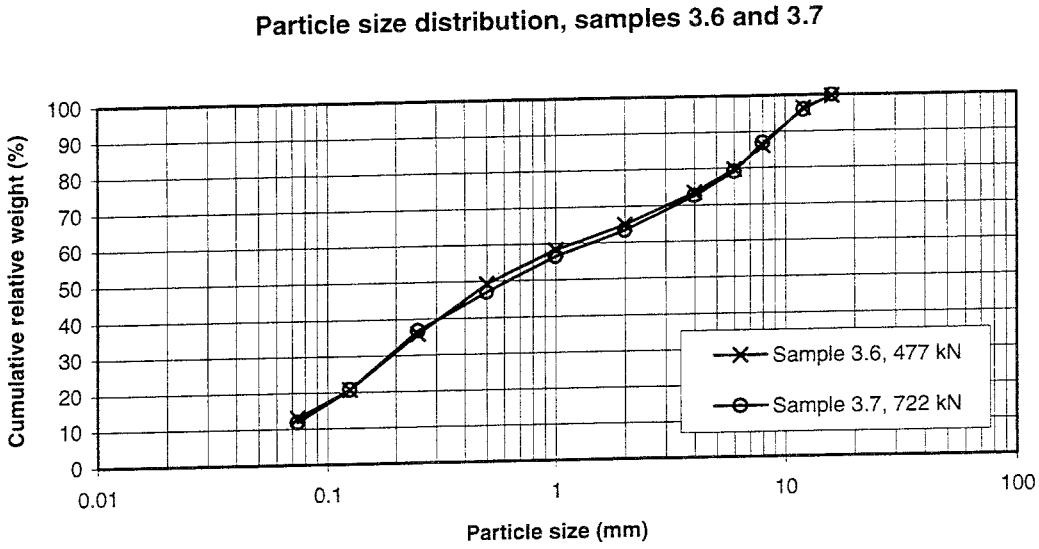

***Figure 6.4-5**. Particle size distribution for samples with different levels of thrust, 4 & 5 row cutters, rotation speed about 8 rpm and maximum thrust of 477 - 722 kN. Samples 3.6 and 3.7.*

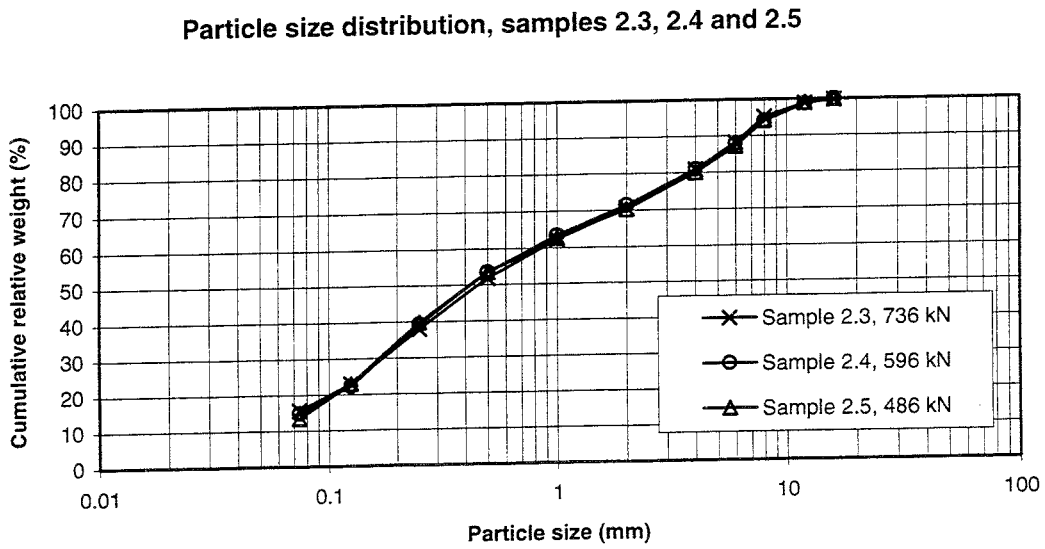

***Figure 6.4-6**. Particle size distribution for samples with different levels of thrust, 5 & 6 row cutters, rotation speed about 8 rpm and maximum thrust of 486 - 736 kN. See Figure 6.4-9 for the different particle size fractions in Sample 2.3.*

The difference in particle size resulting from different rotation speeds is presented in Figures 6.4-7 and 6.4-8. In general, particle size falls as rotation speed is lowered. The difference is evident with both types of cutters. It was observed during boring that the efficiency of vacuum cleaning decreased as the rotation speed was increased - an obvious result of more regrinding and smaller particle size. The result also implies that there are other factors which may affect particle size such as the technique used for sampling.

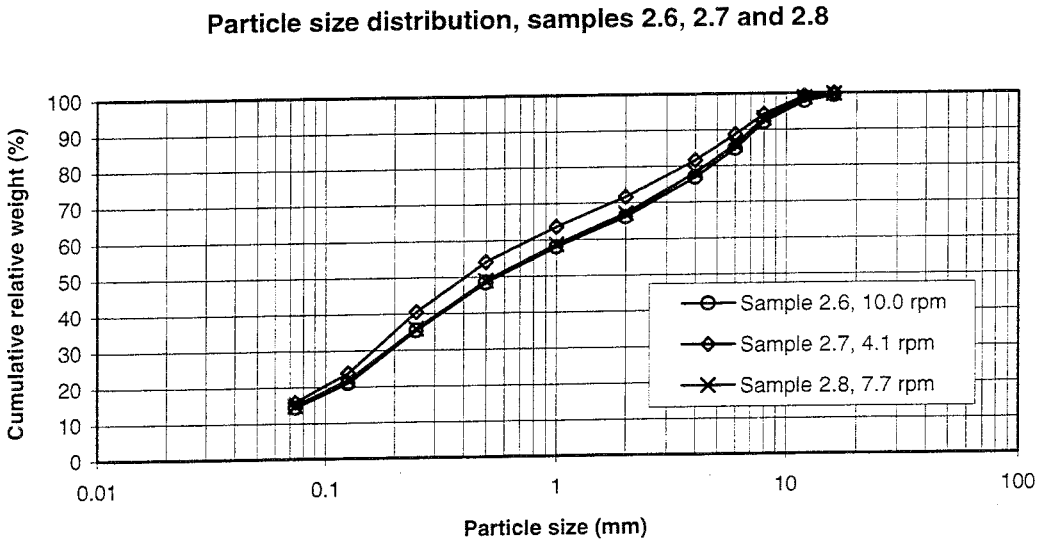

Figure 6.4-7. Particle size distribution for samples with different rotation speeds, 5 & 6 row cutters, rotation speed 4 - 10 rpm and thrust of about 730 kN.

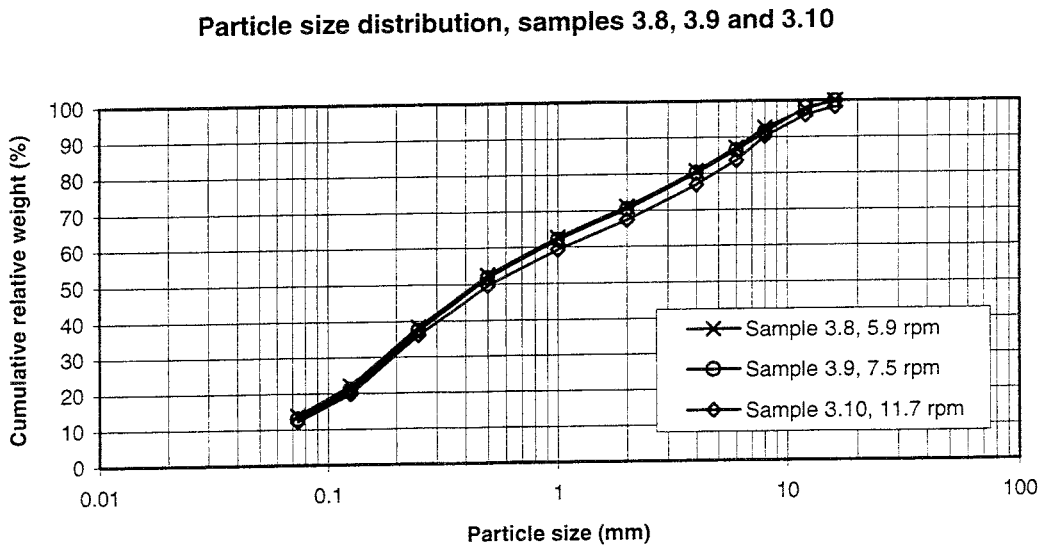

Figure 6.4-8. Particle size distribution for samples with different rotation speeds, 4 & 5 row cutters, rotation speed 6 - 12 rpm and thrust of about 730 kN.

The results of the determinations of particle size distribution show that the quantity of fine particles of size less than 1 mm in the crushed rock is large - about 60 weight-% - when compared to a reference curve for boring in granite, see Figure 6.4-10.

The large quantity of fine particles is indicative of some regrinding of crushed rock. The ideal particle size distribution for cutters used in the boring test is not known and the extent of regrinding cannot be determined precisely. The particle fraction diagram (Figure 6.4-11), shows that the difference is caused mainly by the larger number of smaller 0.063 - 0.125 mm fractions.

The quantity of larger particles is greater with 4 and 5 row cutters which could be expected when using cutters with larger spacing between the buttons.

Particle sizes were larger with larger levels of thrust which is also to be expected, since larger indentation forces cause the rock to break into larger fragments.

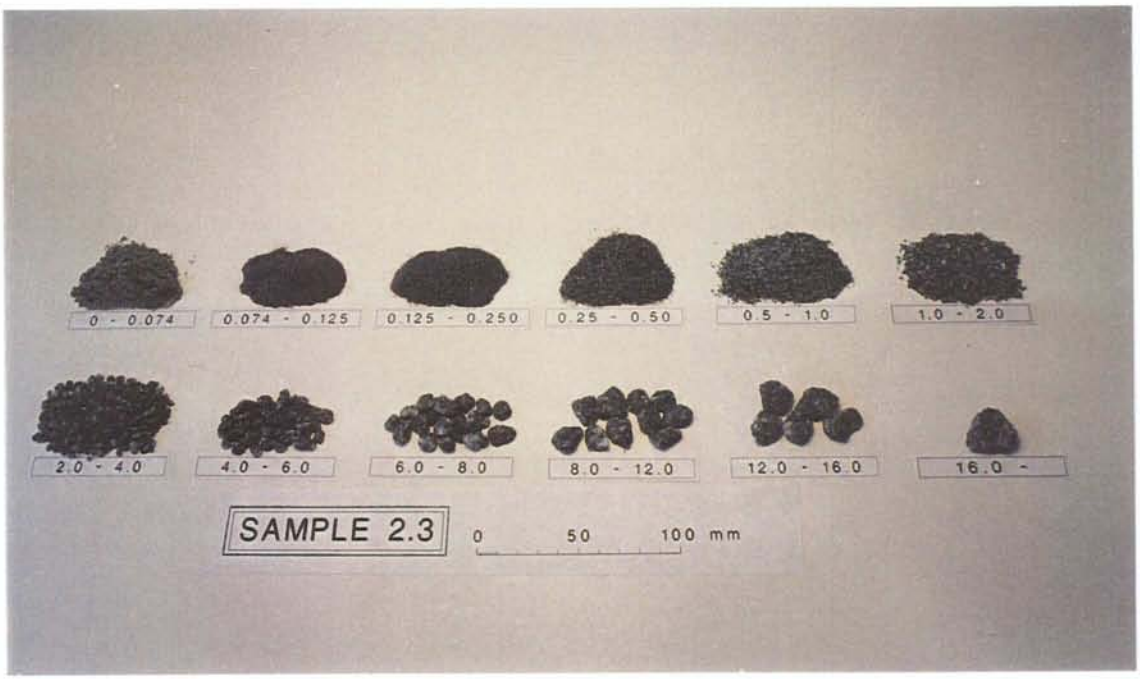

***Figure 6.4-9**. The different particle size fractions in a sample of crushed rock.*

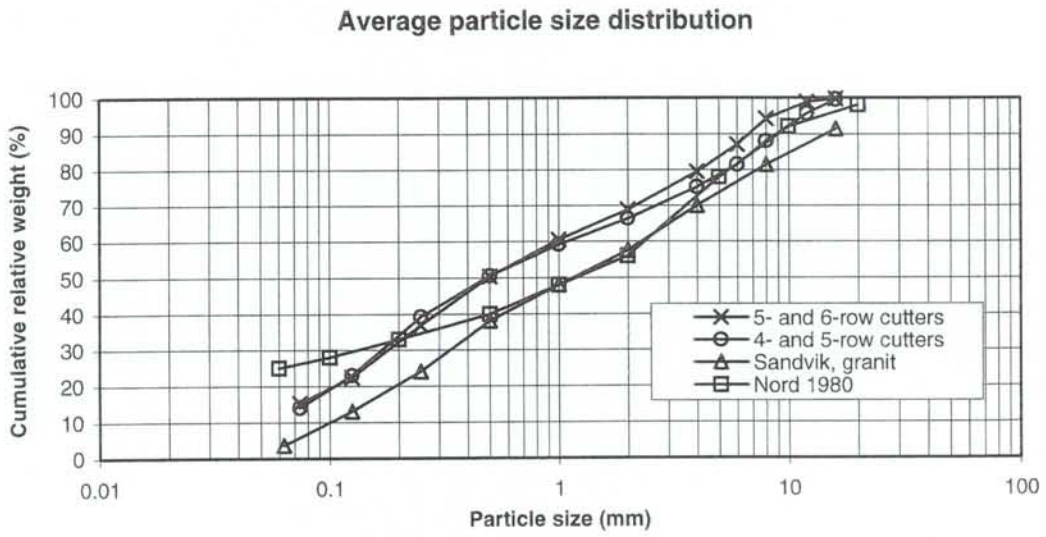

***Figure 6.4-10**. Particle size distribution for samples at maximum thrust and a rotation speed of 8 rpm for both types of cutter configurations and a reference result for granite (6 button rows, 2 cutters, row spacing 51 mm, thrust 200 kN, AB Sandvik Rocktools 1980).*

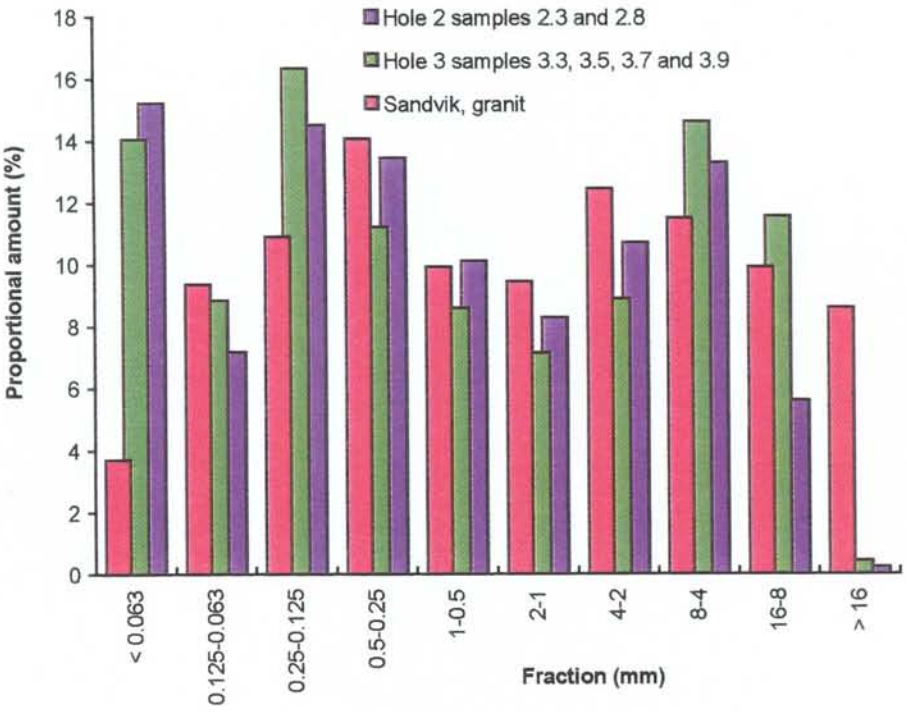

***Figure 6.4-11**. Particle fraction diagram showing the proportion of different fractions of crushed rock and a reference result for granite (6 button rows, 2 cutters, row spacing 51 mm, thrust 200 kN, AB Sandvik Rocktools 1980).*

6.4.2 Particle shape

The dimensions and shape factors were determined as the average values of one hundred rock chips taken from the largest particle fractions. The size (width, thickness and length) distribution of the chips in the different tests was quite irregular as shown for example by Samples 2.8 (5 and 6 row cutters) and 3.3 (4 and 5 row cutters) in Figures 6.4-12, 13 and 14.

The average thickness of the particles was 5.5 mm, the average length was 16.9 mm and the average width was 13.2 mm. With the 4 and 5 row cutters (row and kerf spacing 25.5 mm) the average particle length of 17.6 mm and width of 13.4 mm was slightly larger than with the 5 and 6 row cutters (row and kerf spacing 19.8 mm) where the corresponding dimensions were 16.1 mm and 12.8 mm. The difference in length is clearer in results where a constant rotation speed of 8 rpm was used, see Figure 6.4-16 and Table 6.4-1.

The thickness of the largest particles seems to be slightly reduced when the thrust is increased, as seen in Figure 6.4-15. This change is more evident when comparing the ratio of length and thickness (elongation), see Figure 6.4-17. The elongation of 4 and 5 row cutters seems to be higher than with 5 and 6 row cutters and this value rises as the thrust is increased.

Table 6.4-1. Average dimensions of the samples.

Sample	Average size			Average elongation	Average flakiness
	Thickness **a** (mm)	Width **b** (mm)	Length **c** (mm)	c/a	b/a
2.3	5.27	12.88	16.01	3.14	2.54
2.4	5.53	13.08	16.43	3.06	2.44
2.5	5.59	12.54	15.65	2.90	2.33
2.6	5.50	12.92	16.20	3.06	2.46
2.7	5.53	12.51	15.60	2.92	2.36
2.8	5.60	13.08	16.70	3.09	2.42
Average	5.50	12.84	16.10	3.03	2.43
3.3	5.41	13.00	17.63	3.37	2.50
3.4	5.71	13.30	17.70	3.18	2.41
3.5	5.43	13.05	18.16	3.44	2.49
3.6	5.35	13.27	16.51	3.15	2.54
3.7	5.56	13.82	18.44	3.41	2.58
3.8	5.81	13.84	17.69	3.11	2.45
3.9	5.59	13.54	17.52	3.21	2.50
3.10	5.30	13.32	16.93	3.27	2.58
Average	5.52	13.39	17.57	3.27	2.51
Tot.avg.	5.51	13.15	16.94	3.17	2.47

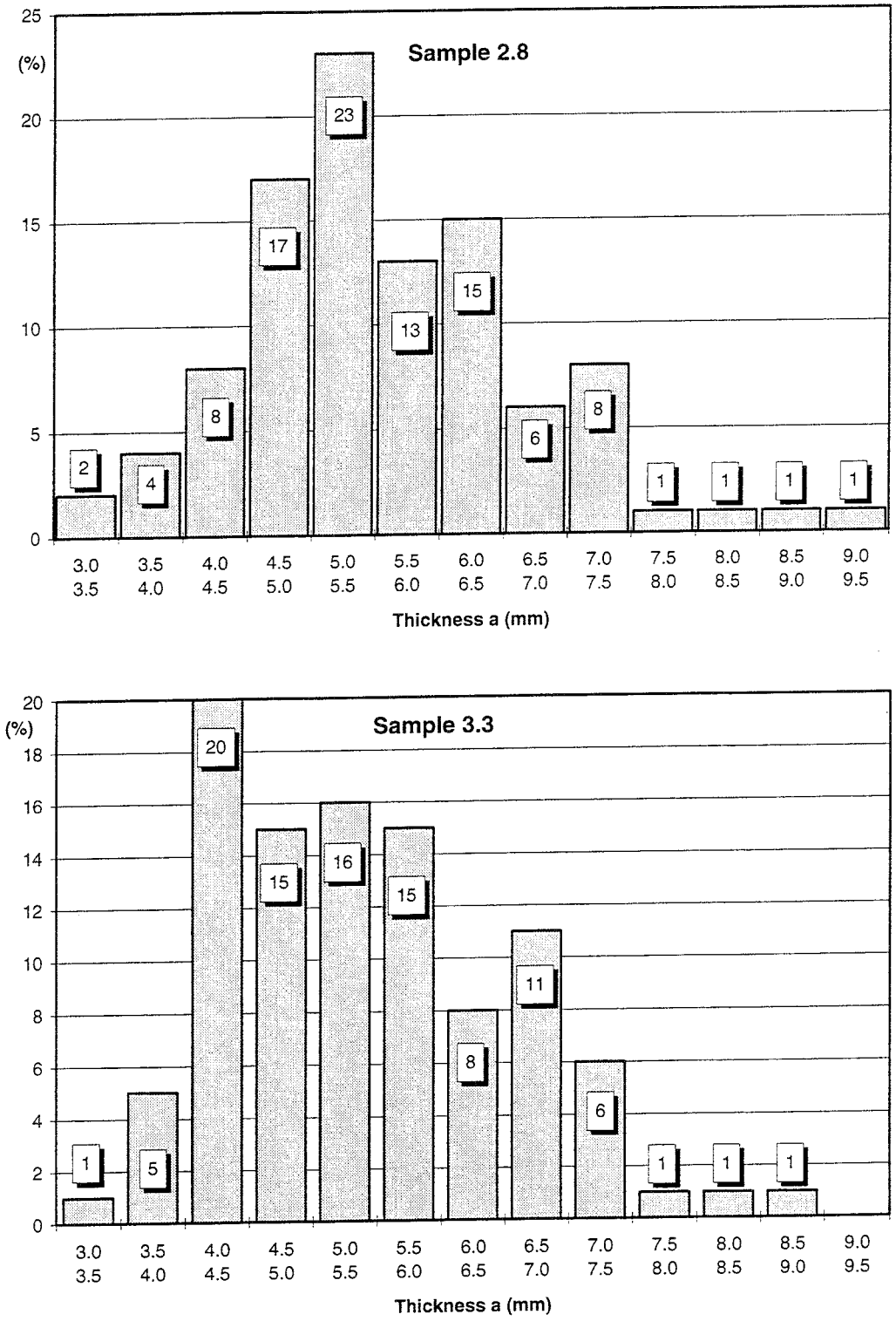

Figure 6.4-12. *Particle thickness frequency distribution curves for the fraction of 100 largest particles in samples 2.8 and 3.3.*

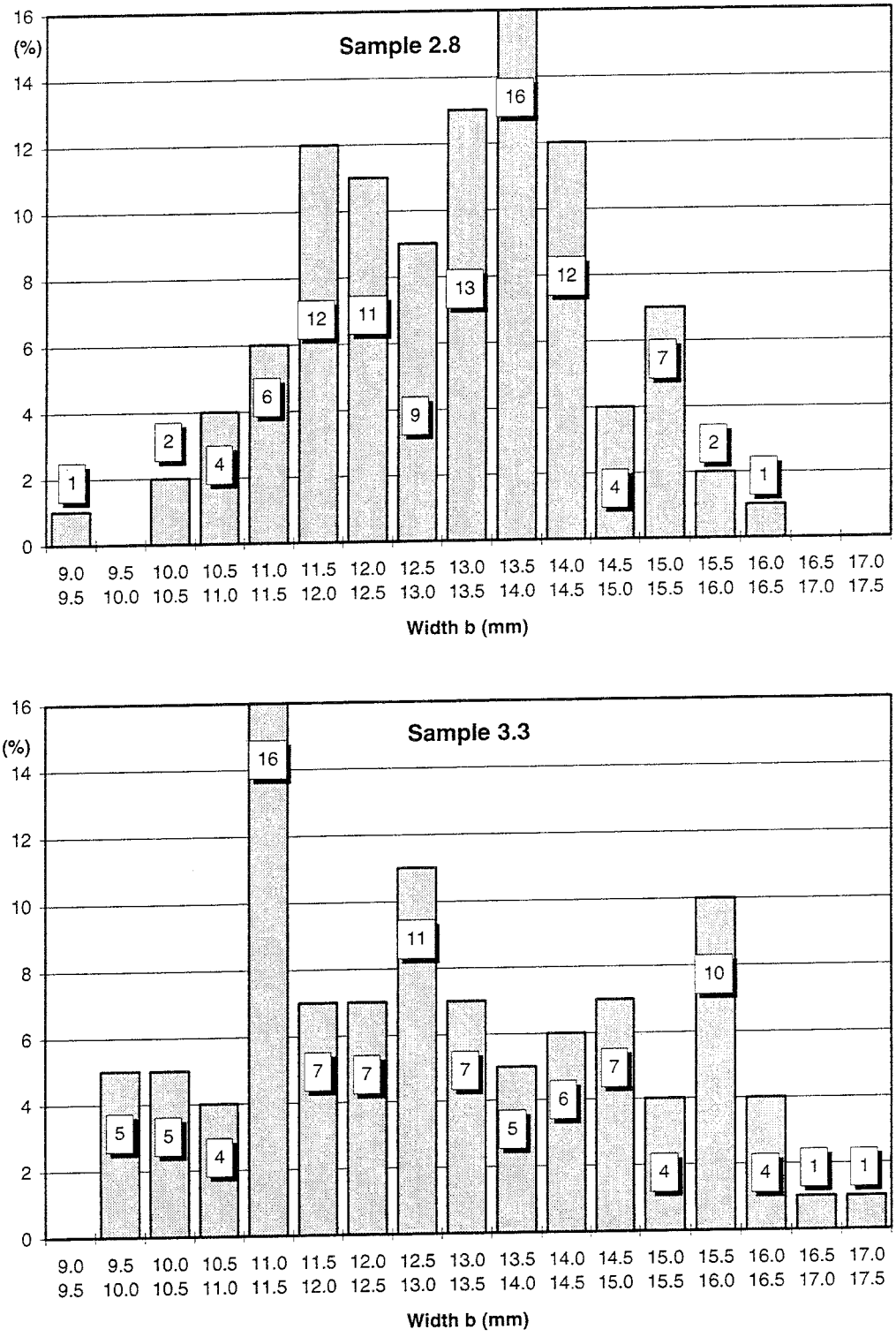

***Figure 6.4-13**. Particle width frequency distribution curves for the fraction containing the 100 largest particles in Samples 2.8 and 3.3.*

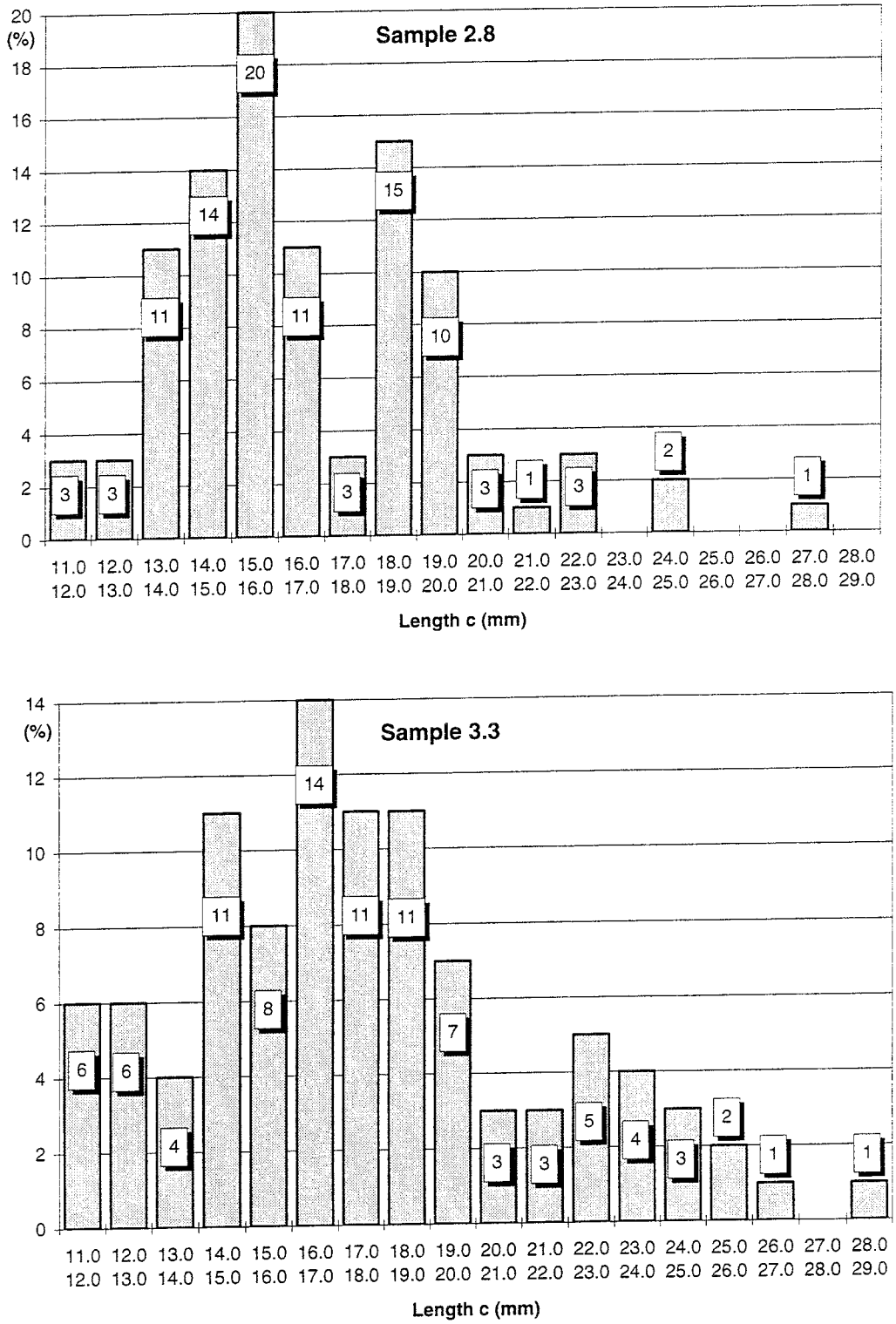

Figure 6.4-14. *Particle length frequency distribution curves for the fraction containing the 100 largest particles in Samples 2.8 and 3.3.*

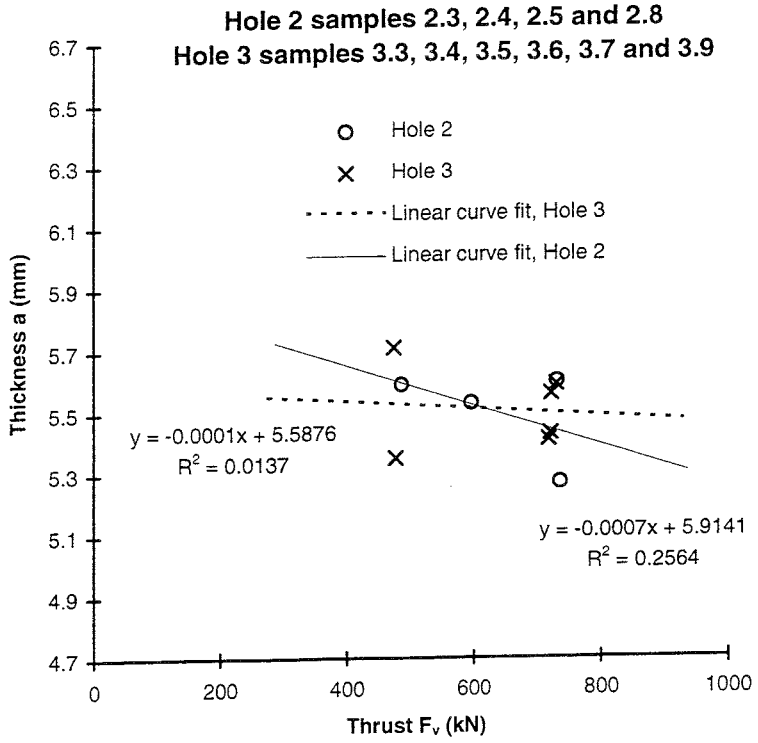

Figure 6.4-15. Thickness of the largest particles plotted against thrust at a rotation speed of 8 rpm.

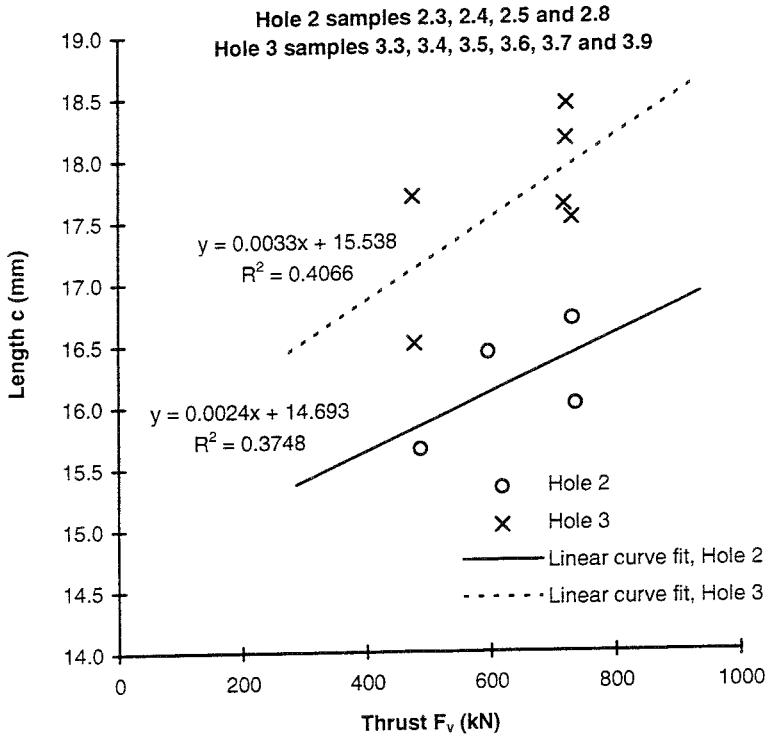

Figure 6.4-16. Length of the largest particles plotted against thrust at a rotation speed of 8 rpm.

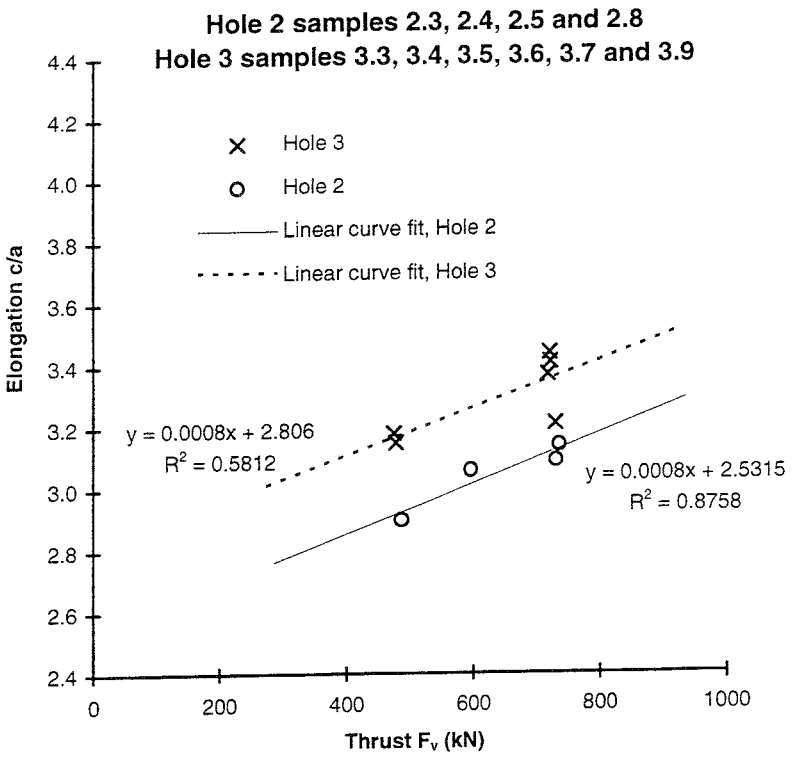

Figure 6.4-17. Elongation of the largest particles plotted against thrust at a rotation speed of 8 rpm.

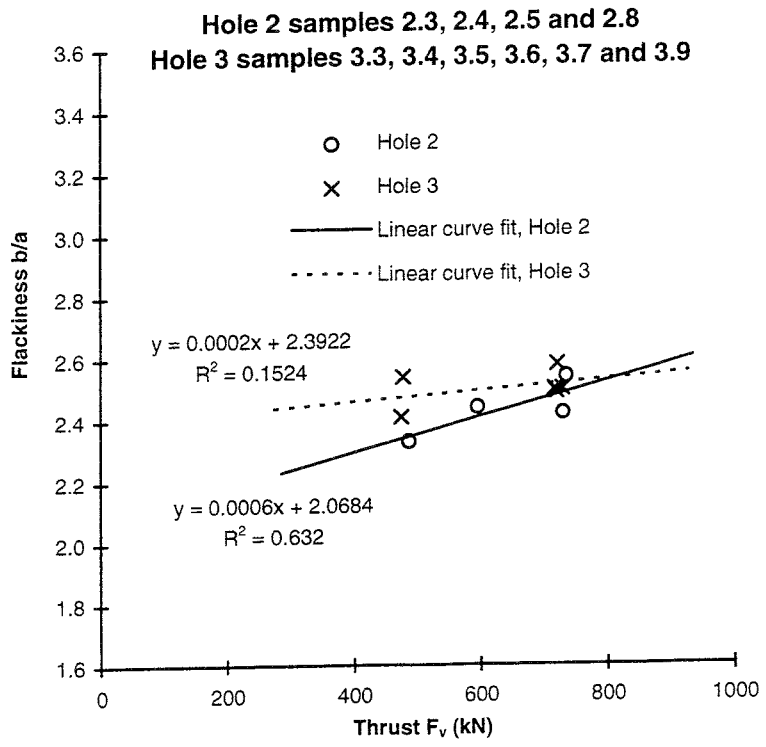

Figure 6.4-18. Flakiness of the largest particles plotted against thrust.

The flakiness of the largest particles (Figure 6.4-18) seems to increase slightly when the thrust is raised. In general, it can be stated that as the thrust is increased the largest particles grow wider, longer and slightly thinner (Figure 6.4-16).

An increase in rotation speed seems to have an effect on the size of the largest particles. Surprisingly, the change seems to be different for the two types of cutters.

When using the 5 and 6 row cutters (large hole 2), the width and length of particles increased while thickness remained unchanged as rotation speed was increased, see Figures 6.4-19, 6.4-20 and 6.4-21.

When using the 4 and 5 row cutters (large hole 3), the width, length and thickness of particles became smaller as rotation speed was increased, see Figures 6.4-19, 6.4-20 and 6.4-21.

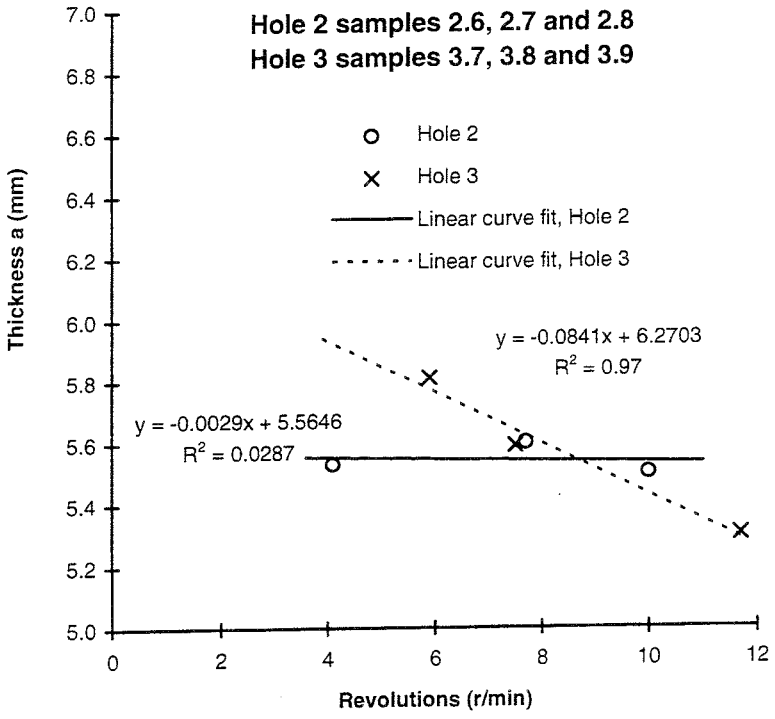

Figure 6.4-19. *Thickness of the largest particles plotted against rotation speed of the cutter head.*

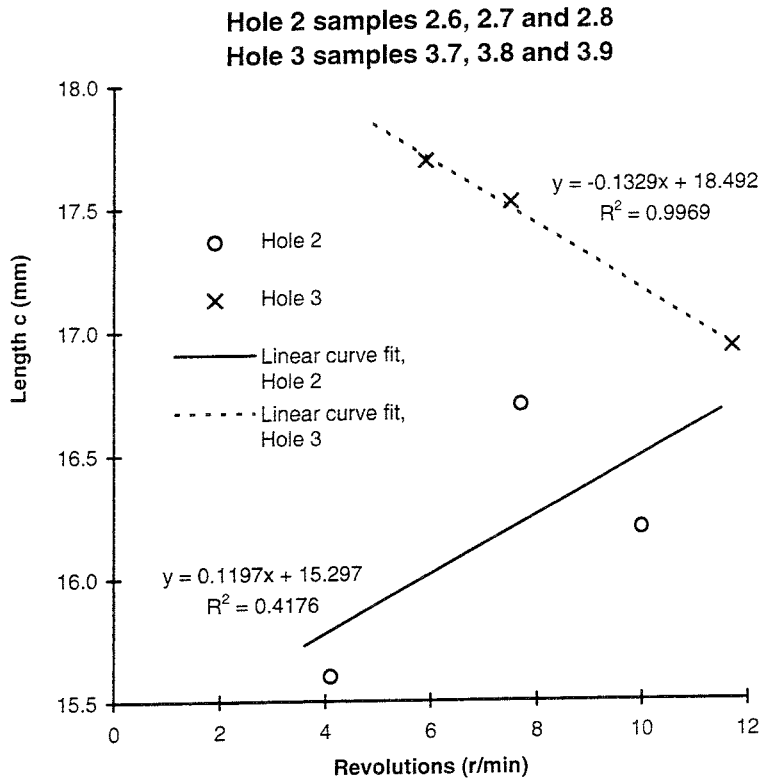

Figure 6.4-20. Length of the largest particles plotted against rotation speed of the cutter head.

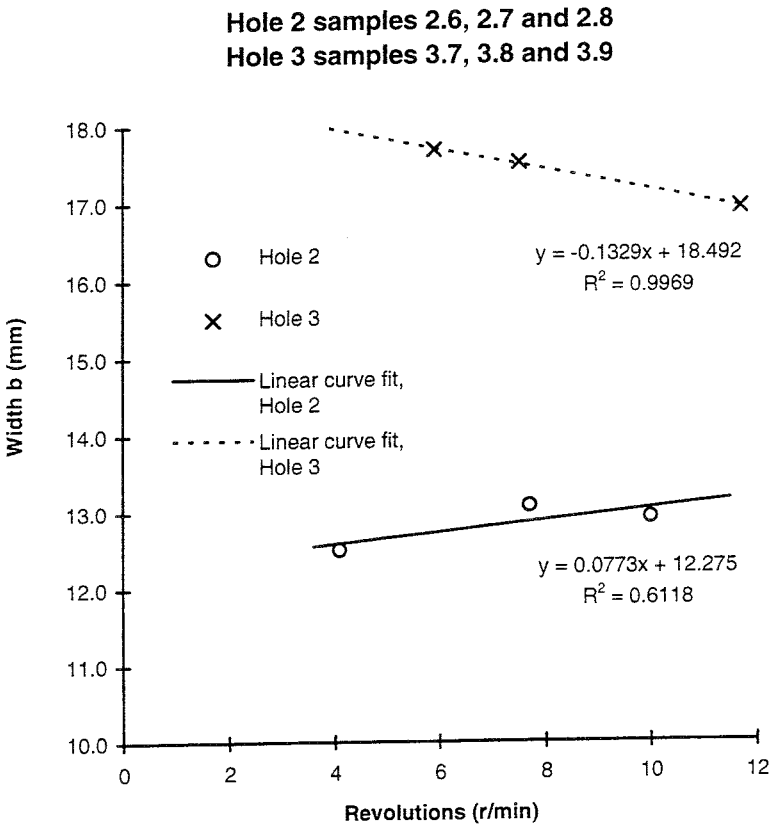

Figure 6.4-21. Width of the largest particles plotted against rotation speed of the cutter head.

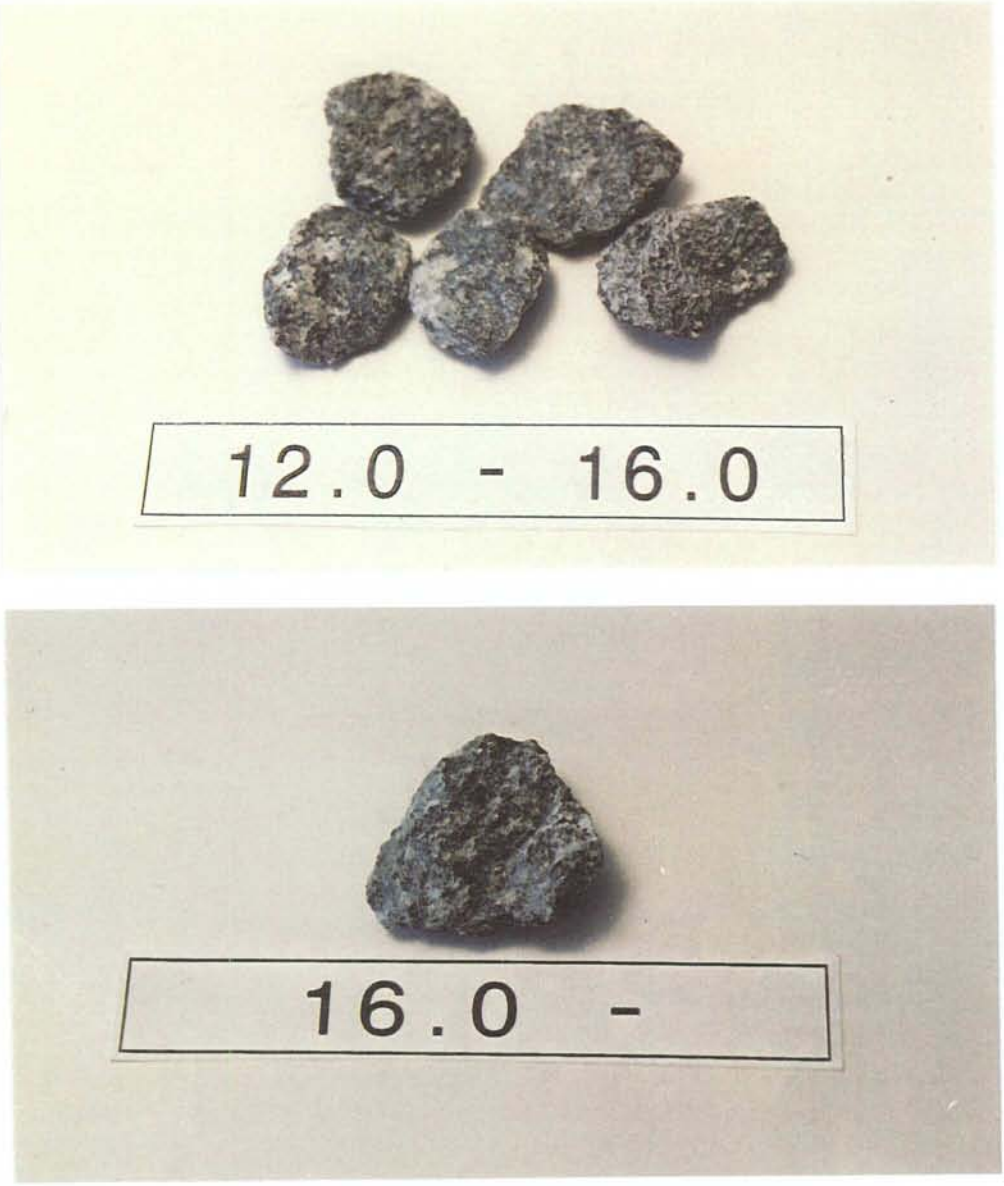

Figure 6.4-22. *Typical sample of the largest particles (chips) in the crushed rock.*

The average thickness of the largest particles (Figure 6.4-22) was about 5.6 mm (Figure 6.4-15 and 6.4-19) and indicates that the cutter head must have rotated several times before chipping occurred. The corresponding number of rotations is between five and six if the advance per rotation is assumed to be 1 mm, which was a typical value when boring.

Figures 6.4-23 and 6.4-24 show a comparison of the size of the largest particles, button configuration and topography of the surface, and indicates that the longitudinal direction of the rock chips is most likely to be either diagonal to, or parallel to, the direction of the button row. When looking at the width of the chips the distance between the button rows is not as important as the distance between the edges of the contact area, see Figure 6.4-25.

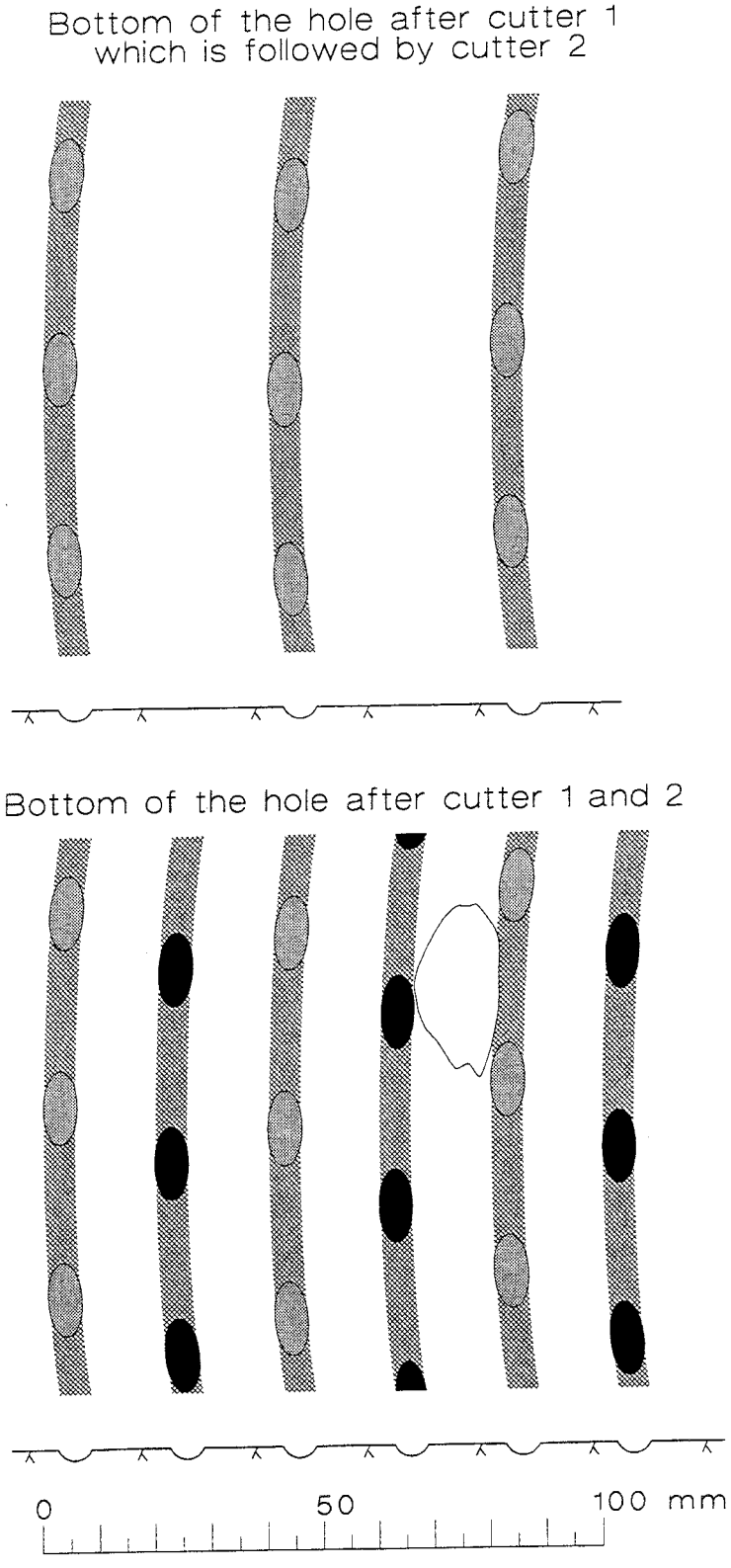

Figure 6.4-23. *Diagram showing an average large particle (chip) and the geometry of the contact points of the buttons on the bottom of the hole, 5 & 6 row cutters.*

The proportion of the area where the buttons of a cutter are in direct contact with the rock (i.e. the kerfs), is about 30 % of the total area under the cutters, see Figure 6.4-25. It is the area under the buttons which is being crushed in the boring process and the proportion of fine particles of size less than 0.5 mm should be 30 volume-% (equal to weight-%) or more if it is assumed that the buttons crush the surface of the kerf and thus form a continuous crushed groove. The result is consistent with the particle size distribution found which shows, as seen in Figure 6.4-10, that the size of about 50 weight-% of the crushed rock is less than 0.5 mm. This, together with the comparison shown in Figure 6.4-10, implies that some degree of regrinding has taken place.

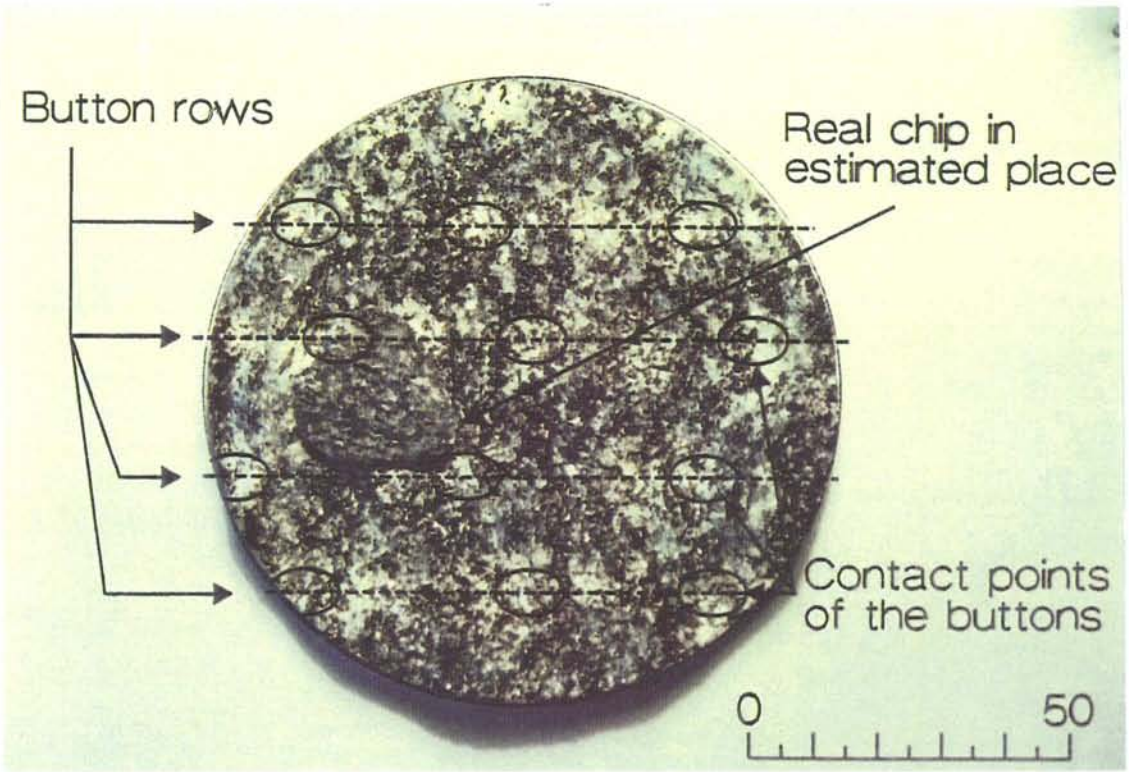

Figure 6.4-24. *Photographs of a sample taken from the bottom of a large hole. The location of the button rows, contact points and a chip are shown. As seen, the positions of contact points form an irregular pattern with varying spacing between successive contact points.*

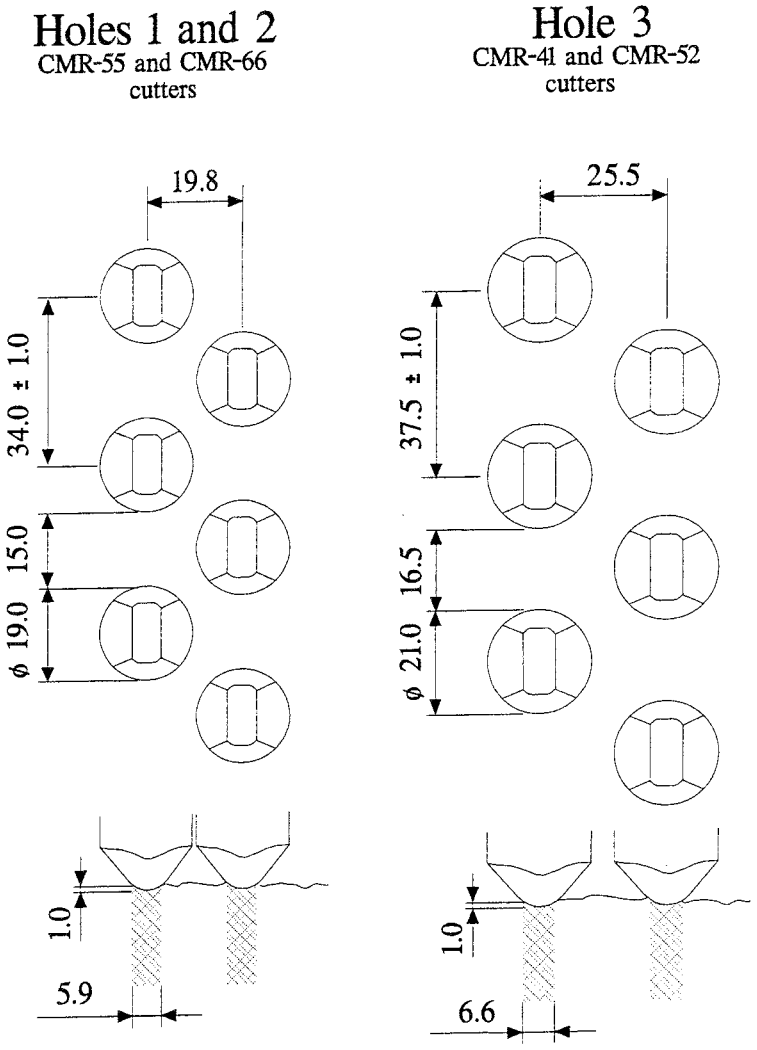

Figure 6.4-25. *Contact area of the button rows.*

7 PROPERTIES OF THE LARGE HOLES

7.1 DIAMETER

The diameter of the holes was measured (Äikäs 1995) as the minimum peak-to-peak diameter in different directions at a depth interval of 1 m. The holes were found to be slightly elliptical. The average diameters of the holes ranged from 1.527 - 1.528 m, see Table 7.1-1. Variations in the average radii of the holes were less than 3 mm. The ratio of the north-south and east-west radius were determined in the upper part of the holes at a depth of about 0.5 m and 6.5 m. The variations in the ratio of the diameters were small as seen in Table 7.1-2.

The average diameter of the holes was 0.26 % larger than the design diameter of the holes i.e. 1524 mm. The minimum diameter measured was the same as the design value.

Table 7.1-1. Diameters and radii of the large holes [m].

Depth of hole [m]	Hole 1	Hole 2	Hole 3	Average radius	Average diameter
0.5	0.762	0.763	0.766	0.764	1.527
1.0	0.764	0.764	0.764	0.764	1.527
2.0	0.764	0.763	0.764	0.764	1.527
3.0	0.764	0.764	0.764	0.764	1.528
4.0	0.764	0.763	0.765	0.764	1.528
5.0	0.764	0.763	0.764	0.764	1.527
6.0	0.764	0.763	0.764	0.763	1.527
7.0	0.764	0.764	0.764	0.764	1.528
Average radius	0.764	0.763	0.764	0.764	1.527
Average diameter	1.527	1.527	1.528		

Table 7.1-2. Ratio of north-south diameter to east-west diameter.

Depth of hole [m]	Hole 1	Hole 2	Hole 3	Average
0.5	0.998	0.998	0.998	0.998
1.0	0.997	0.998	0.998	0.998
2.0	0.996	0.998	0.998	0.997
3.0	0.998	0.998	0.998	0.998
4.0	0.998	0.998	0.998	0.998
5.0	0.998	0.998	0.998	0.998
6.0	0.998	0.998	0.998	0.998
7.0	0.998	0.998	0.998	0.998
Average	0.998	0.998	0.998	0.998

7.2 STRAIGHTNESS

The coordinates of the centerline of each large hole were measured and the straightness and curvature of the holes determined (Äikäs 1995). Measurements were carried out at a depth interval of 1 m.

The deviation in the direction of the holes expressed as the horizontal distance between the theoretical centerline at the bottom of the hole and the true centerline were 32 mm, 27 mm and 17 mm for holes 1, 2 and 3 respectively which are equal to deviations between 0.2 - 0.4% of the hole length as seen in Figure 7.2-1 and Table 7.2-1. Large holes 1 and 2 were inclined in a northwest direction and large hole 3 was inclined towards the southwest.

The large holes were found to be slightly curved as shown by Figures 7.2-1 and 7.2-2. Hole 1 shows greater curvature in the bottom section which was bored without a guiding pilot hole. Hole 2 is evenly curved and Hole 3 is curved in the upper part but fairly straight in the lower part.

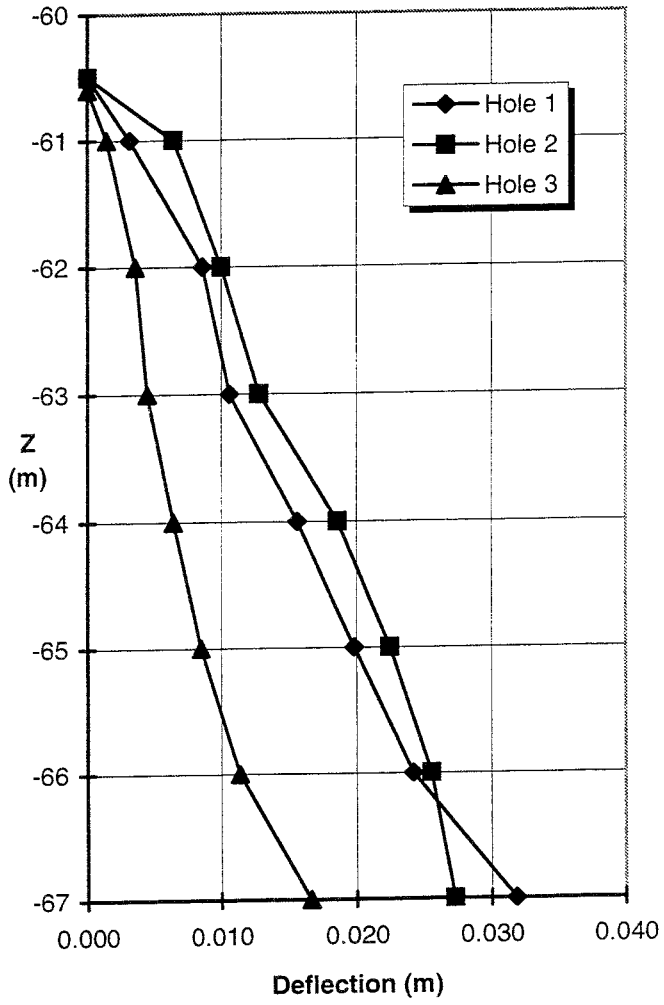

Figure 7.2-1. *The deviation of the holes at different depths between the -60.500 and -67.000 levels in a vertical section. The concrete floor was at the -60.000 level.*

The average radius of curvature of the centerline of the large holes calculated from the deflection was 960 m. This calculation was based on the simplified assumption that the curvature of the large holes is circular.

The deviations which occur already in the upper parts of the large holes are assumed to be primarily the result of misalignment at the beginning of the boring process.

Table 7.2-1. Deviation of the holes expressed as the horizontal distance between the actual centerline at the bottom of the hole and the true centerline.

Large hole	Direction	Deviation
1	316°	32 mm
2	298°	27 mm
3	237°	17 mm

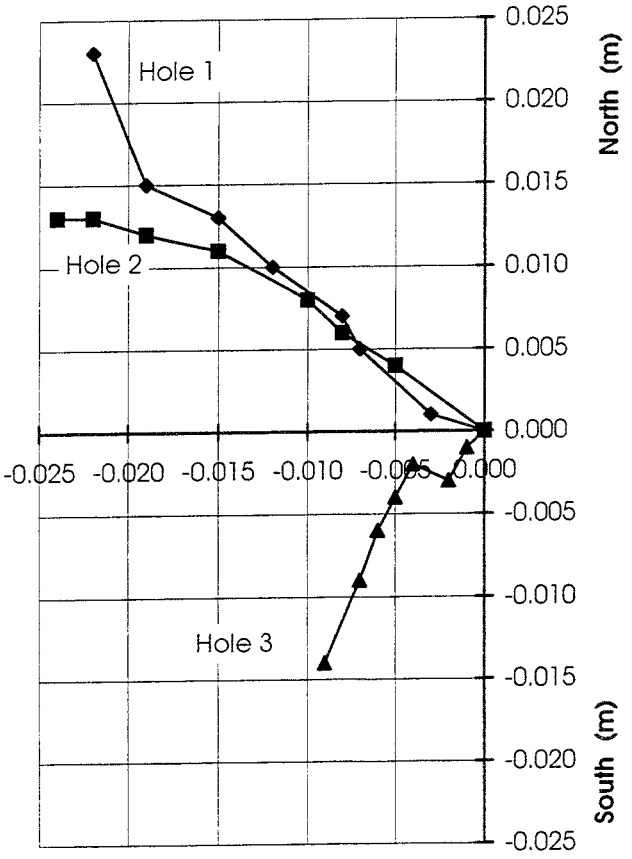

Figure 7.2-2. The deviation of the holes at different depths between -60.500 and the -67.000 levels projected on horizontal plane. The vertical distance between succesive points in the curves is 1 m. The concrete floor was at the -60.000 level.

7.3 SURFACE ROUGHNESS

The surface roughness of the three large holes was measured using an optical linear laser profilometer, see Figure 7.3-1 and 7.3-2 (Halttunen 1995).

Figure 7.3-1. *The optical laser profilometer (Halttunen 1995).*

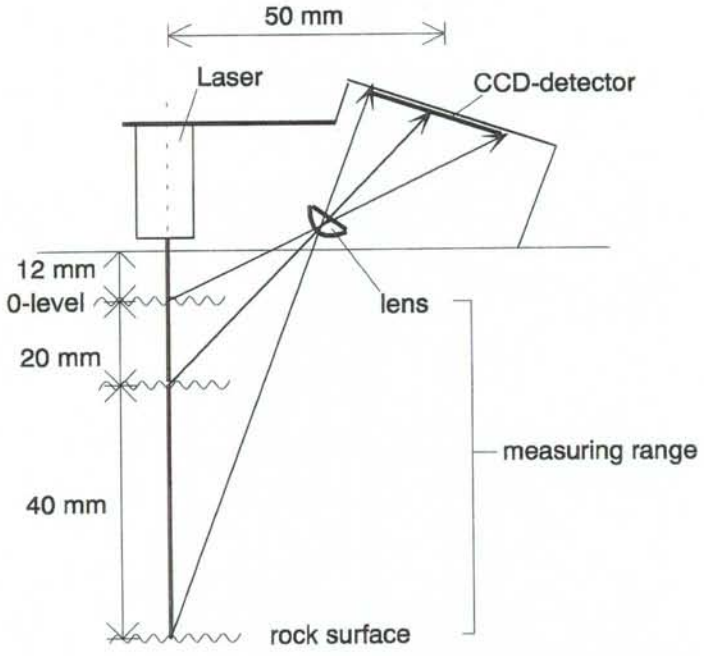

Figure 7.3-2. *The principle of measurement using the laser profilometer.*

The roughness parameters calculated from measurements of the surface topography were: R_a and R_z (ISO), which describe differences in profile height; and S_m, which describes the differences between the spacings of peaks in the profile, see Figures 7.3-3 and 7.3-4. An example of the section of roughness profile is shown in Figure 7.3-5.

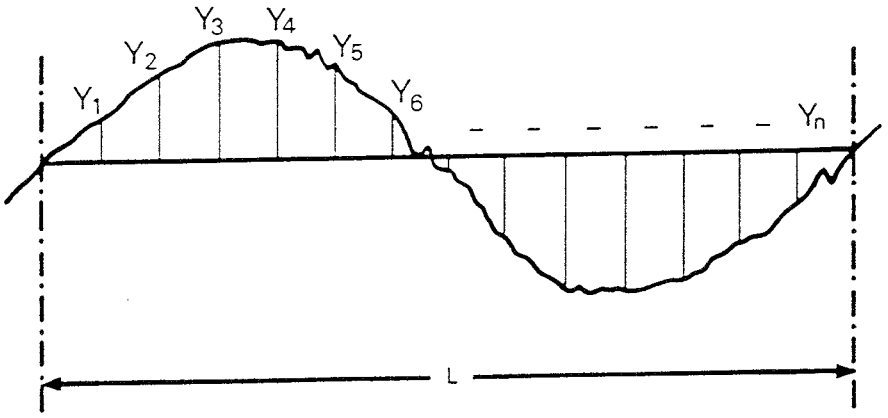

$$R_a = \frac{|y_1| + |y_2| \ldots |y_n|}{n}$$

Figure 7.3-3. *R_a (Dagnall 1986).*

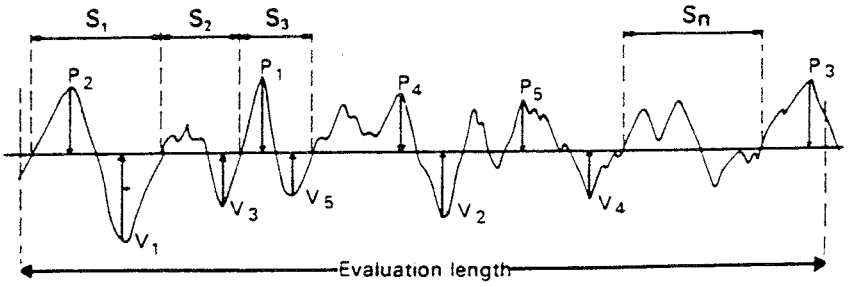

$$R_z(ISO) = \frac{(p_1 + p_2 + p_3 + p_4 + p_5) + (v_1 + v_2 + v_3 + v_4 + v_5)}{5}$$

$$S_m = \frac{s_1 + s_2 + s_3 + s_4 + \ldots\ldots + s_n}{n}$$

Figure 7.3-4. *R_z(ISO) and S_m (Dagnall 1986).*

The values of R_a varied from 0.25 mm to 2.37 mm (the average of all the measured profiles was 0.56 mm) and R_z from 1.63 mm to 9.38 mm (average value 2.74 mm). The values of S_m are from 3.46 mm to 49.60 mm (average value 8.71 mm).

Furthermore, two R_q parameters (the root mean square parameters of amplitude), determined from the filtered profiles were included. These so called mega and macro roughness values were calculated from two filtered profiles. The macro-value is estimated by eliminating wavelengths smaller than 0.5 mm and greater than 50 mm from the measured profiles. The filters used for mega-values were 50 mm and 500 mm. The mega-values varied from 0.18 mm to 2.65 mm (the average mega-value was 0.62 mm) and the macro-values varied from 0.15 mm to 1.50 mm (the average macro-value was 0.37 mm).

The average values of the roughness parameters in the different holes did not differ significantly, as can be seen from Table 7.3-1. Distinct variations were however found in the amplitude parameters of holes in relation to hole depth, as seen in Figure 7.3-6. The most distinct variations were found in the R_z parameter although consistent variations also occurred in the parameters for R_a and mega-roughness. Most of the culmination points of the roughness parameter curves corresponded to points where the boring machine drill string had been extended. This required that the boring was stopped, the thrust released and the cutter head lifted slightly before a new drill pipe was installed.

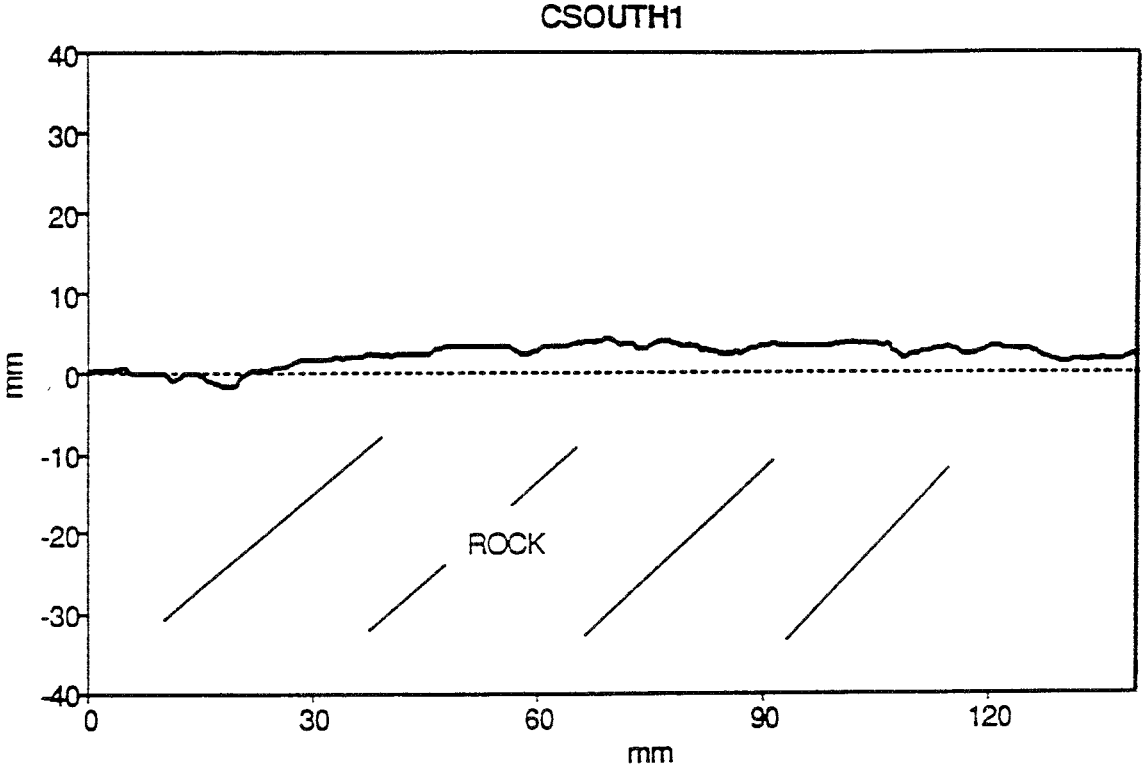

***Figure 7.3-5** . An actual-size example of a section of roughness profile. The mean line shown dotted is the average line for the measured section of profile of length 512 mm (Halttunen 1995).*

Table 7.3-1. Average roughness parameters of the holes.

Hole	R_a	R_z	S_m	mega	macro
1, average	0.58	2.84	8.83	0.62	0.36
range	0.34-1.39	2.10-4.00	4.14-46.08	0.31-1.50	0.26-0.53
2, average	0.57	2.72	9.52	0.63	0.38
range	0.25-1.53	1.63-4.93	4.08-33.93	0.18-1.74	0.23-0.88
3, average	0.52	2.65	7.78	0.61	0.37
range	0.30-1.32	1.67-9.38	4.31-26.50	0.27-1.94	0.15-1.50
Total average	0.56	2.74	8.71	0.62	0.37

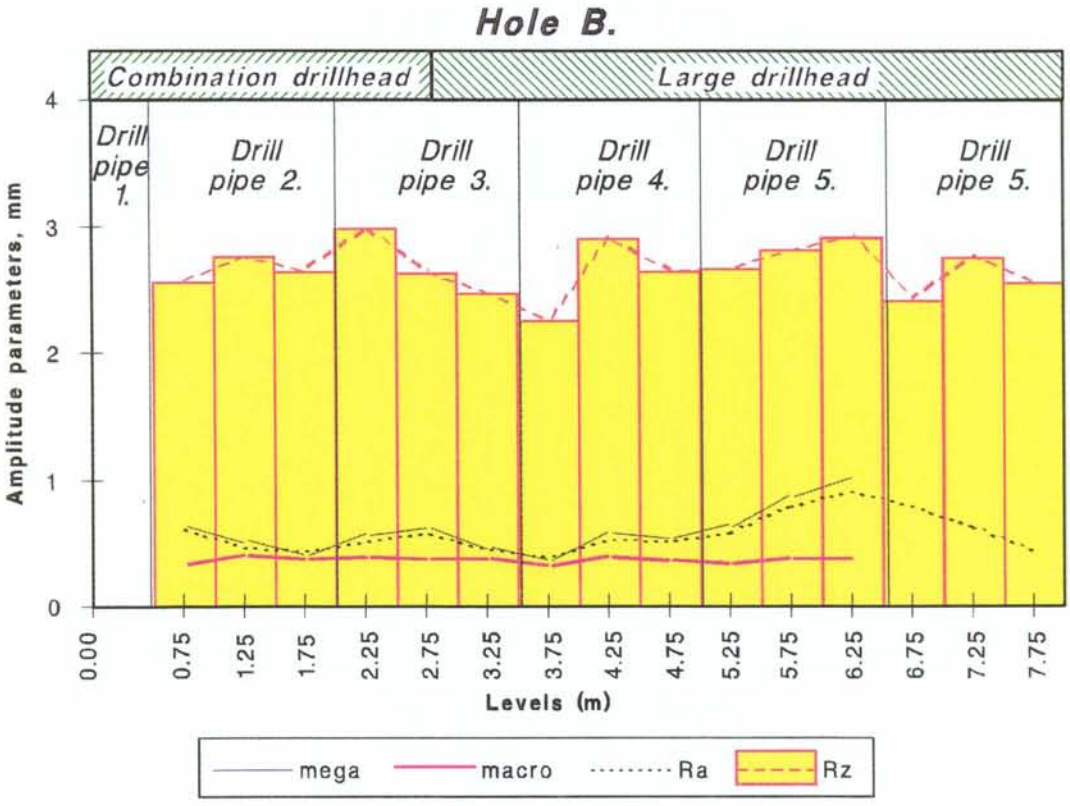

Figure 7.3-6. Amplitude parameter values at different levels in large hole 2. These values are averages of four vertical lines.

7.4 EXCAVATION DISTURBANCE CAUSED BY BORING

7.4.1 General

The disturbance of the rock caused by boring was studied using two novel methods: the ^{14}C-Polymethylmethacrylate (^{14}CPMMA)-method (Siitari-Kauppi 1995); and the He-gas method (Hartikainen et al. 1995). Studies of disturbance took place in the laboratory by examining 98 mm diameter core samples representative of different boring parameters and taken from different parts of the large holes, see Figure 7.4-1.

The methods, techniques and results of these examinations are presented in greater detail by Siitari-Kauppi 1995 (in regard to the ^{14}CPMMA-method) and by Hartikainen et al. 1995 (in regard to the He-gas method). A more detailed description and summary of all the studies is presented by Autio 1996.

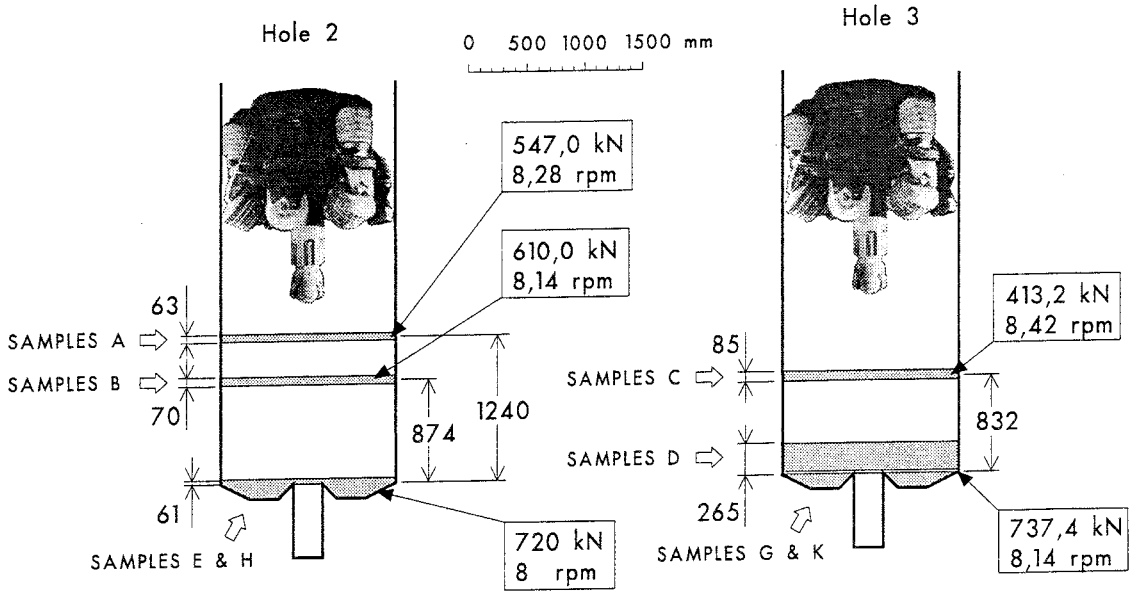

Figure 7.4-1. *The location of the sampling points in the large holes and the corresponding boring parameters (Autio et al. 1995).*

7.4.2 ^{14}CPMMA-method

The ^{14}CPMMA-method was used to study the mechanical disturbance of the rock in the side walls in terms of the geometry of microfractures and porosity profiles (Siitari-Kauppi 1995).

The method involves impregnation of the rocks with ^{14}C-methylmethacrylate, irradiation polymerization, sample partitioning (see Figure 7.4-2), autoradiography and optical densitometry using digital image processing techniques, see Figure 7.4-4. Scanning electron microscopy (SEM) and energy dispersive X-ray analysis (EDX) were used to investigate the pore apertures and minerals in porous regions in greater detail. SEM/EDX measurements were conducted on ^{14}CPMMA impregnated samples.

The disturbed zone appeared as a zone of increased porosity and a zone of distinct porous tracelines which extended deeper into the rock matrix than the zone of increased porosity, see Figure 7.4-3.

The total porosities of rock increased to a depth of about 11 mm from the disturbed surface in samples cored from the walls of the holes. The maximum average values of porosities adjacent to the disturbed surface of the walls excluding the bottom of the hole and corner sections ranged from 0.5 to 1.6 vol.%. The corresponding range of porosity in individual profiles was slightly larger. The average values of porosity in a zone from the disturbed surface to a depth of 5 mm ranged from 0.2 to 1.2 vol.%. The porosities of the undisturbed rock ranged from 0.10 to 0.15 vol.%.

The porous tracelines extended to depths of 15 - 25 mm from the wall surface. These did not significantly increase the total porosity of the disturbed zone at depths of 15 - 25 mm, see Figure 7.4-5 and 7.4-6.

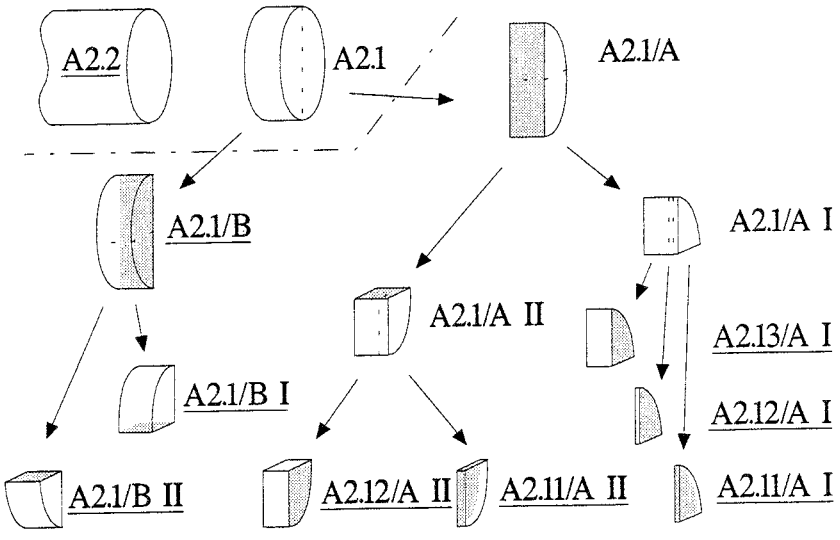

Figure 7.4-2. *Partition diagram for the 98 mm diameter core sample A2 for the ^{14}CPMMA study from large hole 2. The exposed surfaces were examined.*

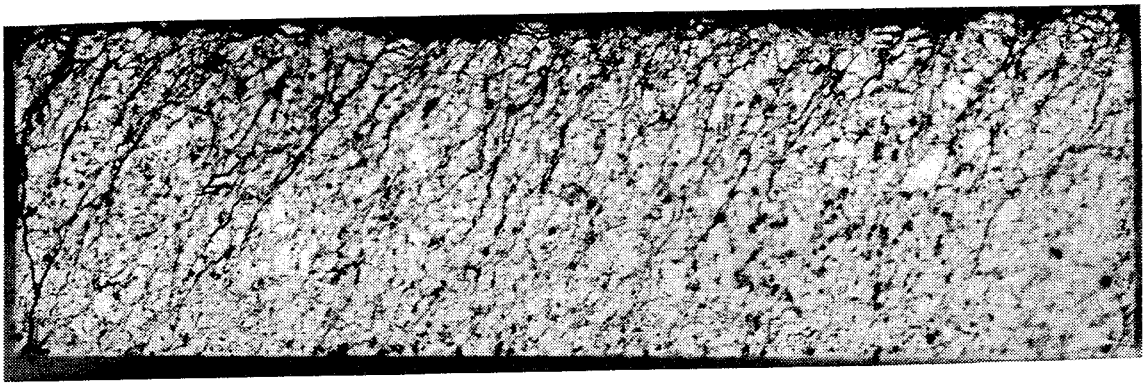

Figure 7.4-3. *Example of a autoradiograph, sample C2 (Siitari-Kauppi 1995). The upper surface of the sample is a section of the surface of large hole 3. The plane of the section is perpendicular to the surface. Different levels of gray shades represent different levels of porosity.*

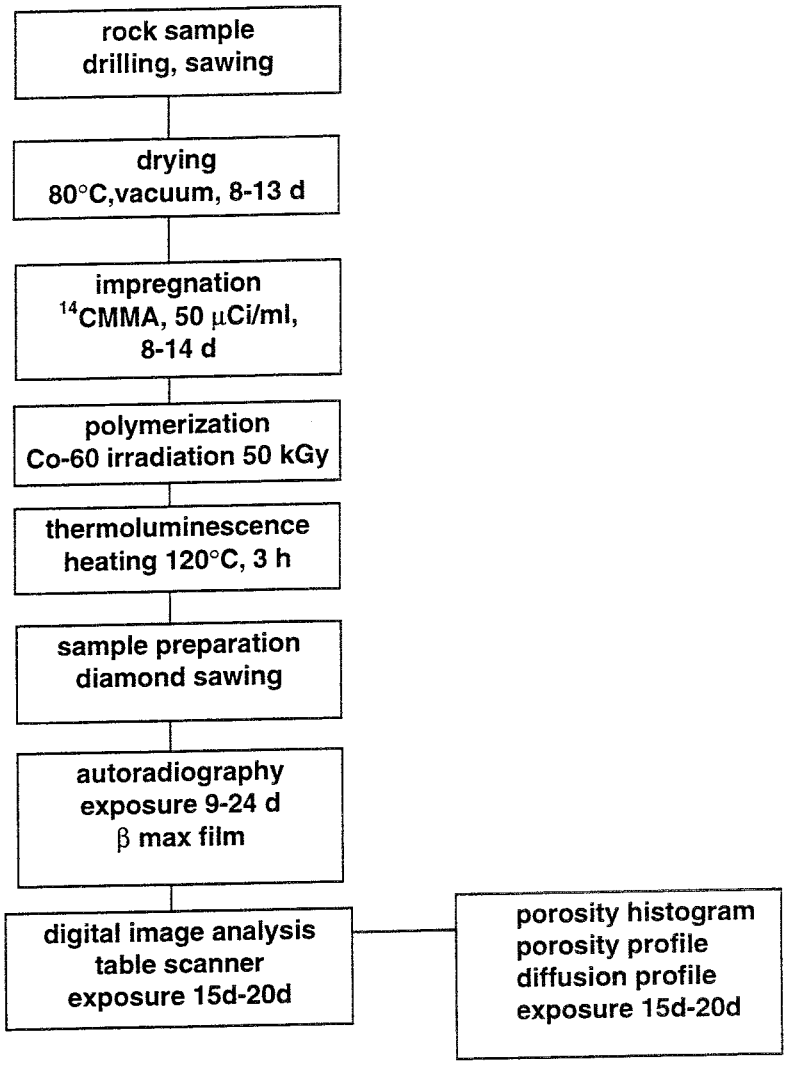

Figure 7.4-4. *The ^{14}CPMMA -method.*

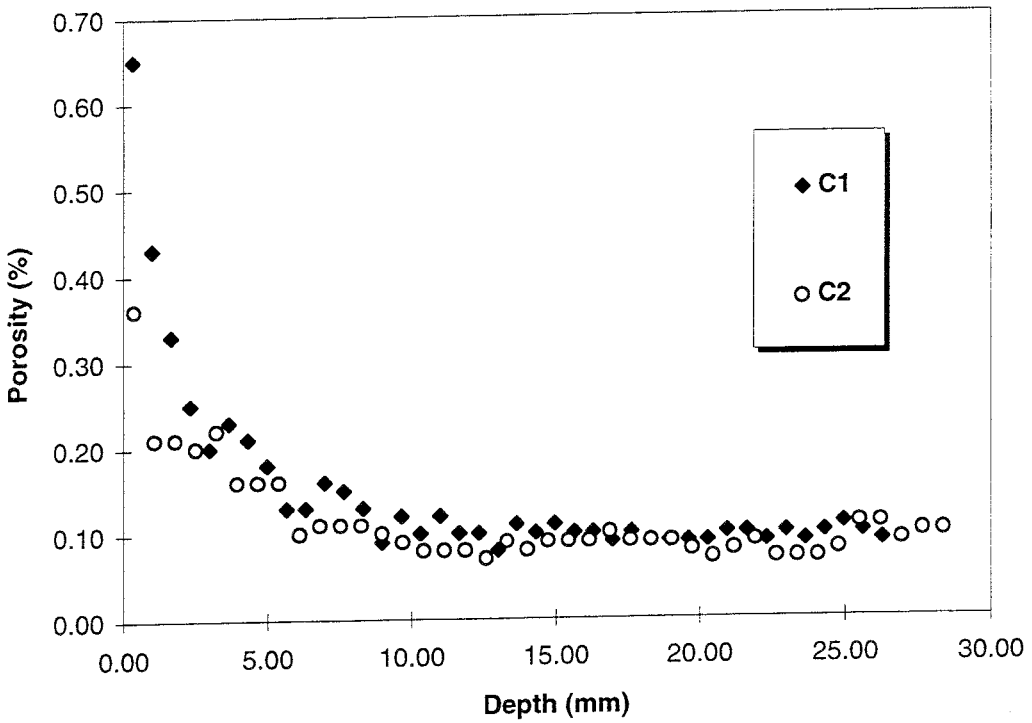

Figure 7.4-5. *Porosity profiles of samples from the C-series. A section of sample C2 is shown in Figure 7.4-3. The porosity value is presented in relation to distance from the disturbed surface of the wall of the hole (Siitari-Kauppi 1995).*

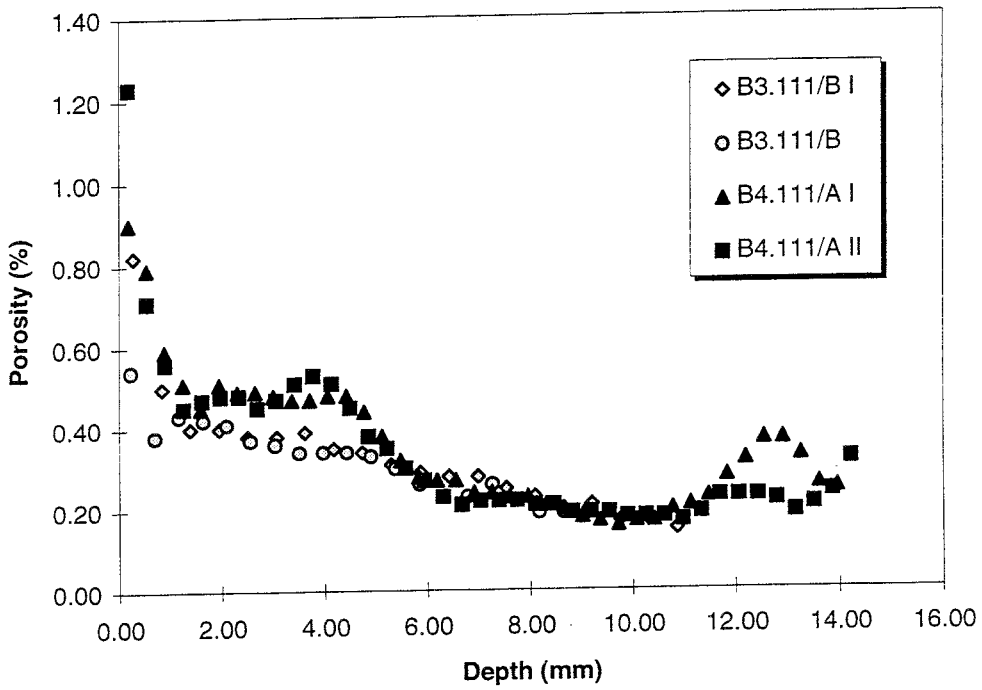

Figure 7.4-6. *Porosity profiles of samples from the B-series. The porosity value is presented in relation to distance from the disturbed surface of the wall of the hole (Siitari-Kauppi 1995).*

7.4.3 He-gas method

The He-gas method was used to investigate the disturbance in terms of the effective diffusion coefficients as shown in Figure 7.4-7, and the permeabilities as shown in Figure 7.4-8 (Hartikainen et al. 1995).

The diffusion coefficients (D_e) and permeabilities (k) were measured from 30 samples of both disturbed and undisturbed rock taken from six positions in the holes. Some of the samples were investigated also with the ^{14}CPMMA-method. The measurements showed a zone of higher conductivity and diffusitivity next to the surface of the holes.

The estimated thickness of this zone was from 17 to 21 mm from the surface, see Table 7.4-1. The maximum extent of separate microcracks was estimated to be some 12 mm.

The ratio of the diffusion coefficients in the disturbed zone and in the intact rock was found to vary between 5 and 31, and the corresponding ratio of the permeabilities varied between 10 and 90, see Table 7.4-1.

The estimated thickness of the disturbed zone was different when defined as the depth of the zone of anomalous porosity or diffusion coefficient and permeability or microfracturing as seen in Figure 7.4-9.

Table 7.4-1. Diffusion coefficient (D_e) and permeability (k) of disturbed and undisturbed rock, the ratio between these and the estimated thickness of the disturbed zone.

sample	intact rock		disturbed zone		depth	relative change	
series	D_{e1} [m^2/s]	k_1 [m^2]	D_{e2} [m^2/s]	k_2 [m^2]	h [mm]	D_{e2}/D_{e1}	k_2/k_1
B4	1.10×10^{-10}	3.60×10^{-21}	1.45×10^{-9}	7.40×10^{-20}	17	13	21
B8	3.50×10^{-10}	6.23×10^{-21}	1.70×10^{-9}	6.27×10^{-20}	20	5	10
D2	2.30×10^{-10}	4.65×10^{-21}	5.20×10^{-9}	4.00×10^{-19}	18	23	86
D4	4.00×10^{-10}	8.46×10^{-21}	7.20×10^{-9}	7.59×10^{-19}	19	18	90
D7	1.40×10^{-10}	2.47×10^{-21}	4.30×10^{-9}	1.84×10^{-19}	21	31	74

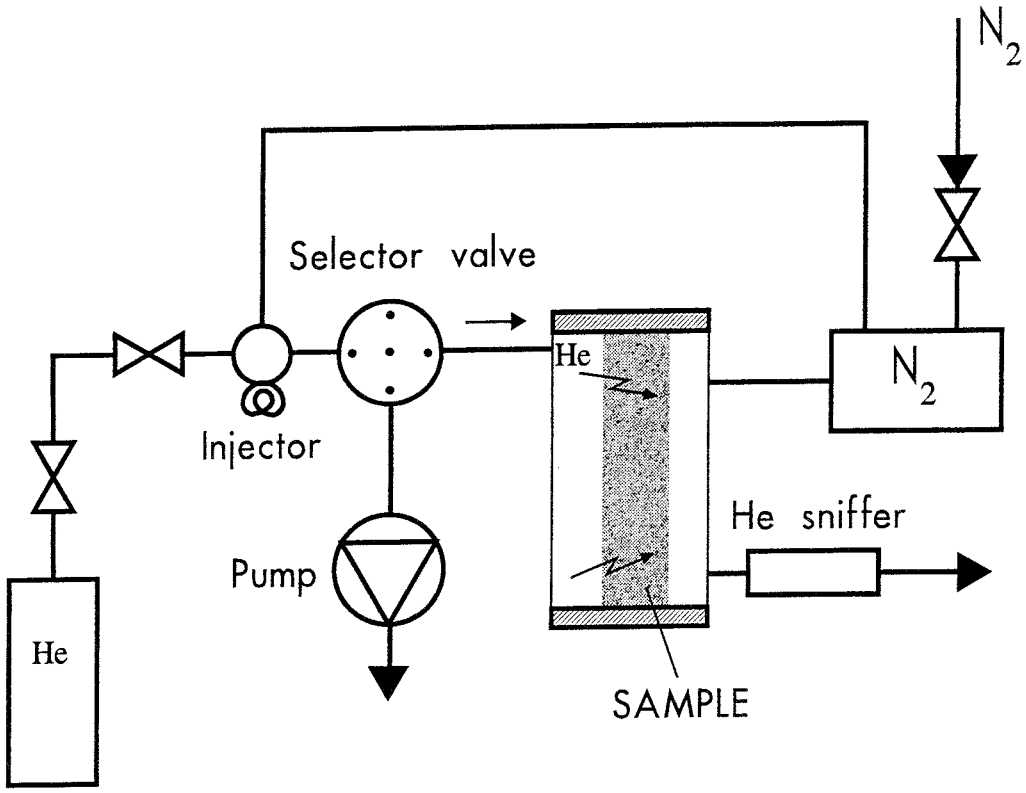

Figure 7.4-7. *The experimental apparatus used for measurement of through-diffusion.*

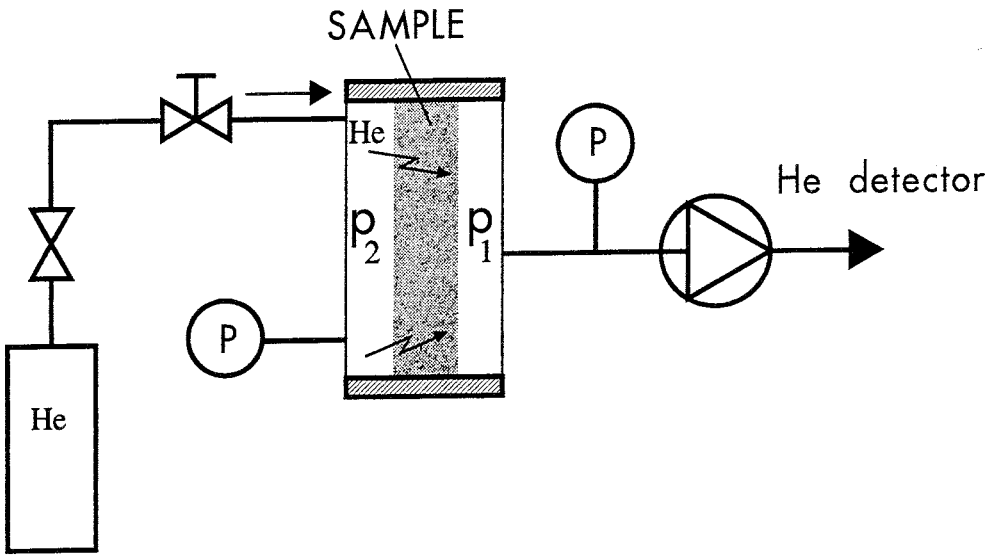

Figure 7.4-8. *The experimental apparatus used for measurement of permeability.*

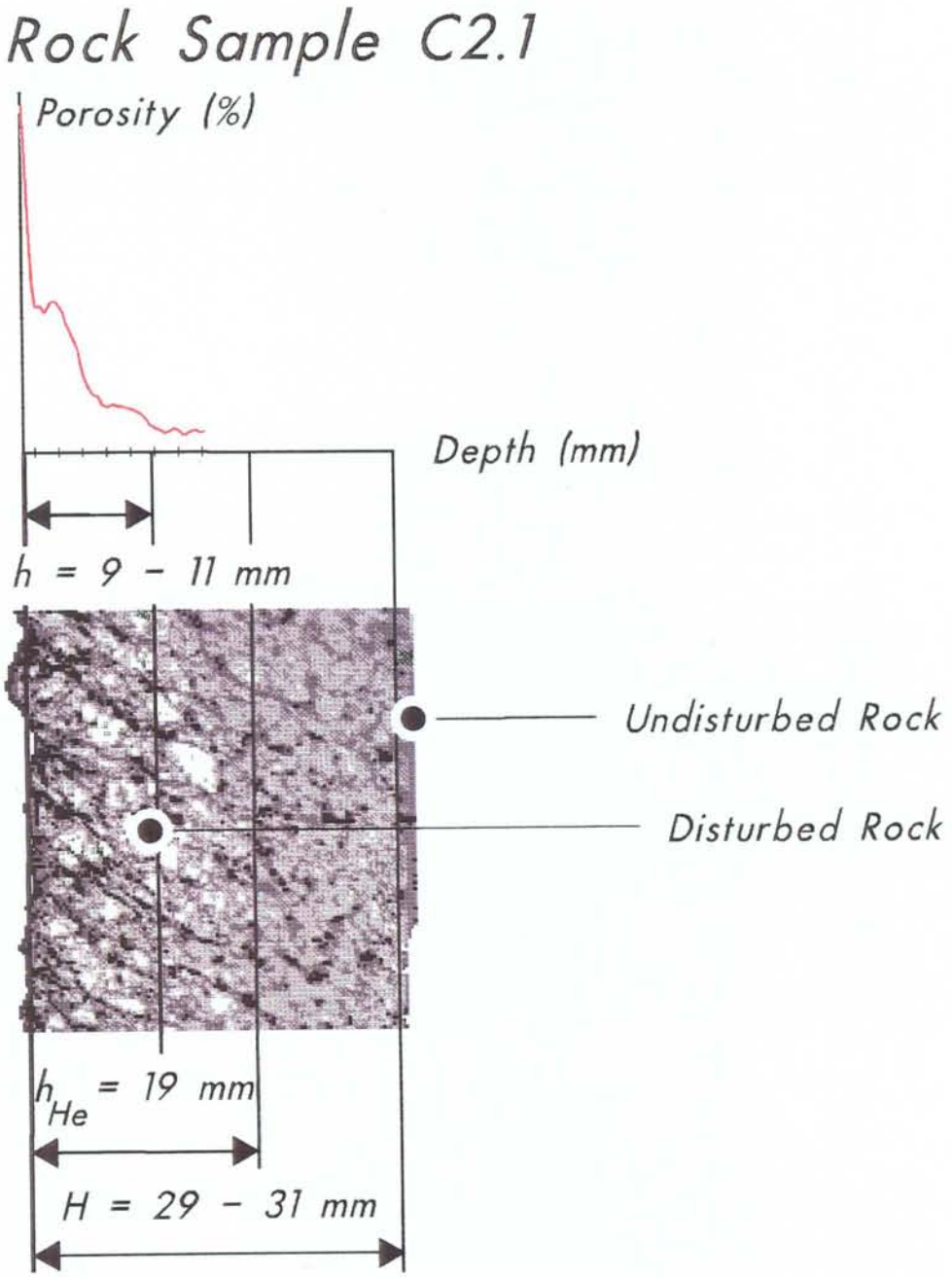

Figure 7.4-9. *The thickness of the disturbed zone (h_{He}) determined by the He-method, the thickness of the zone of increased porosity (h) determined by the ^{14}CPMMA-method and the thickness of the zone of extended microfractures (H) interpreted visually from the autoradiographs.*

8 SUITABILITY OF THE METHOD FOR BORING DEPOSITION HOLES

8.1 PERFORMANCE

8.1.1 Performance of the existing equipment

Good boring performance close to that of raise boring was achieved when the equipment was in good operating condition.

The average advance rate of the boring machine tested at the maximum machine thrust of about 600 kN and rotation speed of 8 rpm with 5 and 6 row cutters was about 1.9 mm/rev. which is equivalent to 91 cm/h. The observed advance rate measured at a flushing air flow ratio of less than 1.7 is quite close to the values which have been measured in the laboratory for single cutters and this implies that the boring process worked efficiently. The highest advance rate of 1.23 m/h was measured during boring with a rotation speed of 12 rpm and thrust of 700 kN.

The observed thrust-advance range did not represent the best performance of the cutter head in regard to the rock-breaking process. The highest loading rate of the buttons was 18 - 20 kN which is only about 30 - 38 % of the maximum loading rate allowed and just 35 % higher than the critical thrust.

Rock crushing results from button impacts which cause the formation of a crushed zone below the button impact area and chipping of the rock between the impact points, see Figure 8.1-1. The formation of chips is the most effective method of rock crushing. The larger the size of chips the less energy is spent on breaking and grinding the rock and the higher the advance rates achieved, see Figure 8.1-2.

It is evident that the efficiency of the boring process with the tested equipment would have been higher if the thrust and corresponding torque could have been increased since the chipping efficiency is increased as the thrust force is raised. The optimum design load for the cutters is governed by the cutter shape and rock factors.

Boring performance can be improved by using a more powerful machine specially modified for this purpose. As boring performance is improved, the flow of crushed rock will be increased. According to the test results obtained, the efficiency of the method of vacuum cleaning the bottom of the hole is sensitive to the level of boring performance which governs the mass flow of crushed rock and this may in fact become the limiting factor when using a design similar to that employed in the Research Tunnel.

An increase in the rotation speed of the cutter head was observed to result in a clear drop in the advance rate per rotation, this in turn being caused by a fall in efficiency of the vacuum cleaning process. This was assumed to be the result of

the reduction in pick-up time as the speed of the nozzles was increased. The low flow ratio of the vacuum suction system was still at an effective level and presumably could not have caused the inefficiency.

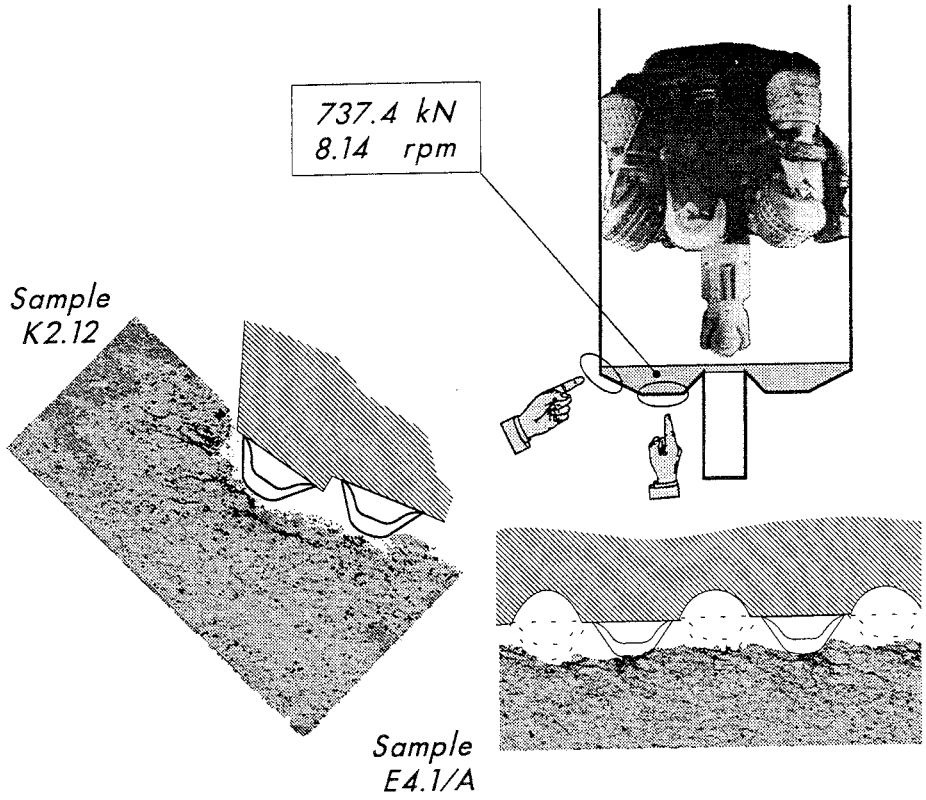

Figure 8.1-1. *Fracturing of rock under the cutters as seen in particular test sections.*

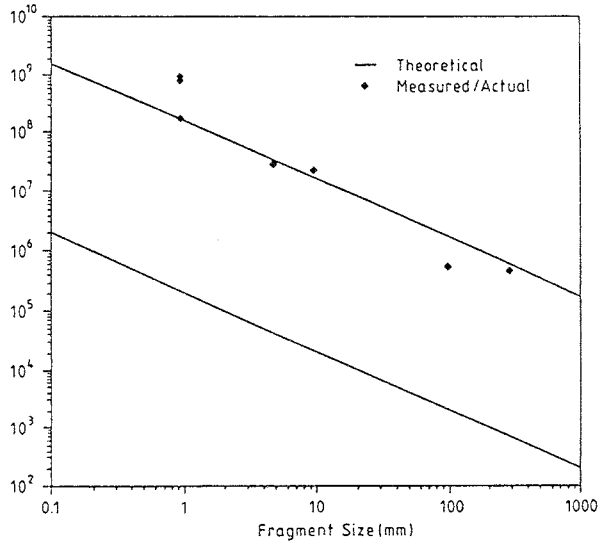

Figure 8.1-2. *Size of crushed rock in relation to specific energy (Hartman 1992).*

8.1.2 Influence of rock type

The efficiency of boring is affected by the resistance of rock to failure (strength) and weaknesses such as fractures and fissures in the rock and the orientation of these. The estimated basic rates of advance must therefore be modified if different types of rock are involved. The rock in the Research Tunnel was very sparsely fractured and it was assumed that the test results would not be affected significantly by fracturing.

The strength of the rock in regard to the efficiency of boring has been described by using the compressive strength, tensile strength and drilling rate index (DRI-value). Of these, the DRI-value, a function of the brittleness value S_{20} and Siever's J value, has been developed to describe the level of performance of percussive drifters, but has also been applied when estimating advance rates for tunnel boring.

Compressive strength and indirect tensile strength (point load strength) are useful supplementary parameters but they are not by themselves sufficient to determine rock drillability (NTH 1994).

If rock drillability is assessed by using figures for compressive strength, results will be biased away from the true values by indicating an easier drillability (i.e. a larger DRI-value) for granitic rocks and more difficult drillability (i.e. a smaller DRI-value) for schistose and foliated rocks such as mica gneiss and the anisotropic tonalite typical of the Research Tunnel. In other words, as seen in Figure 8.1-3, the drillability can be the same for schistose rocks of low compressive strength and granite rocks of high compressive strength.

According to laboratory penetration tests using linear test rigs the thrust required for chipping is proportional to the contact area of the cutter (NTH 1994) and the compressive strength of the rock according to the following Equation 8-1, which is valid for a constant cross section cutter:

$$F_v = K_p \, \sigma_{ucs} \, A_{contact} \qquad 8\text{-}1$$

where, σ_{ucs} is the unconfined compressive strength of the rock
$A_{contact}$ is the contact area of the cutter
K_p is the proportionality factor
F_v is the thrust applied.

The relation between the contact area and the advances of hard metal buttons achieved in the tests was established for the 5 and 6 row cutters used in the work. A toroid was used to approximate the surface geometry of the button. The following Equation 8-2 for the contact area of the button was obtained

$$A_{contact} = 56.4 \, i \qquad 8\text{-}2$$

where, i is the advance of a hard metal button [mm]
$A_{contact}$ is the contact area of the button [mm^2].

The relationship between the contact area and the advance rates achieved in the tests is therefore linear, which also explains the good regression coefficients obtained with linear curve fits. The same was true of the 4 and 5 row cutters, for this case the relationship was both measured and calculated. The Equation 8-3 gives a simple correlation between critical thrust and compressive strength for the 5 and 6 row cutters if I = 1 mm,

$$F_c = K_p \sigma_{ucs} 56.4 \qquad 8\text{-}3$$

The Equation 8-3 can be written in a new form,

$$F_c = K_p \sigma_{ucs} A_c \qquad 8\text{-}4$$

where,
- b is the penetration coefficient
- F_v is the thrust
- F_c is the critical thrust
- K_p is the proportionality factor
- A_c is the contact area of the button at critical thrust (i=1 mm)

For the same type of buttons the contact area in different rock types is the same at the same depth of penetration. According to Equation 8-4 the ratio of critical thrust forces is therefore equal to the ratio of compressive strengths in different rock types and the effect of compressive strength can be taken into account by modifying the critical thrust in Equation 8-3 or the constant ´a´ in Equation 5-3.

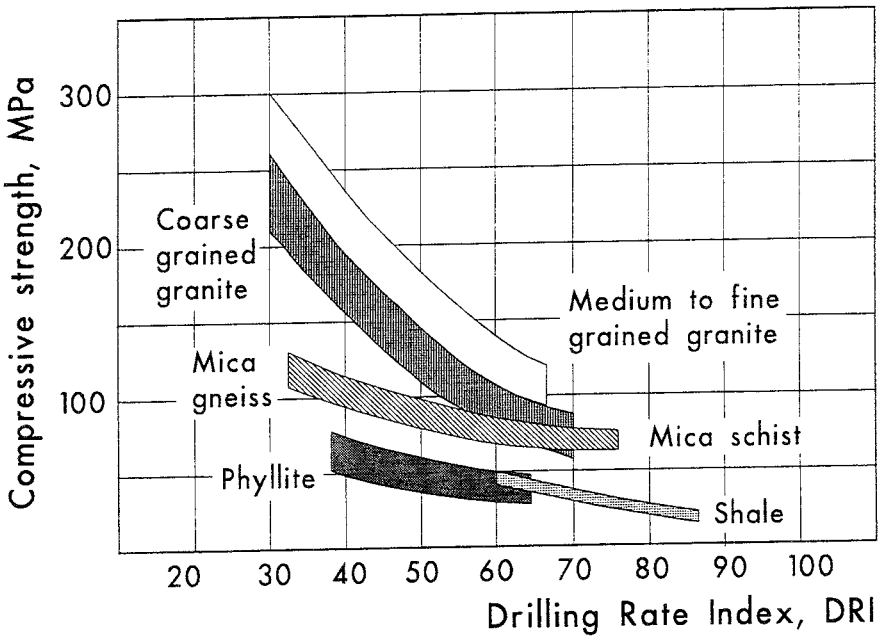

Figure 8.1-3. *Relation between DRI-value and compressive strength for granitic, schistose and foliated rock (NTH 1994). Note that smaller DRI-values indicate rock which is more difficult to drill.*

The penetration coefficient and critical thrust were established as described in Chapter 5 for the anisotropic tonalite in the Research Tunnel. If the penetration coefficient b is independent of the rock type and the critical thrust is dependent on the compressive strength of rock, the effect of rock strength can therefore be estimated using Equation 8-3 and the known compressive strength of the rock in the Research Tunnel.

According to laboratory determinations, the compressive strength of the ansiotropic tonalite was 75 MPa. The value for compressive strength calculated from the test results on the basis of Equation 8-3 and the critical thrust was found to be in the range from 170 to 200 MPa. The factor of proportionality was assumed to be one, as in the case of constant cross section cutters. The inconsistency of these results is likely to result from the fact that the compressive strength is not an ideal parameter for use when estimating boring performance, and in this respect a higher than true value of compressive strength (effective compressive strength) would give a better estimate of performance in anisotropic tonalite.

The thrust-advance curves for 5 and 6 row cutters in rocks of different compressive strengths are shown in Figure 8.1-4. At a thrust of about 2000 kN a penetration rate of 3 mm/rev. is achieved in rock with a compressive strength almost double that of the ansiotropic tonalite (150 MPa) in the Research Tunnel. The corresponding penetration rate in anisotropic tonalite is about 8 mm/rev. At a cutter head rotation speed of 8 rpm these values are equal to 3.8 m/h and 1.44 m/h respectively.

The average DRI-value of 55 for the anisotropic tonalite is typical for this type of rock but indicates a rock of more difficult drillability than the compressive strength would, on average, imply. Therefore the effective compressive strength which corresponds to the actual drillability of the rock is assumed to lie somewhere between the calculated and measured values.

Corresponding rates of advance can also be estimated for rock types with different drillability if it is assumed that the advance rate in different types of rock is linearly dependent on the DRI-value, as implied by NTH 1994. A correlation between DRI-value and penetration rate has been established in the form of a correlation factor for advance rate, k_{DRI} (NTH 1994) shown in Figure 8.1-5, which gives the modified advance rate. This correlation can be approximated as shown in Equation 8-5.

$$k_{DRI(x)} = -0.0001(x)^2 + 0.0256\,(x) + 0.0105 \qquad 8\text{-}5$$

$$i_{DRI(x)} = i_{49}\, k_{DRI(x)} \qquad 8\text{-}6$$

where, $i_{DRI(49)}$ is the advance rate at a DRI-value of 49
$i_{DRI(x)}$ is the advance rate for a different DRI-value (x)
$k_{DRI(x)}$ is the advance rate correlation factor for DRI-value (x) with respect to DRI-value 49.

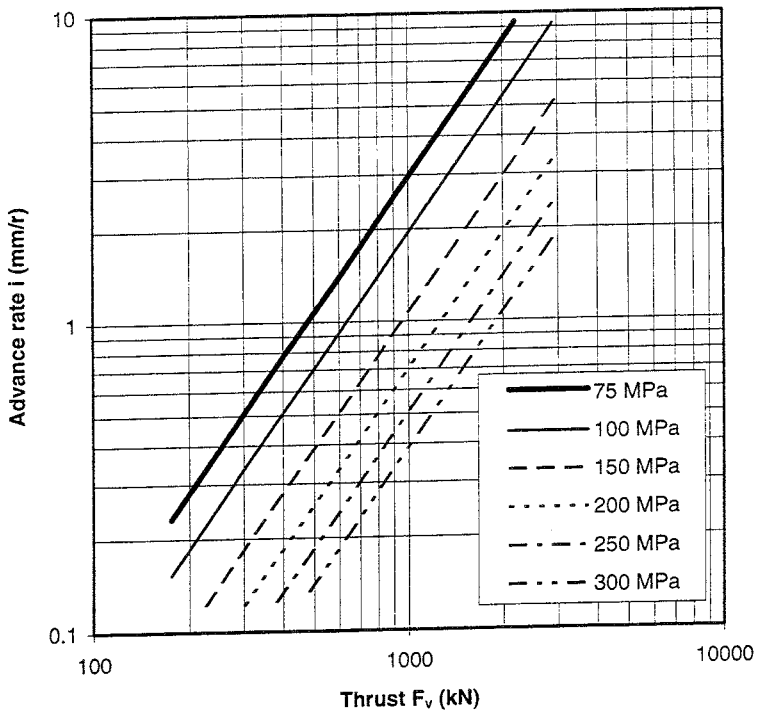

Figure 8.1-4. *Thrust-advance curves for 5 & 6 row cutters with different compressive strengths of 100 %, 133 %, 200 %, 270 %, 330 % and 400 % of the uniaxial compressive strength of the rock in the Research Tunnel. The corresponding rock compressive strengths are 75, 100, 150, 200, 250 and 300 MPa. It has been assumed that the compressive strength is in linear proportion to the critical thrust.*

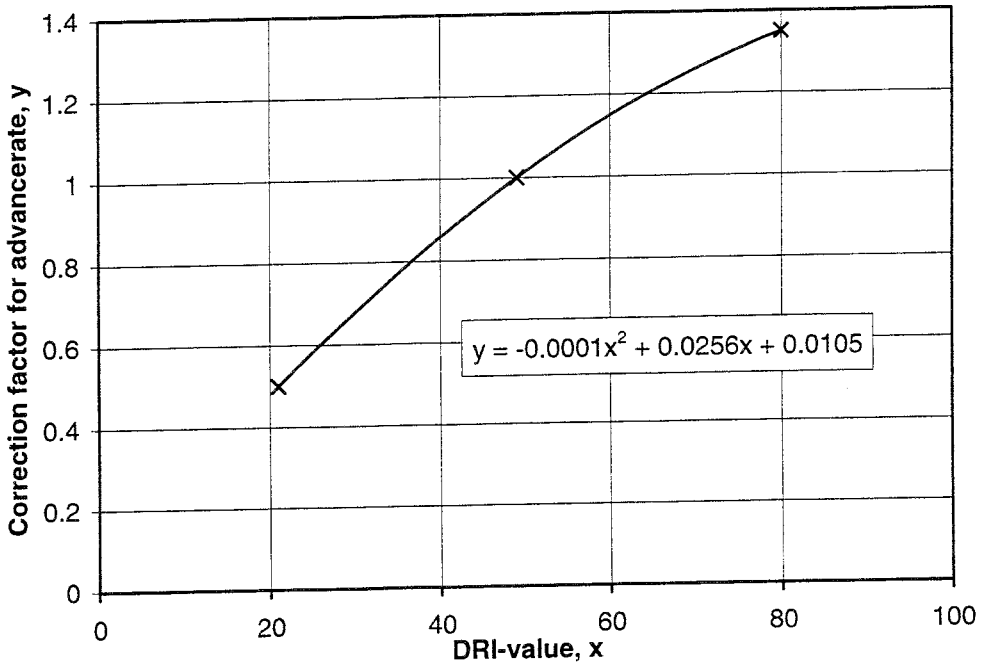

Figure 8.1-5. *The correlation between DRI-value and a correction factor for advance rate in compact rock, modified from (NTH 1994). The regression equation has been estimated using the principle of the sum of least squares.*

In the case of the anisotropic tonalite in the Research Tunnel, Equation 8-6 can be rewritten as:

$$i_{DRI\,(x)} = i_{DRI(55)}\, k_{DRI(x)}/k_{DRI(55)} \qquad 8\text{-}7$$

where, $i_{DRI(55)}$ is the advance rate in anisotropic tonalite (DRI=55).

Using Equations 8-5 and 8-7 for calculation, $k_{DRI(55)}$ is 1.09, $k_{DRI(41)}$ is 0.87, and $k_{DRI(69)}$ is 1.27.

Therefore:

$$i_{DRI\,(41)} = 0.80\, i_{DRI(55)} \qquad 8\text{-}8$$

$$i_{DRI\,(69)} = 1.16\, i_{DRI(55)} \qquad 8\text{-}9$$

The calculated thrust-advance diagrams shown in Figure 8.1-6 show that the effect of changes in the DRI-value is not as significant as the estimated effect of changes in the compressive strength (note that small DRI-values represent rock in which it is difficult to bore and vice-versa).

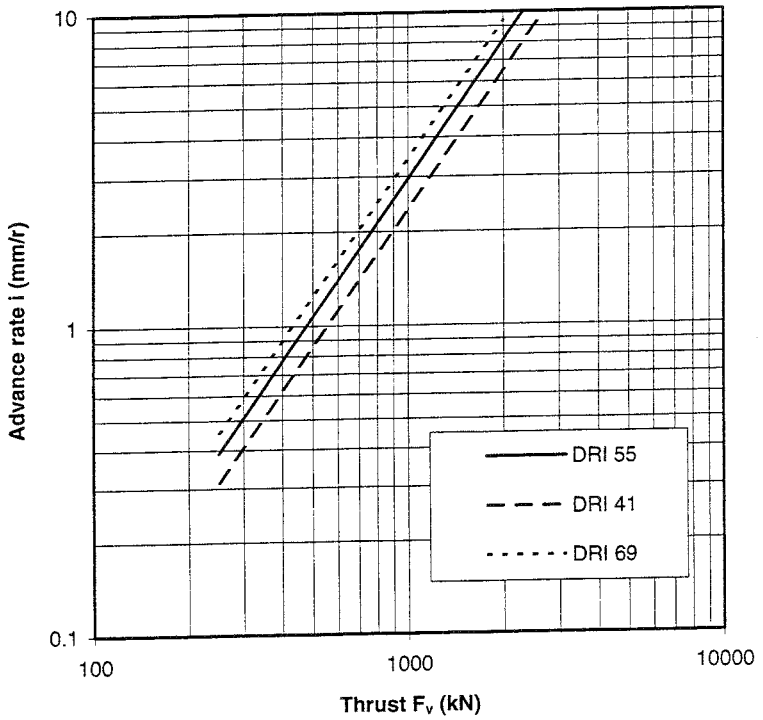

Figure 8.1-6. *Thrust-advance curves for 5 & 6 row cutters with different DRI-values which are 75 %, 100 % and 125 % of the DRI-value in the Research Tunnel. The corresponding DRI-values are 41, 55, 69 and these cover the range for most common granitic rocks.*

Corresponding rates of advance were also estimated for rock types with different drillability in a similar manner assuming that the critical thrust in different types of rock is linearly dependent on the DRI-value. A correlation between DRI-value and thrust has been established in the form of a correlation factor for critical thrust, K_{DRI} (NTH 1988), which gives the modified thrust. The result obtained was consistent with the one shown in Figure 8.1-6.

It is assumed that the DRI-value describes boring performance better than compressive strength and therefore the behaviour shown in Figure 8.1-6 can be regarded as being more proper than that shown in Figure 8.1-4.

8.1.3 Performance estimate for the method

In respect to the optimum performance achievable with the method, both the thrust exerted and the torque of the boring machine used in this boring demonstration were low, as was the efficiency of vacuum suction.

If it is assumed that the thrust force and torque could be raised without limitation, the theoretical upper limit of performance is determined by the cutter capacity.

The maximum bearing capacity of the cutter is 300 kN. The maximum thrust divided by the largest number of rows in a single cutter gives a maximum possible thrust of 50 kN per button row. According to Equation 5-9, the maximum thrust which could be applied to the cutter head used in this work would therefore be 1750 kN. The corresponding torque would then be 114 Nm. That would give an advance rate of about 7 mm/rev. which is equivalent to 3.2 m/h at a rotation speed of 8 rpm.

At high advance rates, and even at an advance rate of 3.5 m/h, the air flow ratio would rise to the upper limit of the current dilute vacuum suction system and cleaning of the bottom of the hole would become less effective. Also, the test results obtained suggest that the pick-up efficiency of the nozzles would be reduced significantly if the rotation speed of the cutter head is increased. Therefore the performance of the method is limited by the efficiency of the vacuum cleaning in keeping the bottom of the hole clean. The results indicate that the thrust on a similar type of cutter head to that used in the test could be raised to improve the boring efficiency significantly. The possibility of improving performance by increasing the rotation speed is a more open question, but probably, such a change to the operating parameters could to some extent be utilized if the efficiency of the vacuum flushing system is also improved.

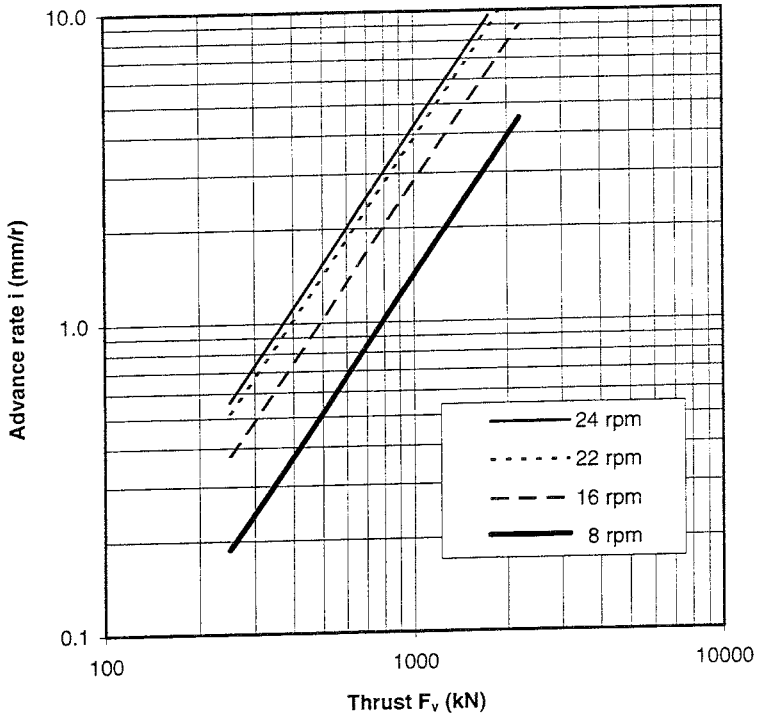

Figure 8.1-7. *Advance rate (m/h) plotted against thrust (kN) for 5 & 6 row cutters with different rotation speeds of 8 rpm (as used in the Research Tunnel), 16 rpm and 24 rpm.*

The normal rotation speed of the cutter head, 8 rpm, used in the work is low. The rotation speed could be doubled to 16 rpm or increased to the maximum of 22 rpm (determined by the maximum rotation speed, 100 rpm, of the roller cutters). The corresponding theoretical advance rate at the maximum thrust force of 1750 kN would be 6.4 m/h or 8.8 m/h (Figure 8.1-7), assuming that the vacuum flushing system is functioning properly - which most likely shall not be the case.

8.2 OPERATIONAL EXPERIENCES

The boring equipment is compact and easy to transfer since the only fixed connections needed are those providing a supply of electricity.

The space requirement of the boring equipment used in the Research Tunnel is greater than the space that will be available in deposition tunnels. It will be easy to modify the equipment to fit the space available in the deposition tunnels - this is in turn determined by the space required for canister emplacement.

The occupational conditions were judged to be acceptable. The impact of the method on the environment is limited and consists primarily of emissions of hydraulic oil. These emissions can be reduced by proper equipment design and operation.

The problems encountered in the work which were manifested by the low degree of equipment utilization achieved were primarily related to the technical design and implementation of the method.

The performance of the large diameter cutter head was disturbed by problems which were mainly related to the filling of the pilot hole during the boring of the large hole, breakage or clogging of the nozzles and wear of the components in the vacuum flushing system. The operations of detaching the large cutter head for pilot boring and its subsequent reattachment were quite labour-intensive tasks.

The principle of boring the large diameter hole in a single run was demonstrated by the boring of a section of the second large hole without a separate pilot hole in a so called 'single pass' test. Technically, the boring equipment performed well.

The vacuum suction system performed well although some problems were encountered which were in the main related to the monitoring of the equipment, extensive wear of the components in the vacuum suction line and rapid filling of the dust compartment of the vacuum unit.

The principle of vacuum flushing and transportion of crushed rock using a flow of air was found to be advantageous. Both direct and reverse flushing using either water or air as transport media can be used to remove crushed rock from beneath the cutter head. The advantages of vacuum air flushing compared to water flushing is that the equipment required is compact and easy to move, and that the technique makes it possible to observe the surface and bottom of the hole while boring. Another major advantage is that the flushing media, air, is available everywhere. It should however be noted that extensive cleaning of the outflow air from the vacuum unit is required in order to provide a good working environment for personnel.

The main problems which should be addressed when improving the method are: filling of the pilot hole; extensive wear of the vacuum suction system; set-up and transfer characteristics of the boring equipment; cleaning of filters and emptying of the tank for crushed rock.

Wear on the cutters as a result of the boring of the three large holes was below the limit of measurement, but according to the performance data and particle size distribution of the crushed rock, some regrinding of the crushed rock took place during the boring and therefore, compared to normal raiseboring, somewhat increased cutter wear is expected. Information provided by contractors and manufacturers suggests that the lifespan of a single cutter dressing is at least 500 m of boring in granitic rock. If the lifespan is taken to be only half this estimate (i.e. taking a conservative view), this is equivalent to 250 m of boring or 32 holes of a depth of 7.5 m.

The results of the work time analysis imply that the best way to improve the degree of utilization when boring relatively short holes is to reduce the time spent on set-up and transfer of the equipment (19 %) and preparation for boring (15 %) so that maintenance and service work is carried out during these activities.

Although the observed overall performance of the boring equipment was hampered by the low degree of utilization achieved, the operating experience gained from the current tests can be used to make an approximate estimate of the overall performance of a similar piece of equipment modified so that the parts most vulnerable to wear are strengthened sufficiently to last for at least the time required to bore a single hole. The estimated total time required for boring a hole of depth 7.5 m (in rock) without interruptions and maintenance work on the vacuum suction line would be as shown in Table 8.2-1, i.e. 40 hours for a two person crew or about 6 normal underground shifts. This is equivalent to 80 manhours.

Table 8.2-1. An estimated time division between the basic work phases (excluding repair, maintenance, transport, transfer etc.) for a single hole of depth 7.5m.

Activity	Hours
Boring of pilot hole	6.0
Boring of large hole	15.0
Extension of pipes (l=152 cm)	1.3
Change of large cutter head	4.7
Emptying, rock tank and vacuum unit	13.0
The total	40.0

8.3 QUALITY OF THE HOLE

The main measurements used when assessing the quality of the holes were surface roughness, straightness, geometry, and the disturbance of the rock caused by boring. It should be remembered that the boring equipment used had not been designed to meet any particular quality requirements and there are ways of modifying the boring equipment to produce a different quality of hole, if this is deemed favourable.

For example, the disturbance caused by boring can be ameliorated by adjusting the thrust on the buttons in the outermost button row of the cutter head which finishes the surface. The surface roughness can be influenced by more rigid stabilization of the cutter head and the design and configuration of the gauge rollers used. Similar considerations also apply to the geometrical properties of the hole.

The surface roughness of the hole and the deflection of the hole have an effect on the total surface area and the volume of the hole when compared to a totally even surface presented by an ideal geometrical cylinder with a diameter of 1524 mm. The increase in the surface area of the walls of the full scale experimental deposition holes in comparison to a totally even surface was estimated to be 15 % and the increase in volume was estimated to range from 0.4 % to 1.1 % depending on the deflection of the axis of the hole from 0 to 22 mm, see Figure 8.3-1. The values can be applied to hole diameters from 1.5 to 1.6 m.

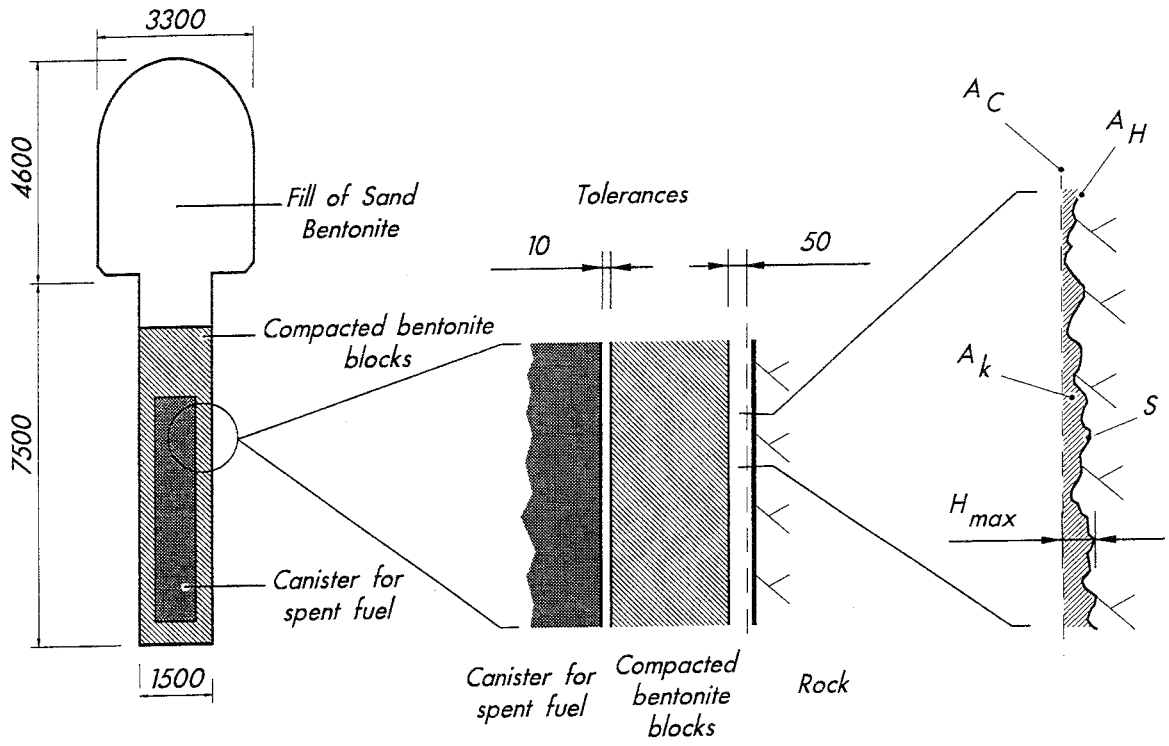

Figure 8.3-1. *Effect of surface roughness on the volume and surface area of a KBS-3 type deposition hole. A_C is the surface of the ideal cylinder, A_H is the surface of the hole, S is the length of the surfaceline of the profile, A_k is the cross-sectional area between the hole and the ideal cylinder surface and H_{max} is the maximum amplitude of the highest peak in the surface profile, which determines the radius of the ideal cylinder.*

8.4 EFFECT OF THE STATE OF STRESS

The considerations which apply to rock mechanics for raiseboring in hard rock are also applicable to the boring of deposition holes. Practical aspects may differ since the depth of deposition holes (7.5 m) is shallow when compared to holes made in normal raiseboring applications. In very good quality rock which is under a moderate stress field (the relevant assumption when designing a repository for spent nuclear fuel) problems are not usually encountered although the combination of a high stress field, unfavourable stress direction and low rock strength can cause failures in the walls of deposition holes at depths of 500 meters (Tolppanen et al. 1995).

In cases where sporadic failures occur, the following matters should be taken into consideration when evaluating the mechanical behaviour of rock which is subject to boring:

- The boring of a hole is a dynamic process. The stress distribution changes as the boring proceeds. The diameter of the upper stem section of the hole is deformed more than the lower section as a consequence of high stresses in rock.

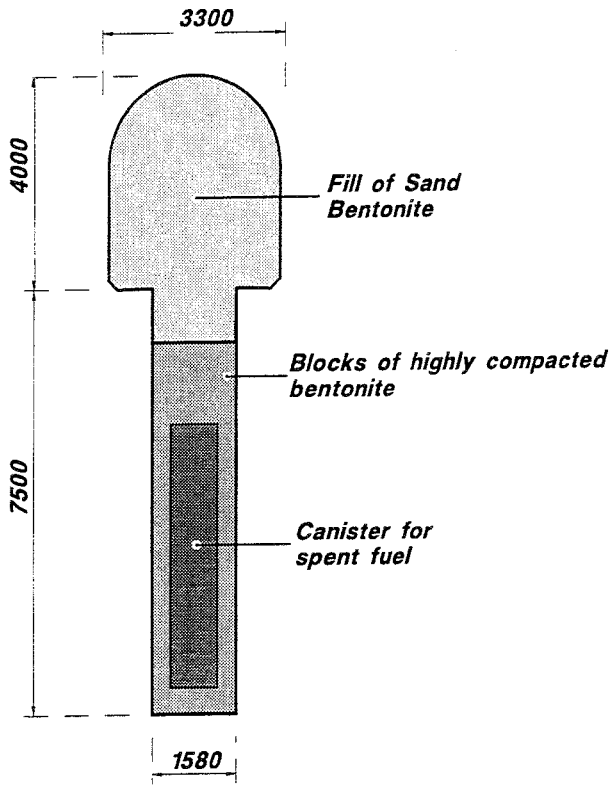

Figure 8.4-1. Section through the deposition tunnel and deposition hole (TVO 1992).

- The deposition tunnel affects stress redistribution around the deposition holes. The stress field around the hole close to floor level is higher than the stress field in the stem part of the hole. The highest compressive stresses appear close to the tunnel floor, see Figures 8.4-1 and 8.4-2.

- If the deposition tunnel is excavated by drill and blast, a zone of excavation disturbance and stress release will exist in the upper part of the hole and this affects the stress distribution. If the deposition tunnel is excavated using a tunnel boring machine the stress concentrations will be closer to the floor of the deposition tunnel and of higher magnitude.

- The mechanical excavation damage caused by boring is very limited and stresses are therefore concentrated close to the walls of the holes.

The possible modes of deformation of rock around deposition holes are elastic deformations, spalling and slabbing, and block failures.

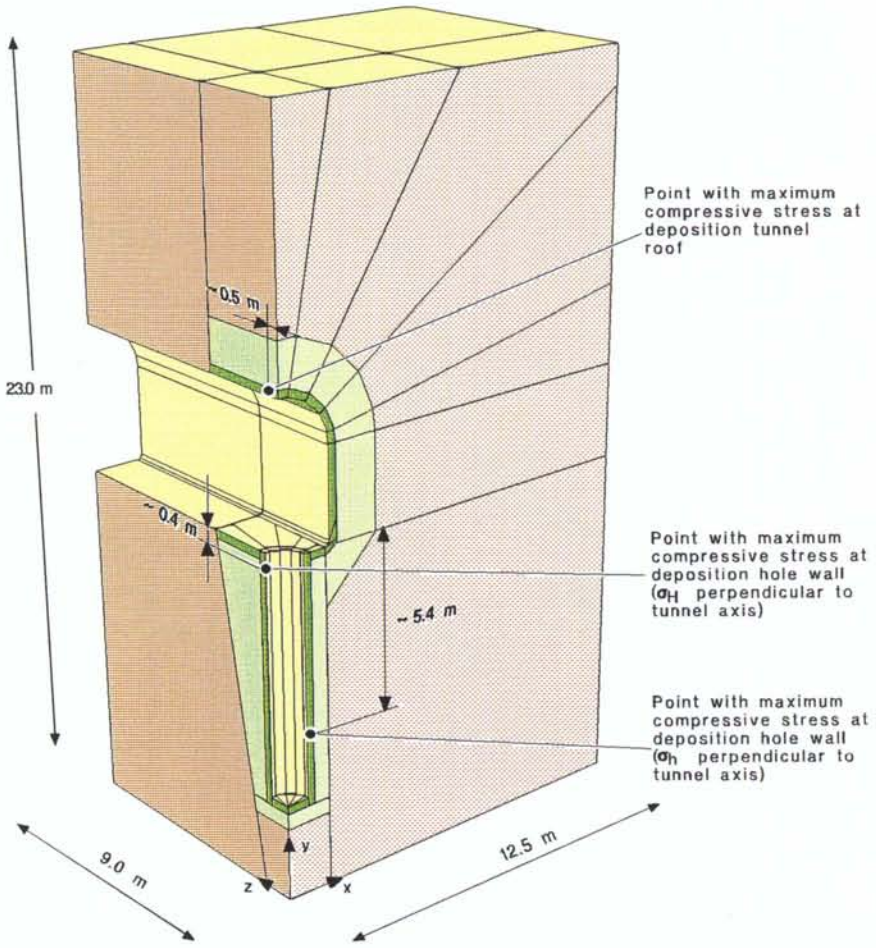

Figure 8.4-2. *A model of the deposition hole and the locations where the maximum compressive stresses occur in regard to the direction of principal stresses (Tolppanen et al. 1995).*

Elastic deformations cause the diameter of the holes to be reduced by a few millimeters depending on the exact state of the stress. The deformation of the hole diameter is of the same order as the variations in hole diameter measured in the experimental deposition holes. The cutter head used for boring of deposition holes should therefore be furnished with side rollers which makes it possible to backream the hole to a more accurate final diameter since the deformations will be larger above the cutter head. Deformations of the elastic type are therefore not expected to pose significant problems.

Under high stress occasional spalling or slabbing may occur (Kaiser & McCreath 1994, Tolppanen et al. 1995), which can result in "dog earing" type breakouts. The rock around deposition holes is assumed to be of very good quality and the state of stress is assumed to be moderate even though some differences are expected between different sites and also locally within sites. This possible spalling and slabbing will cause fragmented rock to fall to the bottom of the hole and will not pose an obvious problem.

It is also possible that sporadic block type failures will occur. In most cases the unfavourable fracturing which might cause wedge failures will probably be detected during the characterization of the deposition tunnels. The same applies also to local peak variations in the stress field which will probably also be detected during the characterization period.

The area of greatest potential for block failures is located in the upper part of the hole where the floor of the deposition tunnel forms a free plane of the block, see Figure 8.4-3. Other failures will be very limited in size because of the sparse fracturing and hole geometry. The deformed blocks can be removed from the hole or reamed by using side rollers.

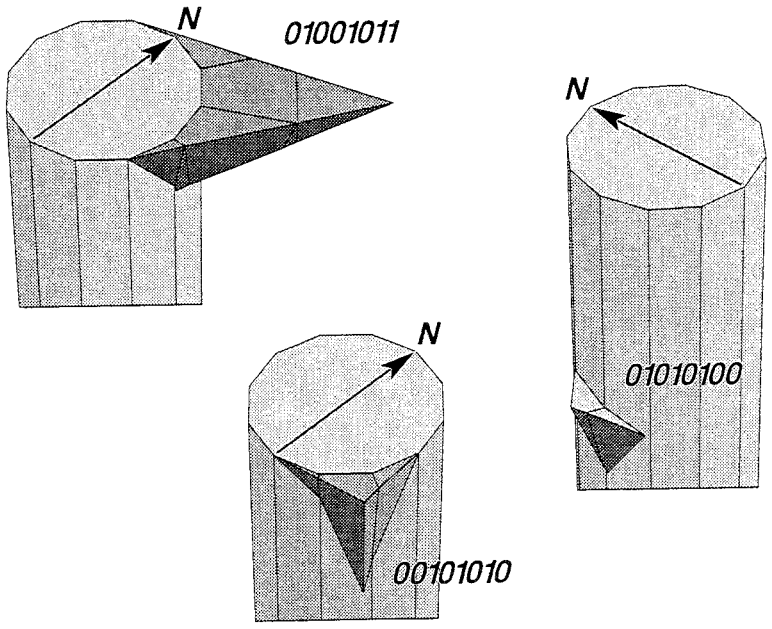

Figure 8.4-3. *An example of three types of possible critical block structures around deposition holes based on field data, KEYBLOCK and 3DEC-analyses.*

8.5 DISCUSSION OF FUTURE DEVELOPMENT

The following factors are significant when assessing the feasibility of a deposition hole boring machine and design aspects:

- The deposition tunnel where the boring must be carried out offers very limited space (width about 3.4 m and height about 4 m).

- Cutter wear is not as significant a factor as it is in raise boring since cutters can be changed frequently and without difficulty.

- The machine will be moved frequently since each deposition hole requires only 7.5 to 8.0 m of boring.

- The design of the cutter head must be based on the quality of the hole required and the boring performance expected.

The key to the quality of the hole and the boring performance is the placement of cutters in the cutter head and the cutter geometry employed. Also, it seems obvious that the shape of the bottom of the hole should be changed from that achieved in the experimental deposition holes. The shape of the hole bottom depends on whether the hole is made in a single run without a separate pilot hole, or by boring a smaller pilot hole before boring the large hole.

If a pilot hole of about 310 mm is required, the minimum number of 5 and 6 row cutters needed to produce the same number of rows and the same distance between rows as in the cutter head studied in these tests is 6, which is equivalent to a total of 30 rows. The total thrust which can be utilized is 50 kN per button row which is equivalent to a total thrust on the cutter head of about 1500 kN. The same advance rates can be achieved with this design at a smaller thrust and using less cutters than with the cutterhead used at the Research Tunnel. The performance of the cutter head would be increased and there would be additional room for nozzles in the cutter face. A disadvantage of this approach is that wear on the outer cutters would be increased and they would have to be replaced more frequently.

The degree of utilization of the boring machine can be improved by proper selection of materials and good design as discussed in Chapter 4. The transport, transfer and set-up of the machine takes a large proportion of time and therefore the boring equipment should be designed as a single unit which can be moved in one piece in the same manner as current tunnel boring machines. The method used for transfer can be based on wheels, rails or a track. The set-up and support as well as lifting of the machine for attachment of the cutter head can be achieved using hydraulic cylinders.

The handling and treatment of crushed rock can be arranged in the same manner as in tunnel boring by the use of continuous unloading. The main difference is that in this method of deposition hole boring the crushed rock is collected under vacuum pressure which favours the use of closed tanks.

A major limitation on the efficiency of the boring machine is, according to these tests, the efficiency of the vacuum suction system which is sensitive to an increase in the cutter head rotation speed. The efficiency of the vacuum suction system could be raised in different ways:

- improved design of nozzles and cutter placement
- addition of extra nozzles to the cutter head
- increasing the diameter of the suction line to raise the airflow rate and reduce the flow ratio.

An important part of the design of the equipment should be the monitoring and control system. The flow of air should be monitored to detect possible blocking of nozzles or other types of malfunction. To cope with the problem of blocked nozzles, a system should be constructed which is able to open the nozzles by using a blast of compressed air.

The inflow rate of air into the vacuum suction system should also be adjusted to the advance rate to achieve an optimum flow ratio which will also reduce the speed of the air and consequent wear on the elements of the suction pipeline.

Wear of the suction pipeline is affected by the particle size of the crushed rock and the velocity of the rock particles. Experimental observations (Marcus et al. 1990) show a clear increase in wear with increase in particle size, this being governed by the efficiency of the boring and the rock breaking process. The efficiency of the boring process increases as the particle size is raised and therefore it is not beneficial to reduce wear by reducing the particle size.

A much more effective means of reducing wear is to control the speed of the airflow. The relationship between wear and particle velocity which is dependent on the air speed can be written in the following form (Marcus et. al. 1990):

$$W = C\,V^{n} \qquad 8\text{-}10$$

where,
- W is the wear or erosion
- V is the air speed
- C is an experimental constant
- n is an experimental constant.

The value of n derived from experiments on brittle materials is 6. The effect of particle velocity and air speed is therefore significant.

The filters and related compartments for handling the crushed rock should be designed to minimize the need for stops during operation. This should be achieved by employing a system which continuously cleans the filters during the boring operation and by using a cyclone separation arrangement which prevents large quantities of crushed rock entering the filter unit.

Suitable mechanical concepts for deposition hole boring equipment, such as those shown in Figures 8.5-1, 8.5-2 and 8.5-3, have been proposed. These could be modified in various ways to meet different standards.

The wheel-mounted boring equipment concept shown in Figure 8.5-1 was developed on the basis of experience gained. Hydraulics are used to raise the wheels of the boring machine and to support it during boring. After boring the boring machine is lifted back onto the wheels and is then ready for transfer to the next hole. All units can be changed for repair and maintenance and the unloading of crushed rock can be carried out on a continuous basis.

The most critical part in the design of a boring system for deposition holes is the flushing system. Water, air, or both can be employed as the flushing medium. Flushing can be based either on suction through the drill string, blasting, spraying, or a combination of these techniques.

In general, a blast of air is more effective than suction for the cleaning of surfaces. The same is true when using water as a flushing medium. A cleaning system based on blasting could therefore be more efficient when boring.

In the boring of deposition holes the use of air as the flushing medium has advantages.

The proposed flushing concepts for use in the boring of deposition holes are:

- Flushing based on the same principle as the equipment described in this report (patent pending, Kroll-Disab et al. 1994) but employing additional nozzles or suction openings which are positioned closer to the centre of the hole. One such design has been proposed by Robbins (Tahvanainen & Matikainen 1983), see Figure 8.5-4.

- Flushing based on both blasting and suction. One such type design has been patented (Sinclair & Lively 1993), see Figure 8.5-5. A draft describing the principle is shown in Figures 8.5-6 and 8.5-7.

- Flushing based on high pressure spraying of water and suction of air. A draft describing the principle is shown in Figure 8.5-8.

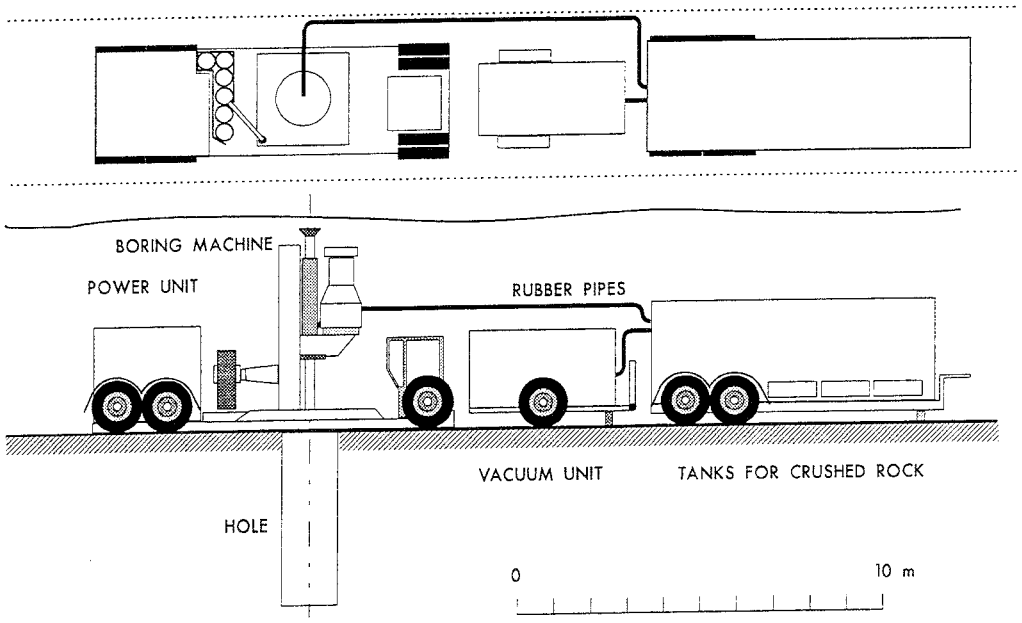

Figure 8.5-1. *One proposed concept for a deposition hole boring machine.*

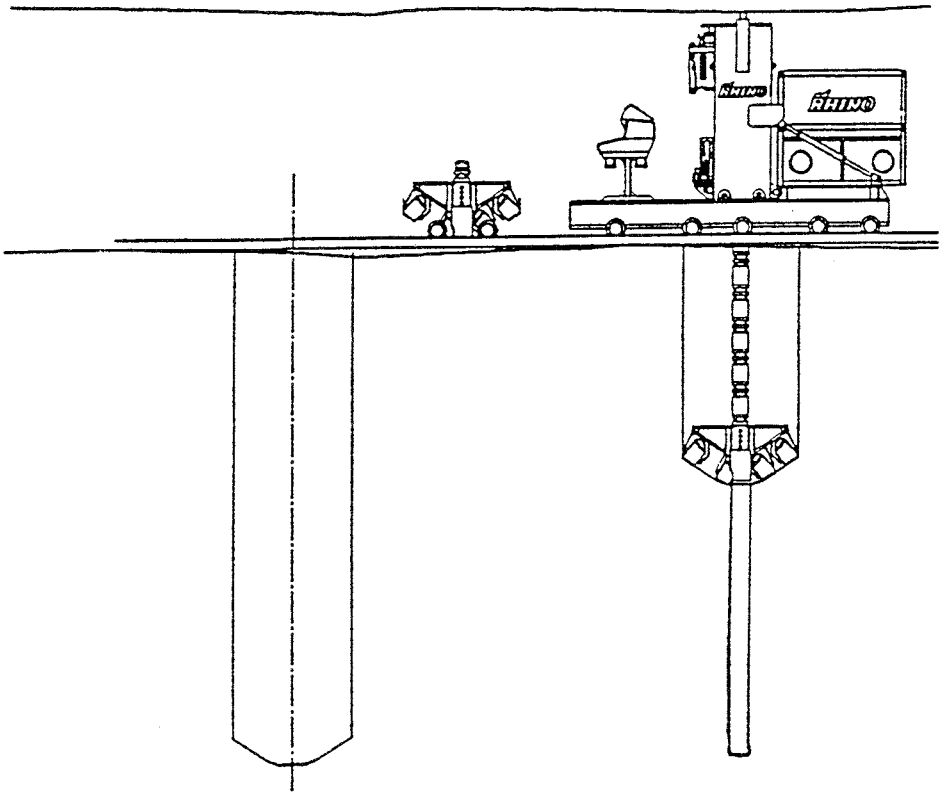

Figure 8.5-2. *The Tamrock concept for a deposition hole boring machine (Autio 1992).*

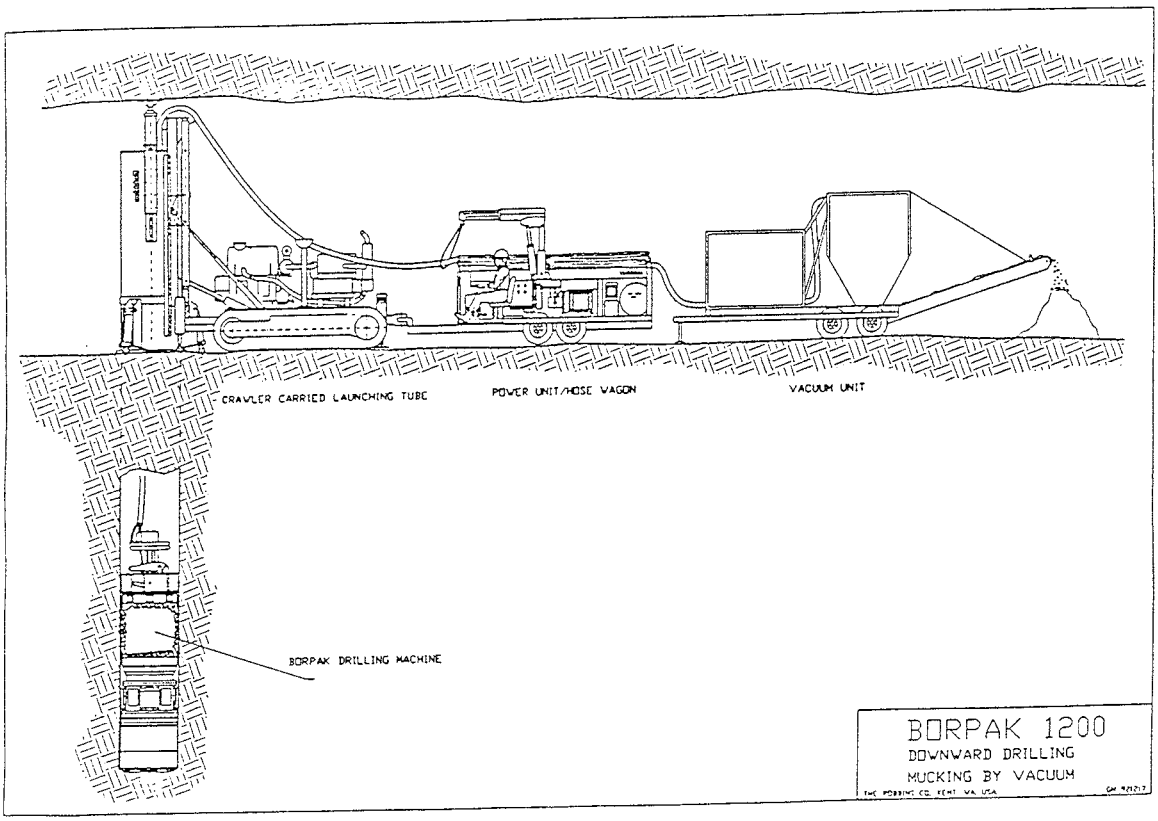

Figure 8.5-3. *The Robbins concept for a deposition hole boring machine (Robbins Ltd).*

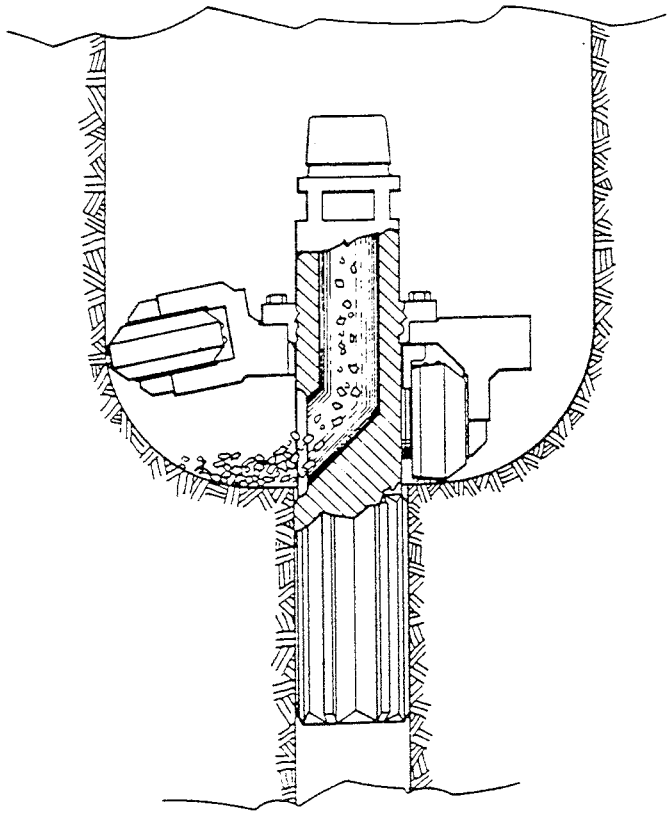

Figure 8.5-4. *Design for suction through the drill string by the Robbins Company (Tahvanainen & Matikainen 1983).*

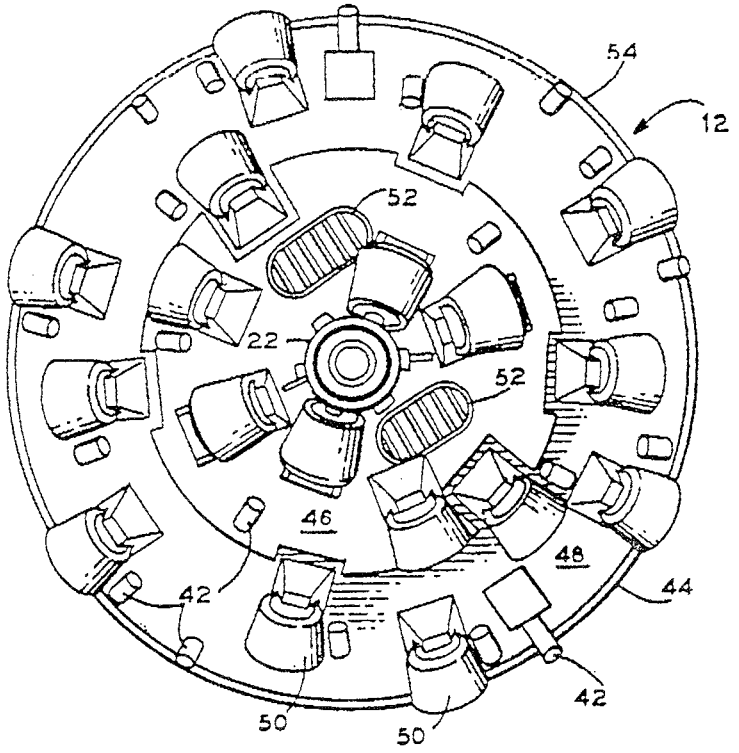

Figure 8.5-5. *Cutter head design based on air blasting and suction (Sinclair & Lively 1993).*

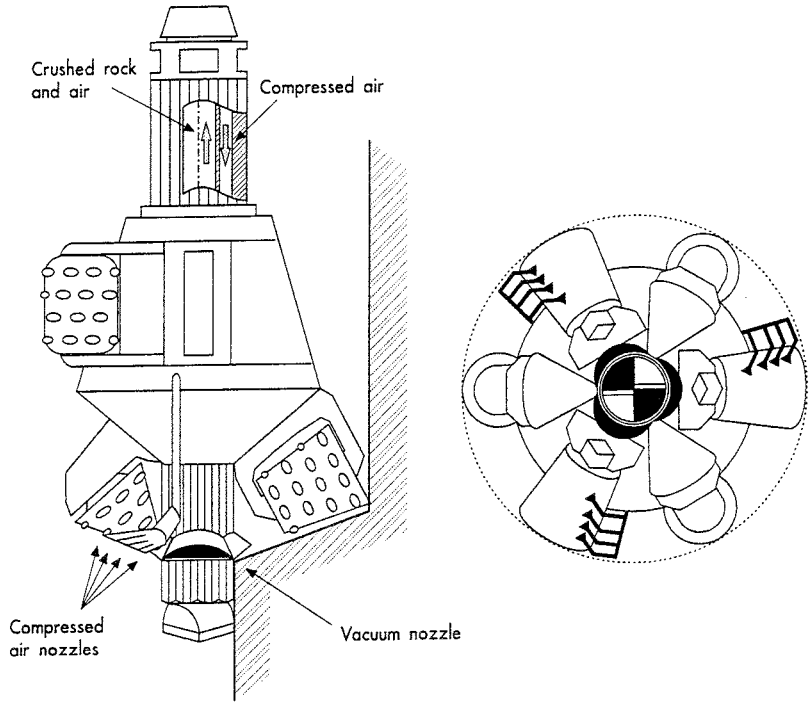

Figure 8.5-6. *Cutter head concept employing suction from the centre of the cutter head.*

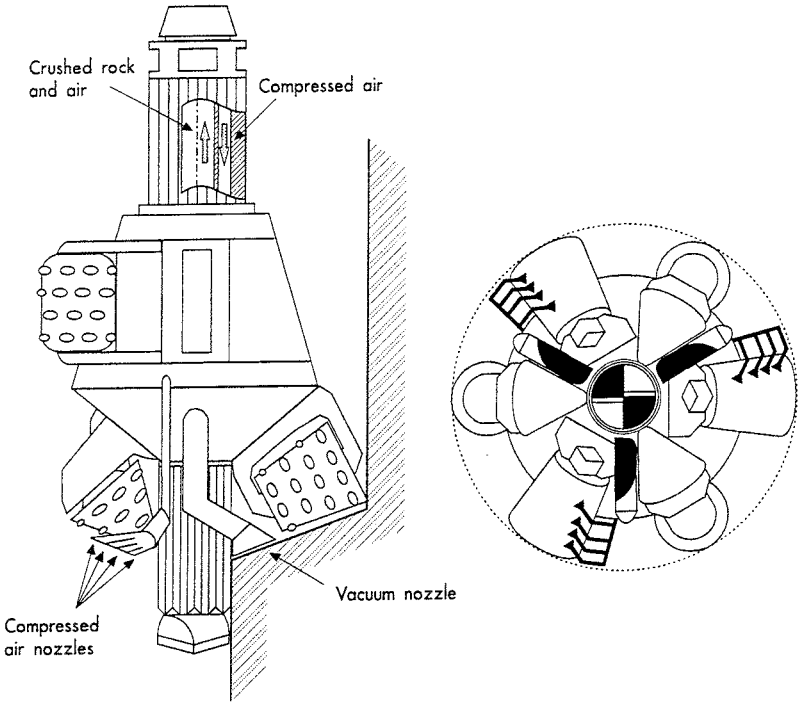

Figure 8.5-7. *Cutter head concept employing both air blasting and suction.*

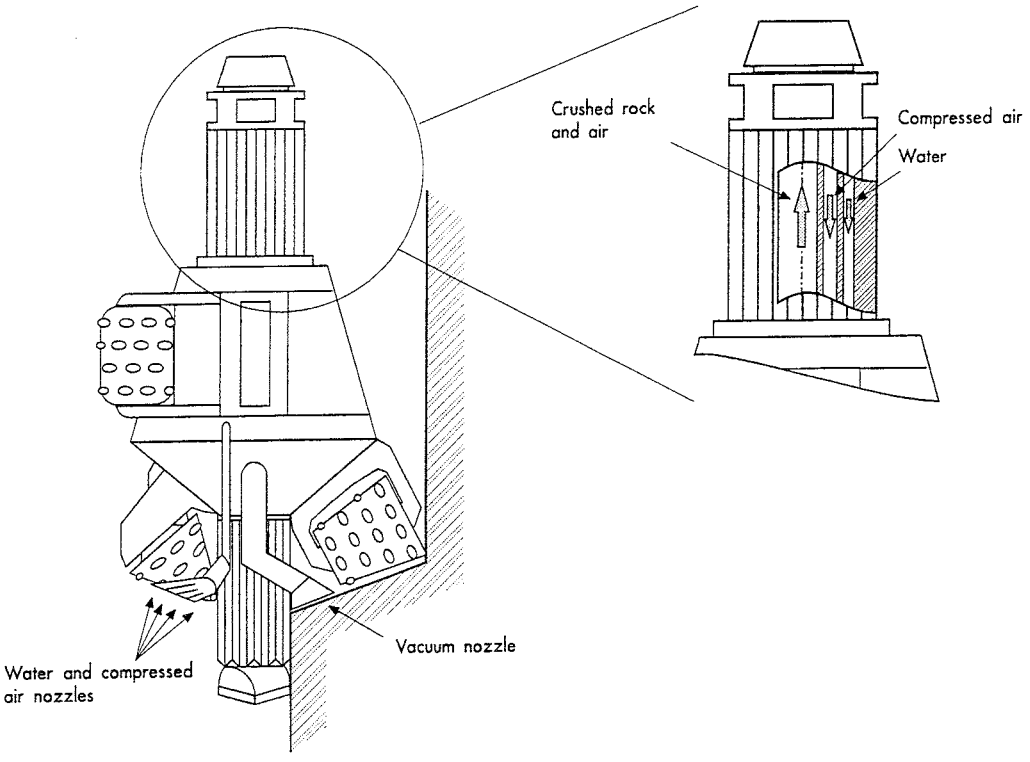

Figure 8.5-8. *Cutter head concept employing a high-pressure water spray, blasting of air and suction.*

REFERENCES

AB Sandvik Rock Tools, 1980. Test data of particle size distribution of granit, 16-December 1980 and 8-Jan 1981 (grov granit).

AB Sandvik Rock Tools. Raise boring equipment, Sandvik modular flat-head Raise Boring System covering raise sizes from 0.6 to 6.1 meters. Booklet HR-12671-ENG)

Autio, J. 1992. Description of Tamrock Equipment for Boring Vertical Deposition Holes. Helsinki. TVO/KPA Turvallisuus ja Tekniikka Work Report 92-02.

Autio, J. 1996. Characterization of the excavation disturbance caused by boring of the experimental full scale deposition holes in the Research Tunnel at Olkiluoto. Report POSIVA-96-09, Posiva Oy, Helsinki and similar report in SKB's (Svensk Kärnbränslehantering AB) report series (in preparation).

Autio, J. & Kirkkomäki, T. 1996. Boring of full scale deposition holes using a novel dry blind boring method. Boring procedure and operational experiences Work report TEKA-96-04e, Posiva Oy, Helsinki and similar report PR D-96-030 in SKB's (Svensk Kärnbränslehantering AB) report series.

Autio, J. & Kirkkomäki, T. 1996a. Test boring at Långdal using a novel dry blind boring method. Work report TEKA-96-03e, Posiva Oy, Helsinki and similar report AR D-96-015 in SKB's (Svensk Kärnbränslehantering AB) report series.

Autio, J., Äikäs, T. & Kirkkomäki T. 1995. Coring and description of samples from the full scale experimental deposition holes at TVO/Research Tunnel. Helsinki. Teollisuuden Voima Oy. Work Report TEKA-95-02 and similar report AR D-95-003 in SKB's (Svensk Kärnbränslehantering AB) report series.

Boisson, J. Y. & Derlich, H. S. 1994. Études de la fissuration et de la microfissuration du granite. Sciences et techniques nucléaires. Commission européenne. Rapport EUR 15185 FR.

CERCHAR 1986. The Cerchar Abrasiveness Index. Charbonnages de France. Report 86-538.

Dagnall, H. 1986. Exploring surface texture. Rank Taylor Hobson Limited.

Halttunen, K. 1995. Linear surface profile measurements with laser profilometer of experimental full scale deposition holes in TVO Research Tunnel. Helsinki. Teollisuuden Voima Oy, Work Report TEKA-95-09 and similar report AR D-95-012 in SKB's (Svensk Kärnbränslehantering AB) report series.

Hartikainen, J., Hartikainen, K., Pietarila, H. & Timonen, J. 1995. Permeability and diffusivity measurements with the He-gas method of excavation-disturbed zone in rock samples cored from the full-scale experimental deposition holes in the TVO Research Tunnel. Helsinki. Nuclear Waste Commission of Finnish Power Companies. Report YJT-95-16 and similar report AR D-95-018 in SKB's (Svensk Kärnbränslehantering AB) report series.

Hartman, H.L. 1992. SME Mining Engineering Handbook. Littleton, Colorado. Society for Mining, Metallurgy and Exploration, Inc.

Johansson, E. 1994. Rock Mechanical Properties of Intact Rock in TVO´s Test Boring Site in Boliden, Sweden. Helsinki. Teollisuuden Voima Oy. Work Report TEKA-94-15.

Johansson, E. & Autio, J. 1993. Rock Mechanical Properties of Intact Rock in TVO´s Research Tunnel. Helsinki. Teollisuuden Voima Oy. Work Report TEKA-93-05.

Johansson, E. & Autio, J. 1995. Properties of Rock in TVO Research Tunnel and Investigation Sites. Helsinki. Teollisuuden Voima Oy. Work Report TEKA-95-10.

Kaiser, P. & McCreath, D., 1994. Rock Mechanics Considerations for Drilled or Bored Excavations in Hard Rock. Tunneling and Underground Space Technology. vol. 9, No. 4., 1994. Pergamon Press.

Knuuttila, T. 1994. Otaniemi. Valtion teknillinen tutkimuskeskus. VTT Tutkimusselostus VAL45139.

Kou, S., Lindqvist, P-A. & Tan, X. 1994. Conceptual Model of Crack Structure in Rock Caused by Mechanical Excavation. Luleå University of Technology. Svensk Kärnbränslehantering AB SKB. Project Report PR 44-94-022.

Kroll-Disab AB, Sandvik AB, Drillcon Contracting AB 1994. Anordning, förfarande och borrhuvud för torr fullareaborrning, Patentansökning nr 9400324-1, Rotel 436. Patent- och Registreringsverket, Sverige.

Kuula, H. & Johansson, E. 1991. Rock mechanical stability of the VLJ repository. Helsinki. Nuclear Waste Commission of Finnish Power Companies. Report YJT-91-03 (in Finnish).

Lappalainen, K. 1994. TVO:n tutkimustunnelin sijoitusreikien porauksessa syntyneen porausmurskeen laboratoriomääritykset. Helsinki. Tielaitos, Geokeskus (in Finnish).

Lien, R. 1980. Classification of Rock Drillability (in Norwegian). Proc. Norwegian Nat. Tunneling Conf., Oslo 1980. Tapir.

Lingvist, P-A., Suarez del Rio, L.M., Montoto, M., Tan, X.C. & Kou, S.Q. 1994. Rock Indentation Database - Testing Procedures, Results and Main Conclusions. Luleå University of Technology. Svensk Kärnbränslehantering AB SKB. Project Report PR 44-94-023.

Lislerud, A. 1994. Tamrock Oy Technology Center. Personal communication.

Marcus, R.D., Leung, L.S., Klinzing, G.E. & Rizk,F. 1990. Pneumatic Conveying of Solids. London. Chapman and Hall.

Nord, G. 1980. Drilling Holes in Rock for Final Storage of Spent Nuclear Fuel. Stockholm. SKBF/KBS. Teknisk raport 80-12.

NTH, Norges Tekniske Hϕgskole, 1988. Hard Rock Tunnel Boring. Trondheim. The University of Trondheim, The Norwegian Institute of Technology, The Division of Construction Engineering. Project Report 1-88.

NTH, Norges Tekniske Hϕgskole, 1994. Fullprofilboring av tunneler, Trondheim. The University of Trondheim, The Norwegian Institute of Technology, The Division of Construction Engineering. Project Report 1-94 (in Norwegian).

Nykyri, M., Riekkola, R., Äikäs, K., Johansson, E. & Kuula, H. 1991. Underground repository for low and intermediate radioactive waste at Olkiluoto. Finland. Proc. of 7th Int. Cong. on Rock Mechanics. A.A. Balkema. Rotterdam.

Nykyri, M., Helenius, J., Johansson, E. & Nieminen, J., 1994. Monitoring of the bedrock in the VLJ Repository in 1992. Work report VLJ 94-02. Teollisuuden Voima Oy, Helsinki (in Finnish).

Pusch, R. & Nilsson, J. 1982. Buffer Mass Test - Rock Drilling and Civil Engineering. Sweden. SKBF/KBS. Stripa Project 82-07.

Rautio, T. & With, E. 1993. Core drilling in the VLJ repository in 1993, boreholes VLJ-KR4...KR8. Helsinki. Teollisuuden Voima Oy. Work Report VLJ-93-01 (in Finnish).

Siitari-Kauppi, M. 1995. Investigation of porosity and microfracturing in a disturbed zone with ^{14}C-PMMA method based on samples from full-scale experimental deposition holes of the TVO Research Tunnel. Helsinki. Nuclear Waste Commission of Finnish Power Companies, Report YJT-95-13 and similar report AR D-96-001 in SKB's (Svensk Kärnbränslehantering AB) report series.

Sinclair, K. & Lively, J. 1993. Dry Pneumatic System for Hard Rock Shaft Drilling. United States Patent. Patent number 5.199.515. April 6, 1993.

Super Products 1993. "Super Sucker"™ industrial vacuum loader , Model 100 specifications.

Tahvanainen, T. & Matikainen, R. 1983. Sijoitusreikien poraus käytetyn polttoaineen loppusijoitustiloihin. Otaniemi, Helsinki. Teknillinen korkeakoulu, Louhintatekniikan laboratorio. Raportti YJT-83-07 (in Finnish).

Tan X.C., Kou, S. & Lindqvist, P-A. 1994. Cracks in Rocks Caused by Mechanical Excavation. Svensk Kärnbränslehantering AB SKB. Work Report AR 44-94-002.

Tolppanen, P., Johansson, E. & Hakala, M. 1995. Rock Mechanical Analyses of in Situ Stress/strength Ratio at the TVO Investigation Sites Kivetty, Olkiluoto and Romuvaara. Helsinki. Nuclear Waste Commission of Finnish Power Companies. Report YJT-95-11.

TVO 1992. Final Disposal of Spent Fuel in the Finnish Bedrock, Technical Plans and Safety Assessment. Helsinki. Teollisuuden Voima Oy. Report YJT-92-31-E.

Työministeriö 1993. HTP-arvot 1993. Turvallisuustiedote nro 25 (1993). Työministeriön kemian työsuojeluneuvottelulautakunta (in Finnish).

Wichmann, C. 1993. Blind hole boring of vertical KBS-3 disposal holes, possible techniques and equipment. Stockholm. Svensk Kärnbränslehantering AB SKB. Work Report AR-93-14.

Äikäs, K. & Sacklén, N. 1993. Fracture mapping in the Research Tunnel. Helsinki. Teollisuuden Voima Oy. Work Report 93-01.

List of SKB reports

Annual Reports

1977-78
TR 121
KBS Technical Reports 1 – 120
Summaries
Stockholm, May 1979

1979
TR 79-28
The KBS Annual Report 1979
KBS Technical Reports 79-01 – 79-27
Summaries
Stockholm, March 1980

1980
TR 80-26
The KBS Annual Report 1980
KBS Technical Reports 80-01 – 80-25
Summaries
Stockholm, March 1981

1981
TR 81-17
The KBS Annual Report 1981
KBS Technical Reports 81-01 – 81-16
Summaries
Stockholm, April 1982

1982
TR 82-28
The KBS Annual Report 1982
KBS Technical Reports 82-01 – 82-27
Summaries
Stockholm, July 1983

1983
TR 83-77
The KBS Annual Report 1983
KBS Technical Reports 83-01 – 83-76
Summaries
Stockholm, June 1984

1984
TR 85-01
Annual Research and Development Report 1984
Including Summaries of Technical Reports Issued during 1984. (Technical Reports 84-01 – 84-19)
Stockholm, June 1985

1985
TR 85-20
Annual Research and Development Report 1985
Including Summaries of Technical Reports Issued during 1985. (Technical Reports 85-01 – 85-19)
Stockholm, May 1986

1986
TR 86-31
SKB Annual Report 1986
Including Summaries of Technical Reports Issued during 1986
Stockholm, May 1987

1987
TR 87-33
SKB Annual Report 1987
Including Summaries of Technical Reports Issued during 1987
Stockholm, May 1988

1988
TR 88-32
SKB Annual Report 1988
Including Summaries of Technical Reports Issued during 1988
Stockholm, May 1989

1989
TR 89-40
SKB Annual Report 1989
Including Summaries of Technical Reports Issued during 1989
Stockholm, May 1990

1990
TR 90-46
SKB Annual Report 1990
Including Summaries of Technical Reports Issued during 1990
Stockholm, May 1991

1991
TR 91-64
SKB Annual Report 1991
Including Summaries of Technical Reports Issued during 1991
Stockholm, April 1992

1992
TR 92-46
SKB Annual Report 1992
Including Summaries of Technical Reports Issued during 1992
Stockholm, May 1993

1993
TR 93-34
SKB Annual Report 1993
Including Summaries of Technical Reports Issued during 1993
Stockholm, May 1994

1994

TR 94-33

SKB Annual Report 1994

Including Summaries of Technical Reports Issued during 1994.
Stockholm, May 1995

1995

TR 95-37

SKB Annual Report 1995

Including Summaries of Technical Reports Issued during 1995.
Stockholm, May 1996

List of SKB Technical Reports 1996

TR 96-01

Bacteria, colloids and organic carbon in groundwater at the Bangombé site in the Oklo area

Karsten Pedersen (editor)
Department of General and Marine Microbiology, The Lundberg Institute, Göteborg University, Göteborg, Sweden
February 1996

TR 96-02

Microbial analysis of the buffer/container experiment at AECL´s Underground Research Laboratory

S Stroes-Gascoyne[1], K Pedersen[2], S Daumas[3], C J Hamon[1], S A Haveman[1], T L Delaney[1], S Ekendahl[2], N Jahromi[2], J Arlinger[2], L Hallbeck[2], K Dekeyser[3]

[1] AECL, Whiteshell Laboratories, Pinawa, Manitoba, Canada
[2] University of Göteborg, Department of General and Marine Microbiology, Göteborg, Sweden
[3] Guigues Recherche Appliquée en Microbiologie (GRAM), Aix-en-Provence, France
1996

TR 96-03

Reduction of Tc (VII) and Np (V) in solution by ferrous iron. A laboratory study of homogeneous and heterogeneous redox processes

Daqing Cui, Trygve E Eriksen
Department of Chemistry, Nuclear Chemistry, Royal Institute of Technology, Stockholm, Sweden
March 1996

TR 96-04

Revisiting Poços de Caldas. Application of the co-precipitation approach to establish realistic solubility limits for performance assessment

Jordi Bruno, Lara Duro, Salvador Jordana, Esther Cera
QuantiSci, Barcelona, Spain
February 1996

TR 96-05

SR 95

Template for safety reports with descriptive example
SKB
December 1995

TR 96-06

Äspö Hard Rock Laboratory Annual Report 1995

SKB
April 1996

TR 96-07

Criticality in a high level waste repository. A review of some important factors and an assessment of the lessons that can be learned from the Oklo reactors

Virginia M Oversby
VMO Konsult
June 1996

TR 96-08

A reappraisal of some Cigar Lake issues of importance to performance assessment

John Smellie[1], Fred Karlsson[2]

[1] Conterra AB
[2] SKB
July 1996

TR 96-09

The long-term stability of cement. Leaching tests

Ingemar Engkvist, Yngve Albinsson, Wanda Johansson Engkvist
Chalmers University of Technology, Göteborg, Sweden
June 1996

TR 96-10

Lake-tilting investigations in southern Sweden

Tore Påsse
Sveriges geologiska undersökning, Göteborg, Sweden
April 1996

TR 96-11
Thermoelastic stress due to an instantaneous finite line heat source in an infinite medium
Johan Claesson, Göran Hellström
Depts. of Building Physics and Mathematical Physics, Lund University, Lund, Sweden
September 1995

TR 96-12
Temperature field due to time-dependent heat sources in a large rectangular grid
– Derivation of analytical solution
Johan Claesson, Thomas Probert
Depts. of Building Physics and Mathematical Physics, Lund University, Lund, Sweden
January 1996

TR 96-13
Thermoelastic stress due to a rectangular heat source in a semi-infinite medium
– Derivation of an analytical solution
Johan Claesson, Thomas Probert
Depts. of Building Physics and Mathematical Physics, Lund University, Lund, Sweden
May 1996

TR 96-14
Oklo: Des reacteurs nucleaires fossiles (Oklo: The fossil nuclear reactors). Physics study (R Naudet, CEA)
– Translation of chapters 6, 13, and conclusions
V O Oversby
VMO Konsult
September 1996

TR 96-15
PLAN 96
Costs for management of the radioactive waste from nuclear power production
Swedish Nuclear Fuel and Waste Management Co
June 1996

TR 96-16
Diffusion of I^-, Cs^+ and Sr^{2+} in compacted bentonite
– Anion exclusion and surface diffusion
Trygve E Eriksen, Mats Jansson
Royal Institute of Technology, Department of Chemistry, Nuclear Chemistry, Stockholm
November 1996

TR 96-17
Hydrophilic actinide complexation studied by solvent extraction radiotracer technique
Jan Rydberg
Department of Nuclear Chemistry, Chalmers University of Technology, Gothenburg, Sweden
and Radiochemistry Consultant Group AB, V. Frölunda, Sweden
October 1996

TR 96-18
Information, conservation and retrieval
Torsten Eng[1], Erik Norberg[2], Jarl Torbacke[3], Mikael Jensen[4]
[1] Swedish Nuclear Fuel and Waste Management Co (SKB)
[2] National Swedish Archives
[3] Department of History, Stockholm University
[4] Swedish Radiation Protection Institute (SSI)
December 1996

TR 96-19
Application of space geodetic techniques for the determination of intraplate deformations and movements in relation with the postglacial rebound of Fennoscandia
Hans-Georg Scherneck, Jan M Johansson, Gunnar Elgered
Chalmers University of Technology, Onsala Space Observatory, Onsala, Sweden
April 1996

TR 96-20
On the characterization of retention mechanisms in rock fractures
Jan-Olof Selroos, Vladimir Cvetkovic
Div. of Water Resources Engineering, Dep. of Civil and Environmental Engineering, Royal Institute of Technology, Stockholm, Sweden
December 1996